

FLUOROUS ZIRCONIUM PHOSPHONATES AS NOVEL
MATERIALS FOR CATALYST SEPARATION AND RECOVERY

Thesis submitted for the degree of

Doctor of Philosophy

At the University of Leicester

by

James Andrew Bennett MChem (Leicester)

Department of Chemistry

University of Leicester

March 2007

UMI Number: U226935

All rights reserved

INFORMATION TO ALL USERS

The quality of this reproduction is dependent upon the quality of the copy submitted.

In the unlikely event that the author did not send a complete manuscript and there are missing pages, these will be noted. Also, if material had to be removed, a note will indicate the deletion.



UMI U226935

Published by ProQuest LLC 2013. Copyright in the Dissertation held by the Author.
Microform Edition © ProQuest LLC.

All rights reserved. This work is protected against
unauthorized copying under Title 17, United States Code.



ProQuest LLC
789 East Eisenhower Parkway
P.O. Box 1346
Ann Arbor, MI 48106-1346

Fluorous Zirconium Phosphonates as Novel Materials for Catalyst Separation and Recovery

James Andrew Bennett

Abstract

A series of new perfluoroalkylated aryl- and alkyl-diethylphosphonates [RP(O)(OEt)₂] have been synthesised respectively *via* either a palladium catalysed coupling reaction (R = aryl) or a Michaelis-Arbusov reaction (R = alkyl). The compounds have been characterised by ¹H, ¹³C, ¹⁹F and ³¹P NMR spectroscopic studies, mass spectrometry and elemental analysis. Hydrolysis of the diethyl phosphonates in strong acid allowed formation of the corresponding phosphonic acids [RP(O)(OH)₂], which have been characterised as above.

A series of platinum coordination complexes [Pt(O₃PR)(PPh₃)₂] have been prepared from the phosphonic acids, which act as dianionic bidentate ligands. These complexes have been fully characterised by ¹H, ¹³C, ¹⁹F and ³¹P NMR spectroscopies, mass spectrometry, elemental analysis and X-ray crystallographic studies.

Reaction of the phosphonic acids with a Zr(IV) salt yields amorphous zirconium phosphonate. Crystalline material can be acquired by use of HF, which forms a Zr precomplexing agent and allows slow release of Zr⁴⁺ ions. The zirconium phosphonates are insoluble and, therefore, characterisation has been limited to SEM, EDAX and solid-state IR spectroscopy and powder X-ray studies.

Amorphous fluorous zirconium phosphonates (FZrP) with varying degrees of fluorination have been successfully synthesised and their ability to recover fluorous catalysts assessed in three catalytic systems; a dirhodium perfluorobutyrate cyclopropanation of styrene, a perfluorooctyl seleninic acid oxidation of *p*-nitrobenzaldehyde and a fluorous BINAP palladium catalyst enantioselective fluorination of methyl and butyl cyclopentanone-2-carboxylate. Catalytic conversions were established by GC, enantioselectivities by chiral HPLC and metal leaching levels by ICP-OES analysis.

Conversions of 60 – 70% were attained for the cyclopropanation of styrene after 4 hours in toluene at 100 °C using 0.017 mol % of dirhodium perfluorobutyrate. The catalyst was recovered up to 6 times in both supported and homogeneous/solid phase extraction systems, with no observable drop in activity. Rhodium leaching levels were lowest when the catalyst was supported on [Zr(O₃P-C₆H₄-C₆F₁₃)₂].

A solid-supported seleninic acid precatalyst for the oxidation of *p*-nitrobenzaldehyde was recycled 3 times under optimised conditions, with accumulative Se leaching of 2.0%. Conversions fell slightly over the 3 runs, from 94 to 82%. A comparison of support materials showed that, as for the rhodium system, catalyst leaching was lowest with the FZrP material, [Zr(O₃P-C₆H₄-C₆F₁₃)₂].

In the enantioselective fluorination system, the Pd BINAP catalyst was most effectively separated and reused using a column of FZrP. The catalyst was recycled over 3 runs, with conversions over 90% and ees in excess of 88%. Due to further purification of the product by column chromatography, necessary for chiral-GC analysis, ICP-OES analysis was not performed and Pd leaching data was, therefore, unavailable for this system.

Statement of Originality

The experimental work in this thesis has been carried out by the author in the department of chemistry at the University of Leicester between September 2003 and November 2006. The work has not been submitted, and is not presently being submitted, for any other degree at this or any other university.

Signed.....

Date.....

James Bennett

University of Leicester

University Road,

Leicester.

LE1 7RH

Acknowledgements

I would firstly like to thank my project supervisor, Professor Eric Hope, for giving me the opportunity to work in a diverse and stimulating research area and for his guidance, support and trust in my ideas and my work. I also thank Dr Alison Stuart, Dr Andrew West, Jose Vidal, Pedro Villuendas, Daniel Duncan and the rest of the Leicester Fluorine Group for their help, friendship and for making the lab an enjoyable place to work. Thanks to Maria Velon for her support and for keeping me smiling. Thanks to Gerry Griffiths, Graham Eaton and Mick Lee for their assistance with spectroscopy and chromatography and to the departmental technicians and stores staff. I must also thank my industrial sponsors, Dr Julian Vaughan-Spickers and Dr Martin Pellatt, and John Whittall of Crystal Faraday for allowing me the opportunity to present my work at a number of meetings and conferences. Lastly, thanks go to my parents for their love, trust, and support in all aspects of my life.

Contents

Abstract	i
Statement of Originality	ii
Acknowledgements	iii
Contents	iv
List of Abbreviations	xi
1. Introduction to Catalyst Recovery Methodologies	1
1.1. Green Chemistry and Catalysis	1
1.2. Homogeneous and Heterogeneous Catalysts	1
1.3. Solid-Supported Catalysis	2
1.3.1. <i>Organic Supports</i>	3
1.3.2. <i>Inorganic Supports</i>	4
1.4. Liquid Phase Immobilisation	5
1.4.1. <i>Biphasic Systems</i>	5
1.4.2. <i>Thermomorphic Catalysts</i>	8
1.4.3. <i>Ionic Liquids</i>	9
1.4.4. <i>Supercritical Reaction Media</i>	11
1.5. Dendrimers	13
1.6. Fluorous Solid-Phase Extraction	15
1.7. Supported Liquid Phase Catalysis	17
1.7.1. <i>Supported Aqueous Phase Catalysis</i>	17
1.7.2. <i>Supported Organic Phase Catalysis</i>	18
1.7.3. <i>Supported Ionic Liquid Phase Catalysis</i>	19
1.7.4. <i>Supported Fluorous Phase Catalysis</i>	20
1.8. Conclusion of Support Methodologies	23
1.9. Objectives	24
References for Chapter 1	25
2. Metal Phosphonates	29
2.1. Applications	29
2.2. Structure	30
2.2.1. <i>Zirconium Phosphates and Phosphonates</i>	30
2.2.2. <i>Mixed-Component Phosphonates</i>	32

2.2.3.	<i>Pillared Bisphosphonates</i>	33
2.3.	Synthesis	35
2.3.1.	<i>Diethyl Phosphonates and Phosphonic Acids</i>	35
2.3.2.	<i>Amorphous and Crystalline Zirconium Phosphonates</i>	36
2.3.3.	<i>Proposed Synthetic Route to Fluorous Zirconium Phosphonates</i>	36
2.4.	Synthesis of Fluorous Diethyl Phosphonates and Phosphonic Acids	37
2.5.	Characterisation of Fluorous Diethyl Phosphonates and Phosphonic Acids	42
2.6.	Amorphous Fluorous Zirconium Phosphonates	44
2.6.1.	<i>Synthesis</i>	44
2.6.2.	<i>Separation Studies</i>	44
2.6.3.	<i>Swellability Investigation</i>	45
2.7.	Crystalline Fluorous Zirconium Phosphonates	46
2.8.	Platinum Complexes of Phosphonic Acids	50
2.9.	Conclusions for Chapter 2	53
	References for Chapter 2	54
3.	Olefin Cyclopropanation Catalysed by Fluorous Rhodium Carboxylates	56
3.1.	Dirhodium(II) Tetracarboxylate Catalysts	56
3.1.1.	<i>Rhodium-Catalysed Cyclopropanation with Diazo Compounds</i>	56
3.1.2.	<i>Recovery Techniques for Dirhodium Carboxylate Catalysts</i>	57
3.2.	Results and Discussion	62
3.2.1.	<i>Catalyst Recycle via Fluorous Solid Phase Extraction</i>	66
3.2.2.	<i>Catalyst Recycle using Solid Supports</i>	69
3.2.3.	<i>Comparison of Fluorous and Non-fluorous Zirconium Phosphonate Solid Supports</i>	73
3.2.4.	<i>Catalyst Loading Studies</i>	76
3.2.5.	<i>Investigation into the Effect of Perfluoroalkyl Chain Length on Catalyst Leaching</i>	77
3.2.6.	<i>Optimisation of the Solid-Supported Catalyst</i>	79
3.3.	Supported Cyclopropanation of Cyclooctene	80
3.4.	Conclusions for Chapter 3	81
	References for Chapter 3	83
4.	Selenium Catalysed Oxidations	85
4.1.	Introduction to Selenium Chemistry	85
4.1.1.	<i>Selenium-activated Oxidations</i>	85

4.1.2.	<i>Recovery and Reuse of Selenium-based Oxidation Catalyts</i>	86
4.2.	Results and Discussion	88
4.2.1.	<i>Synthesis of Fluorous Selenium Catalysts</i>	88
4.2.2.	<i>Oxidation of para-Nitrobenzaldehyde with Perfluorooctyl Seleninic Acid</i>	89
4.2.3.	<i>Oxidation of para-Nitrobenzaldehyde with Supported Perfluorooctyl Seleninic Acid</i>	90
4.2.4.	<i>Comparison of Catalyst Support Materials</i>	99
4.3.	Allylic Oxidation of Cyclooctene	103
4.4.	Conclusions for Chapter 4	107
	References for Chapter 4	108
5.	Enantioselective Fluorination Catalysed by Palladium BINAP Complexes	109
5.1.	Introduction to Enantioselective Fluorination	109
5.1.1.	<i>Fluorinating Agents</i>	110
5.1.2.	<i>Chiral Fluorinating Agents</i>	110
5.1.2.1.	Electrophilic Sources of Fluorine	110
5.1.2.2.	Nucleophilic Sources of Fluorine	114
5.1.3.	<i>Fluorinating Agents with Chiral Catalysts; Asymmetric Catalysis</i>	114
5.1.4.	<i>Fluorous Asymmetric Catalysts</i>	117
5.2.	Results and Discussion	118
5.2.1.	<i>Recycling of [Pd(BINAP)(OH₂)₂](OTf)₂ Using Silica Column Chromatography</i>	118
5.2.2.	<i>Synthesis of Perfluoroalkyl-Derivatised BINAP Ligands</i>	119
5.2.3.	<i>Synthesis of Perfluoroalkyl-Derivatised Palladium(II) Complexes</i>	121
5.2.4.	<i>Enantioselective Fluorination with Palladium BINAP Catalysts</i>	121
5.2.4.1.	Recycling of the Palladium BINAP Catalysts Using Column Chromatography with Fluorous Zirconium Phosphonates and FRPSG	123
5.2.4.2.	Recycling of Palladium BINAP Catalysts Supported on Fluorous Zirconium Phosphonates and FRPSG	125
5.5.	Conclusions for Chapter 5	127
	References for Chapter 5	129
6.	Experimental Details	131
6.1.	General Experimental Details	131
6.1.1.	<i>Nuclear Magnetic Resonance Spectroscopy</i>	131

6.1.2.	<i>Mass Spectrometry</i>	131
6.1.3.	<i>Elemental Analysis</i>	131
6.1.4.	<i>Inductively Coupled Plasma Optical Emission Spectroscopy</i>	131
6.1.5.	<i>Infrared Analysis</i>	131
6.1.6.	<i>X-Ray Crystallography</i>	132
6.1.7.	<i>Scanning Electron Microscopy and Energy Dispersive X-ray Analysis</i>	132
6.1.8.	<i>X-Ray Powder Diffraction</i>	132
6.1.9.	<i>Gas Chromatography</i>	132
6.1.10.	<i>High Pressure Liquid Chromatography</i>	132
6.1.11.	<i>Starting Materials</i>	132
6.2.	Experimental Details for Chapter Two	133
6.2.1.	<i>Synthesis of Diethyl Phosphonates via Simeon Protocol</i>	133
6.2.1.1.	Synthesis of PhPO(OEt) ₂	133
6.2.2.	<i>Synthesis of Diethyl Phosphonates via Michaelis-Arbuzov Reaction</i>	133
6.2.2.1.	Synthesis of F ₃ C-C ₂ H ₄ PO(OEt) ₂	133
6.2.2.2.	Synthesis of F ₉ C ₄ -C ₂ H ₄ PO(OEt) ₂	134
6.2.2.3.	Synthesis of F ₁₃ C ₆ -C ₂ H ₄ PO(OEt) ₂	134
6.2.2.4.	Synthesis of F ₁₇ C ₈ -C ₃ H ₆ PO(OEt) ₂	135
6.2.3.	<i>Synthesis of Diethyl Phosphonates via Beletskaya Protocol</i>	135
6.2.3.1.	Synthesis of PhPO(OEt) ₂	135
6.2.3.2.	Synthesis of 4-F-C ₆ H ₄ -PO(OEt) ₂	136
6.2.3.3.	Synthesis of 4-F ₁₃ C ₆ -C ₆ H ₄ -PO(OEt) ₂	136
6.2.4.	<i>Synthesis of Diethyl Phosphonates via Hirao Protocol</i>	137
6.2.4.2.	Synthesis of 4-F ₃ C-C ₆ H ₄ -PO(OEt) ₂	137
6.2.4.3.	Synthesis of 4-F ₁₃ C ₆ -C ₆ H ₄ -PO(OEt) ₂	138
6.2.5.	<i>Synthesis of Phosphonic Acids</i>	138
6.2.5.1.	Synthesis of PhPO(OH) ₂	138
6.2.5.2.	Synthesis of 4-F-C ₆ H ₄ -PO(OH) ₂	139
6.2.5.3.	Synthesis of 4-F ₃ C-C ₆ H ₄ -PO(OH) ₂	139
6.2.5.4.	Synthesis of 4-F ₁₃ C ₆ -C ₆ H ₄ -PO(OH) ₂	139
6.2.5.5.	Synthesis of F ₉ C ₄ -C ₂ H ₄ -PO(OH) ₂	140
6.2.5.6.	Synthesis of F ₁₃ C ₆ -C ₂ H ₄ -PO(OH) ₂	140
6.2.6.	<i>Synthesis of Amorphous Zirconium Phosphonates</i>	141
6.2.6.1.	Synthesis of [Zr(O ₃ PPh) ₂]	141
6.2.6.2.	Synthesis of [Zr(O ₃ P-C ₆ H ₄ -4-CF ₃) ₂]	141

6.2.6.3. Synthesis of $[\text{Zr}(\text{O}_3\text{P}-\text{C}_6\text{H}_4-4-\text{C}_6\text{F}_{13})_2]$	141
6.2.6.4. Synthesis of $[\text{Zr}(\text{O}_3\text{P}-\text{C}_2\text{H}_4-\text{C}_4\text{F}_9)_2]$	141
6.2.6.5. Synthesis of $[\text{Zr}(\text{O}_3\text{P}-\text{C}_2\text{H}_4-\text{C}_6\text{F}_{13})_2]$	142
6.2.7. <i>Synthesis of Crystalline Zirconium Phosphonates</i>	142
6.2.7.1. Synthesis of Crystalline $[\text{Zr}(\text{O}_3\text{PPh}_2)_2]$ in Glass Apparatus	142
6.2.7.2. Synthesis of Crystalline $[\text{Zr}(\text{O}_3\text{P}-\text{C}_2\text{H}_4-\text{C}_6\text{F}_{13})_2]$ in Glass Apparatus	142
6.2.7.3. Synthesis of Crystalline $[\text{Zr}(\text{O}_3\text{PPh}_2)_2]$ in Plastic Apparatus	143
6.2.7.4. Synthesis of Crystalline $[\text{Zr}(\text{O}_3\text{P}-\text{C}_6\text{H}_4-4-\text{C}_6\text{F}_{13})_2]$ in Plastic Apparatus	143
6.2.8. <i>Synthesis of Platinum bis-Triphenylphosphine complexes of Phosphonic Acids</i>	143
6.2.8.1. Synthesis of $[\text{Pt}\{\text{OP}(\text{O})(\text{Ph})\text{O}\}(\text{PPh}_3)_2]$	143
6.2.8.2. Synthesis of $[\text{Pt}\{\text{OP}(\text{O})(\text{C}_6\text{H}_4-4-\text{F})\text{O}\}(\text{PPh}_3)_2]$	144
6.2.8.3. Synthesis of $[\text{Pt}\{\text{OP}(\text{O})(\text{C}_6\text{H}_4-4-\text{CF}_3)\text{O}\}(\text{PPh}_3)_2]$	144
6.2.8.4. Synthesis of $[\text{Pt}\{\text{OP}(\text{O})(\text{C}_6\text{H}_4-4-\text{C}_6\text{F}_{13})\text{O}\}(\text{PPh}_3)_2]$	145
6.2.8.5. Synthesis of $[\text{Pt}\{\text{OP}(\text{O})(\text{C}_2\text{H}_4-\text{C}_4\text{F}_9)\text{O}\}(\text{PPh}_3)_2]$	145
6.2.8.6. Synthesis of $[\text{Pt}\{\text{OP}(\text{O})(\text{C}_2\text{H}_4-\text{C}_6\text{F}_{13})\text{O}\}(\text{PPh}_3)_2]$	145
6.3. Experimental Details for Chapter Three	146
6.3.1. <i>Synthesis of $[\text{Rh}_2(\text{O}_2\text{C}_4\text{F}_7)_4]$</i>	146
6.3.2. <i>Synthesis of $[\text{Rh}_2(\text{O}_2\text{C}_7\text{F}_{13})_4]$</i>	146
6.3.3. <i>General Procedure for Alkene Cyclopropanation Under Homogeneous Conditions</i>	147
6.3.4. <i>Preparation of 10 % Loaded Supported Rhodium Catalyst</i>	147
6.3.5. <i>General Procedure for Alkene Cyclopropanation with Supported 1 mol % $[\text{Rh}_2(\text{O}_2\text{CC}_3\text{F}_7)_4]$</i>	147
6.4. Experimental Details for Chapter Four	148
6.4.1. <i>Synthesis of $\text{H}_9\text{C}_4\text{-Se-C}_8\text{F}_{17}$</i>	148
6.4.2. <i>Synthesis of $\text{F}_{17}\text{C}_8\text{SeO}_2\text{H}$</i>	148
6.4.3. <i>Preparation of 10 % Loaded Supported Perfluorooctyl Seleninic Acid</i>	149
6.4.4. <i>General Procedure for Oxidation of para-Nitrobenzaldehyde Catalysed by Supported Perfluorooctyl Seleninic Acid</i>	149
6.4.5. <i>General Procedure for Allylic Oxidation of Cyclooctene Catalysed by Supported Perfluorooctyl Seleninic Acid</i>	149
6.4.6. <i>General Procedure for Allylic Oxidation of Cyclooctene Catalysed by Perfluorooctyl Seleninic Acid under Homogeneous Conditions</i>	149

6.5.	Experimental Details for Chapter Five	150
6.5.1.	<i>Non-fluorous BINAP</i>	150
6.5.1.1.	Synthesis of (<i>R</i>)-2,2'-di-(trifluoromethane-sulphonyloxy)-1,1'-binaphthyl	150
6.5.1.2.	Synthesis of (<i>S</i>)-2,2'-di-(trifluoromethane-sulphonyloxy)-1,1'-binaphthyl	150
6.5.1.3.	Synthesis of (<i>R</i>)-2,2'-bis-(diphenylphosphino)-1,1'-binaphthyl	151
6.5.1.4.	Synthesis of (<i>S</i>)-2,2'-bis-(diphenylphosphino)-1,1'-binaphthyl	151
6.5.1.5.	Synthesis of [PdCl ₂ {(<i>R</i>)-BINAP}]	152
6.5.1.6.	Synthesis of [PdCl ₂ {(<i>S</i>)-BINAP}]	152
6.5.1.7.	Synthesis of [Pd(OH ₂) ₂ {(<i>R</i>)-BINAP}](OTf) ₂	153
6.5.1.8.	Synthesis of [Pd(OH ₂) ₂ {(<i>S</i>)-BINAP}](OTf) ₂	153
6.5.2.	<i>Fluorous BINAP</i>	154
6.5.2.1.	Synthesis of (<i>R</i>)-6,6'-Dibromo-1,1'-bi-2-naphthol	154
6.5.2.2.	Synthesis of (<i>S</i>)-6,6'-Dibromo-1,1'-bi-2-naphthol	154
6.5.2.3.	Synthesis of (<i>R</i>)-6,6'-Dibromo-2,2'-diacetoxy-1,1'-binaphthyl	155
6.5.2.4.	Synthesis of (<i>S</i>)-6,6'-Dibromo-2,2'-diacetoxy-1,1'-binaphthyl	155
6.5.2.5.	Synthesis of (<i>R</i>)-6,6'-Bis-(perfluoro-n-hexyl)-2,2'-diacetoxy-1,1'-binaphthyl	156
6.5.2.6.	Synthesis of (<i>S</i>)-6,6'-Bis-(perfluoro-n-hexyl)-2,2'-diacetoxy-1,1'-binaphthyl	156
6.5.2.7.	Synthesis of (<i>R</i>)-6,6'-Bis-(perfluoro-n-hexyl)-1,1'-binaphthol	157
6.5.2.8.	Synthesis of (<i>S</i>)-6,6'-Bis-(perfluoro-n-hexyl)-1,1'-binaphthol	157
6.5.2.9.	Synthesis of (<i>R</i>)-6,6'-Bis-(perfluoro-n-hexyl)-2,2'-di(trifluoromethane-sulphonyloxy)-1,1'-binaphthyl	158
6.5.2.10.	Synthesis of (<i>S</i>)-6,6'-Bis-(perfluoro-n-hexyl)-2,2'-di(trifluoromethane-sulphonyloxy)-1,1'-binaphthyl	158
6.5.2.11.	Synthesis of (<i>R</i>)-6,6'-Bis-(perfluoro-n-hexyl)-2,2'-bis(diphenylphosphino)-1,1'-binaphthyl	159
6.5.2.12.	Synthesis of (<i>S</i>)-6,6'-Bis-(perfluoro-n-hexyl)-2,2'-bis(diphenylphosphino)-1,1'-binaphthyl	160
6.5.2.13.	Synthesis of [PdCl ₂ {(<i>R</i>)-RfBINAP}]	160
6.5.2.14.	Synthesis of [PdCl ₂ {(<i>S</i>)-RfBINAP}]	161
6.5.2.15.	Synthesis of [Pd(OH ₂) ₂ {(<i>R</i>)-RfBINAP}](OTf) ₂	161
6.5.2.16.	Synthesis of [Pd(OH ₂) ₂ {(<i>S</i>)-RfBINAP}](OTf) ₂	162

6.5.3. <i>Preparation of 10 % Loaded Supported Palladium Catalyst</i>	162
6.5.4. <i>General Procedure for Enantioselective Fluorination With NFSI Under Homogeneous Conditions</i>	162
6.5.5. <i>General Procedure for Enantioselective Fluorination With NFSI With Supported Catalyst</i>	163
References for Chapter 6	164
Appendix	I
Crystal data for $[\text{Pt}\{\text{OP}(\text{O})(\text{Ph})\text{O}\}(\text{PPh}_3)_2]$	I
Crystal data for $[\text{Pt}\{\text{OP}(\text{O})(\text{C}_6\text{H}_4\text{-4-F})\text{O}\}(\text{PPh}_3)_2]$	II
Crystal data for $[\text{Pt}\{\text{OP}(\text{O})(\text{C}_6\text{H}_4\text{-4-CF}_3)\text{O}\}(\text{PPh}_3)_2]$	III
Crystal data for $[\text{Pt}\{\text{OP}(\text{O})(\text{C}_2\text{H}_4\text{-C}_6\text{F}_{13})\text{O}\}(\text{PPh}_3)_2]$	IV
Seminars Attended	V
Conferences Attended	VIII
Presentations	IX
Publications and Awards	IX
Lecture Courses Attended	IX

Abbreviations

ABC	Aqueous biphasic catalysis
acac	Pentane-2,4-dionate
Ar	Aryl fragment
BAST	bis(2-methoxyethylaminosulphur trifluoride)
BCPC	^t Butyl 2-oxo-cyclopentanonecarboxylate
BINAP	2,2'-Bis(diphenylphosphino)-1,1'-binaphthyl
BINOL	1,1'-Bi-2-naphthol
Bipy	2,2'-bipyridine
BMIM	1- <i>n</i> -butyl-3-methyl-imidazolium ion
BTF	Benzotrifluoride
Cp*	Pentamethylcyclopentadienyl
Cy	Cyclohexyl
d	Doublet
DABCO	1,4-Diazabicyclo[2.2.2]octane
DAST	Diethylaminosulphur trifluoride
DCE	Dichloroethane
DCM	Dichloromethane
dd	Doublet of doublets
DMAP	4-Dimethylaminopyridine
DMF	<i>N,N</i> -Dimethylformamide
DMSO	Dimethyl sulphoxide
dppe	Diphenylphosphinoethane
EDAX	Energy dispersive X-ray analysis
ee	Enantiomeric excess
EI	Electron impact
ES	Electrospray
FAB	Fast atom bombardment
FBC	Fluorous biphasic catalysis
Fc	Ferrocene
FRPSG	Fluorous reverse phase silica gel
FSPE	Fluorous solid phase extraction
FZrP	Fluorous zirconium phosphonate
GC	Gas chromatography

hfacac	1,1,1,6,6,6-hexafluoropentane-2,4-dionate
HMDS	Hexamethyldisilazide
Hz	Hertz
HPLC	High pressure liquid chromatography
ICP-OES	Inductively coupled plasma optical emission spectroscopy
IL	Ionic liquid
IR	Infrared
<i>J</i>	Coupling constant
<i>m</i>	Multiplet
MCPC	Methyl 2-oxo-cyclopentanonecarboxylate
mp	Melting point
NFSI	<i>N</i> -fluorobenzenesulfonimide
NMR	Nuclear magnetic resonance
NR	Not recorded
pfb	Perfluorobutyrate
PFH	Perfluorohexane
Ph	Phenyl fragment
PP3	Perfluoro-1,3-dimethylcyclohexane
ppm	Parts per million
PS	Polystyrene
Rf	Perfluoroalkyl group
Rf-BINAP	6,6'-Bis(perfluoro- <i>n</i> -hexyl)-2,2'-bis(diphenylphosphino)-1,1'-binaphthyl
RT	Room temperature
<i>s</i>	Singlet
<i>ss</i>	Singlet with satellites
SAPC	Supported aqueous phase catalysis
scCO ₂	Supercritical carbon dioxide
SCF	Supercritical fluid
SEM	Scanning electron microscopy
SOPC	Supported organic phase catalysis
<i>t</i>	Triplet
TADDOL	trans- α,α' -(Dimethyl-1,3-dioxolane-4,5-diyl)bis(diphenylmethanol)
TBAB	Tetrabutylammonium bromide

T_c	Critical temperature
Tf	Triflate
THF	Tetrahydrofuran
TOF	Turnover frequency
TON	Turnover number
TPPTS	Triphenylphosphine trisulphonate, sodium salt
wt	Weight
ZrP	Zirconium phosphonate

1. Introduction to Catalyst Recovery Methodologies

1.1. Green Chemistry and Catalysis

The chemical industry is responsible for creating vast quantities of different materials, ranging from pharmaceuticals to polymers and fuels. Were it not for the use of catalysts many of the processes involved in the formation of these products would be hugely wasteful.

A catalyst is defined as a substance that increases the rate of a chemical reaction without itself being consumed.^[1] Catalysts allow thermodynamically feasible reactions to occur *via* pathways of lower Gibbs activation energy, ΔG^\ddagger , and thus often at lower temperatures. The use of catalysts, therefore, allows industrial processes to be more energy efficient and economical. Increasing levels of legislation^[2] are forcing the chemical industry to become more conscious of reducing its energy costs and keeping waste products to a minimum.

The term *green chemistry*^[3] describes an approach that aims to constantly improve the efficiency and safety of a given system. It encompasses ideas such as prevention of waste being superior to treatment, maximising atom economy, reduction of solvents and derivatisation and the preference for catalytic reagents over stoichiometric ones. Using catalysts can clearly aid industry to become more energy efficient but introduces another substance that must be separated from the final product and suitably disposed of. For a process to be truly 'green', the catalyst should not be discarded after it is separated but instead recycled. This not only minimises waste but also financial costs.

The development of separation technology is a substantial area of chemistry and the separation and recycling of catalysts is significant to both industry and academia. The focus of this work is the development of materials and methodologies that allow the isolation of catalysts from synthetic products for their reuse.

1.2. Homogeneous and Heterogeneous Catalysts

Catalysts fall into two major classes: homogeneous and heterogeneous. A homogeneous catalyst exists in the same phase as that of the reagents, typically in the liquid phase. These catalysts tend to give high activities and selectivities. This is due to their mobility in solution and the fact that they have a single active site. They can be well characterised by common solution phase techniques and mechanistic details of their catalytic reaction cycles may also be elucidated. The use of different ligands with metal-based catalysts can transmit various steric and electronic effects to the active site. This can influence the regio- and/or stereo-chemistry of reactions. All of these factors allow homogeneous catalysts to be engineered to suit the needs of a specific reaction.

A heterogeneous catalyst exists in a separate phase to that of the reagent, typically a solid in a liquid/gaseous substrate. As most heterogeneous catalysts are insoluble solids they are generally not well characterised and the mechanisms of their action are often poorly understood. They exist as catalytically active irregular surfaces with numerous active sites, which can result in a loss of selectivity. Also, much of their surface can be inaccessible to reagents, even when they are divided finely into powders. This makes them less efficient per gram than homogeneous catalysts, which are accessible to all substrate molecules dissolved in a solution. Heterogeneous systems generally require harsher reaction conditions than those in homogeneous ones and the use of higher temperatures/pressures makes them less energy efficient and less “green”. Their major advantages, however, are catalyst/product separation is facile, which prevents contamination of the product, and their robust chemical nature.

Industrial processes tend to favour homogeneous catalysts, due to their higher activities, selectivities and adaptability. Despite these advantages, recycling a catalyst in the same phase as the reagents and products can prove to be expensive, difficult or even impossible. Heterogeneous catalysts are readily separated from products by simple liquid-solid extraction techniques, such as filtration, but their reduced dispersal amongst the substrate molecules decreases their performance relative to their homogeneous counterparts.

Much work has been undertaken on combining the advantages of both systems by creating a “heterogenised” homogeneous state. Many approaches towards this aim have been taken but most are dependent on altering the solubility properties of the catalyst. This can be effected permanently, as with solid supports, or temporarily during the reaction, as with biphasic solvent systems. The following sections discuss the advantages and disadvantages of various approaches investigated for catalyst/product separation, including solid supports (1.3), liquid phase immobilisation (1.4), fluororous solid-phase extraction (1.5) and supported liquid-phase catalysis (1.6).

1.3. Solid-Supported Catalysis

The field of catalyst immobilisation through solid-supports emerged in the late 1960s.^[4] This technique involves immobilising a homogeneous catalyst upon the surface of an insoluble solid support. This may be achieved in a number of ways, most commonly through covalent interactions of donor ligands attached to the support, although some examples of ionic bonding are known.^[5, 6] A variety of both organic and inorganic supports have been developed. Each class has its own relative advantages and disadvantages.

1.3.1. Organic Supports

Organic supports typically consist of polymers modified with functional groups, such as diphenylphosphino,^[7] tertiary amino,^[8] cyanomethyl,^[9] thiol^[10] or cyclopentadienyl,^[11] that coordinate to the soluble metal complex catalyst. Most cases involve this donor-acceptor interaction, although there are a few examples of the metal being directly bonded to a carbon atom in the polymer backbone.^[12]

Polystyrene and styrene-divinylbenzene copolymer beads are the most widely used organic supports. These systems are highly tuneable and, therefore, different structures may be designed for specific applications. The amount of cross-linker within the polymer matrix can have an effect on the catalysts properties; too little and the chains become flexible enough for functional groups to interact with one another, preventing catalyst coordination.^[13] Excessive cross-linking prevents the support from absorbing solvents, or swelling, and substrate entry becomes inhibited thus reducing the observed catalytic activity.^[14]

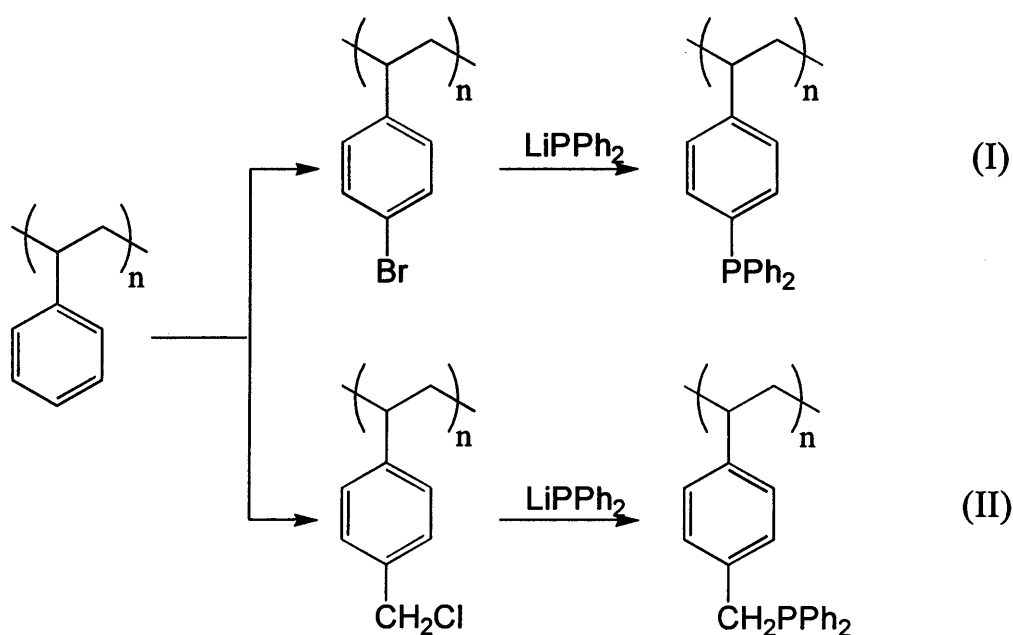


Figure 1.1. Synthesis of polymer-bound ligands

A polymer-anchored catalyst may be formed by displacement of a ligand coordinated to a soluble metal complex by a polymer-bound ligand,^[14] or by cleavage of a weakly bridged dimeric metal complex.^[10] An example of polymer-bound ligand synthesis is shown in Figure 1.1.

A variety of catalytic systems have been investigated utilising polymer-immobilised catalysts. Reaction types studied include hydroformylation,^[15] hydrogenation,^[15] oligomerisation,^{[16,}

^{17]} polymerisation^[18] and metathesis.^[19] Generally, these systems may be recycled several times and show comparable yields to their homogeneous counterparts. However, their reaction rates are often decreased, as diffusion of reagents into the solvent-swollen polymer matrix becomes a limiting factor.^[20] Also, the surrounding polymer environment may detrimentally affect the stereoselectivity of the catalyst; if the metal centre is tightly bound within a rigid matrix then catalytically important conformational changes may be prevented. However, these restrictions can also, occasionally, prevent undesired rearrangement during the catalytic mechanism, thus increasing selectivity.^[21]

The use of soluble polymer supports can circumvent the problems mentioned above. The catalyst is coated upon the surface of the support material, which is then dissolved in the reaction media, allowing catalysis to occur under homogeneous conditions.^[12] Addition of a suitable solvent at the end of the reaction induces precipitation of the supported catalyst, which may then be separated from the product solution by filtration. Other methods of separation include membrane filtration, centrifugation and chromatographic techniques.^[22] However, separation is rarely straightforward; the product is often contaminated and reuse is complicated.^[23]

Another major disadvantage of organic supports are their poor thermal and mechanical stabilities, which reduce their longevity in catalytic applications. This low stability issue may be avoided by the use of more durable inorganic supports.

1.3.2. Inorganic Supports

Although inorganic supports lack some of the desirable chemical characteristics of their organic analogues, inorganic support-materials are highly thermally stable and do not degrade quickly in solvents or over time. Inorganic supports cannot accommodate as many functional groups as organic polymers; up to ten times less per gram of material.^[24] As the density of ligands is lower, a greater amount of support is required per mmol of catalyst. However, their robust physical nature compensates for these disadvantages, and the range of catalytic reactions investigated with inorganic supports is as diverse as that for organic systems.^[25-28]

A number of inorganic materials including glass, ceramics,^[29] zeolites^[30] and clays,^[31] have been employed, but the most widely used support is silica due to its commercial availability and versatility. Catalysts may be attached to the material via reaction with silanol groups, either directly with a metal complex (Figure 1.2, I) or with a suitable ligand-containing reagent (Figure 1.2, II).^[32]

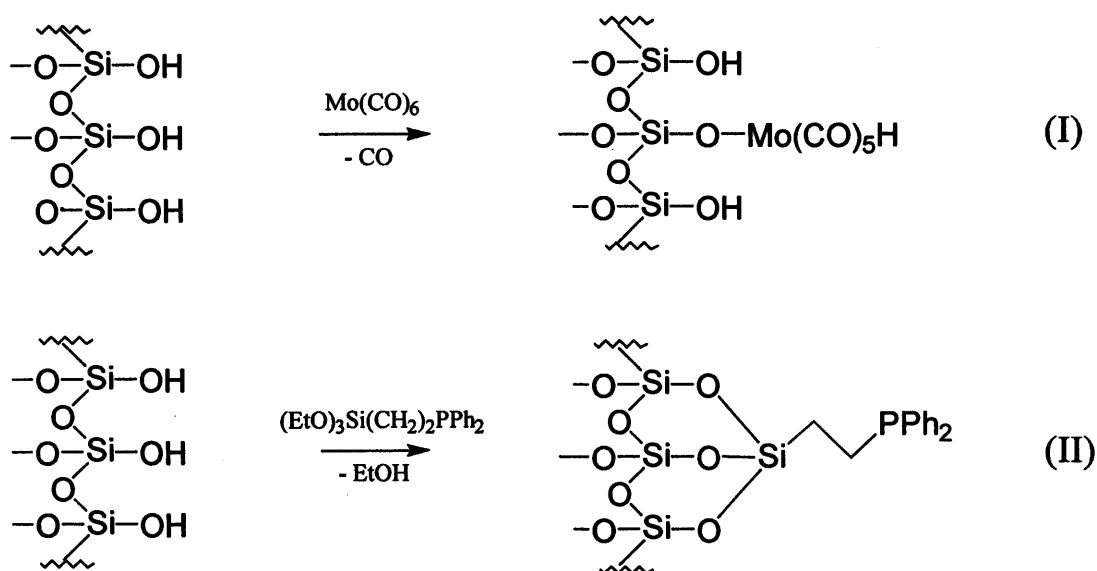


Figure 1.2. Modification of silica for use in supported catalysis

If route (II) is adopted, then the catalyst is coordinated to the ligand-functionalised silica in a second step. Exchange of a ligand coordinated to a soluble metal complex affords the supported catalyst,^[32] in the same way as seen for organic systems. Route (I) is the most direct route to a supported catalyst but the silanol linkage may deactivate some catalysts and route (II) guarantees a more uniform catalytic surface.

To overcome the problem of destructive binding to catalysts, the support may be reacted with a coupling agent, such as *t*-butyldimethylchlorosilane, to block, or cap, the reactive silanol groups. This creates a more lipophilic surface. However, even when using short chain capping-agents, such as Me_3SiCl ,^[33] it is impossible to ensure that all the silanol groups are capped, thus utilisation of the support may result in a small loss of catalyst in each run.

1.4. Liquid Phase Immobilisation

1.4.1. Biphasic Systems

This catalyst separation technique relies on the immiscibility of one solvent with another, to form a biphasic system. The catalyst is engineered to make it preferentially soluble in one phase, and the reagents and products are preferentially soluble in the other phase. Catalysis occurs at the interface between the two phases. After the reaction is complete, the layers may be separated; the product isolated from one solvent and the phase containing the catalyst can be reused in further reaction cycles. A significant advantage of these liquid-liquid systems over surface-anchored methods is the

increased mobility of the catalyst, which allows a closer match to classical homogeneous conditions.

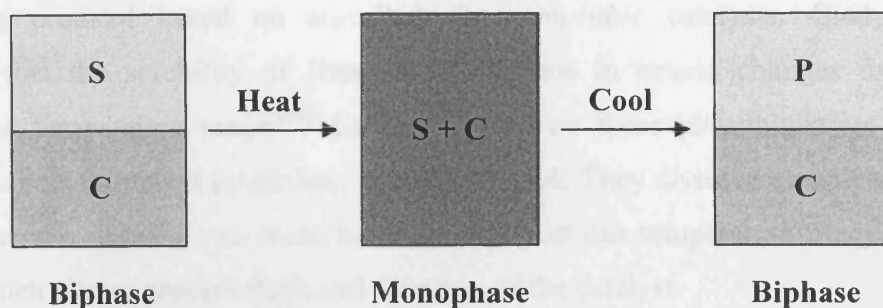
The creation of a biphasic system is possible by using solvents with sufficiently different polarities. One obvious approach is to use polar and non-polar conventional organic solvents. This organic/organic biphasic system is already used by industry, for example in the SHOP oligomerisation process.^[34] However, the number of catalysts and reagents with the required combination of solubilities is currently limited and this restricts the applicability of this type of biphasic system.

Water is a readily available, cheap solvent with no associated environmental or safety concerns. As it is highly polar, it may be used in conjunction with a non-polar organic solvent to create a biphasic system. A variety of polar functionalities can be used to anchor the catalyst in the aqueous phase, typically $-\text{SO}_3\text{H}$,^[35] $-\text{COOH}$, $-\text{OH}$ or $-\text{NH}_2$, or their salts.

The concept of aqueous biphasic catalysis (ABC) was introduced in 1973 and by the early 1980s it had found its first industrial application in the field of hydroformylation.^[36] Despite its rapid development, ABC suffers fundamental drawbacks. The major disadvantage of an aqueous/organic system is that the reaction media will affect reagents or products that undergo hydrolysis, possibly interfering with the catalytic reaction. Additionally, the rate of reaction is dependent on the miscibility of the organic substrate in the aqueous, catalyst-containing phase. These mass transfer rates will be extremely limited for higher molecular weight organic molecules.

Perfluoroalkylated organic moieties have been found to possess novel properties including increased solubility for gases and low miscibility with most organic solvents. The low miscibility of organic and fluorinated solvents enables the creation of a biphasic system. It is from this premise that fluorinated biphasic catalysis (FBC) was developed^[37] as a successor to existing biphasic systems. The term 'fluorinated' was first introduced by Horváth as an analogue to 'aqueous', for highly fluorinated solvents. There are now numerous commercially available fluorinated solvents.³⁸ If the catalyst is made preferentially fluorinated phase soluble then it is possible to use a biphasic system to catalyse a reaction between reagents in the organic phase. Catalyst fluorophilicity may be achieved by the addition of perfluoroalkyl chains, or 'ponytails', and numerous routes to fluorinated ligands are now documented in the literature.^[39-43] A value of 60% wt fluorine is generally accepted as the required quantity of fluorine to achieve preferential solubility in a fluorinated solvent over an organic solvent.^[44] Thus, larger ligands require increasing amounts of fluorine. The fluorinated ponytails may have considerable impact upon molecular mass and, above a certain limit, the catalyst will exhibit poor solubility in all solvents.

The main advantage of FBC is that the system may be genuinely homogenised through increased temperature or pressure (Figure 1.3). This overcomes the mass transfer problems associated with aqueous biphasic systems.



S = substrate, P = product, C = preferentially fluorinated soluble catalyst

Figure 1.3. The concept of fluorinated biphasic catalysis

Careful selection of solvents is necessary, as some organic and fluorinated solvents are partially soluble in one another at room temperature. The temperature required to achieve a monophasic system can be influential on the reaction. There are a number of solvent systems available³⁸ requiring temperatures ranging from room temperature to over 126 °C to achieve monophasic conditions, allowing a range of reaction conditions to be achieved. However, the added expense of the fluorinated solvent and catalyst modification must also be considered when evaluating the benefits of a fluorinated biphasic system. Another consideration is the electron-withdrawing effect of the 'ponytails' on the donor capability of the ligand.^[45] Organic spacer groups may be used in an attempt to insulate the donor atom from the fluorine atoms and prevent a decrease in the coordination strength of the ligand.^[46]

Nonaqueous biphasic systems suffer a common problem of catalyst leaching. This is contamination of product due to a small affinity of the catalyst for the product phase. Not only does this leaching reduce catalyst concentration, and, therefore, yields over successive runs, it also has product toxicity implications. The acceptable level of contamination depends on the product's function, health and environmental concerns and catalyst cost. Pharmaceuticals, for example, clearly require exceedingly high purity, and the associated cost of fluorinated catalysts means that leaching tolerances in this sector are very low.

1.4.2. Thermomorphic Catalysts

In the same fashion that it affects the miscibility of organic and fluoruous solvents, temperature may affect the solubility of a solid in an organic solvent. This allows the creation of a new recycling protocol based on so-called *thermomorphic* catalysts. Gladysz *et al.* have demonstrated that the solubility of fluoruous phosphines in octane changes drastically over a relatively small temperature range.^[47] Catalysts based on these phosphines are effective in the addition of alcohols to methyl propiolate, as in Figure 1.4. They dissolve completely in *n*-octane at 65 °C and, thus, the reaction can occur homogeneously at this temperature. Recycling is achieved by cooling, which allows precipitation, and filtration of the catalyst.

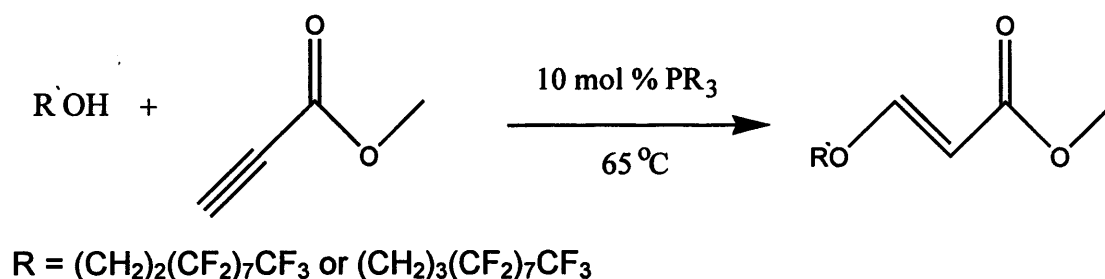


Figure 1.4. An alcohol addition reaction catalysed by thermomorphic phosphines

The use of thermomorphic catalysts allows for fluoruous separation techniques without the use of fluoruous solvents, which are expensive and can leach in small amounts to the organic phase. Clearly, this makes this a ‘greener’ system than the liquid-liquid organic-fluoruous biphasic systems.

The thermomorphic concept was made yet greener by Vincent’s group,^[48] who replaced the perfluoroalkylated chains with cheaper long, alkyl chains. The amine-based polymerisation catalyst (Figure 1.5) showed an exceptionally large temperature-dependent solubility in 1,4-dioxane, over an even narrower range than that of Gladysz’s fluoruous catalyst. The solubility of the CuBr/ligand complex increased by approximately 10,000 times when raising the temperature from 23 °C to 50 °C. The success of this system shows that, for reactions conducted in polar solvents, addition of lengthy alkyl groups seems an effective and economical route to the recovery of the catalyst.

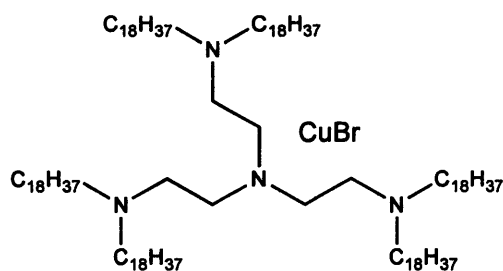


Figure 1.5. A thermomorphic amine-based polymerisation catalyst

Bergbreiter *et al.* applied the thermomorphic principle to a number of soluble polymer-bound catalysts to enable recovery by liquid-liquid phase separation,^[49] as opposed to the solid-liquid filtration based separation methods normally associated with polymer-supported catalysts. The group used a biphasic solvent system which became monophasic upon gentle heating. The catalyst had a strong phase preference for the non-product phase under biphasic conditions. Thus, after post-reaction cooling, the product may be isolated from the catalyst by liquid-liquid separation and subsequent removal of the solvent. The group developed an air-stable palladium catalyst bound to polyethylene glycol *via* an SCS pincer ligand (Figure 1.6). The catalyst was active in the Heck coupling reaction and could be quantitatively recovered and recycled for three runs. There was no reduction in the activity of the recycled catalyst and isolated yields were observed to increase over subsequent runs.

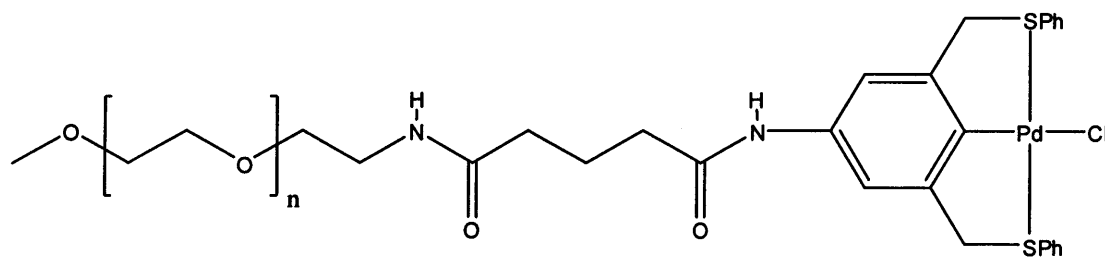


Figure 1.6. A thermomorphic palladium catalyst based upon polyethylene glycol

The group also reported a poly(*N*-isopropylacrylamide)-bound catalyst, which was also air stable and active in the Heck and Suzuki coupling reactions for a range of substrates.

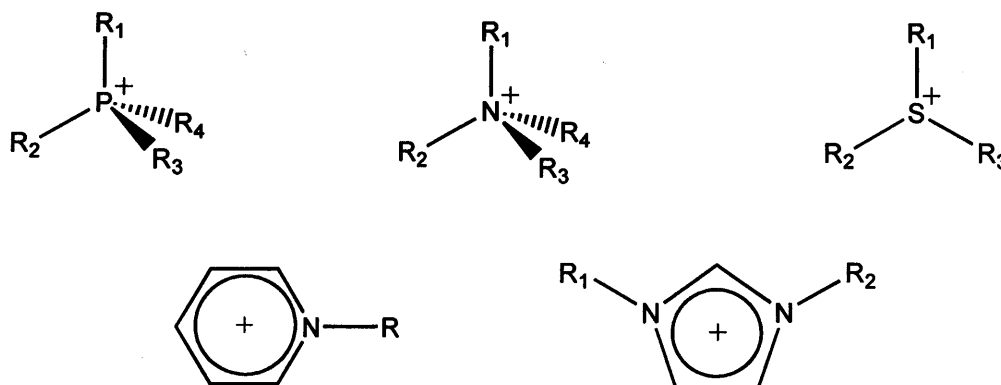
1.4.3. Ionic Liquids

Ionic liquids are salts that are liquid at or below 100 °C, unlike conventional high melting point ionic compounds. They have very different properties to molten salts, such as sodium chloride

at 800 °C, and these properties make them potential solvents for industrial catalysis. Ionic liquids are immiscible with most organic solvents but readily dissolve metals that are commonly used as catalysts. This makes them ideal candidates for biphasic catalysis. The catalyst can be contained in the ionic liquid and the reagents and products in an organic solvent. Prolonged stirring enables the formation of a monophasic long enough for the reaction to occur. After the product is formed, the layers are separated and the catalyst may be recycled, as in conventional solvent biphasic systems.

The ability to tune the solvent by altering the anion or cation implies ionic liquids could have a vast scope for industrial use. A great deal of research has been conducted utilising ionic liquids in reactions with commercial applications,^[50] with the aim of developing an inert, room temperature ionic liquid with low viscosity and volatility. Several commonly used ionic liquids are illustrated in Figure 1.7.

Cations:



Anions: BF_4^- , PF_6^- , SbF_6^- , NO_3^- , CF_3SO_3^- , $(\text{CF}_3\text{SO}_2)_2\text{N}^-$, CF_3CO_2^- , CH_3CO_2^- , Al_2Cl_7^-

Figure 1.7. Common cations and anions of ionic liquids

By altering the anion and the R groups of the cation, it is possible to create a series of ionic liquids with a spectrum of physical properties.^[50] Unfortunately, recent investigations on hydroformylation have shown that none of the tested combinations of ligands and ILs afforded the desired blend of high activity, complete retention of catalyst in the ionic liquid and high selectivity for the desired linear product.^[51, 52] Although ionic systems can be adapted to yield high activities, this inevitably comes at the cost of increased catalyst leaching into the organic phase.

There are examples of successful uses of ionic liquids as solvents for biphasic catalysis in hydrogenation,^[53] hydroformylation^[54] and Heck reactions^[55] where activities are comparable or superior to those for single phase studies and where the catalyst may be separated and recycled with no loss of activity and with negligible leaching of metal to the organic phase. However, the low

solubility of many organic substrates in ionic liquids prevents their more general application and means activities will be restricted by phase transfer limitations.

1.4.4. Supercritical Reaction Media

A supercritical fluid^[56] (SCF) is formed when a substance is heated and pressurised above its critical temperature and pressure. The critical temperature, T_c , is the temperature, above which a substance cannot exist as a liquid. Above a substance's critical pressure, P_c , it cannot exist as a gas. When these two concepts are applied in unison, the substance is somewhere between the two states, and this unusual form of matter is known as a supercritical fluid. In this region, materials have the low viscosity of a gas combined with the density of a liquid, giving them ideal properties as solvents for homogenous catalysis.

The solvent properties of supercritical fluids may be drastically altered by minor changes in temperature and pressure and this has led to an extensive exploration of their possible applications. To date, they have been utilised in extraction,^[57] chromatography^[58] crystallisation^[59] and chemical reaction.^[60]

CO₂ is commonly used in supercritical form due to its non-toxic nature and the relatively modest critical temperatures and pressures.^[61] As scCO₂ is non-polar, for the catalyst to be solubilised it also needs to be non-polar. This can be achieved by replacement of a ligand's polar/aryl groups for alkyl or perfluoroalkyl chains, which are found to have significant solubility within scCO₂.^[62] Thus, by coordinating these ligands to a catalyst, the catalyst is also solubilised in the supercritical phase. This approach was well demonstrated by Smith *et al.*,^[63] who reported that the solubility of [Cu(hfacac)₂] is 200 times greater than that of its non-fluorous analogue [Cu(acac)₂] (acac = pentane-2,4-dionato, hfacac = 1,1,1,6,6,6-hexafluoropentane-2,4-dionato). The addition of co-solvents, such as methanol,^[54] counterions^[64] or surfactants^[65] has also been shown to increase the solubility of polar catalysts or reagents in scCO₂.

When all the components are dissolved in the sc fluid, catalysis occurs under homogeneous conditions. The catalyst may be separated from the product by alteration of pressure or temperature and recycled. Leitner and co-workers have developed a scCO₂-soluble transition-metal complex by addition of fluorinated ponytails to phosphine ligands.^[42, 66] The catalyst was active in the hydroformylation reaction and gave rates and selectivities comparable or superior to those for similar systems in alternative solvents (Figure 1.8).

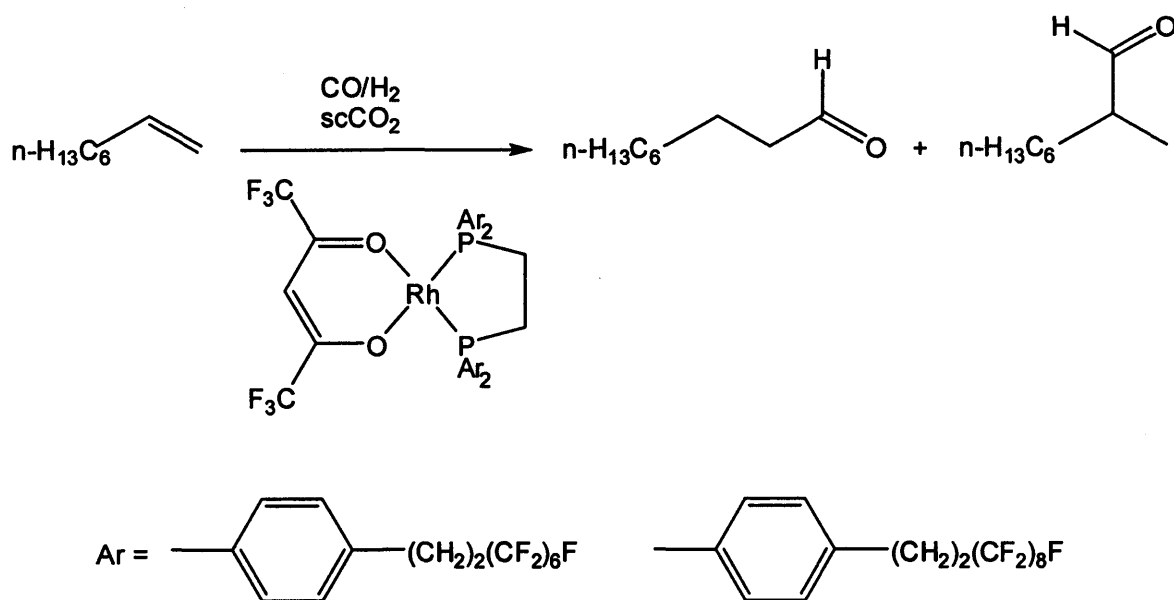


Figure 1.8. Hydroformylation of 1-octene in scCO₂ with a fluorinated Rh catalyst

Two types of biphasic systems are documented for the recycle of catalysts in sc systems (Figure 1.9).^[61] In the first, the catalyst is immobilised in the sc phase and water is used as the substrate-containing phase. This combination allows for reaction of highly polar reagents. The second case involves immobilisation of the catalyst in an ionic liquid and sc fluid is the mobile phase. In this approach the reagents must exhibit sufficient solubility in the sc phase, and thus is only suitable for low molecular weight organics.

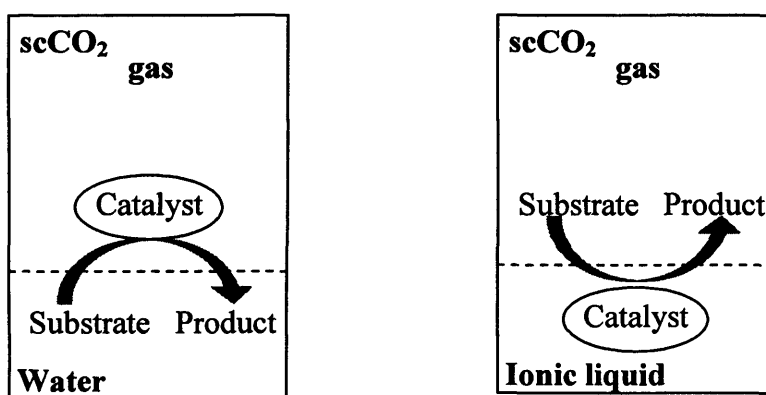


Figure 1.9. Biphasic systems with super critical CO₂

Supercritical fluids have found applications in industry. The majority of these are in the field of extraction, such as in the decaffeination of coffee.^[67] Despite the various advantages in activity, separation and environmental compatibility, the number of large-scale catalytic reactions conducted

in SC media is low. Industry seems hesitant to adopt new methodologies requiring the scale up of high-pressure equipment. However, collaboration between Nottingham University and Thomas Swan & Co resulted in the successful development of a hydrogenation process utilising fixed bed continuous-flow reactors and supercritical carbon dioxide which could be easily scaled up from laboratory to plant-scale.^[68] This process is now in use by Thomas Swan & Co. and demonstrates both the potential of supercritical solvents at an industrial scale and the willingness of industry to develop new green technologies.

1.5. Dendrimers

Dendrimers are macromolecules that, unlike polymers, are well defined at the molecular level with a polydispersity of 1. They have tree-like structures, with many long branches that encourage the formation of globular arrangements and may encapsulate metal nanoparticles. These branches normally contain heteroatoms, which act to coordinate and stabilise any metal particles trapped within the dendritic cage. The termini of the branches can be modified to act as gates, allowing small substrate molecules to enter the dendrimer and have access to the metal centre. Thus, dendrimer and metal may act as a selective catalyst. Careful selection of the termini end-group may provide the dendrimer with solubility in aqueous, organic or fluorous media. Where the molecular mass is sufficiently high, dendrimers may be recovered by membrane filtration and thus reused.

Catalytic dendrimers have been applied to numerous reactions, including Suzuki coupling,^[69] ester hydrolysis,^[70] asymmetric hydrogenation^[71, 72] and amination^[73] and Kharasch addition.^[74] The catalytic site, or sites, may be located in the centre of the dendrimer or at its periphery and many ligand structures may be incorporated into the macromolecular scaffold.

Carbosilane-based dendrimers used as molecular scaffolds for nickel “pincer” complexes (Figure 1.10) were tested as catalysts for the addition of polyhaloalkanes to carbon-carbon-double bonds, the so-called Kharasch reaction.^[74] The macromolecule contained 12 active sites but was found to have greatly reduced activity than the parent mononuclear catalyst. It was suggested that, as the nickel atoms are located in close proximity to one another, electron transfer between Ni^{II} and Ni^{III} atoms was taking place in preference to electron transfer with the substrate molecules. Despite the poor product yields attained, the work did demonstrate the excellent durability of dendrimer-based catalysts. The macromolecule was separated from the organic products by membrane filtration and recycled 100 times with a loss in mass of just 20%.

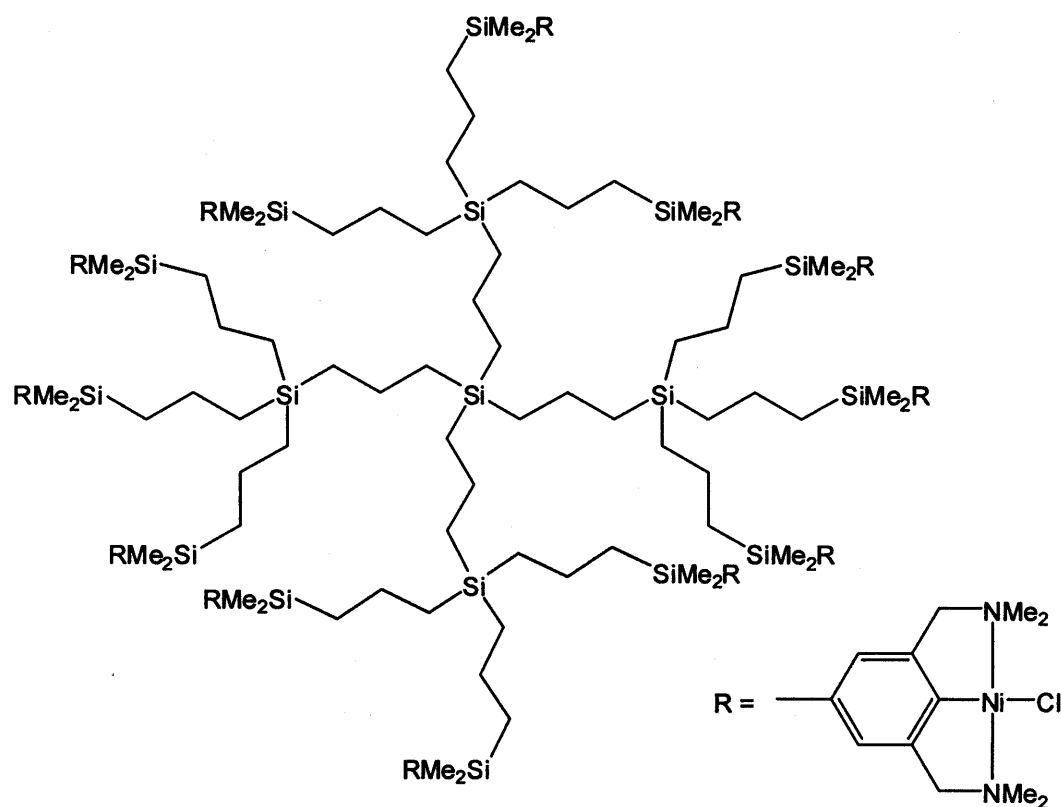


Figure 1.10. An example of a multi-site carbosilane dendritic catalyst

An alternative approach was adopted by Chan's group, who grew dendrimer scaffolds from a single, central BINAP ligand (Figure 1.11). The resulting ruthenium complex was used in the asymmetric hydrogenation of phenylacrylic acid.^[72] The catalysis was conducted in a monophasic solvent system composed of a 1:1 mixture of hexane and ethanol. This allowed a homogeneous reaction of the substrates and the dendritic BINAP complex to afford the product in yields and selectivities comparable to those obtained with the standard BINAP system. By the addition of a small volume of water to the mixture at the end of reaction, a biphasic system was obtained with the macromolecular catalyst immobilised in the hexane layer. The recycled catalyst was successfully recycled for 3 runs with no loss in activity or selectivity. The degree of dendrimer leaching into the aqueous phase was dependent upon its molecular weight, with the heaviest ligand losing less than 1% over the 3 runs.

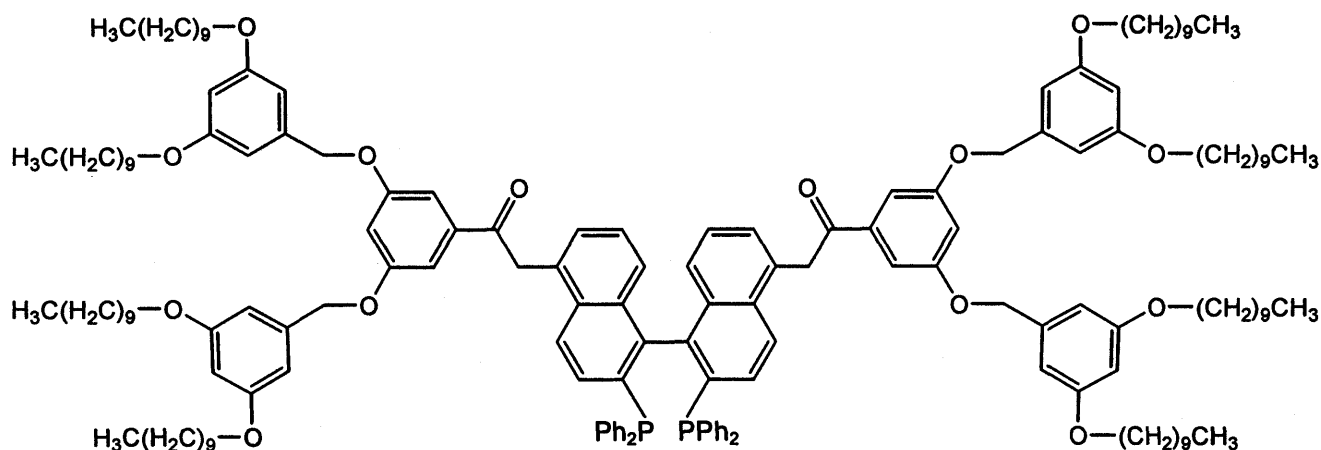


Figure 1.11. A BINAP dendrimer ligand

Dendrimer ligand-based catalysts show good stability and may be recovered *via* a number of alternative methods, such as membrane filtration, thermomorphic separation,^[75] liquid or scCO₂ extraction^[76] and fluorous biphasic catalysis.^[77] However, most require a complicated, multi-step synthesis, which affords the catalyst in poor yield, they are generally difficult to characterise spectroscopically and many display activities and selectivities lower than those of their monomeric equivalents.

1.6. Fluorous Solid-Phase Extraction

The use of FBC requires preferential fluorous solubility for its catalysts. This necessitates the addition of perfluoroalkyl chains to achieve ~60% wt fluorine. This modification can have serious impact on the overall solubility for large compounds, as mentioned in section 1.4.1. Fluorous solid-phase extraction avoids this problem by opting for “light” fluorous-tagged species. In this approach, the fluorous-tagged catalyst that is to be separated and recovered does not need to exhibit preferential fluorous solubility and, therefore, a smaller number of fluorine atoms are sufficient. This reduces the cost of the synthesis of the catalyst. The catalysis is conducted in conventional organic solvents under homogeneous conditions; further reducing cost, as no fluorous solvents are required.

Separation is achieved at the end of the reaction by chromatography. The resultant reaction mixture is passed through a specially customised column. The stationary phase is a finely divided powder that is attributed fluorophilic character by attaching perfluoroalkyl chains to its surface.

In standard chromatography molecules are separated according to their polarity; non-polar compounds have a smaller affinity for the column than polar ones. Thus, by varying the polarity of solvent/solvent mixtures, the compounds may be eluted down the column at different rates and be

separated. In fluorous solid-phase extraction, the polarity of the column is reversed. Therefore, compounds containing increasing levels of fluorine are retained more strongly by the column and non-fluorous products are eluted easily.

Hope and co-workers demonstrated the applicability of this technique with a fluorous reverse-phase silica gel column.^[78] A fluorous-tagged Ni complex was used in the Lewis acid catalysed synthesis of enaminodiones in DCM. Although heavy fluorous catalysts tend to show lower activity than non-fluorous analogues, the light fluorous complex showed superior results in their investigation. The crude reaction mixture was loaded onto the silica column and the enaminodione product was eluted with DCM, whilst the catalyst, containing four $-C_6F_{13}$ ponytails, was retained at the top of the column. The catalyst could then be washed from the column by switching to diethyl ether as eluent. The catalyst was recycled and used in a further four runs. However, despite quantitative recovery of the catalyst, yields still fell with each successive run. This was assumed to be due to deactivation of the catalyst by the support.

Curran and Matsugi^[79] reported the synthesis of light fluorous versions of first- and second-generation Grubbs-Hoveyda metathesis catalysts (Figure 1.12), which could be readily separated from organic product mixtures by fluorous solid-phase extraction and reused up to five times. The activities of the fluorous catalysts were equal to those of the original Grubbs-Hoveyda complexes, demonstrating that the addition of the perfluorooctyl chains had no negative side-effects in terms of reactivity. The catalysts were also recyclable when physically supported upon fluorous silica gel combined with post-reaction filtration.

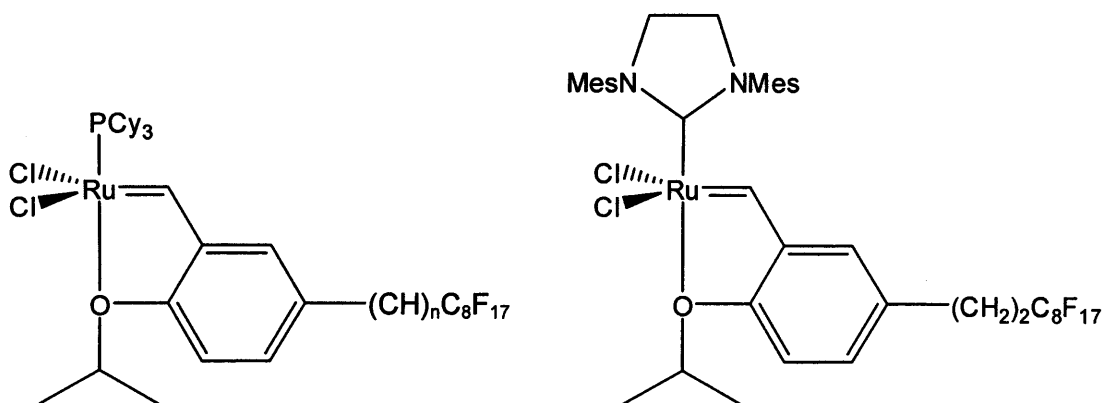


Figure 1.12. Fluorous Grubbs-Hoveyda catalysts

1.7. Supported Liquid Phase Catalysis

1.7.1. Supported Aqueous Phase Catalysis

First proposed by Arhancet *et al.* in 1989,^[80] the concept of supported aqueous phase catalysis (SAPC) involves coating a hydrophilic surface, such as silica or glass, with a small volume of water containing a catalyst (Figure 1.13). The support material is then added to an immiscible organic solvent, which contains the substrate (*S*) and acts as the reaction medium. The substrate is able to diffuse into the porous support and catalysis occurs at the aqueous/organic interface. The catalyst retains a degree of mobility within the supported solvent and may be separated from the final product by filtration.

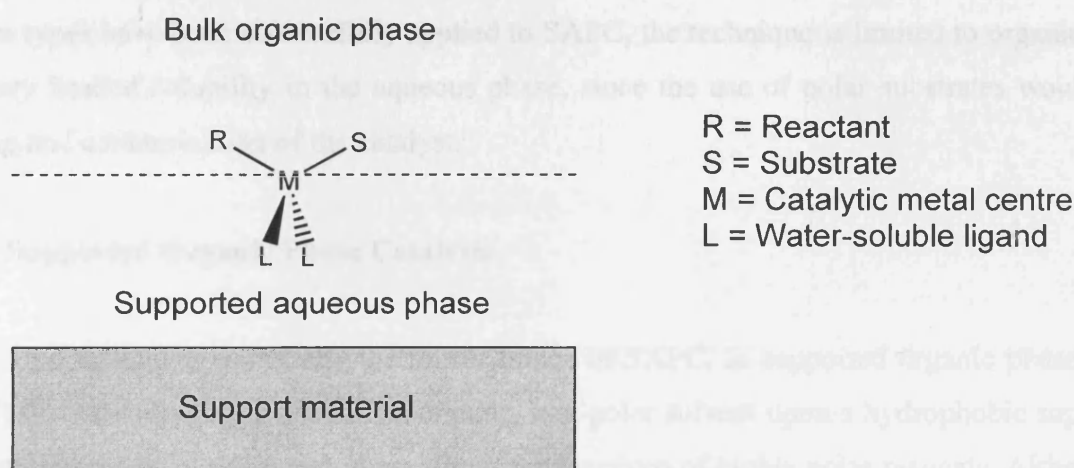


Figure 1.13. Supported aqueous phase catalysis

The supported catalyst may be formed by addition of an aqueous solution of catalyst to a dry, degassed support. The volume of solvent is reduced to yield free flowing powder/beads with the desired water content.

As the surface area of the support material is increased, the solvent interface area is also increased. Thus, SAPC provides a much greater interface between the reagent phase and that of the catalyst when compared to the aqueous biphasic system. This should result in superior catalyst activity. Williams *et al.* showed this to be the case in the hydroformylation of oleyl alcohol,^[81] a water-insoluble substrate that is not hydroformylated under aqueous biphasic conditions. Using a rhodium based, water-soluble catalyst supported on glass beads (Figure 1.14) conversions of 96.6% with SAPC were achieved.

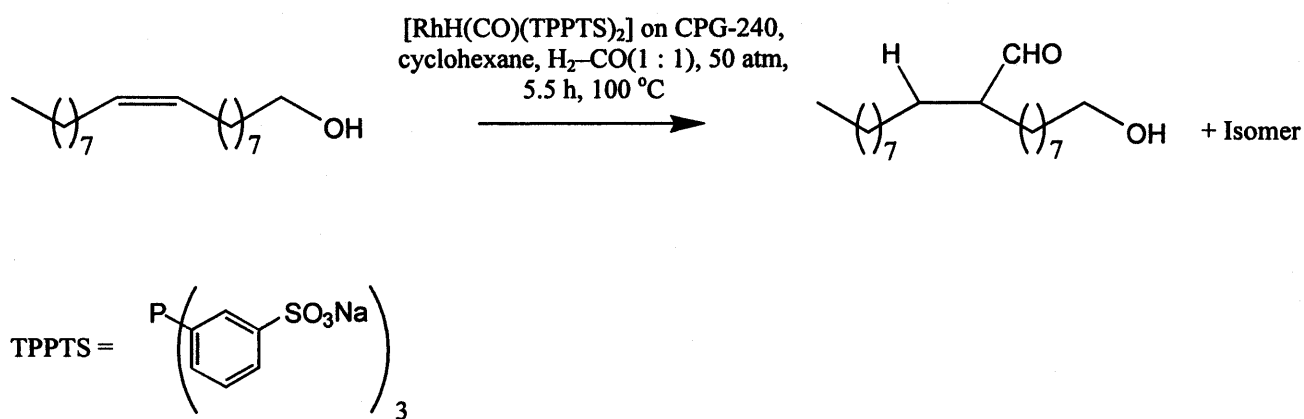


Figure 1.14. Supported aqueous phase catalytic hydroformylation of oleyl alcohol

Several investigations now support these results,^[82, 83] showing that SAPC can overcome the drawback of ABC with respect to substrate solubility in the aqueous phase. Although a number of reaction types have been successfully applied to SAPC, the technique is limited to organic reagents with very limited solubility in the aqueous phase, since the use of polar substrates would lead to leaching and contamination of the catalyst.

1.7.2. Supported Organic Phase Catalysis

This method is essentially the mirror image of SAPC. In supported organic phase catalysis (SOPC) the catalyst is supported in an organic, non-polar solvent upon a hydrophobic support. The bulk reaction media is water and, thus, allows for reactions of highly polar reagents. Although there are abundant ligands suitable for creating a catalyst with the appropriate solubility, the support material itself must be modified to ensure the correct miscibility. It must possess a non-polar surface, which may adsorb the organic catalyst phase yet be immiscible with the bulk solvent. Williams' group^[84] achieved this by attaching long alkyl chains to a silica surface (Figure 1.15).

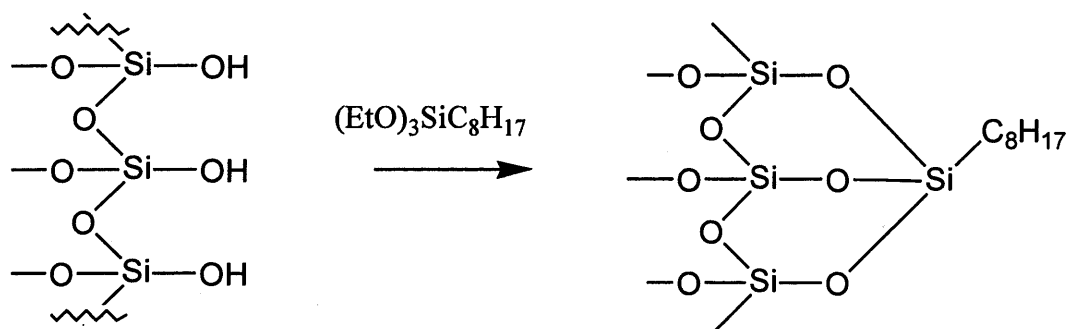


Figure 1.15. Reverse phase silica

The resulting reverse-phase silica was coated with a phosphine-based palladium catalyst in cyclohexane. The supported catalyst was used in a number of Heck coupling reactions in a 1:1 mixture of water/methanol. High yields and acceptable levels of Pd leaching (a maximum of 0.18%) were attained and the support was successfully recovered and recycled in seven consecutive runs with no observable loss in activity.

The group also reported the use of another supported Pd catalyst in an enantioselective allylic substitution reaction (Figure 1.16).^[84] Performed in DMSO, the reaction displayed high yield, good selectivity and low Pd leaching.

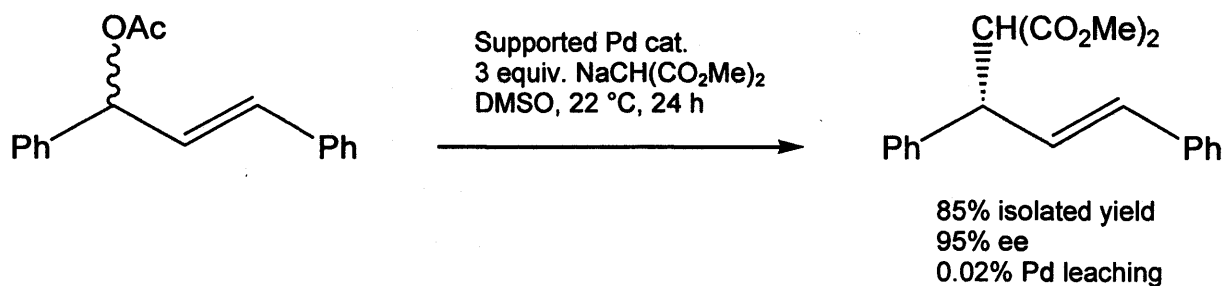


Figure 1.16. Enantioselective allylic substitution catalysed by a supported palladium catalyst

However, despite the accomplishments of both SAPC and SOPC, both systems utilise water. This prevents the use of water-sensitive reagents/catalysts and, thus, the widespread application of these systems.

1.7.3. Supported Ionic Liquid Phase Catalysis

A further evolution of the supported liquid field involved the replacement of the aqueous phase by ionic liquids. These non-volatile solvents may be used as a replacement for water, as they are similarly immiscible with most organic solvents. The same water-soluble catalysts containing polar ligand-functionalities that are used in ABC and SAPC may be solubilised in ionic media. However, the support must be modified with a monolayer of covalently attached ionic liquid fragments.

Mehnert's group recently developed a silica gel that could adsorb a layer of ionic liquid,^[85] shown in Figure 1.17. A rhodium catalyst was dissolved in the ionic liquid (either [bmim][PF₆] or [bmim][BF₄]) and was applied in the hydroformylation of 1-hexene to heptanal. The activity and selectivity were superior to or comparable to those obtained in an ionic liquid biphasic system.

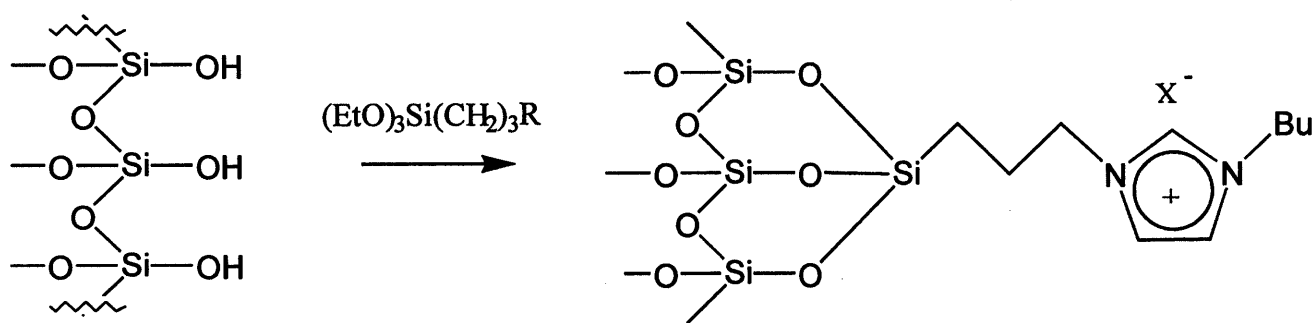


Figure 1.17. Silica gel modified with ionic functionality

Despite the favourable conversions obtained with the supported ionic phase catalyst, significant levels of Rh leaching into the organic solvent were observed. Although the catalysts themselves were insoluble in the organic solvent, the ionic liquid [bmim][BF₄] had some miscibility at high concentrations of the product aldehydes. Thus, the catalyst was carried into the organic phase. The high aldehyde levels also depleted the supported ionic liquid layer and, hence, reduced the longevity of the catalyst.

These problems were overcome by altering the reaction conditions and this work shows the potential of ionic liquids in the heterogenisation of homogeneous catalysis. The absence of an aqueous phase in supported ionic liquid phase catalysis allows separation and further flexibility, and this type of system is likely to receive a great deal of interest in the future.

1.7.4. Supported Fluorous Phase Catalysis

Fluorous solvents offer an alternative replacement for an aqueous phase in supported liquid phase catalysis. This methodology requires the modification of both the catalyst and the support. Both are adapted to allow miscibility with fluorous solvents through the use of perfluoroalkyl chains. Silica may be altered in a manner similar to SOPC. The surface silanols are capped with fluorous ponytails instead of alkyl chains, creating fluorous reverse phase silica gel (FRPSG). Thus, the support may be coated with a fluorous solvent, containing a fluorous soluble catalytic metal complex. When added to bulk organic media, catalysis now occurs at the fluorous/organic interface.

The University of Leicester fluorine chemistry group has recently achieved some success with this approach.^[86, 87] The group evaluated micro- and meso-porous perfluoroalkylated silicas as a solid supports for a perfluoroalkylated analogue of Wilkinson's catalyst (Figure 1.18).^[88]

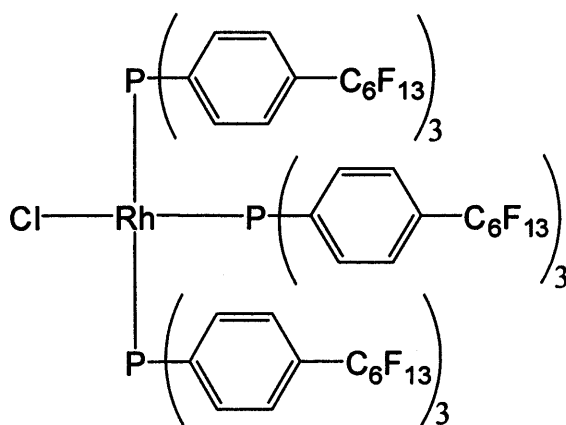


Figure 1.18. Fluorous analogue of Wilkinson's catalyst

The catalyst was immobilised in a thin film of fluoruous solvent, perfluoro-1,3-dimethyl cyclohexane (PP3), on the surface of the support and was utilised in the hydrogenation of styrene. Varying volumes of PP3 were used and reaction rates measured to determine an optimum surface area:volume ratio. As the volume of PP3, and hence catalyst solvation, was increased a gradual rise and subsequent fall in activity was observed. Addition of a small volume of PP3 was shown to substantially decrease catalyst leaching levels compared to when no fluoruous solvent was used at all.

Tsang^[89] developed an interesting technique using fluoruous silica in which a fluoruous tin compound could be trapped upon the surface of the solid support material when in an organic solvent at room temperature and then released by increasing the temperature to 60 °C. When released into a solution of NaBH₄ in 1-butanol, the tris(perfluorohexylethyl) tin bromide formed a tin hydride, which acted as a catalyst for the hydrocyclisation of 6-bromo-1-hexene to methylcyclopentane. However, product yields acquired in the presence of fluoruous silica were lower than in its absence. The group observed a correlation between the amount of unreleased tin compound and the decrease in yield, both around 20%, and suggested that a higher temperature would allow more effective release of the catalyst precursor from the support, thereby increasing the yield. Results of these experiments, or of attempts at recycle, were not reported.

Considerable success using perfluorinated silica as a solid support was achieved by Bannwarth *et al.* in their work with fluoruous palladium-based catalysts.^[90] Three phosphine ligands containing perfluorooctyl chains (Figure 1.19) were prepared and evaluated in the Suzuki and Sonogashira C-C coupling reactions.

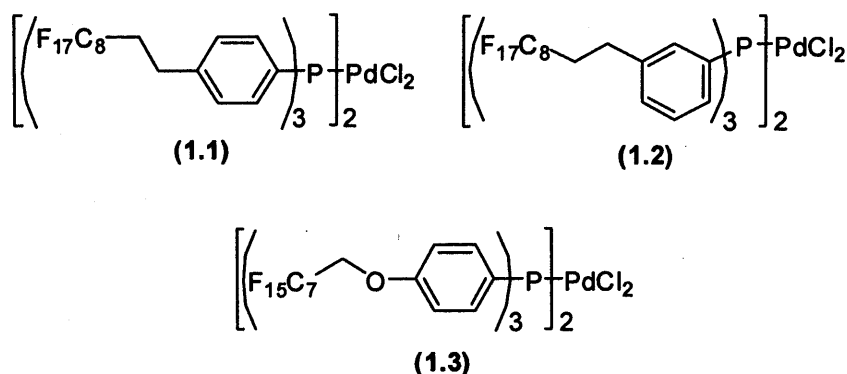


Figure 1.19. Three palladium complexes of different fluorinated phosphines

Diethyl ether/hexafluorobenzene solutions of catalysts were stirred with the required amount of fluorosilica gel and the solvent removed to yield the supported catalyst as an air-stable, free flowing powder. Varying catalyst loadings were tested in the Suzuki cross-coupling of phenylboronic acid and *para*-nitrobromobenzene and in the Sonogashira coupling of phenylacetylene and *para*-nitrobromobenzene. The catalyst could be recovered by facile filtration. In the Suzuki reaction, complete conversions were obtained with catalyst loadings as low as 0.01 mol %, with only small reductions in yield in successive runs. At 0.001 mol % the yield of the first run was 86%, falling to 45% after just one recycle. Recycling results for runs 1 to 4 for each of the immobilized catalysts at 0.1 mol % are shown in table 1.20.

Pd Complex	Yield (%)
(1.1), [PdCl ₂ {P(C ₆ H ₄ -4-C ₈ F ₁₇) ₃ } ₂]	>98, 93, 93, 93
(1.2), [PdCl ₂ {P(C ₆ H ₄ -3-C ₈ F ₁₇) ₃ } ₂]	96, 98, 93, 91
(1.3), [PdCl ₂ {P(C ₆ H ₄ -4-OCH ₂ -C ₇ F ₁₅) ₃ } ₂]	>98, 96, 95, 95

Table 1.20. Yields for the Suzuki coupling of phenylboronic acid and *para*-nitrobromobenzene

Leaching levels in the first run were determined for catalyst (1.1) by inductively coupled plasma optical emission spectroscopy (ICP-OES). Using two different variants of fluorinated silica, 1.9% and 1.6% of the total palladium were lost from the support to the organic product. The catalyst was also tested with a wide range of substrates in the Suzuki reaction and was found to be highly active for all electron-deficient aryl halides.

Results for the Sonogashira reaction were less successful. At loading levels below 0.02 mol % the catalyst was rendered completely inactive after the first run and even at 2 mol % catalyst, yields fell from >98 to 71% after just two recycles.

Silica based supports, from all the aforementioned systems, suffer a common problem. As already described, uncapped –OH groups on the support materials surface can bind irreversibly to the catalytic metal centre. This can impact upon activity/selectivity or even render the catalysts inactive. As it is impossible to ensure that all the silanol groups are protected, the long-term stability of catalysts employing these supports will be adversely affected.

1.8. Conclusion of Support Methodologies

Although the examples given in this chapter are by no means a comprehensive review of all separation and recovery methodologies, all of the aforementioned approaches to catalyst/product separation have their own associated advantages and disadvantages; catalysts bound to organic solid supports, although efficiently recovered, tend to yield lower reaction rates than their homogeneous analogues and the supports themselves are relatively thermally and mechanically unstable. Their inorganic counterparts offer increased stability but, in the case of the most commonly used material, silica, surface functionalities such as hydroxyl groups can destructively bind to the catalyst. Biphasic systems allow conditions closest to the homogeneous case but often involve catalyst leaching due to some miscibility between the two phases used. Selection of suitable solvent/reagent systems is also a limiting factor in this approach.

1.9. Objectives

The goal of this project is to develop alternative support materials for the heterogenisation of homogeneous catalysts *via* fluororous separation techniques. The main criteria for such a support are the ability to separate a fluororous catalyst from organic products at the end of reaction and the absence of free hydroxyl groups, or other potentially reactive functionalities, upon the surface. This would enable the maximisation of catalyst activity by facile, quantitative recovery and recycle in numerous successive catalytic runs.

Separation may be achieved either by fluororous solid-phase extraction, where the material acts as a stationary phase similar to that of silica or alumina in column chromatography, or by supported fluororous phase catalysis.

The following chapter explains why zirconium phosphonates could be a suitable material for such a role, and how they may be adapted to confer them with fluororous character.

In this thesis, fluororous α -zirconium phosphonates were targeted as the support material. In Chapter 2, the synthesis of new fluorinated diethyl phosphonates, phosphonic acids and zirconium phosphonates, as well as platinum coordination complexes of the phosphonic acids, is described.

In Chapters 3, 4 and 5 the application of the zirconium phosphonates supports in three catalytic reactions, a cyclopropanation, an oxidation and an enantioselective fluorination, will be discussed. Chapter 6 summarises all the experimental details.

Overall, this work seeks to establish whether zirconium phosphonates can be reliable robust materials that allow effective product/catalyst separation combined with catalyst reuse.

References for Chapter 1

- [1] G. C. Bond, 'Principles of Catalysis', Royal Institute of Chemistry, 1963.
- [2] *Green Chemistry Research and Development Act of 2004*, 2004, H.R. 3970.
- [3] P. Anastas, J. Warner, 'Green Chemistry Theory and Practice', Oxford University Press, 1998.
- [4] B. Cornils, W. A. Herrmann, 'Applied Homogeneous Catalysis with Organometallic Compounds', VCH, Weinheim, 1996, 605.
- [5] R. S. Drago, E. D. Nyberg, A. El A'mma, A. Zombeck, *Inorg. Chem.*, 1981, 20, 641.
- [6] J. M. Fraile, J. I. Garcia, M. A. Harmer, C. I. Herrerias, J. A. Mayoral, *J. Mol. Cat. A.*, 2001, 165, 211.
- [7] Y. M. A. Yamada, K. Takeda, H. Takahashi, S. Ikegami, *Tetrahedron Lett.*, 2003, 44, 2379.
- [8] K. Oono, M. Sato, *International Patent WO 2004011140*, 2004.
- [9] H. G. Tang, D. C. Sherrington, *J. Mol. Cat.*, 1994, 94, 7.
- [10] L. D. Rollmann, *Inorg. Chim. Acta*, 1972, 6, 137.
- [11] W. D. J. Bonds, C. H. J. Brubaker, E. S. Chandrasekaran, C. Gibbons, R. H. Grubbs, L. C. Kroll, *J. Am. Chem. Soc.*, 1975, 97, 2128.
- [12] T. J. Dickerson, N. N. Reed, K. D. Janda, *Chem. Rev.*, 2002, 102, 3325.
- [13] B. Cornils, W. A. Herrmann, 'Applied Homogeneous Catalysis with Organometallic Compounds', VCH, Weinheim, 1996, 608.
- [14] R. H. Grubbs, L. C. Kroll, *J. Am. Chem. Soc.*, 1971, 93, 3062.
- [15] M. M. Mdleleni, R. G. Rinker, P. C. Ford, *Inorg. Chim. Acta*, 1998, 270, 345.
- [16] U. Schuchardt, E. Nicolau dos Santos, F. Santos Dias, *J. Mol. Cat.*, 1989, 55, 340.
- [17] C. L. Ruddick, P. Hodge, A. Cook, A. J. McRiner, *J. Chem. Soc. Perkins Trans. 1*, 2002, 5, 629.
- [18] H. Zhu, G. X. Jin, N. Hu, *J. Organomet. Chem.*, 2002, 655, 167.
- [19] R. M. Kroell, N. Schuler, S. Lubbad, M. R. Buchmeiser, *Chem. Comm.*, 2003, 21, 2742.
- [20] C. U. J. Pittman, L. R. Smith, R. M. Hanes, *J. Am. Chem. Soc.*, 1975, 97, 1742.
- [21] F. R. Hartley, S. G. Murray, P. N. Nicholson, *J. Mol. Cat.*, 1982, 16, 363.
- [22] K. Geckeler, V. N. R. Pillai, M. Mütter, *Adv. Polym. Sci.*, 1995, 121, 31.
- [23] C. A. McNamara, M. J. Dixon, M. Bradley, *Chem. Rev.*, 2002, 102, 3275.
- [24] B. Cornils, W. A. Herrmann, 'Applied Homogeneous Catalysis with Organometallic Compounds', VCH, Weinheim, 1996, 612.
- [25] P. Y. Zhang Zhuangyu, H. Hongwen, *J. Mol. Cat.*, 1990, 62, 297.
- [26] R. L. Espinoza, C. P. Nicolaidis, C. J. Korf, R. Snel, *Applied Catalysis*, 1987, 31, 259.

- [27] A. J. Sandee, J. N. H. Reek, P. C. J. Kamer, P. W. N. M. van Leeuwen, *J. Am. Chem. Soc.*, **2001**, *123*, 8468.
- [28] Z. M. Michalska, *J. Mol. Cat.*, **1977/78**, *3*, 125.
- [29] K. Morimoto, K. Inoue, *International Patent WO 03082771*, **2003**.
- [30] S. Nishikawa, A. Mukai, T. Masuda, *International Patent JP2000126602*, **2000**.
- [31] K. Suzuki, H. Sakami, K. Kawase, S. Iida, *European Patent JP60166217*, **1985**.
- [32] D. C. Bailey, S. H. Langer, *Chem. Rev.*, **1981**, *81*, 109.
- [33] S. Bae, S.-W. Kim, T. Hyeon, B. M. Kim, *Chem. Comm.*, **2000**, *1*, 31.
- [34] B. Reuben, H. Wittcoff, *J. Chem. Ed.*, **1988**, *65*, 605.
- [35] T. G. Southern, *Polyhedron*, **1989**, *8*, 407.
- [36] B. Cornils, *Org. Proc. Res. & Dev.*, **1998**, *2*, 121.
- [37] I. T. Horváth, J. Rábai, *Science*, **1994**, *266*, 72.
- [38] L. P. Barthel-Rosa, J. A. Gladysz, *Coord. Chem. Rev.*, **1999**, *190-192*, 587.
- [39] W. Chen, L. Xu, Y. Hu, A. M. Banet-Osuna, J. Xiao, *Tetrahedron*, **2002**, *58*, 3889.
- [40] E. G. Hope, R. D. W. Kemmitt, D. R. Paige, A. M. Stuart, D. R. W. Wood, *Polyhedron*, **1999**, *18*, 2913.
- [41] B. Betzemeier, P. Knochel, *Angew. Chem. Int. Ed.*, **1997**, *36*, 2623.
- [42] S. Kainz, D. Koch, W. Baumann, W. Leitner, *Angew. Chem. Int. Ed.*, **1997**, *36*, 1628.
- [43] B. Richter, E. de Wolf, G. van Koten, B. Deelman, *J. Org. Chem.*, **2000**, *65*, 3885.
- [44] V. Herrera, P. J. F. de Rege, I. T. Horváth, T. le Husebo, R. Hughes, *Inorg. Chem. Comm.*, **1998**, *1*, 197.
- [45] J. A. S. Howell, N. Fey, J. D. Lovatt, P. C. Yates, P. McArdle, D. Cunningham, E. Sadeh, H. E. Gottlieb, Z. Goldschmidt, M. B. Hursthouse, M. E. Light, *J. Chem. Soc., Dalton Trans.*, **1999**, *17*, 3015.
- [46] I. T. Horváth, *Acc. Chem. Res.*, **1998**, *31*, 641.
- [47] J. A. Gladysz, M. Wende, *J. Am. Chem. Soc.*, **2003**, *125*, 5861.
- [48] G. Barré, D. Taton, D. Lastécouères, J. M. Vincent, *J. Am. Chem. Soc.*, **2004**, *126*, 7764.
- [49] D. E. Bergbreiter, P.L. Osburn, A. Wilson, E. M. Sink, *J. Am. Chem. Soc.* **2000**, *122*, 9058
- [50] R. Sheldon, *Chem. Comm.*, **2001**, *23*, 2399.
- [51] P. Wasserscheid, H. Waffenschmidt, P. Machnitzki, K. W. Kottsieperb, O. Stelzerb, *Chem. Comm.*, **2001**, 451.
- [52] Y. Chauvin, L. Mussmann, H. Olivier, *Angew. Chem. Int. Ed.*, **1995**, *34*, 2698.
- [53] J. Dupont, A. L. Montiero, R. F. de Souza, F. K. Zinn, *Tetrahedron: Asymmetry*, **1997**, *2*, 177.
- [54] T. Ikariya, P.G. Jessop, R. Noyori, *Chem. Rev.*, **1999**, *99*, 475.

- [55] V. P. W. Böhm, W. A. Herrmann, *J. Org. Chem.*, **1999**, *69*, 141.
- [56] R. M. Smith, *J. Chromatogr. A.*, **1999**, *856*, 83.
- [57] M. A. McHugh, V. J. Krukonic, 'Supercritical Fluid Extraction : Principles and Practice', Butterworth-Heinemann, London, **1994**.
- [58] T. Takeuchi, D. Ishii, M. Saito, K. Hibi, *J. Chromatogr. A.*, **1984**, *295*, 323.
- [59] P. G. Jessop, M. M. Olmstead, C. D. Alban, M. Grabenauer, D. Sheppard, C. A. Eckert, C. L. Liotta, *Inorg. Chem.*, **2002**, *41*, 3463.
- [60] K. B. Stallone, F. J. Bonner, *Green Chem.*, **2004**, *6*, 267.
- [61] W. Leitner, *Pure Appl. Chem.*, **2004**, *76*, 635.
- [62] D. Bonafoux, Z. Hua, B. Wang, I. Ojima, *J. Fluorine. Chem.*, **2001**, *112*, 101.
- [63] K. E. Laintz, R. D. Smith, C. R. Yonker, C. M. Wai, *Supercritical Fluids*, **1991**, *4*, 194.
- [64] M. J. Burk, S. Feng, M. F. Gross, W. Tumas, *J. Am. Chem. Soc.*, **1995**, *117*, 8277.
- [65] T. Ikariya, P. G. Jessop, R. Noyori, *Chem. Rev.*, **1995**, *95*, 259.
- [66] W. Leitner, D. Koch, *J. Am. Chem. Soc.*, **1998**, *120*, 13398.
- [67] M. Perrut, *Ind. Eng. Chem. Res.*, **2000**, *39*, 4531.
- [68] P. Licence, J. Ke, M. Sokolova, S. K. Ross, M. Poliakoff, *Green Chem.*, **2003**, *5*, 99.
- [69] M. A. El-Sayed, R. Narayanan, *J. Phys. Chem. B*, **2004**, *108*, 8572.
- [70] E. Delort, T. Darbre, J.-L. Reymond, *J. Am. Chem. Soc.*, **2004**, *126*, 15642 .
- [71] R. Schneider, C. Köllner, I. Weber, A. Togni, *Chem. Comm.*, **1999**, 2415.
- [72] G.-J. Deng, Q.-H. Fan, X.-M. Chen, D.-S. Liu, A. S. C. Chan, *Chem. Comm.*, **2002**, 1570.
- [73] Y. Ribourdouille, G. D. Engel, M. Richard-Plouet, L. H. Gade, *Chem. Comm.*, **2003**, 1228.
- [74] G. van Koten, J. T. B. H. Jastrzebski, *J. Mol. Cat. A*, **1999**, *146*, 317.
- [75] T. Mizugaki, M. Murata, M. Ooe, K. Ebitani, K. Kaneda, *Chem. Comm.*, **2002**, 52.
- [76] E. L. V. Goetheer, M. W. P. L. Baars, L. J. P. van den Broeke, E. W. Meijer, J. T. F. Keurentjes, *Ind. Eng. Chem. Res.*, **2000**, *39*, 4634.
- [77] A.-M. Caminade, C.-O. Turrin, P. Sutra, J.-P. Majoral, *Current Opinion in Colloid and Interface Science*, **2003**, *8*, 282.
- [78] B. Croxtall, E. G. Hope, A. M. Stuart, *Chem. Comm.*, **2003**, 2430.
- [79] M. Matsugi, D. P. Curran, *J. Org. Chem.*, **2005**, *70*, 1636.
- [80] J. P. Arhancet, M. E. Davis, J. S. Merola, B. E. Hanson, *Nature*, **1989**, *339*, 454.
- [81] M. S. Anson, M. P. Leese, L. Tonks, J. M. J. Williams, *J. Chem. Soc., Dalton Trans.*, **1998**, 3529.
- [82] E. Fache, C. Mercier, N. Pagnier, B. Despeyroux, P. Panster, *J. Mol. Cat.*, **1993**, *79*, 117.
- [83] M. S. Anson, L. Tonks, J. M. J. Williams, *Tetrahedron Lett.*, **1997**, *38*, 4319.
- [84] M. S. Anson, L. Tonks, A. R. Mirza, J. M. J. Williams, *Tetrahedron Lett.*, **1999**, *40*, 7147.

- [85] C. P. Mehnert, R. A. Cook, N. C. Dispenziere, M. Afeworki, *J. Am. Chem. Soc.*, **2002**, *124*, 12932.
- [86] J. Sherrington, *Supported Fluorous Phase Catalysis*, Ph.D Thesis, University of Leicester, **2003**.
- [87] J. F. S. Vaughan, M. G. Pellatt, J. Sherrington, E. G. Hope, *International Patent WO 2002004120*, **2002**.
- [88] E. G. Hope, J. Sherrington, A. M. Stuart, *Adv. Synth. Cat.*, **2006**, *348*, 1635.
- [89] P. M. Jenkins, A. M. Steele, S. C. Tsang, *Cat. Comm.*, **2003**, *4*, 45.
- [90] C. C. Tzschucke, C. Markert, H. Glatz, W. Bannwarth, *Angew. Chem. Int. Ed.*, **2002**, *41*, 4500.

2. Metal Phosphonates

Metal phosphonate chemistry is a relatively new field that has grown rapidly due to two exploitable characteristics: their capability for numerous functionalities and their potential for supramolecular assembly.

In the late 1970's, Alberti *et al.* prepared zirconium phosphonate and phosphonate ester derivatives by reaction of Zr(IV) with the corresponding phosphonic acids.^[1] The compounds all shared a common, layered structure with that of the parent zirconium phosphate α -Zr(HPO₄)₂·H₂O. It was later found that a wide variety of both organic and inorganic groups could be introduced into these layers. This made metal phosphonates appealing to chemists, as an abundance of structures could be designed for a variety of applications, ranging from catalysts to non-linear optical materials. The following chapter details some of these applications and describes how the structure of α -zirconium phosphonates may be adapted to create fluororous supports for catalysis.

2.1. Applications

As metal phosphonates can support a great number of different functionalities,^[2] the list of their possible applications is long and varied. One of the first identified applications for zirconium phosphate was ion exchange,^[3] when the amorphous form was used as a sorbant in artificial kidney devices.^[4] Other early uses include water softeners and cation exchangers in radioactive waste streams.

Metal phosphonates also had some early success as catalysts. A vanadium compound, (VO)₂P₂O₇, was used to catalyse the selective oxidation of butanes and butenes to maleic anhydride.^[5] There have since been a range of phosphonate based catalysts/supported catalysts developed and a number of patents submitted for these compounds.^[6-12]

Functionalised zirconium phosphonates have also been shown to be compatible with thin film formation. Multilayer films can be prepared using Langmuir-Blodgett and self-assembly methods.^[13, 14, 15] Due to their conductivities, these materials have many possible roles. Depending upon which pendant group is used, zirconium phosphonates may have applications as electrolytes in high-energy batteries,^[16] optical storage devices,^[17] photochemical switches,^[18] non-linear electrooptic devices,^[19] insulators^[15] and liquid crystal aligners.^[20]

Clearly, the scope for these versatile compounds is vast and too substantial to be discussed in detail here and the reader is referred to two review articles in this area.^[2, 3] Due to their great potential, the structures of metal phosphonates have been studied extensively and are now well known.

2.2. Structure

2.2.1. Zirconium Phosphates and Phosphonates

There are two main classes of zirconium phosphate labelled α -zirconium phosphate, $\text{Zr}(\text{HPO}_4)_2 \cdot 2\text{H}_2\text{O}$, and γ -zirconium phosphate, $\text{Zr}(\text{PO}_4)(\text{H}_2\text{PO}_4) \cdot 2\text{H}_2\text{O}$. These compounds may be obtained either as amorphous or as highly crystalline materials. The following section will concentrate mainly upon structural details; synthetic considerations will be dealt with in a further part of the chapter.

In α -zirconium phosphate (α -ZrP) the two phosphate groups are equivalent, resulting in a simpler repeat unit, compared to the γ -structure. The crystal structure, provided by Clearfield and Smith in 1967,^[21] showed the compound consists of layers of zirconium atoms, bridged by phosphate groups (Figure 2.1). The zirconium atoms lie slightly above and below the mean plane and are 5.3 Å apart and are 5.3 Å apart.

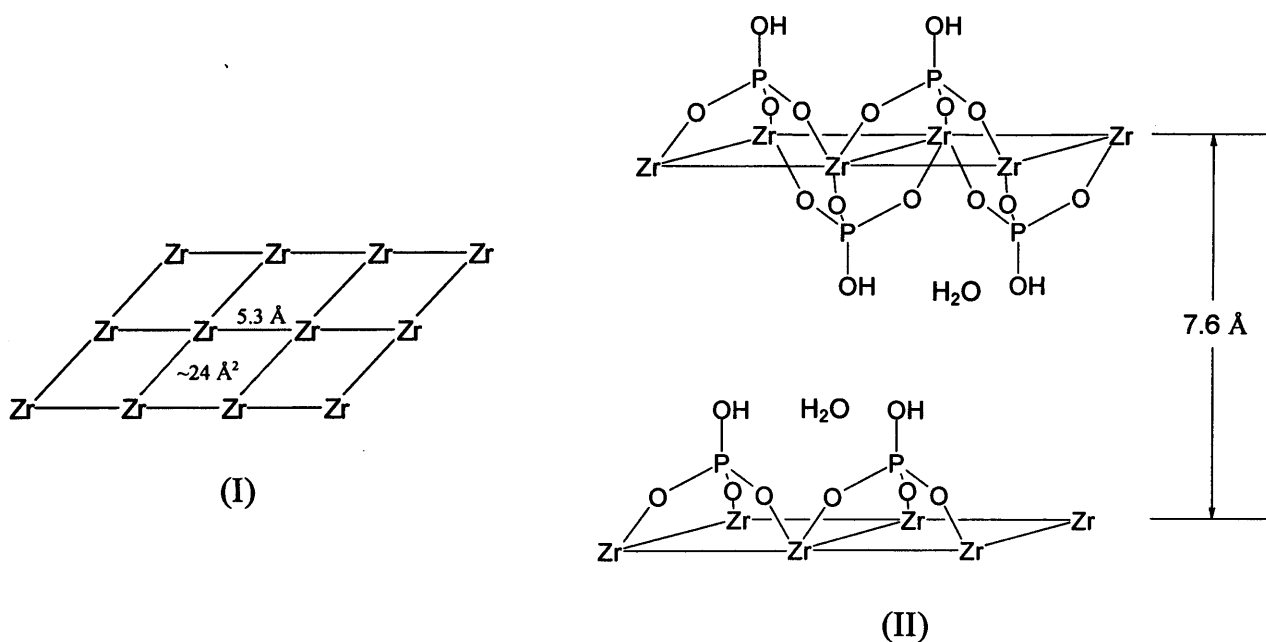


Figure 2.1. (I) The inter-zirconium distances within the plane. (II) Idealised structure of α -ZrP

The phosphates are bonded to both faces of the plane and each group is bound to three separate metal atoms, which form a distorted equilateral triangle. The zirconium atoms are connected octahedrally to six oxygen atoms. The idealised structure is shown in Figure 2.1 (II). The phosphorus atoms lie roughly over the centre of a diamond of four Zr^{4+} , as shown on the following page in Figure 2.2, with its hydroxyl group pointing out into the inter-lamellar space. Water

molecules are contained in the hexagonal cavities between the three hydroxyl groups and are hydrogen-bonded to these groups. There are, however, no hydrogen bonds between the layers and the inorganic sheets are held together solely by Van der Waals attractions.

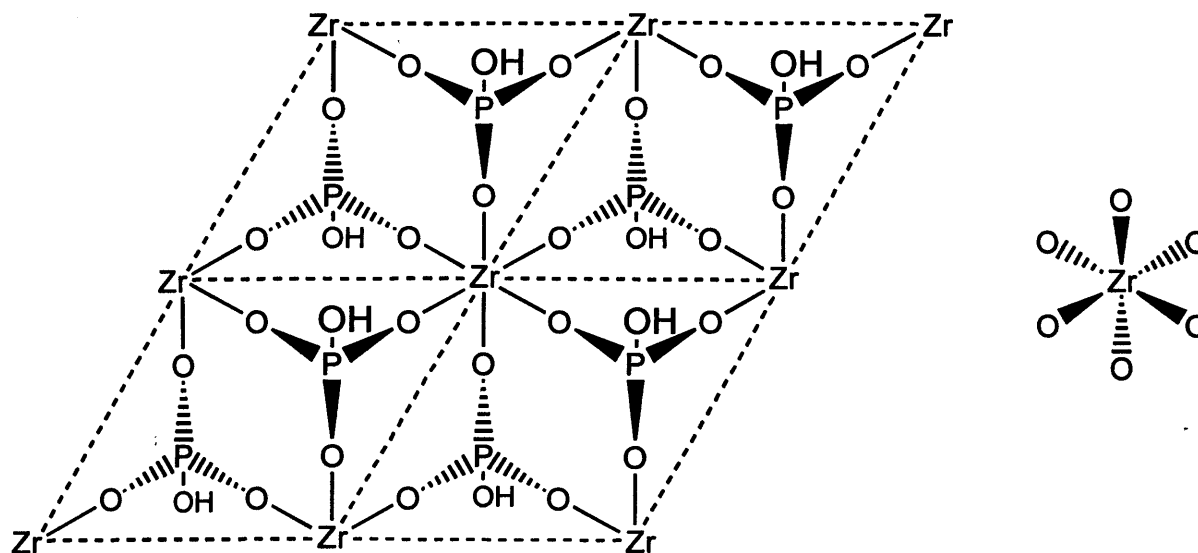


Figure 2.2. Idealised structure of zirconium phosphate

Alberti and co-workers showed that it was possible to replace the hydroxyl group of α -ZrP with alkyl or aryl substituents, by using the corresponding phosphonic acids to create a number of zirconium phosphonates.^[1] Dines and DiGiacomo later expanded the series of functionalities and used a variety of M^{4+} ions.^[22] A report on the behaviour of the material was provided, along with a greater degree of characterisation.

It was found that any pendant group could be incorporated into the α -ZrP architecture, providing its cross-sectional area was less than 24 \AA^2 . The crystallinity of the material was found to decrease as this limit was approached. The phosphonate compounds were also found to be more thermally stable than their phosphate analogues, with no weight change below $300 \text{ }^\circ\text{C}$. The length and type of pendant group affects the inter-lamellar distance. The change in this distance is found to be approximately 2 \AA for each additional carbon atom.^[2] However, the pendant groups are not necessarily perpendicular to the inorganic sheets, as is shown in the idealised structure of Figures 2.1 and 2.2. In phenyl zirconium phosphonate, $\text{Zr}(\text{O}_3\text{PPh})_2$, the phenyl pendant groups lie at an angle of 30° to the zirconium plane.^[23] This explains why the interlayer distance is smaller than expected, at 14.82 \AA . The interlayer distance is also affected by the additional of a suitable solvent that occupies the space between the layers, forcing them apart and causing the materials to ‘swell’.

In γ -zirconium phosphate (γ -ZrP) the two phosphate groups are different and it, therefore, has a more complex structure than the α -ZrP structure. One group is an orthophosphate, PO_4^{3-} , the

other a dihydrogen phosphate, H_2PO_4^- .^[24] The crystal structure^[25] shows that each Zr^{4+} is octahedrally coordinated to four oxygens from four separate PO_4^{3-} groups and two oxygens from two H_2PO_4^- groups.

2.2.2. Mixed-Component Phosphonates

The concept of preparing compounds containing two or more different pendant groups requires several additional considerations. Firstly, the reactivities of the phosphonic acids may not be equal, meaning the ratio of the pendant groups within the products layers may not be equal to the ratio of reagents. For a given compound $[\text{Zr}(\text{O}_3\text{PR})_x(\text{O}_3\text{PR}')_{2-x}]$, the system is discontinuous and not all values of x are possible. Mixed-component structures adopt an interstratified structure,^[26, 27] where one layer consists predominantly of the first pendant group and another layer consists mainly of the second pendant. An example is shown in Figure 2.3.

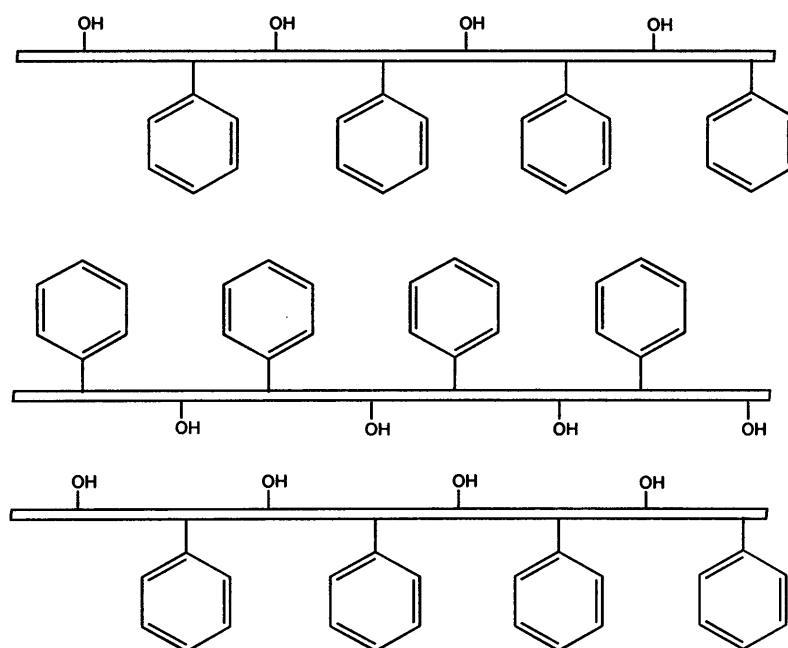


Figure 2.3. A mixed component zirconium phosphonate

Often, more than one phase of product is present, with various values of x . The layers may be well ordered, as in Figure 2.3, or the pendant distribution may be more random. Clearfield *et al.* developed a schematic representation of the possible forms of a metal phosphonate with two different pendant groups, one large and one small.^[27] A reproduction of this schematic is shown in Figure 2.4.

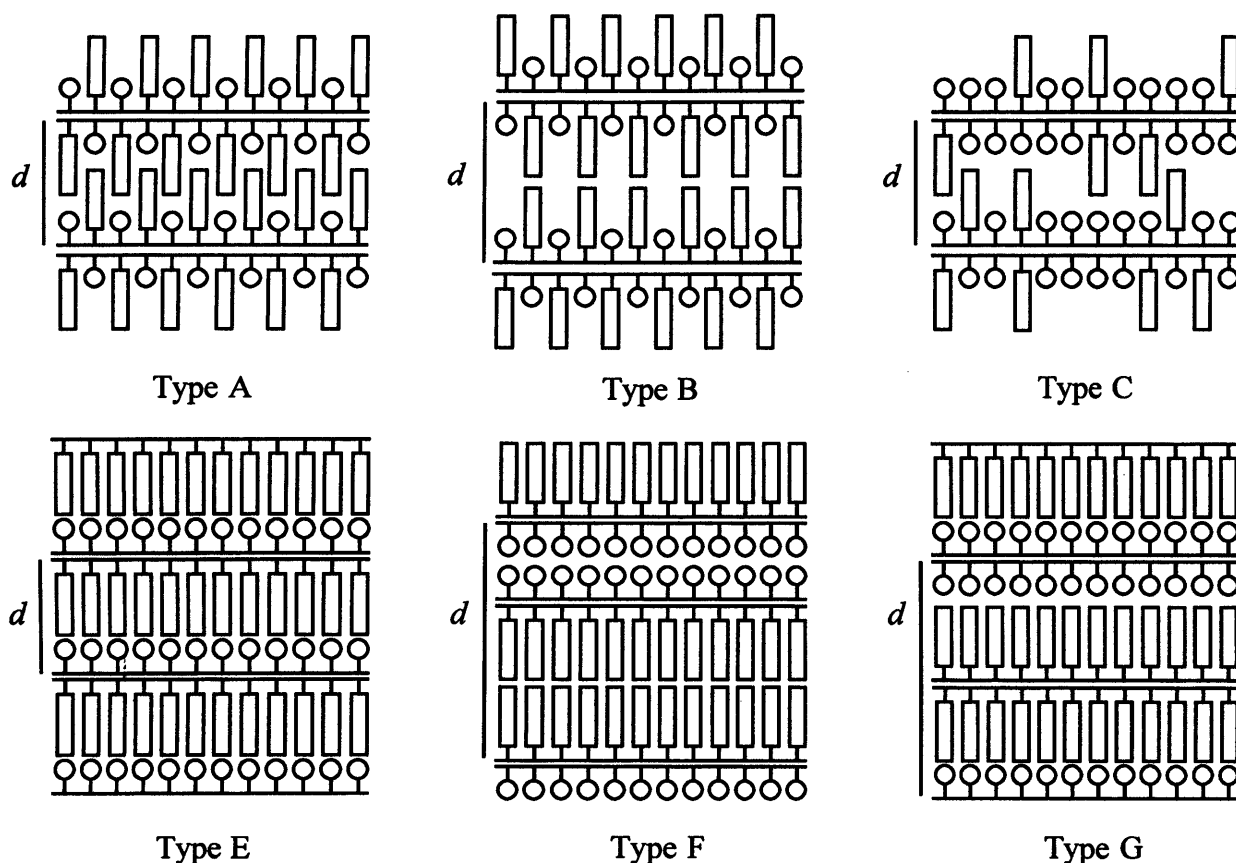


Figure 2.4. Possible configurations of a two component zirconium phosphonate

Figure 2.4 shows that there are three possible interlayer distances, d , that can be attained for a two pendant phosphonate. The smallest value of d is achieved when the large ligands of opposing layers interpenetrate, as in types A and C, or when opposite planes each contain different ligands, as in E. Type B has no interpenetration of ligands, and therefore d is increased. The largest interlayer spacing is found in the interstratified structures of types F and G.

These mixed-component phases allow chemists to design metal phosphonates of increasing complexity, as multiple functionalities and reactive groups may be incorporated simultaneously. Also, if one group is large and one small, microporosity may be introduced into the compound. Thus, by utilising numerous ligands, the versatility of metal phosphonates chemistry may be further increased.

2.2.3. Pillared Bisphosphonates

It is possible to connect the inorganic sheets of a metal phosphonate by using terminal bisphosphonic acids as cross-linkers. Dines *et al.* and Clearfield *et al.* carried out investigations into the microporosity of zirconium biphenylenebis(phosphonate).^[2] No pores were present in the

product when biphenyl-4,4'-bisphosphonic acid was used alone, due to the closeness of the pillars. Therefore, mixed-component phases were created. Small groups, such as H, OH and Me, were used as spacer groups between the pillars in order to create the desired porous material (Figure 2.5).

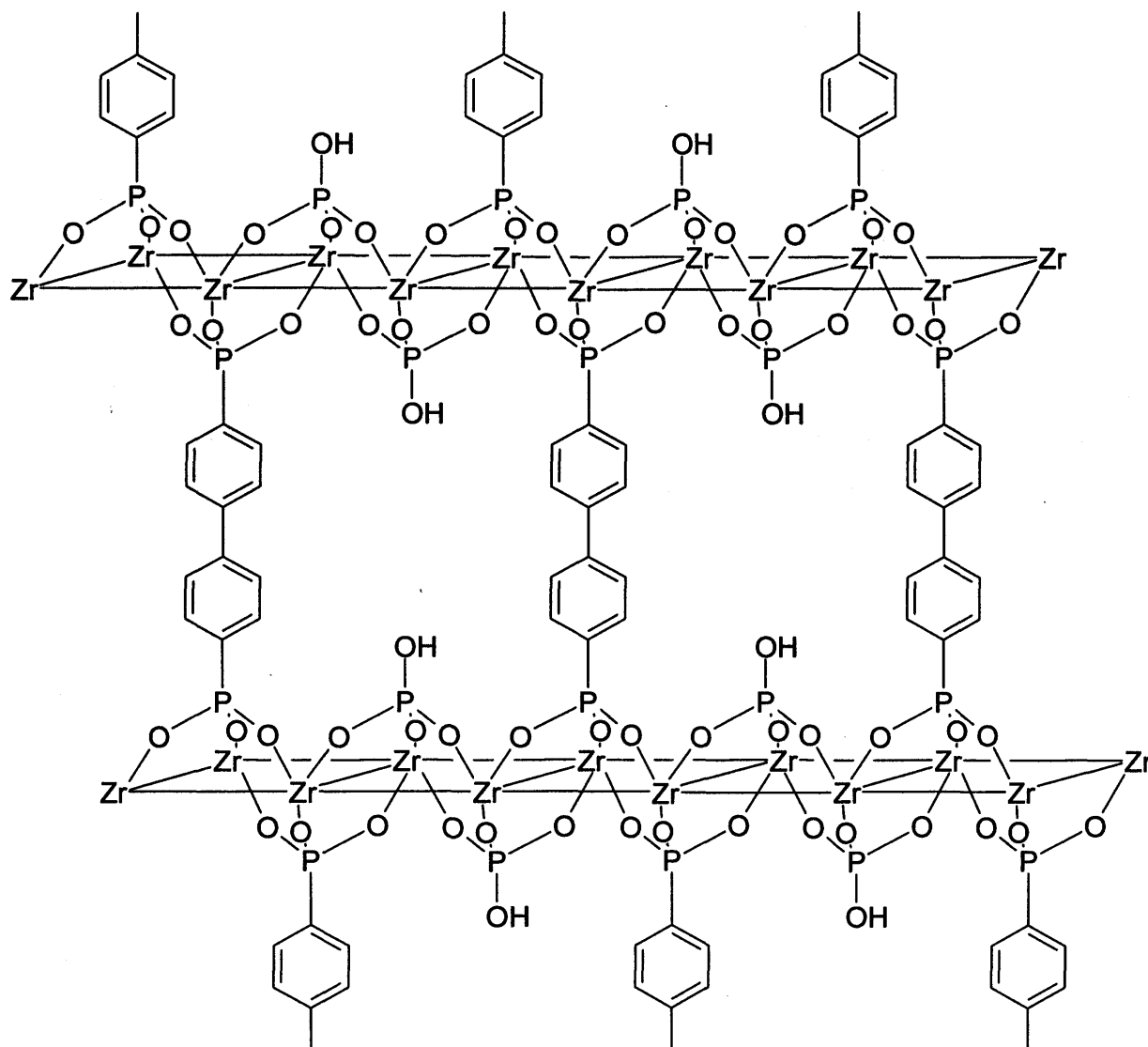


Figure 2.5. A pillared zirconium phosphonate

Another interesting example of pillared phosphonates from Alberti's group utilised flexible bisphosphonic acid derivatives of polyethers to cross-link zirconium sheets.^[28] In the absence of solvent, the non-rigid chains lie almost parallel to the zirconium plane and the layers are thus closely packed. The addition of solvent fills the inter-lamellar cavities and forces the chains to lie perpendicular to the plane, thus increasing the interlayer distance (Figure 2.6). Alberti proposed that the ability to create structures that undergo this 'accordian-like' motion could lead to the possibility of creating molecule-specific adsorbents.

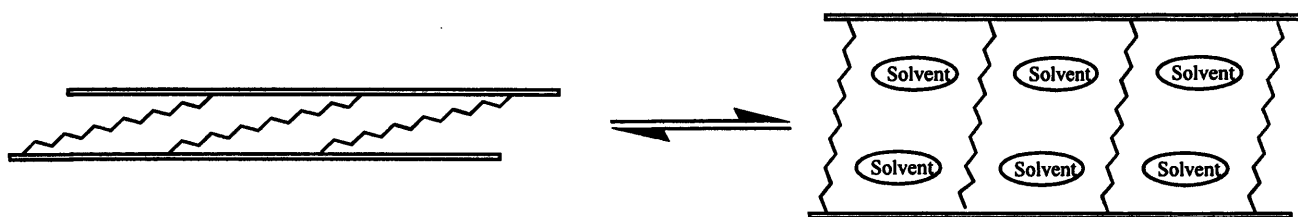


Figure 2.6. Alberti's 'accordion-like' zirconium phosphonate

2.3. Synthesis

2.3.1. Diethyl Phosphonates and Phosphonic Acids

Although there are numerous routes for the synthesis of diethyl phosphonates, perhaps the simplest and most well-documented route is the Michaelis-Arbuzov reaction.^[29] This involves the addition of an alkyl or aryl group to trialkyl phosphite via a phosphonium salt intermediate (Figure 2.7). Where R_1 is an aryl group, a catalyst, typically anhydrous $NiCl_2$, is required.

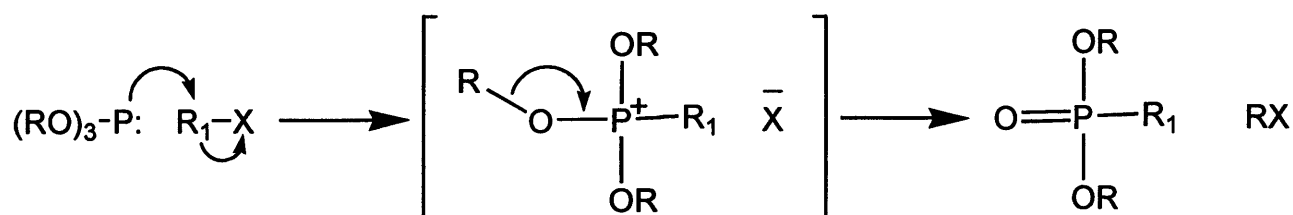


Figure 2.7. The mechanism of the Michaelis-Arbuzov reaction

The alkyl halide product, RX , can also react with the starting material and thus competes with R_1X for the $P(OR)_3$ substrate, forming a mixture of products. This competing, undesired reaction can be controlled by distilling RX out of the reaction mixture. If a suitable trialkyl phosphite, with small R groups is used, the boiling point of RX will be substantially lower than that of R_1X . Therefore, RX can be distilled out of solution as it is formed and cannot react to form side-products.

Recently, Gladysz utilised the Michaelis-Arbuzov reaction to prepare a number of alkyl diethyl phosphonates of the general formula $R_m(CH_2)_nP(O)(OEt)_2$ as precursors in the synthesis of fluoros primary phosphine ligands.^[30]

Conversion of the diethyl phosphonates to phosphonic acids simply requires reflux in concentrated aqueous HCl .

2.3.2 Amorphous and Crystalline Zirconium Phosphonates

Zirconium phosphonate is easily afforded by direct reaction of a Zr(IV) salt and a phosphonic acid in solution. The product rapidly precipitates from the solution as a white amorphous solid.^[31] The crystallinity of these compounds may be increased by drastically slowing the rate of precipitation. One method is to reflux the amorphous material in concentrated phosphoric acid.^[32] Here, the crystallinity is dependent upon the time of reflux and the concentration of acid.

Alternatively, the zirconium ions may be precomplexed with HF, to form ZrF_6^{2-} . This compound, stable at room temperature, is then slowly decomposed by increased temperature in the presence of phosphoric acid.^[33, 1] The rate of precipitation is controlled by the rate of HF removal, which when slow enough leads to highly crystalline materials.

2.3.3. Proposed Synthetic Route to Fluorous Zirconium Phosphonates

The proposed route for the synthesis of a series of zirconium phosphonates containing perfluoroalkyl chains, R_f , is shown in Figure 2.8. Amorphous and crystalline forms will be synthesised. The amorphous material is obtained in step 3 in the absence of acid. R_fX will contain a spacer group to separate the halide from the electronegative ‘ponytails’. Both alkyl (CH_2CH_2) and aryl (C_6H_4) spacers will be employed. A series of R_f groups will be used (F, CF_3 , C_4F_9 , C_6F_{13} , C_8F_{17}) to determine whether the fluorine content of the molecule affects the zirconium phosphonates structure and/or the efficiency of the support material to retain fluorinated catalysts for separation from organic products. Zirconium was selected for the metal phosphonates as the structures and properties of zirconium-based metal phosphonates are well documented in the literature. Platinum coordination compounds of the phosphonic acids will also be prepared and the spectroscopic data of the fluorous complexes will be compared to that of known non-fluorous analogues.

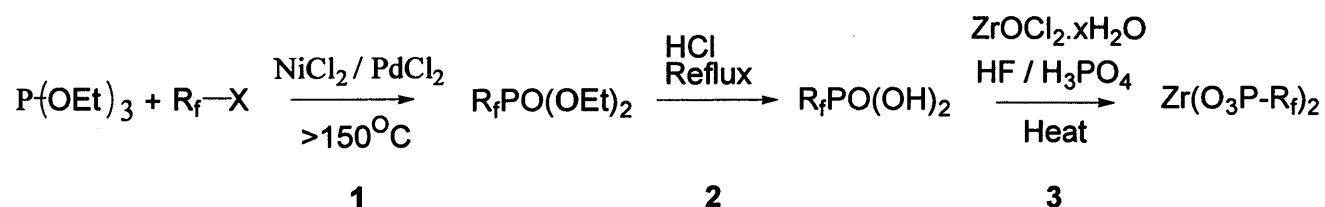


Figure 2.8. Proposed synthetic route to zirconium phosphonates bearing perfluoroalkyl chains

2.4. Synthesis of Fluorous Diethyl Phosphonates and Phosphonic Acids

The synthesis of non-fluorinated diethyl phosphonates is well documented in the literature^[2] and the preparation of compounds containing simple alkyl or aryl groups is suggested to be straightforward. Initial work attempted to repeat the synthesis of $\text{PhPO}(\text{OEt})_2$ ^[34] and its conversion to a crystalline zirconium phosphonate. This would allow the synthetic scheme to be practised and perfected such that any problems with the fluorine-containing analogues could then be attributed to the electronic properties of the fluorinated substituents. The most well cited work regarding $\text{PhPO}(\text{OEt})_2$ ^[34] utilises the Michaelis-Arbuzov^[29, 35] reaction and this was, therefore, the starting point of the project.

The Michaelis-Arbuzov reaction has been used in the synthesis of phosphonates for decades.^[29, 35] It utilises cheap, readily available starting materials and requires no specialist conditions or equipment. As shown in Figure 2.9, triethylphosphite is added dropwise to the appropriate alkyl or aryl halide at a temperature dependent on the R group. When this R group is aryl, a catalyst, such as dry NiCl_2 , is required.

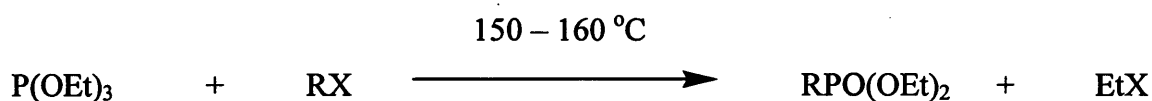


Figure 2.9. Formation of phosphonates *via* the Michaelis-Arbuzov reaction

The preparation of diethyl phenylphosphonate, $\text{PhPO}(\text{OEt})_2$, was attempted first, as the successful synthesis of an aryl containing phosphonate would indicate that alkyl containing analogues should also be attainable, as nucleophilic substitution on an alkyl chain is considerably more energetically favourable than on an aromatic ring.

The general experimental procedure was as follows: Bromobenzene was heated with a catalyst to $160\text{ }^\circ\text{C}$ with stirring, in a flame-dried three neck round bottomed flask. Triethylphosphite was then added dropwise, changing the clear colourless mixture to a deep maroon colour. The flask was fitted with distillation apparatus in order to collect ethylbromide (b.p $\sim 40^\circ\text{C}$), which is a by-product formed in the reaction. However, no bubbling, indicative of ethylbromide evolution, was observed upon addition of triethylphosphite and no liquid was collected in the distillation flask. The ^{31}P NMR spectrum of the crude mixture showed mainly unreacted ($\delta_{\text{P}} \sim 138$) and hydrolysed ($\delta_{\text{P}} \sim 7$) starting material and no trace of the desired product (lit^[36] $\delta_{\text{P}} = 19.4$ ppm).

Despite repeated attempts with numerous alterations to the procedure, including alternative catalysts, reaction times, temperatures and pressures, acceptable yields of product could not be attained using the Michaelis-Arbuzov reaction with aryl halides.

The reaction proved to be more successful with alkylhalide reagents. A series of fluorine-containing diethyl alkylphosphonates, 4-F₃C-C₂H₄PO(OEt)₂, 4-F₉C₄-C₂H₄PO(OEt)₂ and 4-F₁₃C₆-C₂H₄PO(OEt)₂, was prepared *via* the Michaelis-Arbuzov protocol and were purified by Kugelröhr distillation. However, similar problems to those associated with the bromobenzene reactions were identified. Mixtures of products were formed, resulting in low yields (9-57%) of the desired diethylphosphonate.

Hydrolysis products were detectable by ³¹P NMR spectroscopy at ~ -1 ppm and ~7 ppm. These signals can be assigned to diethyl phosphate^[36] (phosphoric acid diethyl ester), (EtO)₂PO(OH), and diethyl phosphite, (EtO)₂PO(H), respectively. A significant amount of EtPO(OEt)₂ was also present in all the crude reaction mixtures. This is formed by reaction of the triethyl phosphite with a catalytic amount of ethyl iodide/bromide (Figure 2.10). This indicates that the ethylhalide reacts with the starting material before it is distilled from the solution, or there is a gas-liquid reaction. The presence of these by-products, although sometimes detectable in significant amounts, does not fully account for the low yields attained (typically ~30%) as triethyl phosphite was used in excess.

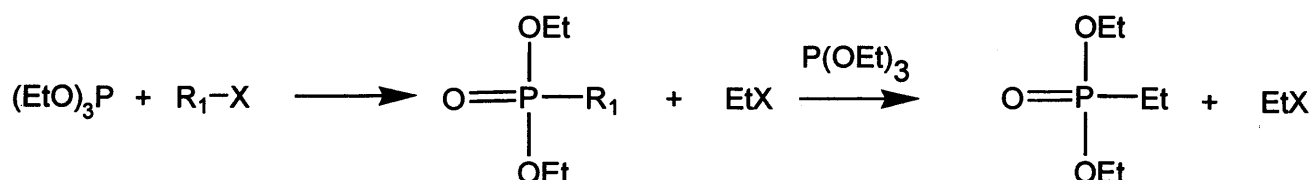


Figure 2.10. Formation of diethyl ethylphosphonate

One possible explanation for the low isolated yields is decomposition of the fluorinated alkylhalides, as shown in Figure 2.11. The resulting olefins would be more volatile than the reagents and may have boiled out of the reaction flask or been lost during distillation at reduced pressure.

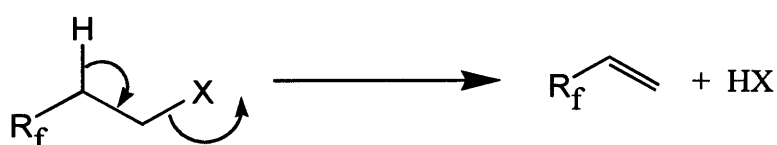


Figure 2.11. Decomposition of fluorinated alkyl halides

To investigate whether this mechanism could account for the low yields, the reaction was carried out with an alkylhalide containing three CH₂ spacer units. This separates the acidic proton on the carbon adjacent to the electron-withdrawing fluorine pendants from the halogen, and hence should prevent the formation of the alkene by-product. 1H, 1H, 2H, 2H, 3H, 3H-perfluoroundecyl iodide, F₁₇C₈-C₃H₆I, was refluxed in excess triethyl phosphite for seven hours. A yield of 62% of the desired product was attained after purification by distillation, which may indicate that reagents with longer spacer groups are more stable in the Michaelis-Arbuzov reaction. If large scale production of perfluoroalkyl diethyl phosphonates was required, the use of perfluoroalkyl halides with propylene organic “spacer groups” would allow more acceptable yields. The additional methylene group also provides the phosphorus with extra insulation from the electron-withdrawing effect of the perfluoroalkyl chain.

Although alkylphosphonates could be prepared, an alternative to the Michaelis-Arbuzov route was required for the preparation of PhPO(OEt)₂ and fluorine containing analogues. Simeon's group^[37] had formed the target compound at room temperature, in the absence of catalyst, by reaction of NaOEt, PhPCl₂ and I₂ in distilled MeOH. The suggested mechanism for the reaction is shown in Figure 2.12.

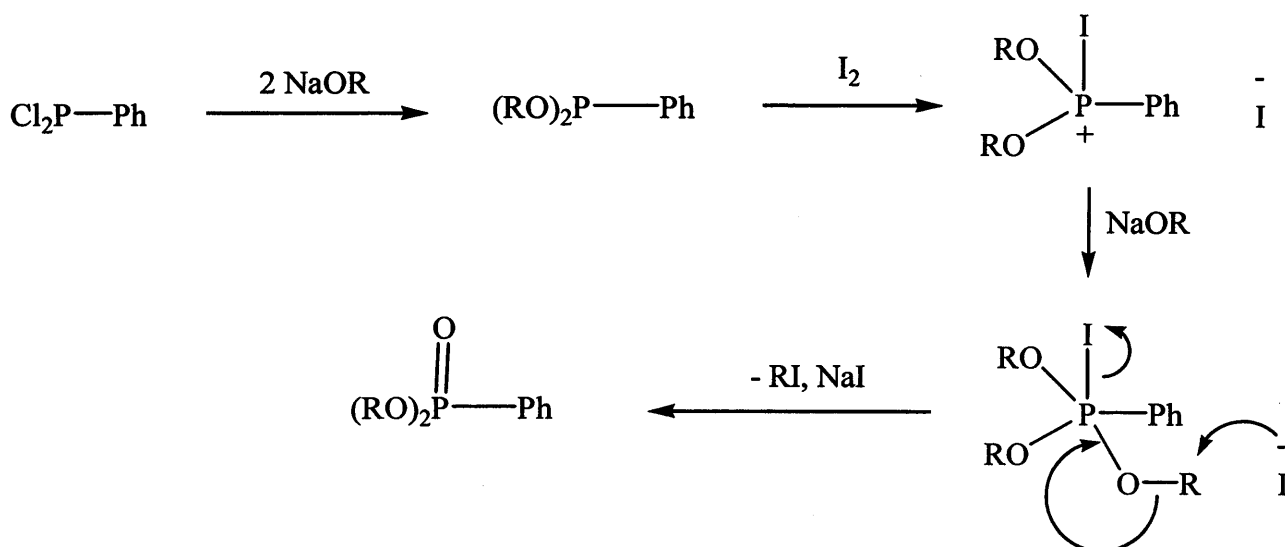


Figure 2.12. Mechanism for the formation of phenyl phosphonates from dichloro phenylphosphine

The procedure was followed and PhPO(OEt)₂ was successfully synthesised and purified. However, to reach the desired fluorinated zirconium phosphonates via this route requires the synthesis of perfluoroalkylated dichlorophosphine intermediates. This introduces two more steps into the overall scheme, which would greatly increase cost and decrease the overall yield of the fluorine α-zirconium phosphonate.

An alternative route, utilised by Beletskaya *et al.*,^[38] involves the reaction of diethyl phosphonate with an aryl iodide or bromide in the presence of a palladium catalyst and ligand. Aryl halides containing both electron-donating and -withdrawing groups had been used successfully in Beletskaya's protocol, suggesting that aryl iodides/bromides containing fluororous moieties could be used successfully in the preparation of diethyl arylphosphonates. A general scheme for the reaction is shown in Figure 2.13.

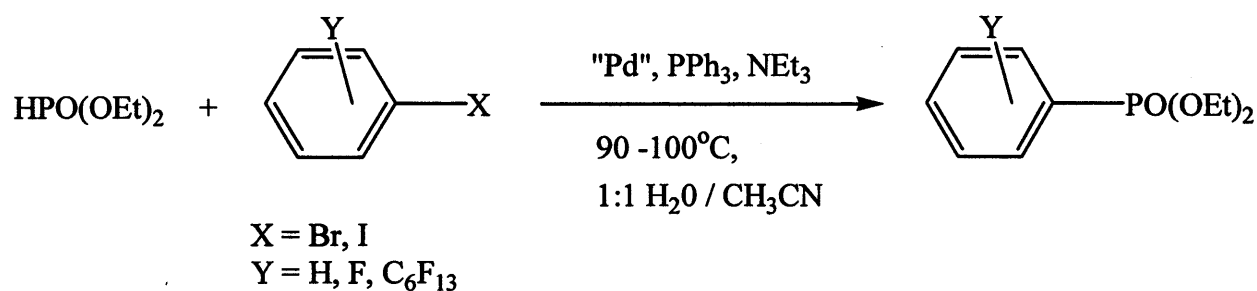


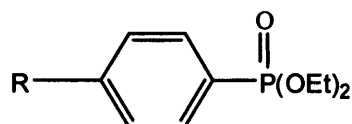
Figure 2.13. Pd-catalysed formation of arylphosphonates from diethyl phosphite

The protocol was used to successfully prepare the three aryl diethyl phosphonates in Figure 2.13 (Y = H, F, C₆F₁₃) in low yields (20-30%). In an attempt to increase the yields attained by the Beletskaya protocol, prolonged reaction times were investigated. For non-fluorinated bromobenzene, raising the reaction time from 5 to 24 hours only gave a 9 % increase in yield and even raising it by a factor of over 14 only resulted in a moderate improvement, as can be seen in Table 2.14. Thus a reaction time of several days would be required in order to gain a substantial enhancement in yield. Increasing the reaction temperature from 90 to 150 °C was also tried but no trace of product was detectable by ³¹P NMR spectroscopy in the crude reaction media. However, it is unclear whether this was solely a result of changing the temperature, as DMSO was used in place of the H₂O/CH₃CN mixture.

R	ArX	Time, h	% Yield
Ph	PhBr	5	24
Ph	PhBr	24	33
Ph	PhBr	72	50
<i>p</i> -F-C ₆ H ₄	<i>p</i> -F-C ₆ H ₄ -Br	5	26
<i>p</i> -F ₁₃ C ₆ -C ₆ H ₄	<i>p</i> -F ₁₃ C ₆ -C ₆ H ₄ -Br	3	19

Table 2.14. Yields of aryl phosphonates achieved *via* Beletskaya protocol

A similar protocol, from Hirao *et al.*,^[39] applied the same reagents and conditions as Beletskaya *et al.*, except a Pd⁰ catalyst, [Pd(PPh₃)₄], was used. This method was used to successfully synthesise compounds **1a** to **1d** in Figure 2.15 in high yield and on a larger scale. The phosphonates were easily purified by Kugelröhr distillation. The synthesis of an alkyl diethyl phosphonate was attempted using this method but no product was detectable by ³¹P NMR spectroscopy. Neither increasing the reaction time, from 5 to 24 hours, or the temperature from 90 to 130 °C gave any improvement. Hence, the Michaelis-Arbuzov reaction is still the favoured route for preparing the fluorinated alkyl series.

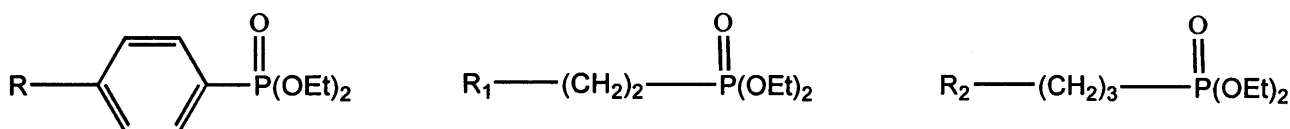


Compound **1a**: R = H, **1b**: R = F, **1c**: R = CF₃, **1d**: R = C₆F₁₃

Figure 2.15. Aryl phosphonates prepared *via* Hirao's approach

The next step of the scheme is to convert the diethyl phosphonates into their acids, by replacing the ethoxy groups with hydroxyl groups. The most direct literature method^[40] is simply to reflux in HCl for several hours and then recrystallise the product from water. Reported yields are virtually quantitative.

The best yields of fluorinated phosphonic acids were attained by reflux in concentrated HCl for ~24 hours, reduction of the solvent in *vacuo* followed by filtration and a chloroform/hexane wash. The pure products are thus isolated as white solids. The library of phosphonates and phosphonic acids synthesised is shown below, in Figure 2.16.



Compound **1a**: R = H, **1b**: R = F, **1c**: R = CF₃, **1d**: R = C₆F₁₃

Compound **1e**: R₁ = CF₃ **1f**: R₁ = C₄F₉, **1g**: R₁ = C₆F₁₃; **1h**: R₂ = C₈F₁₇



Compound **2a**: R = H, **2b**: R = F, **2c**: R = CF₃, **2d**: R = C₆F₁₃

Compound **2e**: R₁ = C₄F₉, **2f**: R = C₆F₁₃

Figure 2.16. Phosphonates and phosphonic acids successfully synthesised

2.5. Characterisation of Fluorous Diethyl Phosphonates and Phosphonic Acids

The diethyl phosphonates and phosphonic acids were characterised by elemental analysis, mass spectrometry and proton, phosphorus and fluorine (where appropriate) NMR spectroscopies. Mass spectrometry studies using the electrospray ionisation method showed the protonated molecular ion for all compounds, and observed elemental analysis values were within 0.2% of calculated values. The ^{31}P NMR chemical shifts observed for the fluorine containing diethyl phosphonates were within the range of 16.3 to 18.4 ppm for aryl spacer group compounds and 28.3 and 30.1 ppm for alkyl spacer group compounds. These values are typical for P^{V} compounds of these types.^[41, 42] The ^{31}P NMR signal is shifted downfield slightly as the amount of fluorine atoms is increased (Table 2.17), as expected, due to deshielding of the phosphorus atom by the electron-withdrawing effect of the fluorine atoms. This is not true for the alkyl series when the C_6F_{13} chain is increased to C_8F_{17} because in this case the length of the spacer group also increases, providing the phosphorus with additional insulation from the fluorine's electronegativity.

Compound	^{31}P NMR Shift in CDCl_3 (ppm)
$\text{C}_6\text{H}_5\text{-PO(OEt)}_2$	19.0
$4\text{-F-C}_6\text{H}_4\text{-PO(OEt)}_2$	18.4
$4\text{-F}_3\text{C-C}_6\text{H}_4\text{-PO(OEt)}_2$	16.4
$4\text{-F}_{13}\text{C}_6\text{-C}_6\text{H}_4\text{-PO(OEt)}_2$	16.3
$\text{MePO(OEt)}_2^{\text{a}}$	27.7
$\text{F}_3\text{C-C}_2\text{H}_4\text{-PO(OEt)}_2$	27.9
$\text{F}_9\text{C}_4\text{-C}_2\text{H}_4\text{-PO(OEt)}_2$	28.4
$\text{F}_{13}\text{C}_6\text{-C}_2\text{H}_4\text{-PO(OEt)}_2$	28.4
$\text{F}_{17}\text{C}_8\text{-C}_3\text{H}_6\text{-PO(OEt)}_2$	30.1

Table 2.17. ^{31}P NMR Shifts for the prepared phosphonates

^a literature value in CDCl_3 ^[42]

The ^{31}P NMR data for the phosphonic acids shows a similar pattern to that of the diethyl phosphonates (Table 2.18). Observed ^{31}P NMR resonances were between 15.2 and 17.1 ppm for the aryl series and 27.6 and 27.8 ppm for the alkyl series. Once again, these values are within the expected range typical for P^{V} compounds of this type.^[42]

Compound	^{31}P NMR Shift in $\text{C}_3\text{D}_6\text{O}$ (ppm)
$\text{C}_6\text{H}_5\text{-PO(OH)}_2$	19.5
$4\text{-F-C}_6\text{H}_4\text{-PO(OH)}_2$	17.1
$4\text{-F}_3\text{C-C}_6\text{H}_4\text{-PO(OH)}_2$	15.4
$4\text{-F}_{13}\text{C}_6\text{-C}_6\text{H}_4\text{-PO(OH)}_2$	15.2
$\text{MePO(OH)}_2^{\text{a}}$	27.8
$\text{F}_9\text{C}_4\text{-C}_2\text{H}_4\text{-PO(OH)}_2$	27.6
$\text{F}_{13}\text{C}_6\text{-C}_2\text{H}_4\text{-PO(OH)}_2$	27.8

Table 2.18. ^{31}P NMR Shifts for the prepared phosphonic acids

^a literature value in D_2O ^[42]

The ^{19}F NMR spectra showed the expected number of fluorine resonances for each of the fluorine containing compounds.

The ^1H NMR spectra of the diethyl phosphonates showed the expected resonances for the ethoxy chains and either the aromatic or aliphatic protons of the spacer groups. The protons of the CH_2 groups in the ethoxy chains are diastereotopic and, therefore, lead to complex multiplets in the ^1H NMR spectra. Figure 2.19 shows a section of the observed proton NMR spectra for $4\text{-F-C}_6\text{H}_4\text{-PO(OEt)}_2$.

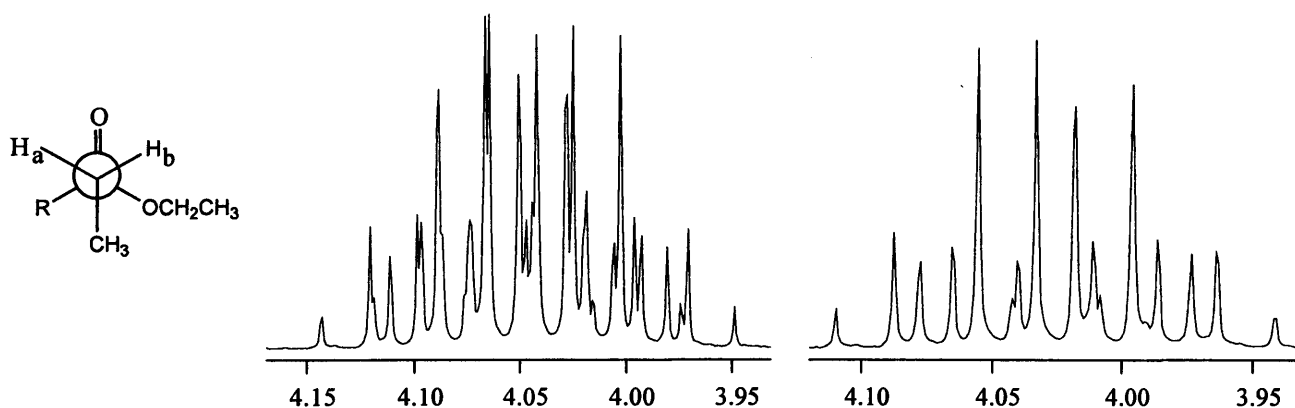


Figure 2.19. ^1H NMR (left) and $^1\text{H} \{^{31}\text{P}\}$ NMR spectra (right) of $4\text{-F-C}_6\text{H}_4\text{-PO(OEt)}_2$

As H_a and H_b are inequivalent, they couple to one another as well as to the CH_3 protons and the phosphorus atom. Thus, a pair of 2H, AB doublet of quartets (dq) appears at approximately 4 ppm for all of the diethyl phosphonate series. In the $^1\text{H} \{^{31}\text{P}\}$ NMR spectrum the signal is reduced to a pair of dq's. The protons of the two terminal methyl groups are equivalent and result in the expected 6H triplet, at approximately 1.3 ppm.

The ^1H NMR spectra of the phosphonic acids were also as expected, containing only the resonances for the aryl/alkyl spacer groups and the broad singlet of the hydroxyl groups.

2.6. Amorphous Fluorous Zirconium Phosphonates

2.6.1. Synthesis

Amorphous zirconium phosphonates are easily prepared by addition of a solution of phosphonic acid to a solution of a soluble Zr(IV) salt, such as $[\text{ZrOCl}_2]$.^[43, 31] A number of fluorinated zirconium phosphonates (FZrP) were synthesised by addition of a THF solution of the phosphonic acid to aqueous $[\text{ZrOCl}_2]$ solutions. The products immediately precipitated from solution as white powders.

The zirconium phosphonates are completely insoluble and, therefore, fewer characterisation techniques are available for the study of these compounds than for their precursors. The products have been analysed by scanning electron microscopy (SEM), EDAX, solid state IR spectroscopy and solid state X-ray powder diffraction. The SEM images showed a broad dispersal of particle sizes, ranging from 5 to 100 μm . EDAX data showed the presence of carbon, hydrogen, oxygen, phosphorus, and fluorine atoms in the expected ratios. IR spectra showed absorptions corresponding to P-O and P=O and the absence of phosphonic acid groups. X-ray spectra of the materials prepared in the presence of HF revealed the zirconium phosphonate to be only partially crystalline, with large amorphous regions.

2.6.2. Separation Studies

The solid-phase extraction potential of these fluorous materials was investigated. Curran^[44] demonstrated the separation of fluorous and non-fluorous compounds by chromatography using a column of reverse phase silica gel (FRPSG). A comparison between the amorphous FZrP and FRPSG modified with $-\text{C}_6\text{F}_{13}$ perfluoroalkyl chains was made. A sample of a fluorous compound ($1\text{-F}_{13}\text{C}_6\text{-C}_6\text{H}_4\text{-4-C}_6\text{F}_{13}$, 0.025 g) was loaded into a Pasteur pipette filled 3 cm deep with either $[\text{Zr}(\text{O}_3\text{PR}_f)_2]$ or fluorous reverse phase silica gel. 5 cm^3 of eluent was passed down the column into a pre-weighed flask. The mass of sample recovered by each solvent is shown in Table 2.20 below. Where low masses were recovered, NMR studies were used to confirm the presence/absence of the fluorous compound.

	Zr(O ₃ P-C ₆ H ₄ -4-CF ₃) ₂	Zr(O ₃ P-C ₂ H ₄ -C ₄ F ₉) ₂	Zr(O ₃ P-C ₆ H ₄ -4-C ₆ F ₁₃) ₂	FRPSG
MeOH	0.002 g ^b	0.000 g ^a	0.000 g ^a	0.001 g ^b
MeCN	0.001 g ^b	>0.001 g ^b	0.000 g ^a	0.001 g ^b
DCM	0.015 g	0.001 g ^b	0.000 g ^a	0.002 g ^b
Ethyl acetate	0.025 g	0.025 g	0.025 g	0.025 g
Et ₂ O	0.025 g	0.025 g	0.025 g	0.025 g

Table 2.20. Mass of fluororous compound eluted from columns of different stationary phases using various solvents

^a No sample detectable by ¹H or ¹⁹F NMR spectroscopy

^b Sample detectable by ¹H NMR and ¹⁹F NMR spectroscopy

The data in Table 2.20 show that the FZrP has potential to replace fluororous silica as the stationary phase in a chromatography column. Zirconium phosphonates have the advantage that they do not contain surface hydroxyl groups, which may react/coordinate to a compound and bind it to the column. However, FZrP does not solvate well with solvents and does not form a gel, like that typically formed with silica. Thus, solvents travel down the column slowly. In the case of the FZrP with perfluorohexyl ponytails, significant pressure from a hand pump was required to force the solvent down the column. The perfluorobutyl derivative appeared to solvate better, and polar solvents travelled down the column at a reasonable rate, and retained the fluororous compound effectively. The perfluoromethyl derivative column, being the least fluororous of the materials, allowed for good solvent flow but did not retain the fluororous compound as successfully. Thus the [Zr(O₃P-C₂H₄-C₄F₉)₂] material appears to be the most suited to act as an alternative to FRPSG.

2.6.3. Swellability Investigation

Crystalline metal phosphonates are known to increase in volume, or 'swell', when in a suspension due to filling of the inter-lamellar spaces between the planes.^[2] If a solvent with sufficient miscibility is used, the solvent is able to penetrate in between the planes, forcing them apart, increasing both the inter-lamellar distance and the overall volume of the material. This property was of great interest to this work as 'swelling' of the material would provide a vast surface area on which to support/immobilise a catalyst. Also by switching solvents it would be possible to close inter-lamellar cavities, trapping the supported catalyst and preventing loss to organic products.

Thus, a series of simple tests was conducted on the amorphous fluororous zirconium phosphonates to determine if these materials also swelled. A measuring cylinder was loaded 1cm deep with fluororous zirconium phosphonate, 3 cm³ of solvent added, the solid was stirred thoroughly

and then allowed to settle completely. The volume of the suspended solid was measured for a number of solvents of varying polarity and fluorine content. The results are shown in Table 2.21.

Solvent Material	PFH	BTF	Et ₂ O	THF	DCM
[Zr(O ₃ PPh) ₂]	20%	20%	20%	30%	10%
[Zr(O ₃ P-C ₂ H ₄ -C ₆ F ₁₃) ₂]	30%	10%	20%	30%	10%
[Zr(O ₃ P-C ₆ H ₄ -4-C ₆ F ₁₃) ₂]	20%	30%	30%	30%	10%

Table 2.21. Percent increase in volume of amorphous zirconium phosphonates in various solvents

Polymers such Merryfield resins (1% polystyrene divinylbenzene) are known to increase in volume by upto 5 times when ‘swelled’ by an appropriate solvent and newer polymers may swell to over 10 times their dry volume.^[45] Amorphous fluorous zirconium phosphonate solids were shown to swell to some degree but the increase in volume was insubstantial. Thus crystalline forms of the support materials were sought, as their ordered structures should allow more effective filling of inter-lamellar spaces and, therefore, offer greater swelling.

2.7. Crystalline Fluorous Zirconium Phosphonates

The formation of crystalline support material was first attempted in standard glass apparatus. An aqueous solution of [ZrOCl₂] and HF was stirred at room temperature for 10 minutes in a 3 neck round bottom flask. This formed the Zr precomplexing agent ZrF₆²⁻, which is stable at room temperature. A solution of the appropriate phosphonic acid in THF was added to the flask and the mixture was then heated to 60 °C. A N₂ flow was introduced to carry any HF evolved into a saturated aq. NaOH trap. The rate of formation of product is dependent upon the concentration of HF used. Increasing the concentration of HF decreases the rate of formation, thereby increasing the crystallinity of the product. The zirconium phosphonate products were analysed by scanning electron microscopy (SEM), energy dispersion of atoms by X-rays (EDAX), and powder X-ray diffraction.

SEM of the support material showed that the method of preparation had little effect on the particle-size distribution. The particles ranged from 5 to 100 μm (Figure 2.22).

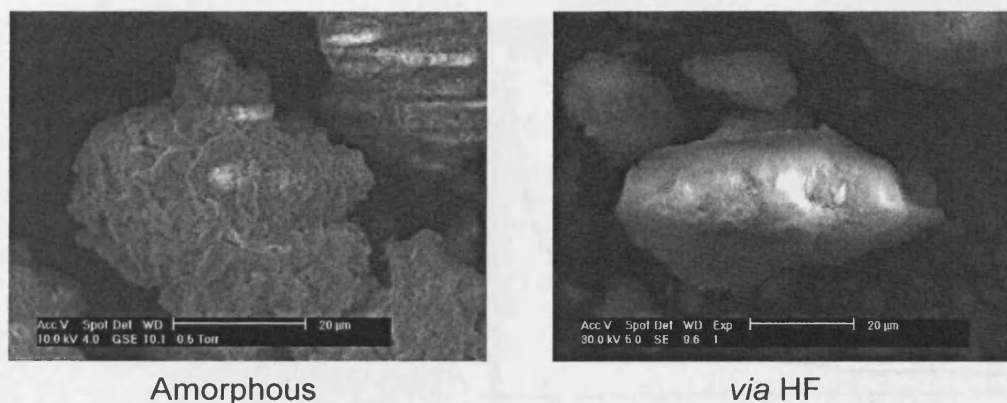


Figure 2.22. Scanning electron microscopy images of zirconium phosphonates

Data obtained from EDAX studies showed that significant amounts of quartz were present in the HF derived samples. This was attributed to the formation of silicates through reaction of HF with the glass walls of the reaction vessel. These insoluble impurities are impossible to remove by standard purification techniques, such as chromatography, recrystallisation or distillation, as the zirconium phosphonates are also insoluble, high-melting point solids. In order to avoid the presence of these contaminants it is necessary to utilise non-glass apparatus.

The X-ray diffraction data of the zirconium phosphonates was the most informative. Firstly, it illustrated the importance of the HF in the reaction. The diffraction spectra of the amorphous material showed no sharp peaks, indicating a lack of crystalline phases. In contrast, the material formed with HF showed definite patterns of peaks resulting from the presence of a crystalline structure. The diffraction pattern library identified $[\text{ZrF}_6\text{H}_2]$ as the major constituent in all these samples. Another common pattern of peaks was discernable in the X-ray diffraction data of all the zirconium phosphonate samples from the HF method. In the case of $[\text{Zr}(\text{O}_3\text{PPh})_2]$, the X-ray diffraction library matched the pattern to that of the crystal form of the product (Figure 2.23). In the absence of HF (Figure 2.23, inset), no crystalline peaks were present. When HF was used, although peaks corresponding to crystalline $[\text{Zr}(\text{O}_3\text{PPh})_2]$ were observed, significant quartz impurities and unreacted H_2ZrF_6 were also present.

Similar peak patterns to that of crystalline $[\text{Zr}(\text{O}_3\text{PPh})_2]$ were found in the other fluorine-containing zirconium phosphonate samples. This is taken as an indication of the formation of crystalline phases of the FZrP.

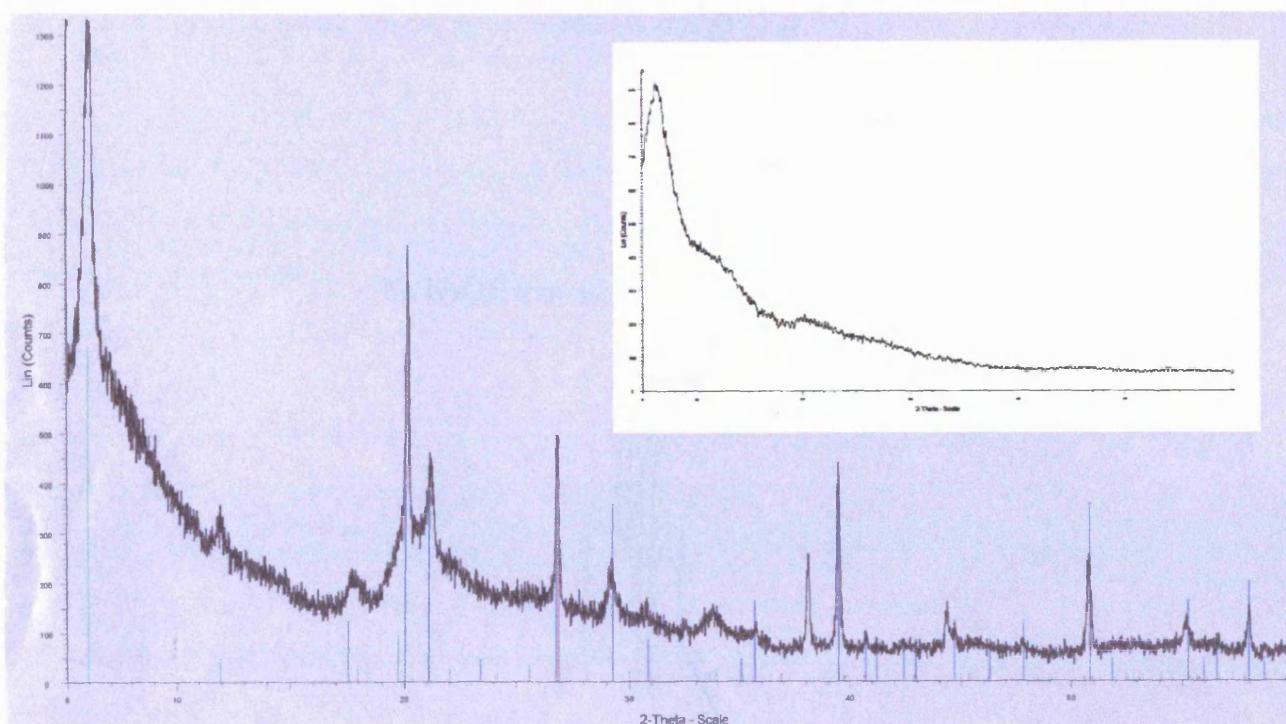


Figure 2.23. Powder X-ray diffraction patterns of amorphous (inset) and attempted crystalline phenyl zirconium phosphonate

Red lines = crystalline SiO_2 ; Green = crystalline $[\text{Zr}(\text{O}_3\text{PPh})_2]$; Blue = crystalline H_2ZrF_6

It was, therefore, clear that the addition of HF to the zirconium starting material did indeed result in the formation of a precomplexing agent, ZrF_6^{2-} . The slow decomposition of this compound allows gradual release of Zr(IV) cations, which then react with the phosphonic acid to form crystalline FZrP. However, even products acquired from reactions of 5 days of heating at $60\text{ }^\circ\text{C}$ contained the H_2ZrF_6 intermediate.

The reaction required adjustment in two ways; firstly, an alternative reaction vessel was required to avoid production of silicate impurities from the glass flask. Secondly, the reaction temperature needed to be increased to ensure all of the precomplexing agent decomposed.

Apparatus as shown in Figure 2.24 was assembled. A plastic conical flask was equipped with a stirrer bar and charged with an aqueous solution of $[\text{ZrOCl}_2]$ and HF. The mixture was stirred gently and heated to $60\text{ }^\circ\text{C}$. The phosphonic acid was added dropwise as a THF solution from a plastic syringe attached to a length of Teflon tubing. A small clamp on the tubing allowed the rate of addition to be controlled. The flow was slowed to allow addition to take place over several hours (6-8 hrs). The temperature was slowly increased ($\sim 5\text{ }^\circ\text{C}$ per hour) to $90\text{ }^\circ\text{C}$ and the mixture was left stirring overnight. The product was centrifuged and the white solid filtered, washed with H_2O (5 cm^3) and THF (5 cm^3) and then dried under vacuum.

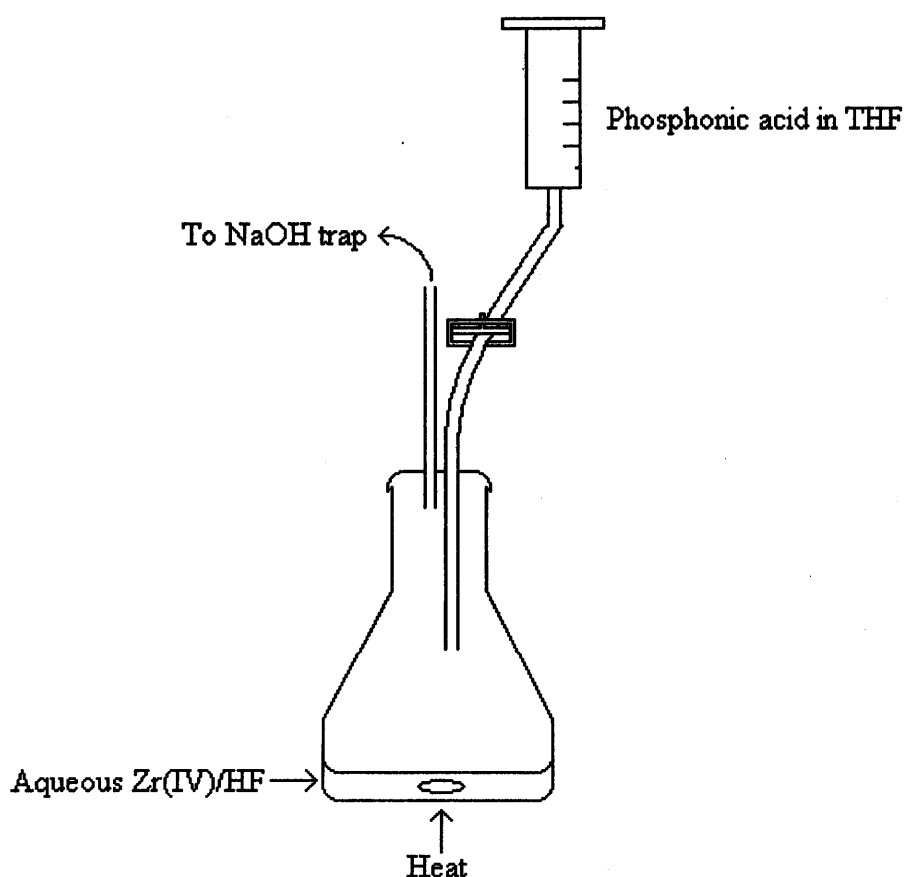


Figure 2.24. Plastic apparatus used for preparation of crystalline zirconium phosphonates

The zirconium phosphonates were studied by IR spectroscopy. All of the amorphous materials showed no broad peaks in the $3000\text{--}4000\text{ cm}^{-1}$ range, indicating the absence of free hydroxyl groups. The observed IR spectrum of phenyl zirconium phosphonate was comparable to the literature spectrum for both the amorphous and HF derived compounds. Although the ‘crystalline’ materials showed peaks at the appropriate wavenumber for ZrF_6^{2-} , these peaks were also found in the spectra of the amorphous materials. Thus, the IR data is inconclusive with respect to identifying unreacted precomplexing agent. The X-ray powder diffraction patterns of the materials formed in plastic apparatus contained no SiO_2 but a substantial amount of unreacted H_2ZrF_6 was observed. Increasing the reaction time to several days had little or no effect on the amount of unreacted precomplexing agent found in the final material.

In an attempt to avoid this contamination, the preparation of the phosphonate was carried out in the absence of HF, with the two reactants in highly diluted solutions. A 0.0005 M THF solution of phosphonic acid was added dropwise to a stirred 0.0005 M aqueous solution of zirconyl chloride in order to try to slow the formation of the metal phosphonate, allowing crystalline material to develop. However, X-ray analysis showed the material was purely amorphous.

Complex	$^2J_{\text{PtP}}$ (Hz)	$^1J_{\text{PtP}}$ (Hz)
[Pt{OP(O)(Ph)O}(PPh ₃) ₂]	127	3872
[Pt{OP(O)(C ₆ H ₄ -4-F)O}(PPh ₃) ₂]	125	3875
[Pt{OP(O)(C ₆ H ₄ -4-CF ₃)O}(PPh ₃) ₂]	122	3879
[Pt{OP(O)(C ₆ H ₄ -4-C ₆ F ₁₃)O}(PPh ₃) ₂]	117	3881
[Pt{OP(O)(C ₂ H ₄ -C ₄ F ₉)O}(PPh ₃) ₂]	114	3865
[Pt{OP(O)(C ₂ H ₄ -C ₆ F ₁₃)O}(PPh ₃) ₂]	118	3862

Table 2.26. Coupling constants for platinum phosphonic acid complexes

Table 2.27 shows the coupling constants for a number of known bis-triphenyl phosphine platinum complexes. The literature and observed J_{PtP} values for the non-fluorous phenyl phosphonic acid complex are identical, which suggests a direct comparison between the literature and observed values is valid. The coupling constants obtained for the fluorous phosphonic acid platinum complexes are in good agreement with those reported for these literature complexes.

Complex	$^2J_{\text{PtP}}$ (Hz)	$^1J_{\text{PtP}}$ (Hz)
[Pt{OP(O)(OPh)O}(PPh ₃) ₂]	147	3936
[Pt{OP(O)(Ph)O}(PPh ₃) ₂]	127	3872
[Pt{OP(O)(Me)O}(PPh ₃) ₂]	122	3848
[FcPO ₃ Pt(PPh ₃) ₂] ^a	125	3850
[FcCH ₂ PO ₃ Pt(PPh ₃) ₂] ^a	116	3895
[FcC ₂ H ₄ PO ₃ Pt(PPh ₃) ₂] ^a	113	3845

Table 2.27. Literature coupling constant values for platinum phosphonic acid complexes

NMR spectra recorded in CDCl₃, Fc = Ferrocene

^a literature value^[48]

Further support that the fluorous zirconium phosphonates have the same structure as their non-fluorous equivalents came from X-ray crystallography data. Suitable crystals of the metal complexes were grown using DCM/petroleum ether and their X-ray diffraction patterns showed their bond lengths, in particular Pt-O and Pt-P, and angles to be virtually identical. Figure 2.28 illustrates the close resemblance of [Pt{OP(O)(Ph)O}(PPh₃)₂] to [Pt{OP(O)(C₆H₄-4-CF₃)O}(PPh₃)₂].

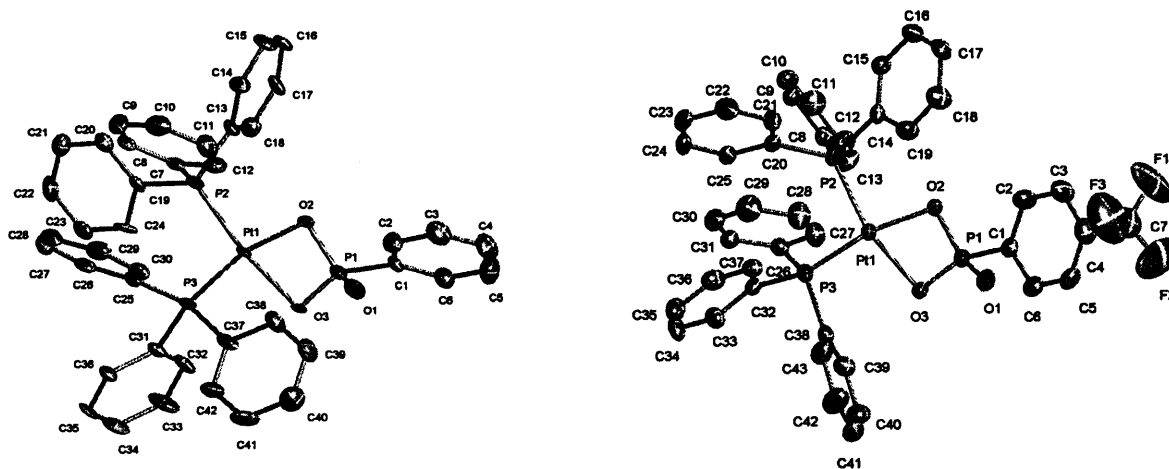


Figure 2.28. Crystal structures of platinum complexes of non-fluorous (left) and fluorinated (right) aryl phosphonic acids

Selected bond lengths for the platinum complexes are shown in Table 2.29. The Pt-O and Pt-P bonds for these metal complexes compare favourably to many literature analogues.^[46, 47]

Complex	Pt(1)-O(2) (Å)	Pt(1)-O(3) (Å)	Pt(1)-P(2) (Å)	Pt(1)-P(3) (Å)
[Pt{OP(O)(Ph)O}(PPh ₃) ₂]	2.061(7)	2.072(7)	2.223(3)	2.239(2)
[Pt{OP(O)(C ₆ H ₄ -4-F)O}(PPh ₃) ₂]	2.064(3)	2.075(2)	2.219(10)	2.239(11)
[Pt{OP(O)(C ₆ H ₄ -4-CF ₃)O}(PPh ₃) ₂]	2.079(3)	2.083(3)	2.223(10)	2.236(10)
[Pt{OP(O)(C ₂ H ₄ -C ₆ F ₁₃)O}(PPh ₃) ₂]	2.077(3)	2.085(2)	2.217(10)	2.243(10)
[Pt{OP(O)(Ph)O}(PMePh ₂) ₂] ^a	2.070(4)	2.102(4)	2.222(1)	2.231(1)
[PtO ₃ PCH ₂ Fc(PPh ₃) ₂] ^b	2.075(3)	2.081(3)	2.225(10)	2.238(10)

Table 2.29. Selected bond lengths for a series of platinum phosphonic acid complexes

^a taken from reference [46].

^b taken from reference [47].

Typical average platinum-oxygen bonds lengths are between 1.996, for aryloxy systems (Pt-O-C_{aryl}), and 2.143 Å, for terminal nitrate systems (NO₃).^[48] The values observed for the phosphonic acid metal complexes fall comfortably within this range. The observed Pt-P bond distances of ~2.22 and ~2.24 Å are slightly shorter than typical average values of between 2.246 and 2.385 Å.^[48] The Pt-O and Pt-P bonds for these metal complexes compare favourably to literature analogues.^[48]

Complex	O(2)-Pt(1)-O(3) (°)	O(2)-P(1)-O(3) (°)
[Pt{OP(O)(Ph)O}(PPh ₃) ₂]	71.40(2)	100.30(3)
[Pt{OP(O)(C ₆ H ₄ -4-F)O}(PPh ₃) ₂]	71.17(10)	100.61(14)
[Pt{OP(O)(C ₆ H ₄ -4-CF ₃)O}(PPh ₃) ₂]	71.61(10)	102.15(15)
[Pt{OP(O)(C ₂ H ₄ -C ₆ F ₁₃)O}(PPh ₃) ₂]	71.80(2)	101.60(3)

Table 2.30. Selected bond angles for a series of platinum phosphonic acid complexes

Table 2.30 contains selected bond angles for the platinum complexes. The data shows that the addition of fluorine-containing groups to the phosphonic acids does not have a significant effect on the bite angle of the chelate.

These data confirms that the fluorous phosphonic acids bond to platinum in the same manner as their non-fluorous analogues. It is reasonable to assume that the structures of the fluorous zirconium phosphonates will not be dissimilar to that of phenyl zirconium phosphonate, a previously synthesised and characterised compound.^[23]

2.9. Conclusions for Chapter 2

A series of novel fluorine containing zirconium phosphonates has been successfully prepared in moderate to good yields *via* their corresponding diethyl phosphonates and phosphonic acids. These precursors have been characterised by ¹H, ¹³C, ¹⁹F and ³¹P NMR spectroscopies, mass spectrometry and elemental analysis. The insoluble zirconium phosphonates have been studied by EDAX, solid state x-ray crystallography and SEM. The solids' ability to increase in volume, or swell, was tested and an assessment was made of their potential to act as a solid phase extraction medium analogous to silica gel.

A series of platinum coordination complexes was also prepared from the phosphonic acids, which act as dianionic bidentate ligands. These complexes were also fully characterised by ¹H, ¹³C, ¹⁹F and ³¹P NMR spectroscopies, mass spectroscopy, elemental analysis and single crystal X-ray diffraction.

The potential of the zirconium phosphonates to act as media for the separation and recovery of catalysts will be assessed for three different systems in the following chapters.

References for Chapter 2

- [1] G. Alberti, U. Constantino, S. Allulli, N. Tomassini, *J. Inorg. Nucl. Chem.*, **1978**, *40*, 1113.
- [2] A. Clearfield, *Progress in Inorganic Chemistry*, **1998**, *47*, 371.
- [3] A. Clearfield, *Chem. Rev.*, **1988**, *88*, 125.
- [4] A. Gordon, O. S. Betler, M. Greenbaum, L. Marantz, T. Gral, M. H. Maxwell, *Trans. Am. Soc. Artif. Int. Organs.*, **1971**, 253.
- [5] G. Centi, F. Trifiro, J. R. Ebner, F. V. M., *Chem. Rev.*, **1988**, *88*, 55.
- [6] N. Krause, A. Hoffmann-Roeder, *Synthesis*, **2001**, 171.
- [7] S. Bischoff, A. Weigt, H. Meißner, B. Lücke, *J. Mol. Cat. A.*, **1996**, 339.
- [8] G. Guillena, C. A. Kruithof, M. A. Casado, M. R. Egmond, G. van Koten, *J. Organomet. Chem.*, **2003**, *668*, 3.
- [9] A. Dokoutchaev, V. V. Krishnan, M. E. Thompson, M. Balasubramanian, *J. Mol. Struct.*, **1998**, *470*, 191.
- [10] M. G. Partridge, R. P. Tooze, J. R. H. Wilson, A. C. Sullivan, *International Patent WO 2004007073 A1*, **2004**.
- [11] K. Mikuni, N. Tanaka, H. Nagaoka, *European Patent EP0778313*, **1997**.
- [12] J. P. Lemmon, R. J. Wroczynski, *U.S. Patent US6395862*, **2002**.
- [13] W. Aiping, D. R. Talhma, *Langmuir*, **2000**, *16*, 7449.
- [14] H. E. Katz, M. L. Schilling, *Chem. Mater.*, **1993**, *5*, 1162.
- [15] L. J. Kepley, D. D. Sackett, C. M. Bell, T. E. Mallouk, *Thin Solid Films*, **1992**, *208*, 132.
- [16] J. R. Owen, S. C. Lloyd-Williams, G. Lagos, P. C. Spurdens, B. C. Steele, 'Lithium Nonaqueous Battery Electrochemistry', Pennington, **1980**.
- [17] Z. Liu, K. Hashimoto, A. Fujishima, *Nature*, **1990**, *347*, 658.
- [18] H. Tachibana, T. Nakamura, M. Matsumoto, H. Komizu, E. Manda, H. Niino, A. Yabe, Y. Kawabata, *J. Am. Chem. Soc.*, **1989**, *111*, 3080.
- [19] H. E. Katz, W. L. Wilson, G. Scheller, *J. Am. Chem. Soc.*, **1994**, *116*, 6636.
- [20] K. Ichimura, Y. Hayashi, H. Akiyama, N. Ishizuki, *Langmuir*, **1993**, *9*, 3298.
- [21] A. Clearfield, G. D. Smith, *Inorg. Chem.*, **1969**, *8*, 431.
- [22] M. B. Dines, P. M. DiGiacomo, *Inorg. Chem.*, **1981**, *20*, 92.
- [23] D. M. Poojary, H.-L. Hu, F. L. Campbell III, A. Clearfield, *Acta. Crystallgr. Sect. B*, **1993**, *49*, 996.
- [24] N. J. Clayden, *J. Chem. Soc., Dalton Trans.*, **1987**, 1877.
- [25] D. M. Poojary, B. Shpeizer, A. Clearfield, *J. Chem. Soc., Dalton Trans.*, **1995**, 111.
- [26] G. Alberti, U. Costantino, G. Perego, *J. Solid State Chem.*, **1986**, *63*, 455.

- [27] A. Clearfield, J. D. Wang, Y. Tian, E. Stein, C. Bhardwaj, *J. Solid State Chem.*, **1995**, *117*, 275.
- [28] G. Alberti, E. Brunet, C. Dionigi, O. Juanes, M. J. de la Mata, J. C. Rodríguez-Ubis, R. Vivani, *Angew. Chem. Int. Ed.*, **1999**, *38*, 3351.
- [29] A. E. Arbuzov, *J. Russ. Phys. Chem. Soc.*, **1906**, *38*, 687.
- [30] C. Emnet, J. A. Gladysz, *Synthesis*, **2005**, *6*, 1012
- [31] G. Alberti, *Acc. Chem. Res.*, **1978**, *11*, 163.
- [32] A. Clearfield, J. A. Stynes, *J. Inorg. Nucl. Chem.*, **1964**, *26*, 117.
- [33] G. Alberti, U. Constantino, R. Giulietti, *J. Inorg. Nucl. Chem.*, **1978**, *42*, 1062.
- [34] P. Tavs, *Chem. Ber.*, **1970**, *103*, 2428.
- [35] A. Michaelis, R. Kaehne, *Chem. Ber.*, **1898**, *31*, 1048.
- [36] J. M. Kuiper, R. Hulst, J. B. F. N. Engberts, *Synthesis*, **2003**, *5*, 695.
- [37] F. Siméon, P.-A. Jaffrés, D. Villemin, *Tetrahedron*, **1998**, 10111.
- [38] I. P. Beletskaya, M. M. Kabachnik, M. D. Solntseva, *Russ. J. Org. Chem.*, **1999**, *35*, 71.
- [39] T. Hirao, T. Masunaga, N. Yamada, Y. Oshiro, T. Agawa, *Bull. Chem. Soc. Jpn.*, **1982**, *55*, 909.
- [40] C. Yuan, H. Feng, *Synthesis*, **1990**, 140.
- [41] K. Blazewska, P. Paneth, T. Gajda, *J. Org. Chem.*, **2007**, *72*, 878.
- [42] J. C. Tebby, 'Handbook of Phosphorus-31 Nuclear Magnetic Resonance Data', CRC, Boca Raton, **1991**, 311.
- [43] G. Alberti and E. Torracca, *J. Inorg. Nucl. Chem.*, 1968, **30**, 1093.
- [44] D. P. Curran, S. Hadida, M. He, *J. Org. Chem.*, 1997, **62**, 6714.
- [45] P. G. Sasikumar, K. S. Kumar, V. N. Rajasekharan Pillai, *J. Appl. Polym. Sci.*, **2004**, *92*, 288.
- [46] R. D. W. Kemmitt, S. Mason, J. Fawcett, D. R. Russell, *J. Chem. Soc. Dalton Trans.*, **1992**, 851.
- [47] W. Henderson, S. R. Alley, *Inorg. Chim. Acta*, **2001**, *322*, 106.
- [48] A. G. Orpen, L. Brammer, F. H. Allen, O. Kennard, D. G. Watson, R. Taylor, *J. Chem. Soc., Dalton Trans.*, **1989**, S1.

3. Olefin Cyclopropanation Catalysed by Fluorous Rhodium Carboxylates

3.1. Dirhodium(II) Tetracarboxylate Catalysts

Dinuclear rhodium complexes (Rh_2L_4) with carboxylate ligands are efficient, versatile catalysts for a number of transformations, including the silylformylation of alkynes,^[1] oxidation of allylic and benzylic alcohols,^[2] C-H,^[3, 4] N-H^[5] and Si-H^[6] insertions and the transfer of carbenes from diazo compounds to a range of substrates.^[7] The dimer molecule is cylindrical with four bridging carboxylate ligands encircling the rhodium-rhodium bond (Figure 3.1). The catalyst has two active sites that are located on opposite ends of the cylinder.

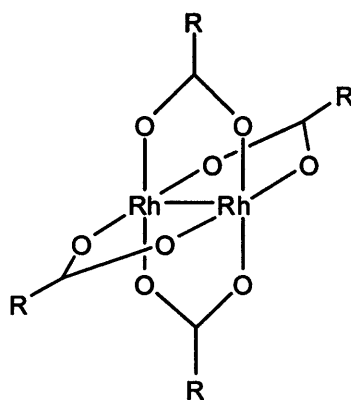


Figure 3.1. The structure of a dirhodium(II) tetracarboxylate

Researchers have adopted a variety of approaches for the recycling of such rhodium catalysts, including fluorous methodologies^[8-11] and covalently binding the catalyst to an ionic liquid^[12] or to a solid support.^[13, 14] A number of relevant examples of these recovery techniques are discussed in section 3.1.2. along with their associated strengths and weaknesses. Many investigations have used the same rhodium-catalysed reaction as a model reaction for recycling studies.

3.1.1. Rhodium-Catalysed Cyclopropanation with Diazo Compounds

The rhodium-catalysed decomposition of ethyl diazoacetate with alkenes, in particular styrene, to form cyclopropanation products (Figure 3.2) is widely documented in the literature^[15-20] and is a commonly used model reaction in catalytic studies.

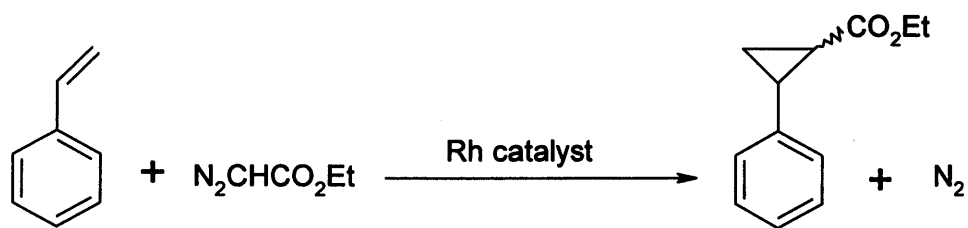


Figure 3.2. Rhodium-catalysed cyclopropanation of styrene with ethyl diazoacetate

Suggested mechanisms^[17, 21, 22] for the reaction involve initial coordination of the carbene to rhodium *via* loss of dinitrogen. One such mechanism is illustrated in Figure 3.3. This is followed by reaction of either the carbene, to yield the desired product as a mixture of *cis* and *trans* enantiomers, or another molecule of ethyl diazoacetate to yield diethyl maleate or diethyl fumarate. In order to reduce this unwanted side reaction, large excesses (typically ten molar equivalents) of alkene are used.

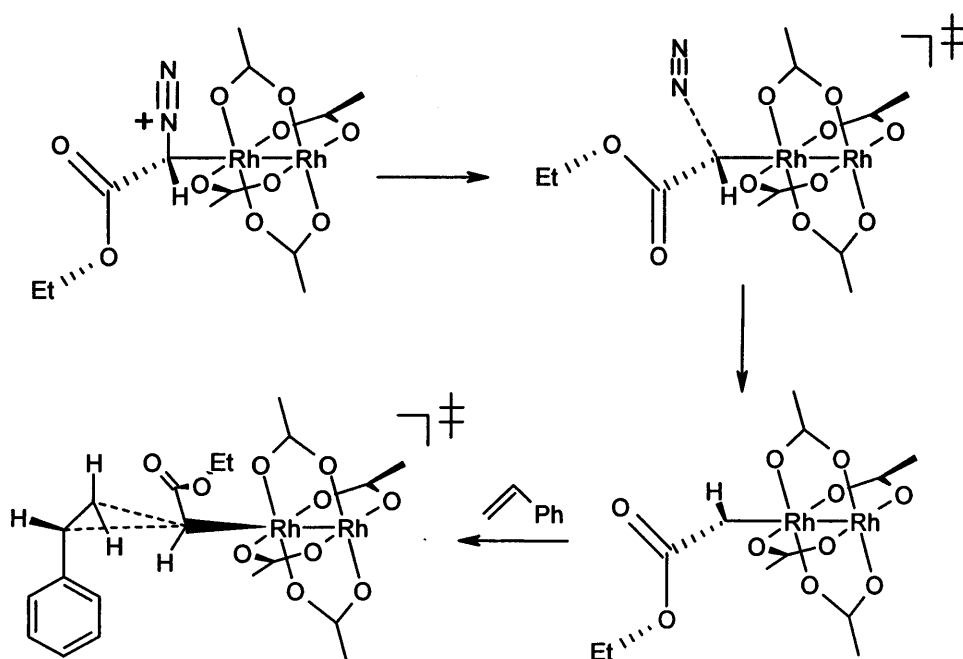


Figure 3.3. Mechanism of the cyclopropanation of styrene with ethyl diazoacetate catalysed by dirhodium(II) tetraacetate

3.1.2. Recovery Techniques for Dirhodium Carboxylate Catalysts

Early studies on these rhodium dimers as catalysts did not consider catalyst recycling and recovery, rather the metal was routinely separated from the organic products by filtration through celite or silica, and disposed of. More recently, fluoruous separation techniques, such as liquid-liquid separations, have been applied in order to recover and recycle rhodium carboxylate catalysts. It is

first necessary to modify the catalyst in order to render it preferentially soluble in a perfluorinated solvent. Addition of perfluorocarboxylate ligands to a rhodium dimer was originally achieved by Hall's group,^[23] in relation to possible antitumor properties, and later by Drago^[24] in a study on synergic bonding effects. The synthesis of these fluoros catalysts is achieved *via* a simple ligand exchange reaction of dirhodium(II) tetraacetate with a perfluorocarboxylic acid, which are common commercially available reagents with chain lengths up to 17 carbon atoms long.

Work on the recycling of dirhodium tetra-perfluorocarboxylate catalysts was conducted by Endres and Maas,^[8] who evaluated the efficiency of a post-reaction fluoros extraction for catalyst separation. The group studied the cyclopropanation of alkenes, including styrene, with methyl diazoacetate. Reactions were carried out in DCM at 20 °C with a 10-fold excess of alkene. At the end of the reaction the solvent and most of the alkene were removed by distillation and perfluoro-1,3-methylcyclohexane added to the resulting residue. The catalyst was extracted into the fluoros solvent and a liquid-liquid phase separation carried out. The fluoros solvent was removed and the catalyst could be recycled up to four times with no loss in activity or selectivity. Two fluoros catalysts of the general formula $[\text{Rh}_2(\text{OOCR})_4]$ were used ($\text{R} = \text{C}_6\text{H}_4\text{-4-C}_6\text{F}_{13}$ and C_7F_{15}). The catalyst containing an aryl spacer group between the perfluoroalkyl chain and the carboxylate carbon was found to give higher yields of cyclopropane products for most of the olefin substrates tested. This was suggested to be due to reduction of the electron-withdrawing effect of the fluorine on the metal centres due to insulation by the aromatic ring. Where $\text{R} = \text{C}_7\text{F}_{15}$, as the catalyst is highly electrophilic, it is more easily deactivated by any donor molecules which are present in the mixture.

Biffis *et al.*^[9-11] also investigated fluoros recovery techniques in their substantial work on alcohol silylation. The group utilised both fluoros biphasic and solid-supported catalysis to recover dirhodium species containing a series of perfluorocarboxylate ligands with varying lengths of perfluoroalkyl chains.

Biffis' group first evaluated fluoros biphasic catalysis with the aforementioned fluoros rhodium dimers.^[11] Three catalysts were prepared, with perfluoroalkylated chains of 7, 9 and 13 carbons atoms (Figure 3.4).

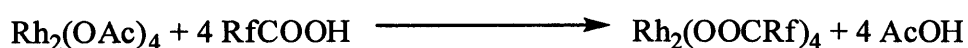


Figure 3.4. Ligand exchange of dirhodium acetate with perfluorocarboxylic acid.

These catalysts were used in the silylation of alcohols with triethyl silane in a biphasic solvent system of DCM and an immiscible fluoruous solvent (perfluorodecalin, perfluoromethylcyclohexane or Fluorinert® FC-77). The two catalysts with shorter perfluoroalkyl chains were both found to leach into the DCM, regardless of which fluoruous solvent was used in the biphasic system. The perfluorotetradecanoate catalyst, the most heavily fluorinated of the three complexes, did not dissolve in the DCM and remained restricted to the fluoruous phase. Thus, efficient separation of this catalyst was achieved and it was recycled for three subsequent runs. However, yields fell from 68 to 45% during these three runs and yields in the first run were lower than those reported for the same reaction in a homogeneous system. The latter observation was not unexpected as mass transport is a known limitation of biphasic catalysis. Although no leaching to the organic product phase was detected, evidence of catalyst decomposition was reported which accounted for the decrease in yield over successive recycles.

Despite some basic problems with the biphasic system, the dirhodium(II) tetra-perfluorocarboxylates did show potential as catalysts for alcohol silylation. Biffis continued work in the area in an attempt to optimise yields and improve the sustainability of the system. Homogeneous reactions were carried out and the fluoruous catalyst was separated by extraction from the DCM solution into a fluoruous solvent. However, yields and activities were only slightly higher than those for the biphasic system and still considerably lower than those found for the benchmark catalyst, dirhodium(II) tetra-perfluorobutyrate, under comparable reaction conditions. The group attributed the reduced activity to aggregation of the highly fluoruous catalysts in the organic phase. As the catalysts were soluble in the substrate olefins following substrate coordination, solventless silylation reactions were also conducted in an attempt to avoid the problem of catalyst deactivation through aggregation. The catalyst was extracted from the product mixture into a fluoruous solvent, which was separated and added to a second batch of substrate, which extracted the catalyst back, thus allowing the reaction to start again. This recovery technique was tested, and although the catalyst could be recycled with no loss in activity, 40% of the catalyst was lost due to inefficient catalyst extraction by the substrate olefin from the fluoruous phase. The product yield also decreased by 21% after a single run.^[11]

Next, the group investigated the application of solid supports for catalyst separation and recovery in a heterogeneous system, utilising a novel approach termed “bonded fluoruous phase catalysis” (Figure 3.5).^[9] A perfluoroalkylated analogue of silica was prepared and used to support the dirhodium(II) tetra-perfluorocarboxylates. The group describe the catalyst as embedded in the fluoruous surface layer of the support material. As the perfluoroalkyl chains surrounding the catalyst repel any immiscible organic solvent that comes into contact with the surface, the embedded catalyst is effectively shielded from the solvent and immobilised on the support. Surface-

immobilised catalysts based on perfluorooctyl carboxylic acid were shown to be highly active in the silylation of 1-octanol under solventless conditions at room temperature. The conversions were up to five times greater than those for the unsupported analogues and less than 3% of the total rhodium was found to be lost to the product phase after the first run. Activities and yields could be improved by increasing the reaction temperature to 50 °C and the supported catalyst was recycled by filtration with no loss in turnover number (TON) or frequency (TOF). By further increasing the temperature to 80 °C activities 50 times those reported for the homogeneous system were observed and the catalyst could still be recycled with no detriment to TON or TOF. However, only one catalyst recycle was reported.

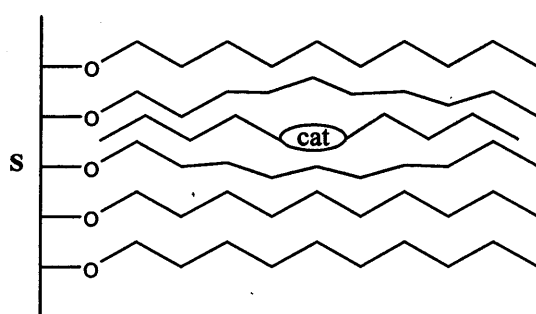


Figure 3.5. The “Bonded fluororous phase catalysis” approach. A catalyst bearing perfluoroalkyl chains is embedded in the surface layer of a solid support S, also bearing fluororous chains.

The cyclopropanation of styrene with ethyl diazoacetate was studied in an ionic liquid medium by Forbes.^[12] The group exchanged the acetate ligands of a dirhodium(II) tetraacetate for carboxylic acids tethered to an imidazolium functionality (Figure 3.6), with a view to heterogenise a homogeneous catalyst for separation and reuse. The imidazolium group acted as the cation in an ionic liquid (IL) with a BF_4^- counter ion. As ILs are immiscible with most organic solvents, separation of products from the catalyst could, in theory, be achieved by liquid extraction at the end of the reaction. The standard rhodium acetate catalyst, $[\text{Rh}_2(\text{OAc})_4]$, was first tested in an ionic liquid medium and was found to give quantitative conversions to the desired product. However, the IL-grafted metal complex was shown to have reduced activity in the cyclopropanation reaction compared to the acetate precursor. Attempts to recycle the catalyst, or analysis of the product for metal content, were not reported.

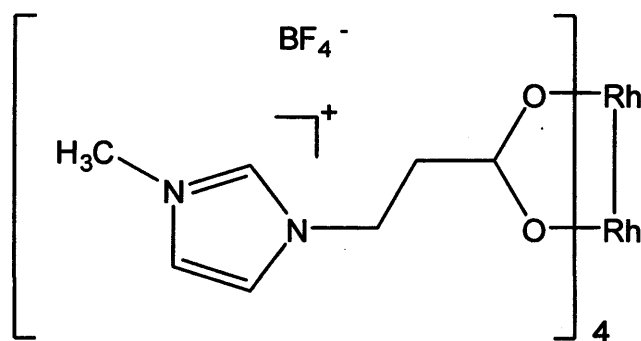
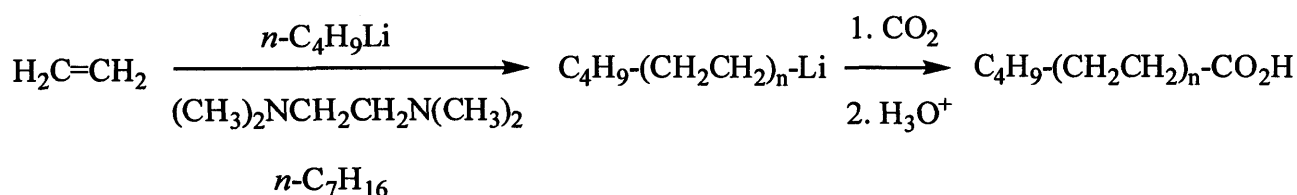


Figure 3.6. Rhodium Complex Covalently Bound to an Organic Salt

A number of supported methods have been applied to rhodium carboxylate catalysts. The activity of a rhodium catalyst covalently bound to the surface of functionalised carbon nanotubes was evaluated for hydroformylation and hydrogenation reactions by Serp *et al.*^[25] Carboxylate groups were grafted onto the surface of the nanotubes, allowing complexation to a rhodium centre. The surface immobilised catalyst was active in the hydroformylation of hex-1-ene to heptanal, giving good to moderate yields of the desired product, depending on the catalyst loading and support type used.

The heterogenised catalyst was also tested in the hydrogenation of *trans*-cinnamaldehyde. Although conversions and activities were found to be considerably lower than those for the commercial palladium on charcoal catalyst, the rhodium catalyst showed far superior selectivity, giving 100% desired product. The nanotubes were recoverable by filtration but no report of recycle or rhodium leaching to the product phase was given.

Bergbreiter^[13] used the cyclopropanation of styrene with ethyl diazoacetate as a model reaction to study the efficacy of polymer-bound rhodium carboxylate catalysts. The catalyst was covalently bound to a polyethylene support *via* terminal carboxylate functionalities (Scheme 3.7). The polymer, which was soluble in toluene at 100 °C and, therefore, could act as a homogeneous catalyst, gave activities and selectivities similar to those for transition metal acetates but was quantitatively recoverable by filtration at 25 °C.

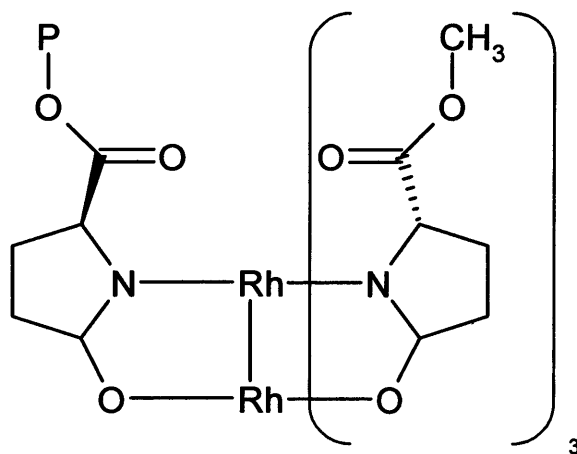


Scheme 3.7. Synthesis of oligomers containing terminal carboxylic acid functionalities

A number of different types of olefin were tested, including styrene, nonene, cyclooctene and 2,5-dimethyl-2,4-hexadiene. Catalytic reactions were carried out in dry toluene under a

dinitrogen atmosphere. A toluene solution of ethyl diazoacetate was added dropwise over 7-8 hours to a mixture of dissolved catalyst (2 mol %) and alkene in toluene at 110 °C. A 10-fold excess of alkene was used to reduce the formation of the maleate/fumarate side products. Although the reaction of styrene with the diazo compound was high yielding (96%), recovery and recycling of the polymer-bound catalyst was not reported for this olefin. The only data concerning catalyst recycling was for the 2,5-dimethyl-2,4-hexadiene substrate, where the catalyst was reused 10 times with no significant observable decrease in activity. However yields for this substrate were considerably lower than those for styrene, between 54 and 59%, and lower than literature yields for the same reaction with a homogeneous rhodium carboxylate catalyst (81%).^[26] The group reported very low levels of rhodium leaching into the organic product (<1% of metal lost in a single run).

More recently, Doyle's group reported the use of polymer-bound chiral dirhodium tetracarboxamidates as catalysts for the cyclopropanation of styrene (Figure 3.8).^[14] The compounds had activities and selectivities comparable or superior to those of homogeneous counterparts, did not require the use of dried/degassed solvents or inert atmospheres and could be separated from the products by simple filtration. However, the catalysts were reused a maximum of two times and in most cases were not recycled at all.



P = polystyrene-PEG or Merrifield resin

Figure 3.8. Polymer-bound chiral dirhodium carboxamidates

3.2. Results and Discussion

We sought to evaluate the fluororous zirconium phosphonates as supports for a dirhodium tetrafluorocarboxylate catalyst used in a model cyclopropanation reaction as an initial model system to establish the veracity and efficacy of the novel materials as catalytic supports.

We envisaged two methods for the recovery and recycling of the catalyst: Firstly, a heterogeneous-type system, where the supported catalyst is inside the vessel during the reaction and then separated post-reaction by filtration, akin to Biffis' "bonded fluororous phase catalysis". Secondly, a homogeneous system where the catalyst is separated from the product by passing through a flash column of the support material and then recovered using a solvent switch.

A number of alternative support materials, including fluororous and non-fluororous zirconium phosphonates, polystyrene beads and silica gels were tested at the same time for direct comparison purposes. The supports are displayed in Figure 3.9.

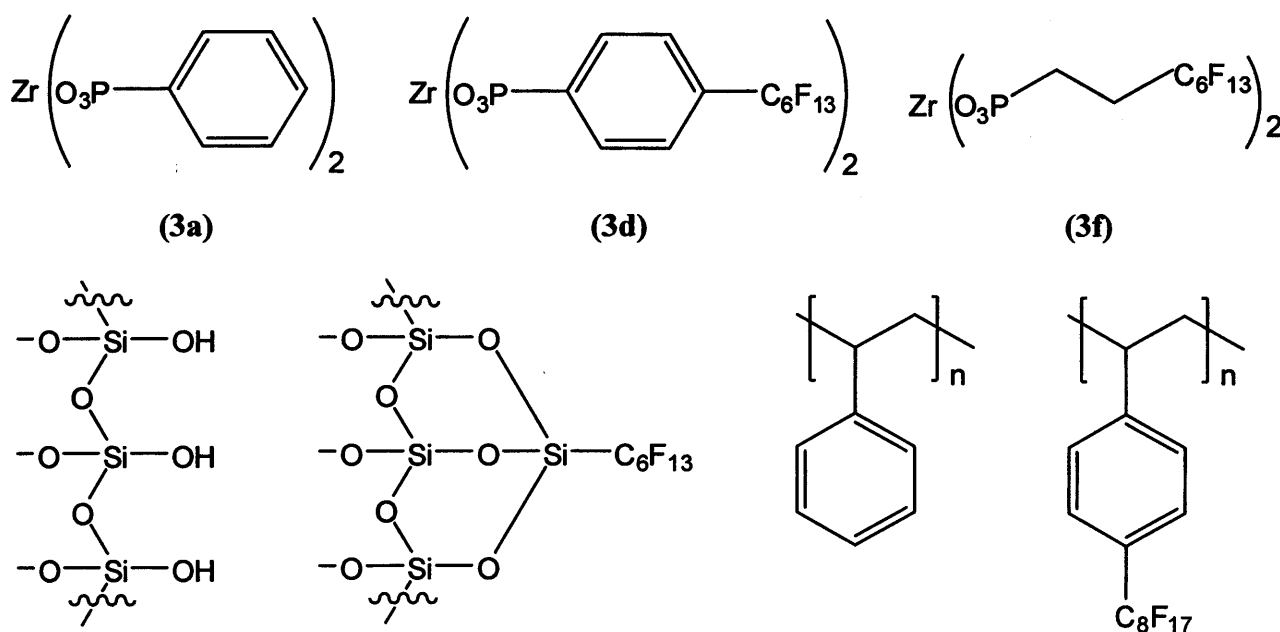


Figure 3.9. Non-fluororous and fluororous zirconium phosphonates (top), silicas (bottom left) and polystyrenes (bottom right) solid supports

The non-fluororous zirconium phosphonate used was phenyl zirconium phosphonate (3a). The fluororous zirconium phosphonates tested possessed perfluorohexyl chains with an aryl (3d) or alkyl (3f) spacer group. The silica used had a particle size of 40 μm , with the fluororous analogue bearing perfluorohexyl chains. The polystyrene beads tested were prepared in our laboratory and were 10% crosslinked with divinylbenzene. The perfluorinated polystyrene possessed perfluorooctyl chains in the *para* position. The beads were separated using a Nickel-Electro sieving outfit and those selected for use in this work were between 10 and 40 mesh.

To obtain benchmark values for comparison with supported results it was first necessary to determine optimal reaction conditions, such as reaction time and temperature, substrate stoichiometry and solvent, in a homogeneous system. Much of the literature work on styrene cyclopropanation uses DCM as solvent, with reaction times ranging from 8 to 24 hours at either

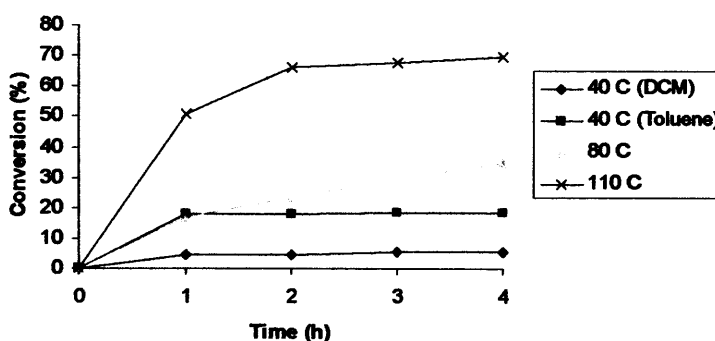
room temperature or reflux. In Bergbreiter's work with polymer-bound dirhodium(II) tetracarboxylates,^[13] the group carried out the reactions in toluene at reflux. However, these high temperatures were used to ensure dissolution of the soluble polymer support and were not necessarily needed to achieve acceptable reaction conversions and product yields. Also, some literature work with dirhodium(II) tetra-perfluorocarboxylates seems to suggest an inert atmosphere is required.^[9, 11, 13] To ensure a sufficient understanding of the reaction before conducting recycling experiments a series of homogeneous cyclopropanation reactions was carried out. The catalyst used was dirhodium(II) tetra-perfluorobutyrate, $[\text{Rh}_2(\text{pfb})_4]$. This perfluorocarboxylate rhodium dimer complex is commercially available and should have an affinity for the surface of a solid support modified with perfluoroalkyl chains. All initial experiments were carried out at room temperature under a N_2 atmosphere in dry solvents. A solution of ethyl diazoacetate was added dropwise to a solution of 10 equivalents of substrate and 0.02 mol % of catalyst and the mixture was stirred for 4 hours. Conversions and selectivities were determined using gas chromatography by integration against an internal standard (biphenyl). The values calculated by this method are accurate to within $\pm 2\%$ error. Selectivities could also be verified by integration of the benzylic protons in the NMR spectra of the products.

Initial testing was conducted in dry DCM as this was the literature precedent. However, conversions to the desired cyclopropane product were very poor at room temperature and even at 40 °C only 5% conversion was observed. The *cis/trans* selectivities, at 55% major isomer, were also lower than those reported in the literature when styrene was used as the substrate (65% major isomer). Results were improved when the reaction solvent was switched to dry toluene, as used in Bergbreiter's polymer work.^[13] At 40 °C conversions and selectivities were raised to 20% and 63% respectively after 4 hours. By further increasing the temperature to 80 °C and 110 °C conversions could be raised to 35 and 69%. These results are summarised in Table 3.10 and Graph 3.11 shows the reaction profile at each temperature.

Temperature (°C)	Conversion (%)
40	5 ^a 20 ^b
80	35
110	69

Table 3.10. Conversion to desired product at different temperatures

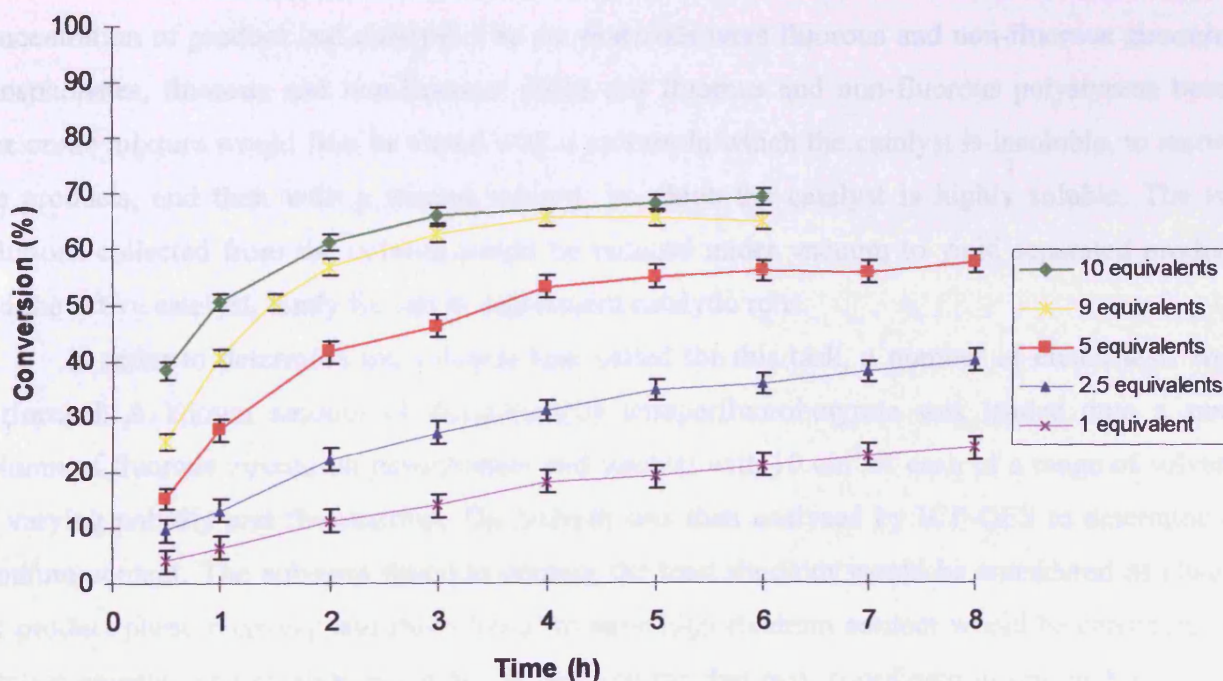
^a in DCM, ^b in toluene



Graph 3.11. Conversion to desired products over time

Based on the above results, toluene was selected as the solvent and a reaction temperature of 110 °C was used for all the subsequent catalytic tests. This allowed a comparison to be made between results collected in this work and those of Bergbreiter.^[13]

Next, a series of experiments was carried out in order to determine the effect of varying the excess of styrene in the reaction. Cyclopropanations reported in the literature typically use 10 molar equivalents of olefin to diazo compound to reduce the formation of diethyl fumarate and diethyl maleate as by-products. Tests with 1, 2.5, 5, 9 and 10 equivalents of styrene were conducted to ascertain if this large excess was required for our system. The data, summarised in Graph 3.12, confirmed that 10 equivalents were necessary to satisfactorily limit the reaction of the diazo reagent with itself. When the excess is halved conversions drop by over 10% and with 2.5 equivalents conversions are almost halved. Therefore, all subsequent catalysis experiments were conducted with 10 equivalents of the alkene.



Graph 3.12. Conversion to desired products with time

Catalytic runs were also carried out in non-dried toluene and in the absence of a dinitrogen atmosphere and these were found to have no negative impacts upon the reaction. Thus, reactions could be conducted in air, making recovery processes simpler to perform as specialised glassware for the exclusion of oxygen was not required.

3.2.1. Catalyst Recycle via Fluorous Solid Phase Extraction

After the reaction conditions for the cyclopropanation had been set recycling studies were initiated. The first recovery technique investigated was fluorous solid-phase extraction. As the catalyst contained four perfluorobutyrate ligands it was reasoned that the catalyst would be retained on the surface of a column with a stationary phase modified with perfluoroalkyl chains when eluted with a suitable solvent. Thus, organic products would be separated from the catalyst, which could then be recovered by elution with a second solvent. To compare the efficiency of the fluorous zirconium phosphonates as a media for this separation method a series of other materials was tested in parallel. A single large-scale homogeneous styrene cyclopropanation reaction was performed at six times the scale of previous experiments. This product mixture was divided into six equal aliquots and each was passed down a column packed with one of six different support materials. Thus, each of the six aliquots had an equal composition after the first run and should have the same concentration of product and catalyst. The six materials were fluorous and non-fluorous zirconium phosphonates, fluorous and non-fluorous silica and fluorous and non-fluorous polystyrene beads. The crude mixture would first be eluted with a solvent in which the catalyst is insoluble, to recover the products, and then with a second solvent, in which the catalyst is highly soluble. The two solutions collected from the column would be reduced under vacuum to yield separated products and the active catalyst, ready for use in subsequent catalytic runs.

In order to determine the solvents best suited for this task, a number of eluant tests were performed. A known amount of dirhodium(II) tetrafluorobutyrate was loaded onto a small column of fluorous zirconium phosphonate and washed with 10 cm³ of each of a range of solvents of varying polarity and fluorination. The solvent was then analysed by ICP-OES to determine its rhodium content. The solvents found to contain the least rhodium would be considered as eluants for product phase recovery and those found to have high rhodium content would be considered as catalyst eluants. The catalyst is soluble in any solvent that may coordinate to one or both of the apical vacant sites of the complex, acting as a ligand. As such, the catalyst is highly soluble in acetonitrile, methanol and tetrahydrofuran, all of which form deep purple/blue solutions upon addition of the deep green dirhodium(II) tetrafluorobutyrate; the colour change perhaps resulting from the now fully saturated coordination sphere. The complex was also found to be soluble in diethyl ether, but a greater volume of solvent was required for total dissolution of a given amount of the solid and the resulting solution was green rather than blue, perhaps indicating that the solvent is not acting as a ligand. Therefore, these three solvents were selected to be tested as possible eluants for recovery of the catalyst from the column. At room temperature the catalyst is poorly soluble in both hexane and toluene and, thus, these solvents were tested for use as the first eluant, to recover

the product phase. A fluorinated analogue of toluene, benzotrifluoride (BTF) was also tested. Despite its fluorination, the catalyst was sparingly soluble in this solvent, with only a trace of green colouration observed.

The percentages of rhodium metal washed from the column with each solvent, calculated from ICP-OES analysis, are shown in Table 3.13.

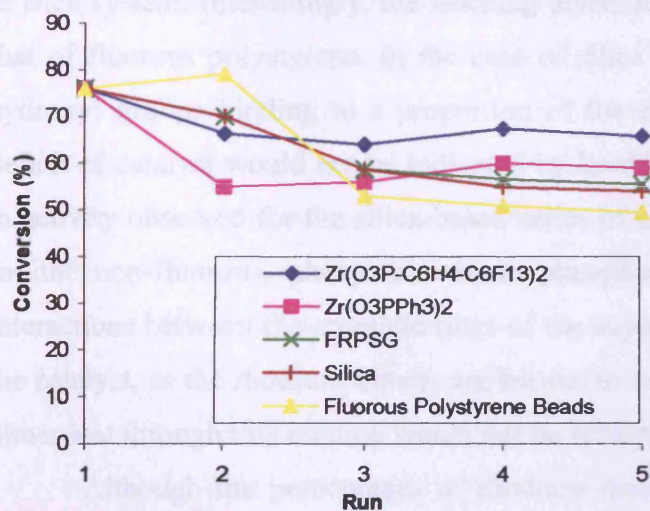
Solvent	Rhodium (%)
Hexane	4.5
Toluene	5.2
BTF	15.9
Diethyl ether	95.1
MeOH	>99.9
Acetonitrile	>99.9

Table 3.13. Rh leaching with various eluants

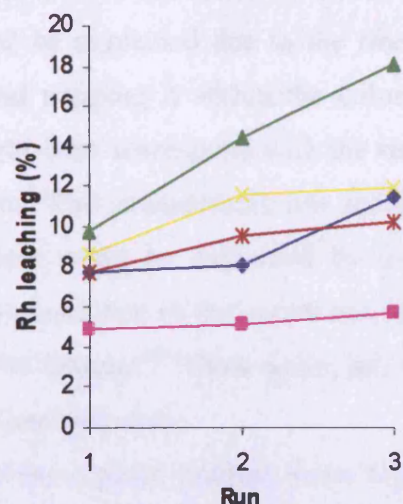
Although slightly lower levels of rhodium leaching were found for the hexane wash, the product mixture showed far superior solubility in toluene and, therefore, the latter was chosen as the first stage eluant. The difference in the elution potential of diethyl ether, methanol and acetonitrile was small but, as it was known that the acetonitrile adduct of dirhodium(II) tetrafluorocarboxylates can be reduced to the free complex upon gentle heating under vacuum,^[27] the latter of the three was selected as the eluant for the catalyst recovery phase.

When the aforementioned solid phase extraction process was attempted with the column composed of standard polystyrene beads, the beads formed a congealed gel, which prevented solvent from being passed down the column. Thus, recycling experiments using this column were not pursued.

The catalysts from the other five fractions were successfully separated and recycled a further four times. The product phase was reduced in vacuum and analysed by GC and ICP-OES to determine conversions/selectivities and rhodium leaching levels respectively. Results are displayed in Graphs 3.14 and 3.15 and are summarised in Table 3.16.



Graph 3.14. Conversion to desired product over subsequent catalytic runs



Graph 3.15. Rh leaching over subsequent catalytic runs

Column Media	Conversion (%) ^a	Rh Leaching ^{a, b}
Zr(O ₃ P-C ₆ H ₄ -4-C ₆ F ₁₃) ₂	76 (66, 64, 67, 66)	4.9 (5.2, 5.7)
Zr(O ₃ PPH) ₂	76 (55, 56, 60, 59)	7.8 (8.1, 11.5)
FRPSG	76 (70, 59, 57, 56)	9.8 (14.4, 18.1)
Silica	76 (70, 59, 55, 54)	7.7 (9.6, 10.2)
Fluorous Polystyrene Beads	76 (79, 53, 51, 50)	8.6 (11.6, 11.9)

Table 3.16. Conversion to desired products over subsequent homogeneous runs

^a Values in parentheses are conversions for 2nd (3rd, 4th and 5th) runs

^b Values indicate total percentage of rhodium metal lost, accumulative over subsequent runs

The data shows that although the catalyst may be recovered using all of the five materials, the lowest Rh leaching levels are found for the column composed of fluorous zirconium phosphonate. The conversion in the first run is the same for all tests as this was the large scale reaction that was divided into the six fractions. Conversions for the second run vary greatly, possibly due to errors in the division of the first crude product mixture, however, after the second run conversions stabilised and fall only slightly over the final three runs. Selectivities were consistent throughout, at around 63% major isomer.

The degree of rhodium loss varies more significantly, with the amount of metal lost to the organic product with FRPSG being almost four times that lost with the fluorous zirconium phosphonate. It is important to note that these leaching levels indicate the amount of rhodium found in the organic product and are not necessarily the absolute values of rhodium which have been lost

in each system. Interestingly, the leaching levels for the non-fluorous materials are almost equal to that of fluorinated polystyrene. In the case of silica this could be explained due to the free surface hydroxyl groups binding to a proportion of the catalyst and trapping it within the column. This deficit of catalyst would not be indicated by leaching data but does correspond with the steady fall in activity observed for the silica-based series of experiments. The unexpectedly low rhodium loss for the non-fluorous, phenyl zirconium phosphonate system could be explained by π -bonding interactions between the aromatic rings of the support material and one of the vacant active sites of the catalyst, as the rhodium dimers are known to coordinate to toluene.^[24] Once again, any rhodium dimer lost through this method would not be reflected in the leaching data.

Although the percentages of rhodium metal lost to the organic product seem high, these correspond to minuscule masses of metal in real terms. The initial reaction used 0.02 mol % catalyst, or 0.011 g for 5.75 g of ethyl diazoacetate substrate. The product mixture was divided into six fractions each theoretically containing 0.0018 g of dirhodium(II) tetrafluorobutyrate. Therefore, the maximum leaching value for a single run of 9.8% corresponds to a mass of 0.00003 g, or 0.03 mg, of rhodium metal. If the reaction were scaled up to a kg of substrate, the same leaching would signify only 5 mg of rhodium in the organic product.

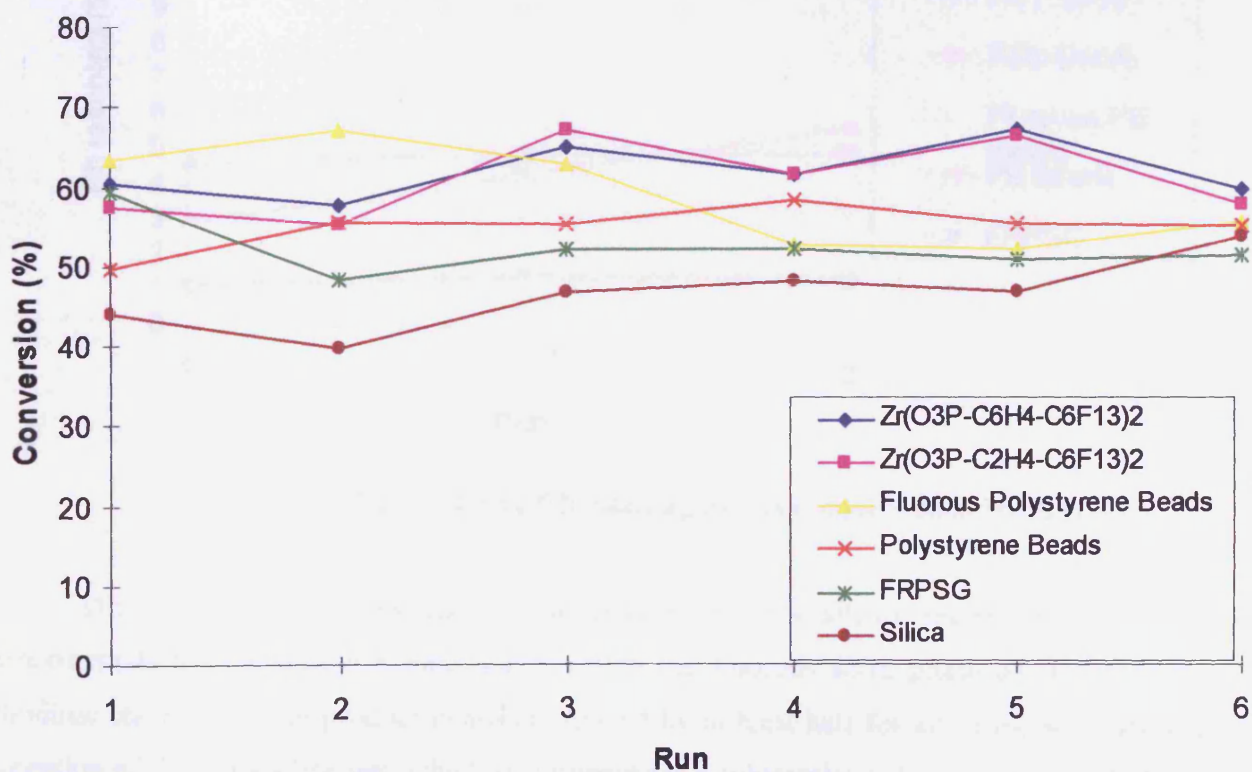
Although these recycling results were encouraging, the percentage of rhodium leaching was still unacceptably high. Therefore, we moved on to investigate the possibility of supporting the dirhodium(II) tetrafluorobutyrate catalyst on the surface of an insoluble material, which could be filtered post-reaction to separate it from organic products and recycled.

3.2.2. Catalyst Recycle using Solid Supports

In a more direct comparison to Bergbreiter's polymer-bound catalytic cyclopropanation,^[13] we next sought to study the dirhodium(II) tetrafluorobutyrate's activity and recyclability when immobilised on a insoluble support material. It was proposed that the fluorinated dimer may be embedded on a perfluorinated surface, as with Biffis' "bonded fluorinated-phase catalysis" described previously.^[9] The affinity of the perfluoroalkyl chains of the catalyst for those of the support should ensure that it remains immobilised upon the surface when in contact with any one of a series of fluorophobic organic solvents, with which they are highly immiscible. An increase in temperature, however, improves fluoro-organic miscibility and thus the catalyst may be able to leave the support during a reaction and act homogeneously. It was proposed that this could allow for an improved catalyst activity than that for the heterogeneous polymer-bound system, as the catalyst would be more mobile as no covalent interactions are involved between the rhodium complex and the solid support.

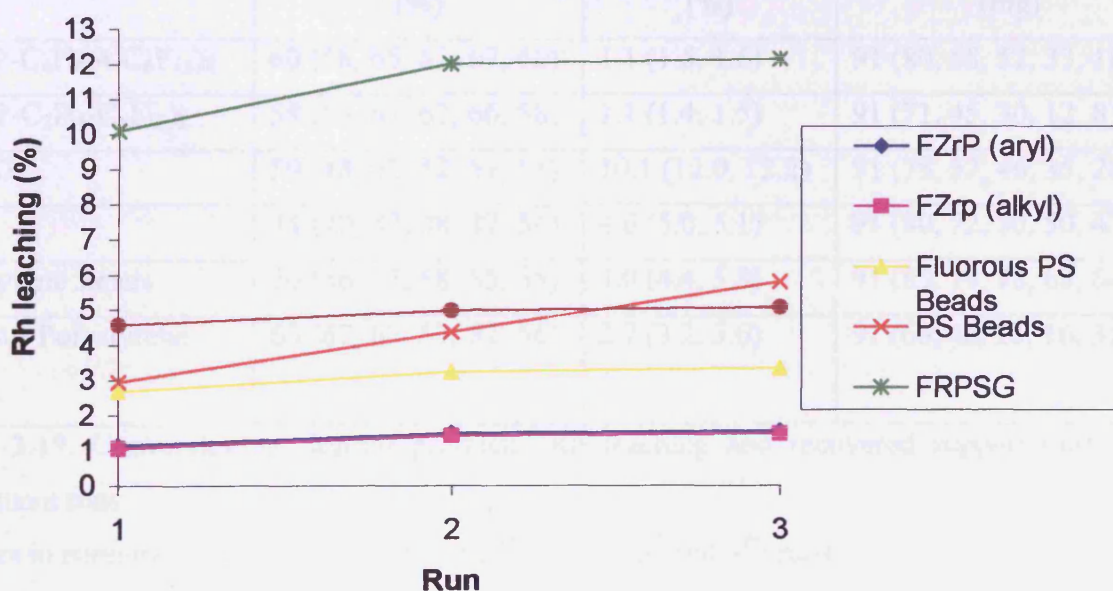
As for the previous homogeneous experiments, several different support materials, both fluorinated and non-fluorinated, were evaluated. The supported catalyst was straightforwardly prepared by stirring a solution of dirhodium(II) tetra-perfluorobutyrate in acetonitrile with the solid support material, removing the solvent and thoroughly drying the material under vacuum. Upon drying, the powder changes from the deep purple colour of the acetonitrile-coordinated complex to the dark green of the free catalyst. A catalyst loading of 1% was used; that is, 0.01 g of catalyst per 1 g of support. This low level of coverage was chosen to help reduce leaching of the rhodium complex into the product phase and to minimise the loss of catalyst through mechanical losses of the support associated with the separation and recovery process.

Six different supports were tested; FRPSG and standard silica gel, polystyrene beads and fluorinated polystyrene beads and fluorinated zirconium phosphonates with an aryl or alkyl spacer group between the perfluoroalkyl chain and the phosphonate group. The perfluoroalkyl chains of the fluorinated zirconium phosphonate and silica supports were six carbons long (perfluorohexyl) and those of the polymer beads were eight carbons long (perfluorooctyl). Catalytic cyclopropanation reactions were carried out using the same conditions as those in the homogeneous experiments. At the end of the reaction the supported-catalyst was filtered, washed with toluene to elute any adsorbed product and dried for use in a successive run. Conversions for each run are shown in Graph 3.17.



Graph 3.17. Conversion to desired products over subsequent runs

The catalyst could be successfully reused five times regardless of the support used and conversions were maintained over the six runs. Conversions in the initial catalytic runs are slightly lower than those for the homogeneous system but this is expected due to mass transport issues associated with the immobilised catalyst. The amount of dried support recovered by filtration was weighed following each cycle to allow consideration to be given to any mechanical losses. An average of around 15 mgs of support was lost mechanically during each recovery, either to the side of the reaction vessel or to the filter frit. It should be noted that as the same reaction vessel was reused after recycling, any solid remaining in the flask would be recycled, and since the recorded masses do not account for this the losses of support are, therefore, exaggerated. Due to the small scale of the reactions the starting mass of the support was 91 mg meaning that at the end of the sixth run, a large proportion of the support and hence the catalyst, had been lost. The fact that this decrease in the amount of catalyst is not reflected in the conversions to desired product suggests that the catalyst is highly active. Indeed, the catalyst loadings used in our work (0.02 mol %) are 100 times smaller than that used by Bergbreiter^[13] and the reaction is virtually complete in under half the reaction time, albeit with reduced product conversions (around 60% as opposed to 90%).



Graph 3.18. Accumulative Rh leaching over subsequent catalytic runs

The ICP-OES data reveals that supported catalysis allows improved recyclability of dirhodium(II) tetra-perfluorobutyrate compared to the fluorosolid phase extraction technique. Rhodium leaching to the product phase is reduced by at least half for all of the supports with the exception of fluorosilica gel, which still undergoes a substantial reduction of around 6%. As for the homogeneous experiments, FRPSG retains the catalyst the least effectively. A coarse silica (40

μm) was chosen for these experiments in an attempt to keep mechanical losses to a minimum. However, the large particle size results in a reduced surface area, which may account for poor retention of the fluoros complex by this silica. Standard silica once again shows lower leaching levels than expected, possibly due to irreversible binding of surface hydroxyl groups to the catalyst's vacant sites. The amount of fluoros rhodium complex lost with the standard polystyrene beads did as one may predict for a non-fluorous support, increase steadily with each run.

The best separation results are obtained for the three remaining supports with fluoros surfaces. The two fluoros zirconium phosphonates and the fluoros polystyrene beads have similar leaching profiles (Graph 3.18), but are distinguished by a larger rhodium loss by the latter in the initial catalytic run. The type of organic spacer group present in the phosphonate group appears to have no impact upon the materials' ability to retain the fluoros catalyst used in this system.

The amount of rhodium found in the organic product during the first run when the catalyst was immobilised on the two fluoros zirconium phosphonates was just 1.5% and 1.6% of the total metal. This equates to 0.000003 g of rhodium in 0.575 g of product, or 0.005 g for a kg.

Support Material	Conversion ^a (%)	Rh Leaching ^{a, b} (%)	Mass of Support Used ^a (mg)
Zr(O ₃ P-C ₆ H ₄ -4-C ₆ F ₁₃) ₂	60 (58, 65, 61, 67, 60)	1.1 (1.5, 1.6)	91 (80, 68, 52, 33, 18)
Zr(O ₃ P-C ₂ H ₄ -C ₆ F ₁₃) ₂	58 (55, 67, 62, 66, 58)	1.1 (1.4, 1.5)	91 (71, 45, 30, 12, 8)
FRPSG	59 (48, 52, 52, 51, 51)	10.1 (12.0, 12.2)	91 (75, 57, 46, 35, 28)
Silica	44 (40, 47, 48, 47, 54)	4.6 (5.0, 5.1)	91 (80, 72, 70, 50, 43)
Polystyrene Beads	50 (56, 55, 58, 55, 55)	3.0 (4.4, 5.8)	91 (85, 79, 78, 68, 64)
Fluorous Polystyrene Beads	63 (67, 63, 53, 52, 56)	2.7 (3.2, 3.6)	91 (66, 48, 25, 10, 3)

Table 3.19. Conversion to desired products, Rh leaching and recovered support masses over subsequent runs

^a Values in parentheses are conversions for 2nd (3rd, 4th, 5th and 6th) runs

^b Values indicate total percentage of rhodium metal lost, accumulative over subsequent runs

An evaluation of which support performed most favourably requires consideration of several factors. Conversions are generally comparable, within the associated error of $\pm 2\%$, for each support. Although the two non-fluorous supports, silica and polystyrene, showed the lowest degree of mechanical losses, their catalyst leaching values were among the highest and conversions in the initial run were slightly poorer.

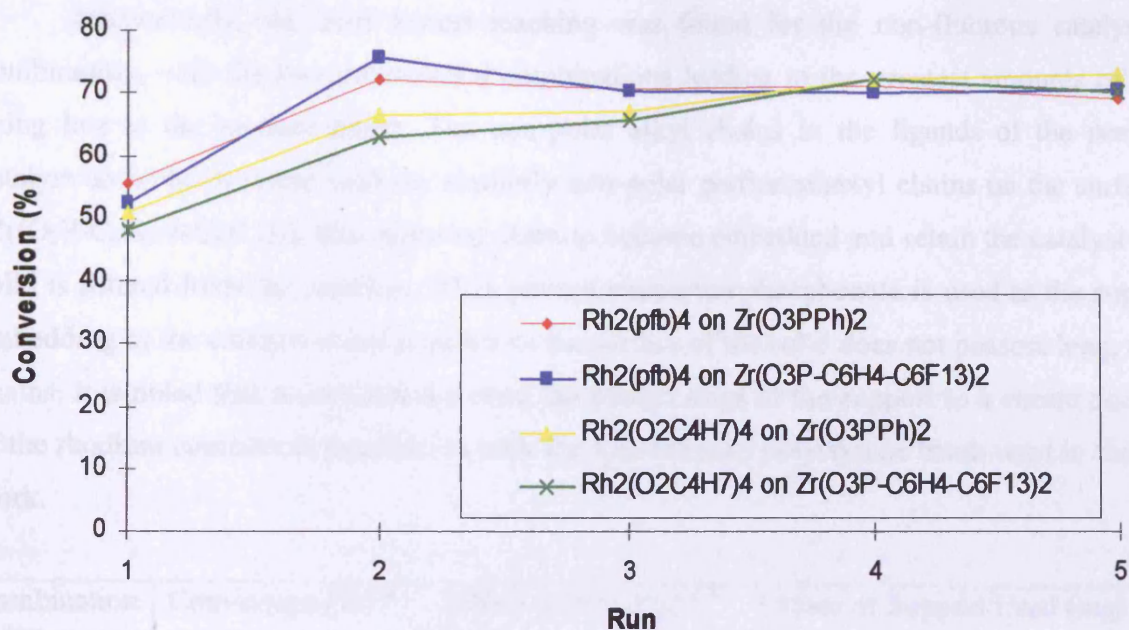
Of the fluorous supports FRPSG gave the highest leaching and lowest, though highly consistent, conversions. As with standard silica, mechanical losses were reduced as compared to the finely powdered zirconium phosphonates. However, although the two fluorous zirconium phosphonates were among the worst for recoverability, with less than 20 mg of the original support retained after filtration in the sixth run, their associated conversions were not adversely affected and were, in fact, the highest for the final four runs. Also, the minimal amounts of metal found in the products of the first three runs make the fluorous zirconium phosphonate more favourable for a large-scale process. Firstly, these supports give the best separation of the metal from the organic product and secondly, on scale up, the mechanical losses of support would be minimised. That is, a loss of around 15 mg of support would clearly be a far smaller proportion of the catalyst in a process of a kilogram scale as opposed to one on a gram scale.

The results obtained in the initial supported catalysis were encouraging and clearly showed that the fluorous catalyst may be immobilised and recycled without covalently binding it to the surface of the solid support. However, as the non-fluorous supports also allowed recycling of the fluorous catalyst, we wished to investigate the affinity of the perfluoroalkyl chains of the catalyst for those of the support in more detail.

3.2.3. Comparison of Fluorous and Non-fluorous Zirconium Phosphonate Solid Supports

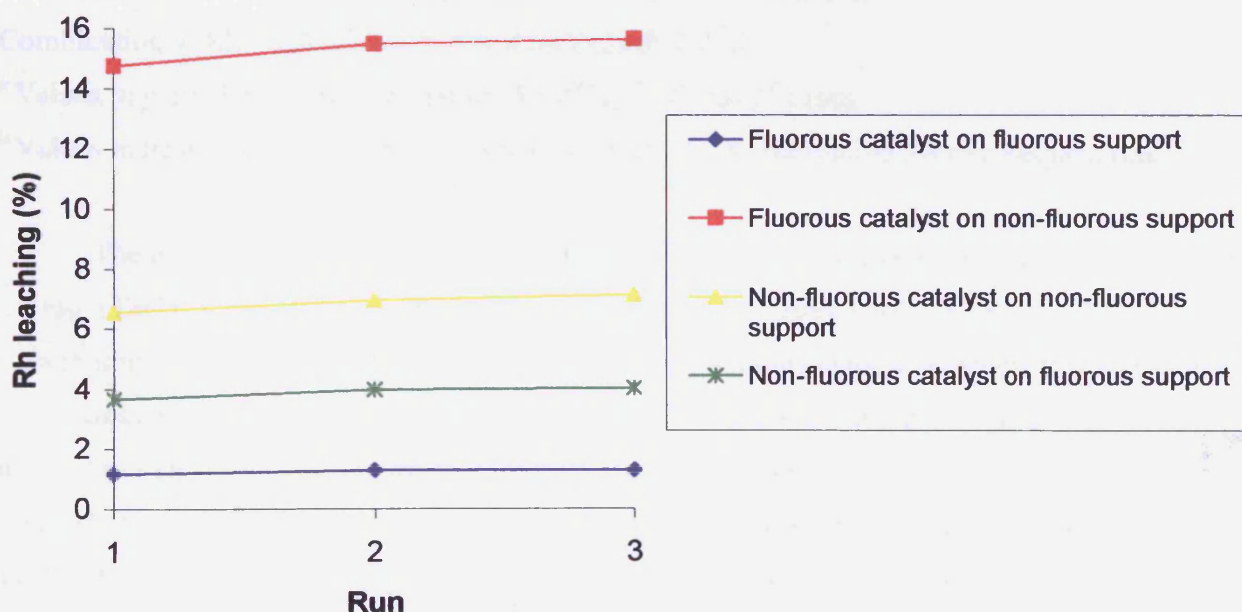
As two non-fluorous solid supports had been shown to allow recovery of an active fluorous catalyst, with almost the same degree of success as the fluorous supports, we sought to determine whether the presence of perfluoroalkyl chains on the support and/or within the ligand structure were improving the retention of the catalyst.

In order to evaluate the effect of the fluorous moieties, a series of solid-supported dirhodium(II) carboxylate catalysts was prepared, with combinations of fluorous/non-fluorous catalysts/supports. Dirhodium(II) tetrabutyrates, $[\text{Rh}_2(\text{O}_2\text{C}_4\text{H}_7)_4]$, and its perfluorinated analogue dirhodium(II) tetra-perfluorobutyrate, $[\text{Rh}_2(\text{O}_2\text{C}_4\text{F}_7)_4]$, were each separately loaded onto both phenyl zirconium phosphonate, $[\text{Zr}(\text{O}_3\text{P}-\text{C}_6\text{H}_5)_2]$, and its fluorous congener, $[\text{Zr}(\text{O}_3\text{P}-\text{C}_6\text{H}_4-4-\text{C}_6\text{F}_{13})_2]$. These four supported catalysts were then utilised in the cyclopropanation of styrene with ethyl diazoacetate and were filtered, washed, dried and recycled as for the previous supported system. The supports were successfully reused a total of five times and conversions are displayed in Graph 3.20.



Graph 3.20. Conversion to desired products over subsequent runs

As can be seen from the data in Graph 3.20, conversions are consistently maintained over the five runs and are in good agreement with one another within the associated $\pm 2\%$ error, with the exception of the first run, which is notably lower. Conversions do not indicate any significant increase in catalyst leaching when the catalyst or support lacks perfluoroalkyl chains. However, the ICP-OES data tells a different story. The degree of Rh leaching for the combination of fluorous catalyst immobilised on a fluorous support is by far the lowest of all the combinations (Graph 3.21).



Graph 3.21. Accumulative Rh leaching over subsequent catalytic runs

Interestingly, the next lowest leaching was found for the non-fluorous catalyst/support combination, with the two mismatched combinations leading to the greatest amounts of Rh metal being lost to the product phase. The non-polar alkyl chains in the ligands of the non-fluorous catalyst could be miscible with the similarly non-polar perfluorohexyl chains on the surface of the $[\text{Zr}(\text{O}_3\text{P}-\text{C}_6\text{H}_4-4-\text{C}_6\text{F}_{13})_2]$, thus allowing them to become embedded and retain the catalyst when the solid is filtered from the reaction. When phenyl zirconium phosphonate is used as the support, this embedding of the catalyst is not possible as the surface of the solid does not possess long, non-polar chains. It is noted that π -coordination from the phenyl rings of the support to a vacant coordination of the rhodium complex is possible, as with the non-fluorous polystyrene beads used in the previous work. However, the phenyl rings do result in a small reduction in conversion to the cyclopropane product. As expected, catalyst losses for the supported reactions are marginally lower

Combination	Conversion (%) ^a	Rh Leaching (%) ^{a, b}	Mass of Support Used (mg) ^a
1	56 (72, 71, 71, 69)	1.2 (1.3, 1.3)	91 (81, 59, 50, 34)
2	52 (76, 71, 70, 70)	14.8 (15.2, 15.6)	91 (76, 52, 37, 23)
3	48 (63, 66, 72, 70)	6.6 (7.0, 7.1)	112 (86, 68, 59, 42)
4	51 (67, 67, 72, 73)	3.7 (4.0, 4.1)	112 (92, 68, 45, 29)

Table 3.22. Conversion to desired products, Rh leaching and recovered support masses over subsequent runs

Combination 1: $\text{Rh}_2(\text{O}_2\text{C}_4\text{F}_7)_4$ supported on $\text{Zr}(\text{O}_3\text{P}-\text{C}_6\text{H}_4-4-\text{C}_6\text{F}_{13})_2$

Combination 2: $\text{Rh}_2(\text{O}_2\text{C}_4\text{F}_7)_4$ supported on $\text{Zr}(\text{O}_3\text{P}-\text{C}_6\text{H}_5)_2$

Combination 3: $\text{Rh}_2(\text{O}_2\text{C}_4\text{H}_7)_4$ supported on $\text{Zr}(\text{O}_3\text{P}-\text{C}_6\text{H}_4-4-\text{C}_6\text{F}_{13})_2$

Combination 4: $\text{Rh}_2(\text{O}_2\text{C}_4\text{H}_7)_4$ supported on $\text{Zr}(\text{O}_3\text{P}-\text{C}_6\text{H}_5)_2$

^a Values in parentheses are conversions for 2nd (3rd, 4th and 5th) runs

^b Values indicate total percentage of rhodium metal lost, accumulative over subsequent runs

The mechanical losses were similar to those of the previous tests, typically between 10 and 20 mg (Table 3.22). Despite the combined catalyst loss from leaching and mechanical losses, conversions in the second run increase for all the combinations used. This seems to suggest that the rate increases once the catalyst concentration has dropped below a certain value. But, leaching in the first run varies for each of the combinations and is generally low, particularly in the all fluorine case, which at only 1% seems unlikely to be the cause for such a pronounced change in conversion. This type of unusual behaviour has also been observed for the cyclopropanation of styrene by Cenini *et al.*^[28] In their work with a cobalt-based catalyst, the group reported that the rate of

cyclopropanation was limited by concentrations of styrene above 0.13 M and of the diazo substrate above 0.05 M.

3.2.4. Catalyst Loading Studies

To investigate the effect of catalyst concentration and determine if high levels actually impede conversion to the desired products, the cyclopropanation was carried out using a series of catalyst loadings, both homogeneously and under supported conditions. Stock solutions of catalyst were prepared and were diluted to the required values. The results shown in Table 3.23, suggest that increasing the catalyst loading does result in a small reduction in conversion to the cyclopropane product. As expected, conversions for the supported reactions are marginally lower than those under homogeneous conditions.

Catalyst Loading (mol %)	Conversion (%)	
	Homogeneous	Supported
0.0001	74 ^a	69
0.001	72 ^a	69 (66, 69, 68, 68) ^b
0.01	66 ^a	65
0.1	57 ^a	57
0	0	0

Table 3.23. Conversions to desired products with various catalyst loadings

^a average of 2 runs

^b Values in parentheses are conversions for 2nd (3rd, 4th and 5th) runs

The tests show that the dirhodium(II) tetrafluorobutyrates is an immensely active catalyst for the cyclopropanation of styrene. Good levels of conversion to the desired cyclopropane product are maintained at extremely low loadings of catalyst. In a control reaction, in the absence of catalyst, no trace of product was observed. In the case of reaction with 0.001 mol % loading, the supported catalyst was recovered and reused for five runs and showed no loss in activity. Although ICP-OES analysis of the product was conducted, masses of metal would be negligible even with high levels of leaching. If the reaction were scaled up to a kg scale, a 0.001 mol % catalyst loading would only correspond to 0.0014 mg. With leaching levels previously observed for the small scale supported catalysis, the organic phase of such a kilogram scale reaction would contain just 0.00002 mg of rhodium. As leaching is observed to fall greatly after the first run, the mass of rhodium in the products of subsequent runs would be substantially smaller again.

3.2.5. Investigation into the Effect of Perfluoroalkyl Chain Length on Catalyst Leaching

All of the catalytic tests conducted thus far had utilised the same combination of perfluoroalkyl chains; the catalyst ligands possessed perfluoropropyl, C_3F_7 , chains and both the fluorous supports possessed perfluorohexyl, C_6F_{13} , chains.

It was proposed that increasing the length of the perfluoroalkyl chains of the catalyst or the support might allow more effective embedding of the dirhodium(II) carboxylate in the fluorous surface of the support. Similarly, it was expected that shortening these chains would have the opposite effect, and leaching levels would rise. Therefore, a comparison was conducted between two supports with different perfluoroalkyl chain lengths. The perfluorobutyrate catalyst was immobilised on a fluorous zirconium phosphonate bearing perfluorobutyl chains with an ethylene spacer group and on one bearing perfluorohexyl chains with a benzene spacer, as used in the previous experiments (Figure 3.24). As the former has a lower degree of fluorination it was predicted that more of the immobilised catalyst would be lost from its surface when filtered and washed in the recovery process.

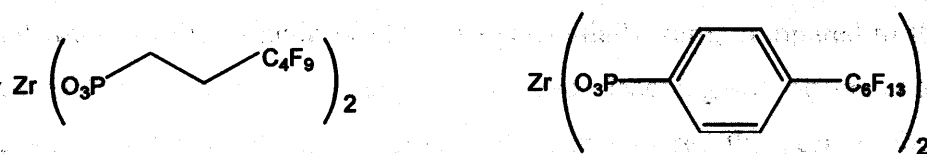


Figure 3.24. Fluorous zirconium phosphonates possessing C_4F_9 and C_6F_{13} perfluoroalkyl chains

A comparison between catalysts of varying fluorination was also conducted. Dirhodium(II) tetra-perfluoroheptanoate was readily prepared *via* a ligand exchange reaction of dirhodium(II) tetraacetate with perfluoroheptanoic acid and was characterised by NMR and IR spectroscopies. This catalyst, with perfluoroalkyl chain length double that of the perfluorobutyrate complex, was also immobilised on the supports above. A catalyst loading of 0.02 mol % was used in these experiments for a direct comparison to the earlier work.

Table 3.25. summarises the results obtained for the two catalysts when supported on the $Zr(O_3P-C_2H_4-C_4F_9)_2$. Conversions are comparable to those previously obtained, with the first run being slightly lower than subsequent runs. Mechanical losses are also of a similar magnitude. The lower degree of fluorination of the C_4F_9 support does appear to have an effect on the amount of perfluorobutyrate catalyst lost to the organic product phase, presumably because the extent of interlacing between the fluorous chains on the surface and the ligands of the dirhodium complex is

reduced. The catalyst, therefore, is less well rooted on the support and more susceptible to becoming dislodged when washing with toluene.

When the perfluoroheptanoate catalyst is supported on the C_4F_9 support, the longer perfluoroalkyl chains of the ligands act to reduce leaching to a level comparable to that obtained for the dirhodium(II) tetrafluorobutyrate when used with the C_6F_{13} based supports.

Catalyst	Conversion (%) ^a	Rh Leaching (%) ^{a, b}	Mass of Support Used (mg) ^a
$Rh_2(O_2C_4F_7)_4$	51 (69, 65)	3.8 (4.0, 4.3)	91 (68, 61)
$Rh_2(O_2C_7F_{13})_4$	48, (75, 62)	1.5 (1.9, 2.2)	140 (125, 111)

Table 3.25. Desired product conversion using $Rh_2(L)_4$ supported on $[Zr(O_3P-C_6H_4-C_6F_9)_2]$

^a Values in parentheses are conversions for 2nd and 3rd runs

^b Values indicate total percentage of rhodium metal lost, accumulative over subsequent runs

The dirhodium(II) tetrafluoroheptyrate catalyst was also supported on the perfluorohexyl based aryl zirconium phosphonate. This combination of longer fluorous chains on both the support and the catalyst led to the lowest level of leaching observed thus far (Table 3.26). In the first run the amount of metal found in the organic product was essentially zero, compared to the 1% typically observed for $Rh_2(O_2C_4F_7)_4$ on the same support. However, leaching still occurs at a consistent rate and over three recycles the leaching is virtually the same as for the perfluorobutyrate catalyst. Although this gradual leaching of the $Rh_2(O_2C_7F_{13})_4$ results in the same overall loss of catalyst as that for $Rh_2(O_2C_4F_7)_4$, it does spread the metal contamination into the product more equally, rather than having a large amount of metal in the product of the first run.

Catalyst	Conversion (%) ^a	Rh Leaching (%) ^{a, b}	Mass of Support Used (mg) ^a
$Rh_2(O_2C_4F_7)_4$	60 (68, 66)	1.1 (1.5, 1.6)	91 (80, 68, 52)
$Rh_2(O_2C_7F_{13})_4$	52 (60, 58, 66)	>0.1 (0.5, 1.1, 1.5)	140 (121, 100, 80)

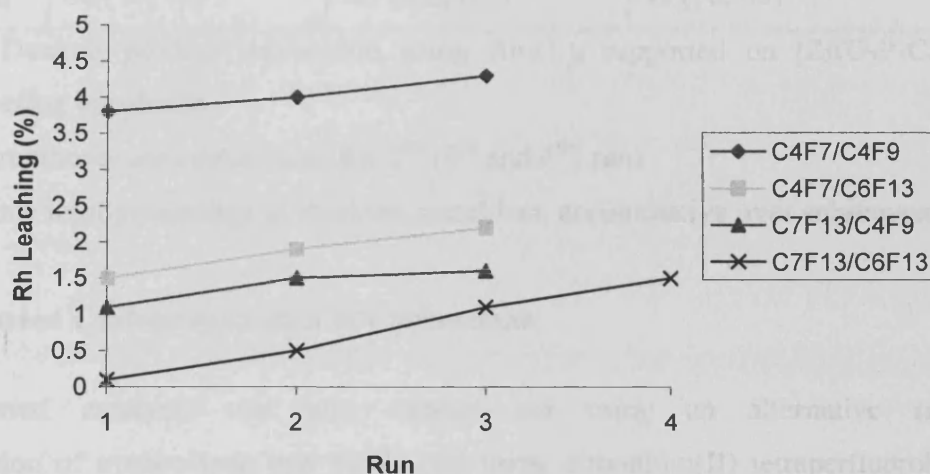
Table 3.26. Desired Product Conversion Using $Rh_2(L)_4$ Supported On $[Zr(O_3P-C_6H_4-C_6F_{13})_2]$

^a Values in parentheses are conversions for 2nd (3rd and 4th) runs

^b Values indicate total percentage of rhodium metal lost, accumulative over subsequent runs

The data indicates that changing the length of the perfluoroalkyl chains of the catalyst or support does have an effect on the degree of leaching to the product phase. As the length of the chains is increased, the amount of rhodium lost from the support is reduced, as shown in Graph 3.27. Although the effect is small for the combinations tested, this is not unexpected, as the

difference in length is also relatively small. It should be noted that when using an even less fluororous zirconium phosphonate support, such as $[\text{Zr}(\text{O}_3\text{P}-\text{C}_6\text{H}_5)_2]$, with the dirhodium(II) tetra-perfluorobutyrate, the degree of catalyst loss increases substantially (14.8, 15.2 and 15.6%, Table 3.22).



Graph 3.27. Accumulative Rh leaching using combinations of catalysts and supports of varying fluorination

It is possible that the reduction in the degree of rhodium leaching into the organic phase when a catalyst bearing C_7F_{13} chains is used results from a reduction in the solubility of the catalyst, rather than an increase in interlacing between the fluororous chains of the catalysts ligands and those of the support.

3.2.6. Optimisation of the Solid-Supported Catalyst

In the supported catalysis conducted thus far, it was observed that the first run showed lower conversions and higher leaching than those for subsequent runs. Generally, leaching levels after the third cycle were negligible. In an attempt to optimise the system, a new procedure for the preparation of the supported catalyst was developed. The dirhodium(II) tetra-perfluorobutyrate and 4-perfluorohexylphenyl zirconium phosphonate were refluxed in toluene for four hours, essentially a blank catalytic run. After cooling, the solid was filtered, dried and used in the cyclopropanation reaction, as before. This method ensured that any rhodium lost from the support during the first run did not contaminate the product phase of the first catalytic reaction and could be disposed of separately. The results show that this method both reduces the amount of metal found in the product of the initial run and also leads to a slightly improved conversion (Table 3.28). It should be noted

that although the data suggests accumulative leaching of a total of just 0.2% rhodium to the product over three runs, this is not the absolute amount of catalyst lost, as a small amount is likely to have been lost during filtration after the supporting process.

Catalyst	Conversion (%) ^a	Rh Leaching (%) ^{a, b}	Mass of Support Used (mg) ^a
Rh ₂ (O ₂ C ₄ F ₇) ₄	66 (72, 71)	0.1 (0.2, 0.2)	89 (76, 65)

Table 3.28. Desired product conversion using Rh₂(L)₄ supported on [Zr(O₃P-C₆H₄-4-C₆F₁₃)₂] prepared *via* reflux in toluene

^a Values in parentheses are conversions for 2nd (3rd and 4th) runs

^b Values indicate total percentage of rhodium metal lost, accumulative over subsequent runs

3.3. Supported Cyclopropanation of Cyclooctene

Supported catalysis was also carried out using an alternative substrate. The

cyclopropanation of cyclooctene was performed using dirhodium(II) tetra-perfluorobutyrate on 4-perfluorohexylphenyl zirconium phosphonate. The ethyl diazoacetate was added dropwise over 1 hour to a toluene solution of catalyst and 10 equivalents of alkene. The mixture was then refluxed for 4 hours. Although conversions were expectedly lower than for styrene, as the substrates are less reactive and generally require longer reaction times to achieve high yields,^[18] the catalyst could still be successfully separated and recycled for three runs. Rhodium leaching levels for these experiments are comparable to those found for the styrene cyclopropanation with the same perfluorobutyrate catalyst supported on 4-perfluorohexylphenyl zirconium phosphonate. Results are shown in Table 3.29.

Conversion (%) ^a	Rh Leaching (%) ^{a, b}	Mass of Support Used (mg) ^a
16 (17, 11)	1.9 (2.1, 2.2)	91 (72, 66)

Table 3.29. Conversion to desired products, Rh leaching and recovered support masses over subsequent runs

^a Values in parentheses are conversions for 2nd and 3rd runs

^b Values indicate total percentage of rhodium metal lost, accumulative over subsequent runs

It should be noted that the reaction conditions were not optimised for these substrates and the tests were primarily to evaluate rhodium leaching to ensure that the retention of the catalyst on the solid-support's surface was substrate independent. With increased reaction time and a slower rate of addition of the diazo compound, conversions would be expected to improve. To support this

suggestion, a single run of the cyclooctene cyclopropanation with a reaction time of 8 hours was conducted and the conversion to the desired product was improved by 10%.

3.4. Conclusions for Chapter 3

Dirhodium(II) tetra-perfluorocarboxylates are highly active catalysts for the cyclopropanation of styrene. This work shows that they may be effectively separated from organic products and recycled by fluororous techniques, such as solid phase extraction or supported catalysis. In particular, fluororous zirconium phosphonates are shown to be superior to other fluorinated supports with regards to catalyst separation and recovery.

Under homogeneous reaction conditions, a dirhodium(II) tetra-perfluorobutyrate catalyst was recovered by passing the crude reaction mixture through a short column of the support material, firstly eluting the product with toluene and secondly recovering the catalyst with acetonitrile. The catalyst could be reused in the cyclopropanation reaction with little or no reduction in activity or conversion. Analysis of the products by ICP-OES showed that the lowest levels of catalyst loss were achieved for the column packed with fluororous zirconium phosphonate. With this column, a total of 5.7% of the rhodium metal was lost accumulatively to the products of the first three catalytic runs.

Under supported conditions, the catalyst was first immobilised on the surface of a series of solids, these supported catalysts were then added to the reaction vessel and at the end of the reaction were filtered from the organic product phase. The recovered solid-supported catalyst could be reused in up to 6 successive runs, with no apparent loss in activity. In an initial comparison of a series of fluororous and non-fluororous materials, zirconium phosphonates bearing perfluorohexyl chains were shown to give the best retention of the catalyst on the surface. With these supports around only 1.5% of the total rhodium used was found to be present in the organic product. This indicated that solid-supported catalysis was a more effective method for the separation of the dirhodium(II) tetra-perfluorobutyrate catalyst from products than solid phase extraction.

It was also shown for the zirconium phosphonate solid-supported system that a combination of fluororous catalyst on a fluororous solid support gave lower rhodium leaching than for a totally non-fluororous or mis-matched fluororous/non-fluororous combination of catalyst and support. This shows that the presence of these chains does have a beneficial effect on catalyst retention and separation.

Finally, levels of catalyst leaching could be reduced further by using a catalyst with longer perfluoroalkyl chains. A dirhodium(II) tetra-perfluoroheptyrate catalyst supported on a perfluorohexyl-bearing zirconium phosphonate was shown to lose less than 0.1% rhodium after the catalytic first run, ten times less than that for dirhodium(II) tetra-perfluorobutyrate on the same

support. The opposite effect is observed when reducing the length of the perfluoroalkyl chains, leading to 3.8% rhodium lost after run one with the least fluoruous catalyst/support combination used. Furthermore, by just conducting an initial blank catalytic run with the supported catalyst, conversions and leaching in the first catalytic run are respectively increased and reduced, thus further optimising the system.

To summarise; in this work, we have demonstrated that amorphous zirconium phosphonates act as an effective medium for the separation of dirhodium(II) tetracarboxylate catalysts from cyclopropanation products, and that these catalyst may be actively recovered and reused without loss of activity or selectivity. The presence of long perfluoroalkyl chains on the catalyst and the support allow for greater embedding into the surface and lead to improved retention of the catalyst.

[1] T. W. Greene, *Protective Groups in Organic Synthesis*, Wiley, New York, 1998.

[2] J. E. McMurry, *J. Am. Chem. Soc.*, 1959, 81, 5763.

[3] A. H. Ewald, *J. Am. Chem. Soc.*, 1961, 83, 431.

[4] A. H. Ewald, *J. Am. Chem. Soc.*, 1962, 84, 173.

[5] A. H. Ewald, *J. Am. Chem. Soc.*, 1963, 85, 1001.

[6] A. H. Ewald, *J. Am. Chem. Soc.*, 1964, 86, 2101.

[7] A. H. Ewald, *J. Am. Chem. Soc.*, 1965, 87, 2001.

[8] A. H. Ewald, *J. Am. Chem. Soc.*, 1966, 88, 2001.

[9] A. H. Ewald, *J. Am. Chem. Soc.*, 1967, 89, 2001.

[10] A. H. Ewald, *J. Am. Chem. Soc.*, 1968, 90, 2001.

[11] A. H. Ewald, *J. Am. Chem. Soc.*, 1969, 91, 2001.

[12] A. H. Ewald, *J. Am. Chem. Soc.*, 1970, 92, 2001.

[13] A. H. Ewald, *J. Am. Chem. Soc.*, 1971, 93, 2001.

[14] A. H. Ewald, *J. Am. Chem. Soc.*, 1972, 94, 2001.

[15] A. H. Ewald, *J. Am. Chem. Soc.*, 1973, 95, 2001.

[16] A. H. Ewald, *J. Am. Chem. Soc.*, 1974, 96, 2001.

[17] A. H. Ewald, *J. Am. Chem. Soc.*, 1975, 97, 2001.

[18] A. H. Ewald, *J. Am. Chem. Soc.*, 1976, 98, 2001.

[19] A. H. Ewald, *J. Am. Chem. Soc.*, 1977, 99, 2001.

[20] A. H. Ewald, *J. Am. Chem. Soc.*, 1978, 100, 2001.

[21] A. H. Ewald, *J. Am. Chem. Soc.*, 1979, 101, 2001.

[22] A. H. Ewald, *J. Am. Chem. Soc.*, 1980, 102, 2001.

[23] A. H. Ewald, *J. Am. Chem. Soc.*, 1981, 103, 2001.

[24] A. H. Ewald, *J. Am. Chem. Soc.*, 1982, 104, 2001.

[25] A. H. Ewald, *J. Am. Chem. Soc.*, 1983, 105, 2001.

[26] A. H. Ewald, *J. Am. Chem. Soc.*, 1984, 106, 2001.

[27] A. H. Ewald, *J. Am. Chem. Soc.*, 1985, 107, 2001.

References for Chapter 3

- [1] M. P. Doyle, M. S. Shanklin, *Organometallics*, **1994**, *13*, 1081.
- [2] C. J. Moody, F. N. Palmer, *Tetrahedron Lett.*, **2001**, *43*, 139.
- [3] K. Hikichi, S. Kitagaki, M. Anada, S. Nakamura, M. Nakajima, M. Shiro, S. Hashimoto, *Heterocycles*, **2003**, *61*, 391.
- [4] P. M. P. Gois, N. R. Candéias, C. A. M. Afonso, *J. Mol. Cat. A.*, **2005**, *227*, 17.
- [5] J. R. Davies, P. D. Kane, C. J. Moody, *Tetrahedron*, **2004**, *60*, 3967.
- [6] R. T. Buck, D. M. Coe, M. J. Drysdale, L. Ferris, D. Haigh, C. J. Moody, N. D. Pearson, J. B. Sanghera, *Tetrahedron: Asymmetry*, **2003**, *14*, 791.
- [7] M. P. Doyle, M. A. McKerverey, T. Ye, 'Modern Catalytic Methods for Organic Synthesis with Diazo Compounds: From Cyclopropanes to Ylides', Wiley, New York, **1998**.
- [8] A. Endres, G. Maas, *Tetrahedron Lett.*, **1999**, *40*, 6365.
- [9] A. Biffis, M. Braga, M. Basato, *Adv. Synth. Catal.*, **2004**, *346*, 451.
- [10] A. Biffis, M. Zecca, M. Basato, *Green Chemistry*, **2003**, *5*, 170.
- [11] A. Biffis, E. Castello, M. Zecca, M. Basato, *Tetrahedron*, **2001**, *57*, 10391.
- [12] D. C. Forbes, S. A. Patrawala, K. L. T. Tran, *Organometallics*, **2006**, *25*, 2693.
- [13] D. E. Bergbreiter, M. Morvant, B. Chen, *Tetrahedron Lett.*, **1991**, *32*, 2731.
- [14] M. P. Doyle, D. J. Timmons, J. S. Tumonis, H.-M. Gau, E. C. Blosssey, *Organometallics*, **2002**, *21*, 1747.
- [15] I. Goldberg, I. Saltsman, L. Simkhovich, Y. Balazs, Z. Gross, *Inorg. Chim. Acta.*, **2004**, *357*, 3038.
- [16] F. Estevan, P. Lahuerta, J. Lloret, D. Penno, M. Sanau, M. A. Ubeda, *J. Organomet. Chem.*, **2005**, *690*, 4424.
- [17] H. M. L. Davies, T. M. Gregg, D. T. Nowlan III, D. A. Singleton, *J. Am. Chem. Soc.*, **2003**, *125*, 15902.
- [18] J. S. Yadav, B. V. S. Reddy, P. Narayana Reddy, *Adv. Synth. Catal.*, **2003**, *346*, 53.
- [19] M. Barberis, J. Perez-Prieto, K. Herbst, P. Lahuerta, *Organometallics*, **2002**, *21*, 1667.
- [20] G. Chelucci, A. Saba, F. Soccolini, D. Vignola, *J. Mol. Cat. A*, **2002**, *178*, 27.
- [21] A. J. Anciaux, A. J. Hubert, A. F. Noels, N. Petiniot, P. Teyssie, *J. Org. Chem.*, **1980**, *45*, 695.
- [22] A. Demonceau, A. F. Noels, J.-L. Costa, A. J. Hubert, *J. Mol. Cat.*, **1990**, *58*, 21.
- [23] L. M. Hall, R. J. Speer, H. J. Ridgway, *Journal of Clinical Hematology and Oncology*, **1980**, *10*, 25.
- [24] R. S. Drago, J. R. Long, R. Cosmano, *Inorg. Chem.*, **1982**, *21*, 2196.

- [25] R. Giordano, P. Serp, P. Kalck, Y. Kihn, J. Schreiber, C. Marhic, J.-L. Duvail, *Eur. J. Inorg. Chem.*, **2003**, 610.
- [26] M. P. Doyle, R. L. Dorow, W. E. Buhro, J. H. Griffin, W. H. Tambllyn, M. L. Trudell, *Organometallics*, **1984**, *3*, 44.
- [27] A. Endres, G. Maas, *J. Organomet. Chem.*, **2002**, *643*, 174.
- [28] A. Penoni, R. Wanke, S. Tollari, E. Gallo, D. Musella, F. Ragaini, F. Demartini, S. Cenini, *Eur. J. Inorg. Chem.*, **2003**, 1452.

4. Selenium Catalysed Oxidations

4.1. Introduction to Selenium Chemistry

Selenium compounds are widely used by synthetic organic chemists for a number of chemical transformations. Sharpless reported the use of the "first organoselenium reagent" in the early 1970's^[1] but selenium dioxide has been used as an oxidising agent since 1932.^[2] Selenium reagents may be nucleophilic or electrophilic and stoichiometric or catalytic in nature. Organoselenium reagents now find application in such areas as olefin preparation,^[3, 4] dehydrogenation of carbonyl^[5] and other functionalities,^[6, 7] halogenation,^[8-10] and the preparation of 1,2 diketones^[11] and α,β -unsaturated carbonyl compounds.^[12] The area has been summarised in a number of comprehensive reviews.^[13, 14]

4.1.1. Selenium-activated Oxidations

Aryl seleninic acids have been used as catalyst precursors for numerous oxidation reactions in the presence of an re-oxidant, such as hydrogen peroxide.^[14-16] The seleninic acid is first oxidised to a perselenic (selenonic) acid, of the general formula $RSeO_3H$, which then acts as the catalyst and oxidises the substrate. The catalyst is reduced back to the seleninic acid and may be reoxidised to continue the catalytic cycle. An example of one such catalytic oxidation cycle is shown in Figure 4.1.

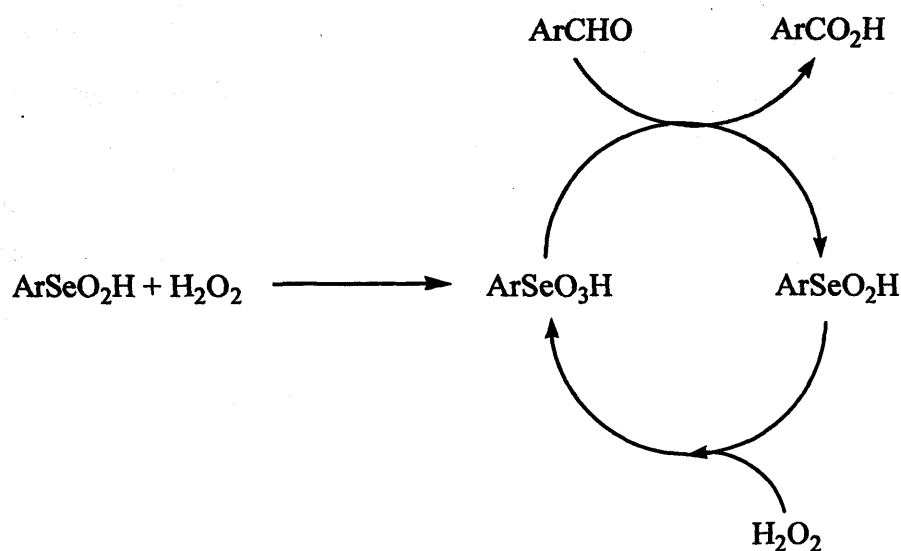


Figure 4.1. Catalytic oxidation of aryl aldehydes to carboxylic acids

4.1.2. Recovery and Reuse of Selenium-based Oxidation Catalysts

Lu and Chen^[17] reported the reuse of a simple, selenium-based carbonylation catalyst. Selenium dioxide was used in the synthesis of a series of pyridyl ureas. The catalyst was successfully recycled in the carbonylation of nitrobenzene and 2-aminopyridine and was shown to be active over 6 runs. Product yields were consistent and no reduction in selectivity was observed. As the urea derivatives were insoluble in the reaction solvent (toluene), filtration of the mixture at the end of the reaction allowed removal of the product and the resulting liquor, containing the catalyst, was recharged with further substrate to start the next cycle. Although the results proved this simple recycling technique to be highly successful, it is clearly limited to products which precipitate upon formation and could not be applied to systems with soluble products.

Sheldon reported the use of *bis-meta* substituted aryl seleninic acids containing two perfluoromethyl or perfluorooctyl chains.^[15] The acids were active catalysts for the conversion of *para*-nitrobenzaldehyde to *para*-nitrobenzoic acid in the presence of hydrogen peroxide (Figure 4.2). The perfluorooctyl derivative was found to have higher activity, which was attributed to the greater electron-withdrawing effect of the more heavily fluorinated chain leading to an enhanced oxidising power. However, work on the electronic properties of a wide variety of triarylphosphines clearly indicates that CF₃ and longer perfluoroalkyl chains are actually very similar, signifying that the length of a perfluoroalkyl chain has no impact on their electron withdrawing properties.^[18]

The fluorous acids used by Sheldon could be recycled using fluorous separation techniques and were active over five cycles. The system used involved triphasic conditions; perfluorodecalin containing 2 mol % of the catalyst, 1,2-dichloroethane containing the substrate and aqueous hydrogen peroxide as the catalyst reoxidant. The mixture was stirred at 80 °C for 4 to 8 hours then cooled to 10 °C and the product phase separated. The perfluorodecalin phase was reused in the subsequent cycle. Although the catalyst remained active until the fifth run, yields fell from 90 to 50%. The use of expensive fluorous solvents and toxic dichloroethane in this system are also of concern.

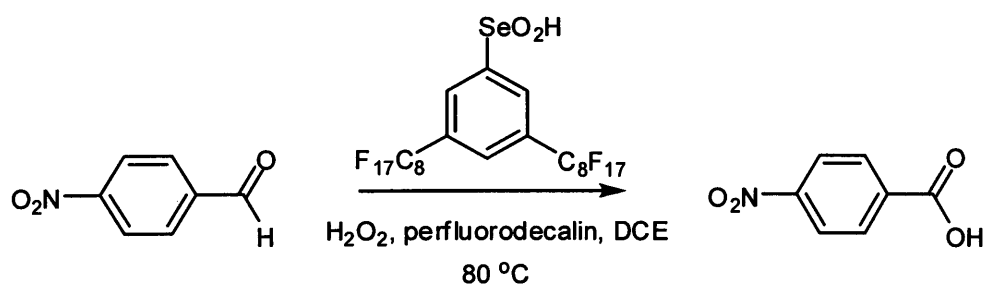


Figure 4.2. Selenium-catalysed oxidation of *para*-nitrobenzaldehyde

A similar fluororous seleninic catalyst was prepared Knochel *et al.*^[16] The group used a 2,4-bis(perfluorooctyl)phenyl butylselenide as the catalyst precursor for the epoxidation of a series of olefins with hydrogen peroxide as reoxidant (Figure 4.3). The reactions were carried out under fluororous biphasic conditions using perfluorooctyl bromide and benzene as the catalyst and reagent phases respectively. In the epoxidation of cyclooctene, the catalyst phase could be recycled ten times with no reduction in yield. The amount of catalyst leaching to the benzene phase, as calculated by ¹⁹F NMR spectroscopy integration against internal fluorobenzene, was shown to be as low as 0.1% per cycle.

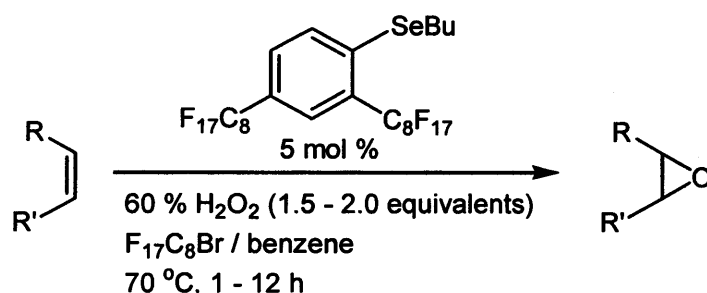


Figure 4.3. Selenium-catalysed olefin epoxidation with hydrogen peroxide

Recently, a simpler seleninic acid precatalyst, perfluorooctyl seleninic acid, was utilised by Crich in the catalytic oxidation of aryl alkylketones to ketoacids^[19] and in a series of allylic oxidations^[20] (Figure 4.4). The group reasoned that as electron poor seleninic acids possessed greater oxidising power, removing the benzene ring and directly attaching a perfluorooctyl chain to the selenium would further improve the acid's catalytic activity. This highly fluororous species was also recovered and reused using fluororous techniques. The recovery method involved reduction of the seleninic acid with sodium metabisulphite to a fluororous diselenide. The crude reaction mixture was washed with water and then partitioned between dichloromethane and perfluorohexanes in a continuous extractor. Separation and evaporation of the fluororous phase allowed the catalyst to be recovered in the form of the diselenide, which was reoxidised *in situ* to the seleninic acid precatalyst at the start of the next cycle. Although the group reported acceptable product yields and recovery of between 86 and 92% of the catalyst, no results from subsequent catalytic cycles were given.

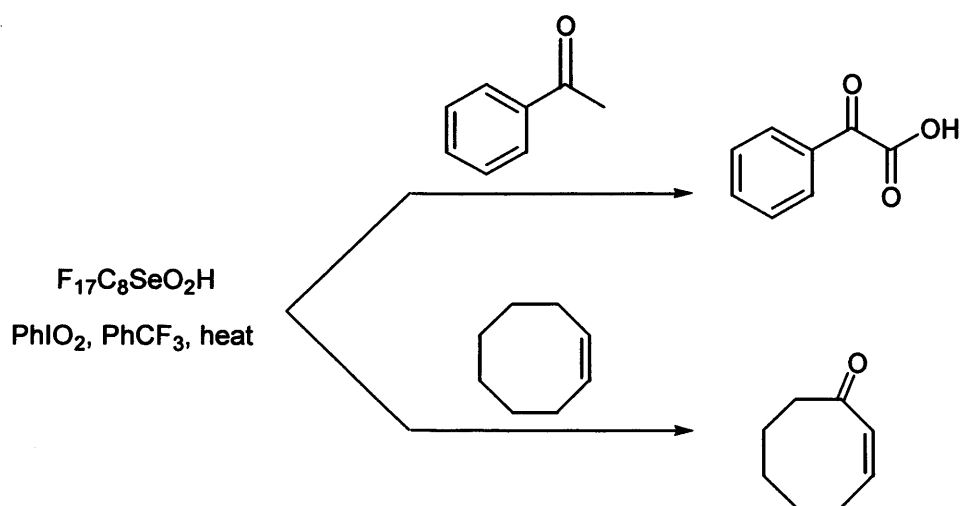


Figure 4.4. Oxidations catalysed by perfluorooctyl seleninic acid

4.2. Results and Discussion

4.2.1. Synthesis of Fluorous Selenium Catalysts

Initially, we sought to conduct a comparison between the efficiency of the fluorous/organic liquid/liquid extraction recycling of Sheldon^[15] and that of fluorous zirconium phosphonates as a catalyst support material in the oxidation of benzaldehyde to benzoic acid. However, attempts to synthesise perfluoroalkylated aryl seleninic acids (Figure 4.5) proved unsuccessful in our laboratory, due to apparent oxidation of the butyl selenium lithiate before reaction with the appropriate perfluoroalkyl halide could occur. Therefore, we turned our attention to the alkyl seleninic acids.

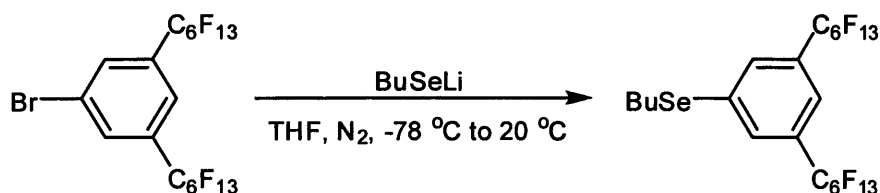
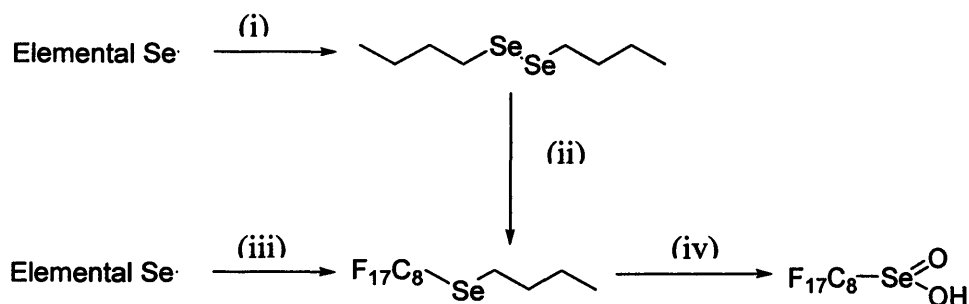


Figure 4.5. Synthetic route to fluorous aryl selenides

Alkyl seleninic acids may be prepared *via* the appropriate alkyl butyl selenide, which are attained by radical-initiated addition of an alkyl iodide to dibutyl diselenide (Scheme 4.6).^[19] We have determined that it is possible to synthesise the perfluoroalkyl butyl selenides in a single step, from elemental selenium, butyl lithium and an alkyl iodide, by *in situ* synthesis of the dibutyl

diselenide. Oxidation of the perfluoroalkyl butyl selenide afforded the seleninic acid. The compounds identities were confirmed by multinuclear NMR spectroscopies, mass spectroscopy and elemental analysis.



Scheme 4.6. (i) NaOH, hydrazine hydrate, TBAB, BuBr (ii) DMF, $F_{17}C_8I$, $Na_2S_2O_5$, Rongalite, N_2 (iii) THF, BuLi, $F_{17}C_8I$, Rongalite (iv) H_2O_2

4.2.2. Oxidation of *para*-Nitrobenzaldehyde with Perfluorooctyl Seleninic Acid

To ensure that the perfluorooctyl seleninic acid was an active catalyst for the reaction, a series of homogeneous oxidations (Figure 4.7) were first carried out. Previous work, conducted using seleninic acids as oxidation catalysts, suggested the use of 1,2 dichloroethane (DCE) as solvent.^[15] The reactions had been carried out in a fluorous triphase system and DCE had been chosen as a non-oxidisable, non-basic, polar liquid that was poorly miscible with perfluorinated solvents.

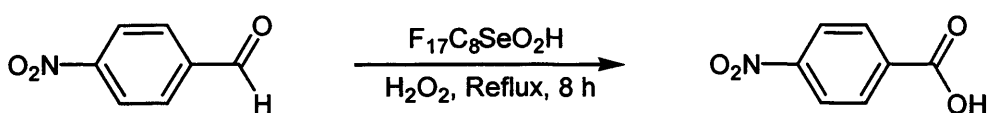


Figure 4.7. Oxidation of *para*-nitrobenzaldehyde with perfluorooctyl seleninic acid

In this work, reactions were first carried out using a procedure based on the triphasic system; 2 mol % catalyst and a five-fold excess of hydrogen peroxide were added to a solution of *para*-nitrobenzaldehyde in 15 cm³ of solvent in a 50 cm³ Schlenk tube. The tube was closed and stirred at reflux for 8 hours. Conversions to the desired carboxylic acid product were determined by ¹H NMR spectroscopy studies and results are shown in Table 4.8. The product was purified by column chromatography and isolated yields corresponded well with the conversions calculated by NMR spectroscopy. These preliminary experiments showed that the perfluorooctyl seleninic acid was an active catalyst in the presence of hydrogen peroxide and, furthermore, that less toxic solvents than

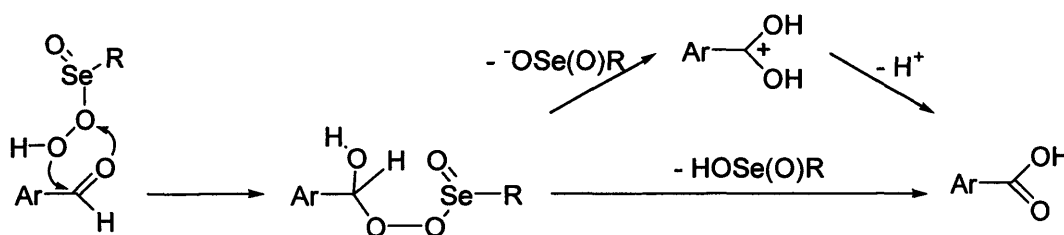
DCE could be employed to give equally high conversions despite reduced solubility of the substrate. Almost quantitative conversions were attained even when the substrate was suspended in a fluoruous solvent, for example PP3, in which it had virtually no solubility.

Entry	Solvent	Time (h)	Temperature (°C)	Conversion to Desired Product	Isolated Yield
1 ^a	DCE	8	80	33%	-
2	DCE	8	80	94%	91%
3	Et ₂ O	8	40	99%	96%
4	MeCN	8	80	99%	99%
5	PP3	8	80	98%	96%
6	DCE/PP3 biphase	8	80	99%	97%

Table 4.8. Homogeneous catalytic oxidation of *para*-nitrobenzaldehyde to *para*-nitrobenzoic acid

^a no catalyst used

The mechanistic scheme for the production of aryl carboxylic acids from aryl aldehydes, as proposed by Mlochowski's group,^[14] is shown below in Scheme 4.9. After oxidation by hydrogen peroxide, the selenonic acid reacts with the aldehyde and is subsequently lost as the seleninic acid catalyst-precursor.



Scheme 4.9. Mechanism for the oxidation of aryl aldehydes

4.2.3. Oxidation of *para*-Nitrobenzaldehyde with Supported Perfluorooctyl Seleninic Acid

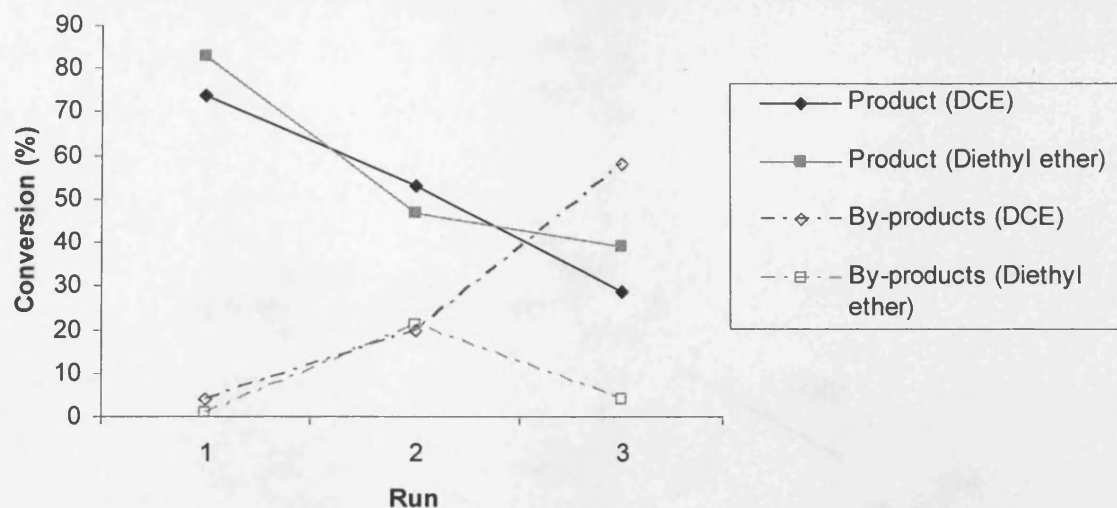
As the previous recycling experiments (see chapter 3) had shown that the solid phase extraction recovery protocol had been less effective than the solid-supported approach, recycling studies for the selenium catalyst focused on the latter system. A series of heterogeneous catalytic runs was conducted using 2 mol % of the seleninic acid supported on amorphous fluoruous zirconium phosphonate, [Zr(O₃P-C₆H₄-4-C₆F₁₃)₂] (Table 4.10). The substrate was added to a 15 cm³

suspension of supported perfluorooctyl seleninic acid and hydrogen peroxide in a 50 cm³ ampoule and refluxed with stirring for 8 hours. After cooling, the reaction mixture was filtered and the solid washed with additional reaction solvent (15 cm³) in order to elute the substrate and product from the catalytic support. The support was then dried under vacuum for use in the next catalytic run. Reactions were carried out in DCE, as a comparison to existing literature work,^[15] and in diethyl ether. This solvent was selected since results under homogeneous conditions were comparable to those in DCE at a higher temperature, it is far less toxic and has desirable miscibility properties with catalyst, i.e. at room temperature the catalyst has very limited solubility but dissolves in ether at reflux, as shown by simple quantitative dissolution tests involving observation of 10 mg of perfluorooctyl seleninic acid in 5 cm³ of solvent at the two aforementioned temperatures. Thus, the catalyst may be made homogeneous during the reaction but after cooling should precipitate onto the support, aiding recovery by filtration. However, ¹⁹F NMR studies of the crude product after filtration show the presence of significant amounts of catalyst.

Entry	Solvent	Time (h)	Temperature (°C)	Conversion to Desired Product (%)	Conversion to By-products (%)
1	DCE	8	80	74	4
2 ^a	DCE	8	80	50	20
3 ^b	DCE	8	80	29	58
4	Et ₂ O	8	40	83	1
5 ^c	Et ₂ O	8	40	47	21
6 ^d	Et ₂ O	8	40	39	4
7	Et ₂ O	8	R.T.	73	13

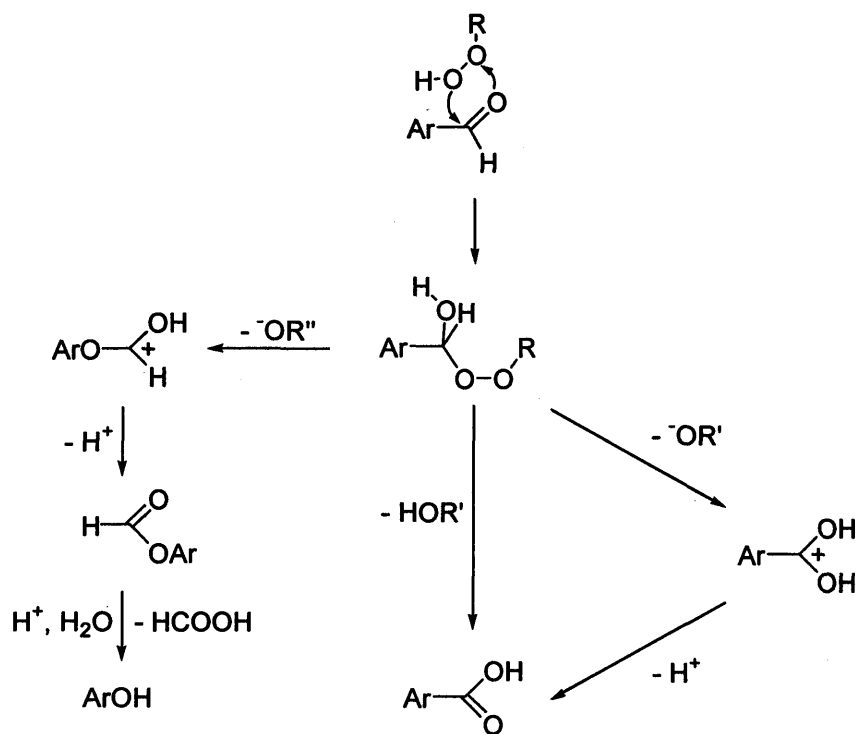
Table 4.10. Heterogeneous catalytic oxidation of *para*-nitrobenzaldehyde to *para*-nitrobenzoic acid with F₁₇C₈SeO₂H supported on amorphous [Zr(O₃P-C₆H₄-4-C₆F₁₃)₂]

^a recycle of entry 1, ^b recycle of entry 2, ^c recycle of entry 4, ^d recycle of entry 5



Graph 4.11. Conversions to desired oxidation product and by-product in DCE and Et₂O

The recycling results for the supported catalysis are summarised in Table 4.10 and in Graph 4.11. A fall in conversion to desired product in the subsequent runs is accompanied by an increase in the formation of a complex mixture of by-products, also suggesting catalyst leaching. Both solvent systems show the same trend but results are marginally better in diethyl ether and a lower reaction temperature is used (~40 °C) in this solvent. It should be noted that the reaction still proceeds at room temperature in Et₂O but here conversion to the desired product is lower and the formation of by-products increased. ¹H NMR spectroscopy showed that the major by-product in the reaction was *p*-nitro-phenol. In their review of selenium-based oxidations,^[14] Mlochowski's group proposed the following scheme for the formation of the desired product and the major by-product (Scheme 4.12).



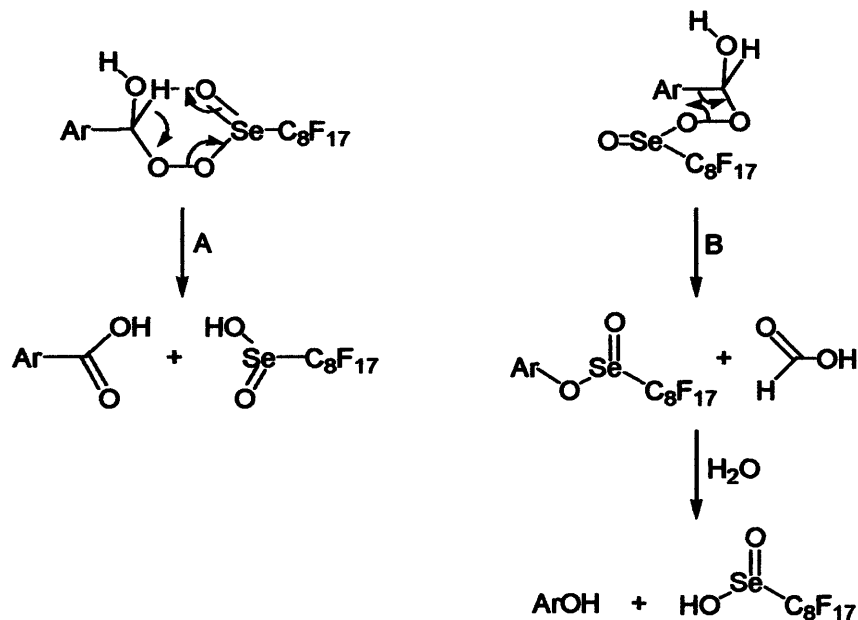
Scheme 4.12. Mechanism for formation of aryl carboxylic acids and phenols from aryl aldehydes

As the amount of phenol increases in subsequent catalytic runs it is proposed that this is the product of an uncatalysed pathway, arising since leaching results in lower concentrations of catalyst in these subsequent runs. The aldehyde substrate may react with either the catalyst ($R = \text{Se}(\text{O})\text{R}$ in Scheme 4.12) or the hydrogen peroxide ($R = \text{H}$ in Scheme 4.12), which is the catalyst reoxidant, to form a peroxy acid. This peroxy acid then undergoes further reaction to form the aryl carboxylic acid or by-products such as phenol.

One explanation for the difference in the products of the two pathways is that the perfluorooctyl group of the seleninic acid introduces selectivity through its steric bulk. Alternatively, hydrogen bonding to the selenium's double bonded oxygen allows the formation of a six-membered transition state, which may undergo a pericyclic rearrangement to form the carboxylic acid product and regenerate the catalyst precursor in a concerted step (pathway A in Scheme 4.13). The catalyst precursor may then be reoxidised by hydrogen peroxide and catalyse the reaction further.

Formation of the phenol by-product (pathway B in Scheme 4.13) is disfavoured with the selenium-based intermediate. Firstly, the bulk of the perfluoroalkyl-bearing selenium sterically hinders the arrangement of the intermediate into the necessary conformation. Secondly, both the double-bonded oxygen and the perfluorooctyl chain of the selenium are electron-withdrawing,

which decreases the nucleophilicity of the peroxide oxygen. Therefore, the three factors; steric, electronic and hydrogen bonding, favour formation of the carboxylic acid product (pathway A in Scheme 4.13) over the phenol by-product with the selenium catalyst-based intermediate.

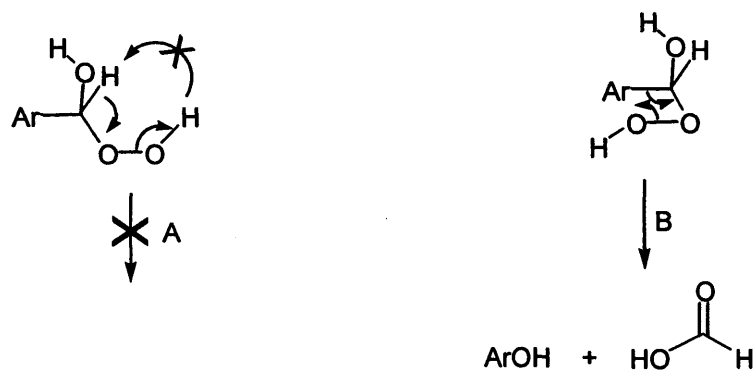


Scheme 4.13. Possible rearrangements of the perfluorooctyl seleninic acid reaction intermediate
Hydrogen bonding shown in red

For the peroxy intermediate, formed by reaction with hydrogen peroxide, the favourable six-membered ring arrangement is not possible, such that the pericyclic reaction leading to the desired product may not proceed (pathway A in Scheme 4.14).

However, the intermediate may rearrange to allow aryl migration and the formation of a phenol and formic acid. The steric problems associated with the selenium, and its perfluoroalkyl chain, do not apply here, thus the conformation necessary for aryl migration is not energetically disfavoured. Also, where as the selenium atom is electron deficient and has an inductive effect on its peroxide oxygen, in the hydrogen peroxide intermediate the effect is reversed, as there is an electron donating inductive effect from the hydrogen to the oxygen.

Thus, pathway B (Scheme 4.14) is favoured for the hydrogen peroxide intermediate and pathway A (Scheme 4.13) is favoured for the catalyst peroxy intermediate and phenol formation is far less probable.



Scheme 4.14. Possible rearrangements of the hydrogen peroxide reaction intermediate

Samples of the products from each run were analysed by ICP-OES to determine the percentage of catalyst which had been lost from the support to the organic phase. The calculated quantities of $F_{17}C_8SeO_2H$ lost to the product phase are shown in Table 4.15. The levels of leaching found for the reactions in diethyl ether were much higher than expected, suggesting that the catalyst did have some solubility in this solvent at room temperature. Leaching levels in dichloroethane were lower but still unacceptably high.

Entry	Mass of Material Recovered by Filtration (g)	Solvent	Loss of Catalyst Per Run (%)	Loss of Catalyst Accumulative (%)
1	0.199	Et ₂ O	11.5	11.5
2 ^a	0.192	Et ₂ O	0.8	12.3
3 ^b	0.215	Et ₂ O	0.4	12.7
4	0.230	DCE	2.6	2.6
5 ^c	0.256	DCE	2.5	5.1
6 ^d	0.279	DCE	0.3	5.4

Table 4.15. Leaching of $F_{17}C_8SeO_2H$ catalyst into product phase determined by ICP-OES

^a recycle of entry 1, ^b recycle of entry 2, ^c recycle of entry 4, ^d recycle of entry 5

A further problem with this protocol arose from the fact that the mass of material recovered by filtration after the catalytic run in the initial testing was greater than the original mass of supported catalyst used (the mass of the supported catalyst used in the first run was 0.210 g). This was attributed to the low solubility of the product, which was not completely eluted from the support during the wash phase of the recovery process. This problem was overcome by running the reaction in a larger volume of solvent (25 cm³), which also led to improved conversions and the reaction was found to be complete after just 4 hours of heating.

In an attempt to minimise catalyst leaching a number of reaction variables were altered. Firstly, an alternative solvent was sought in which the catalyst had no solubility. The surfactant-like nature of the $F_{17}C_8SeO_2H$ afforded it poor solubility in most conventional organic and fluoruous solvents at room temperature, with total dissolution requiring heating in most cases. A series of qualitative solubility tests (results in Table 4.16) determined that acetonitrile was the most suitable solvent for the reaction. The catalyst had very limited solubility in boiling acetonitrile but both the starting material and product were readily soluble.

Entry	Solvent	Soluble at Room Temperature	Soluble in Boiling Solvent
1	DCE	No	No
2	Et ₂ O	No	Yes
3	MeCN	No	No
4	THF	Yes	-
5	DMSO	Yes	-
6	DME	Yes	-
7	MeCH(OH)Me	No	Yes
8	F ₃ CCH(OH)CF ₃	Yes	-
9	F ₃ CCH ₂ OH	No	Yes
10	BTF	No	Yes
11	C ₆ F ₁₄	No	No

Table 4.16. Solubility of 10 mg of $F_{17}C_8SeO_2H$ in 3 cm³ various solvents

The excess of hydrogen peroxide was also reduced from 5 to 2 equivalents due to concerns that the mixture of polar reagents in the solution may be increasing the catalyst's solubility and thus increasing the extent of leaching, since it is possible that the selenium found in the organic phase is in the form of the active catalyst; $F_{17}C_8SeO_3H$. This perfluorooctyl selenonic acid is more polar than the precursor, $F_{17}C_8SeO_2H$, and would, therefore, be more likely to dissolve in polar solvent mixtures. Reducing the excess of hydrogen peroxide may reduce the proportion of selenium present in the selenonic acid form and reduce the polarity of the solvent, thereby reducing leaching. Also, in related selenium-catalysed oxidation work, Crich reported that the use of excesses of hydrogen peroxide as catalyst reoxidant, rather than improving yields, led to complex mixtures of by-products.^[20]

The results from the next series of recycling experiments with the protocol alterations mentioned above are shown in Table 4.17. The use of acetonitrile gave the lowest leaching levels

attained thus far but led to an increase in the formation of by-products. The reason for this is likely to be that, as the catalyst is poorly soluble in acetonitrile, the catalyst remains immobilised upon the surface of the solid support, does not interact with the substrate and, therefore, the non-catalysed pathway dominates. Furthermore, the insoluble by-products may be coating the surface of the support, trapping the catalyst and resulting in further decreases in conversions to the desired product in successive runs.

However, with these conditions the diethyl ether experiments showed more favourable results. The reaction was much cleaner, with less by-product formation and improved recyclability (Table 4.17). Selenium leaching levels were substantially reduced, from 12.7% total selenium in the initial studies down to 4.8%. The improvement in leaching is attributed to the reduction in the volume of H₂O₂ used.

Entry	Solvent	Time (h)	Temperature (°C)	Conversion to Desired Product (%)	Conversion to By-products (%)
1	MeCN	4	40	56	22
2 ^a	MeCN	4	40	24	69
3 ^b	MeCN	4	40	11	81
4	Et ₂ O	4	40	89	0
5 ^c	Et ₂ O	4	40	74	16
6 ^d	Et ₂ O	4	40	45	46

Table 4.17. Heterogeneous catalytic oxidation of *para*-nitrobenzaldehyde to *para*-nitrobenzoic acid with F₁₇C₈SeO₂H supported on amorphous [Zr(O₃P-C₆H₄-4-C₆F₁₃)₂]

^a recycle of entry 1, ^b recycle of entry 2, ^c recycle of entry 4, ^d recycle of entry 5

Entry	Mass of Material Recovered by Filtration (g)	Solvent	Loss of Catalyst Per Run (%)	Loss of Catalyst Accumulative (%)
1	0.204	MeCN	1.4	1.4
2 ^a	0.185	MeCN	0.7	2.1
3 ^b	0.167	MeCN	0.1	2.2
4	0.208	Et ₂ O	3.5	3.5
5 ^c	0.206	Et ₂ O	0.9	4.4
6 ^d	0.195	Et ₂ O	0.4	4.8

Table 4.18. Leaching of F₁₇C₈SeO₂H catalyst into product phase determined by ICP-OES

^a recycle of entry 1, ^b recycle of entry 2, ^c recycle of entry 4, ^d recycle of entry 5

The level of leaching into the product (Table 4.18), despite the catalyst's apparent limited solubility, suggested that an alternative work-up procedure was required for an effective separation. One possible approach would be to carry out the reaction in diethyl ether, to obtain the associated high levels of conversion, remove the solvent under vacuum and wash the resulting solid with acetonitrile to minimise loss of the selenium compounds. Although this method would combine the benefits of each solvent, the level of leaching associated with the acetonitrile would still be unacceptably high. The fact that the seleninic acid catalyst precursor ($F_{17}C_8SeO_2H$) is insoluble in acetonitrile, even at reflux, supports the proposition that selenium is lost as the selenonic acid ($F_{17}C_8SeO_3H$).

Crich^[19, 20] reported that reduction of $F_{17}C_8SeO_2H$ with sodium metabisulfite yields the fluorous diselenide $F_{17}C_8SeSeC_8F_{17}$. In Crich's work this diselenide was separated and recovered using a fluorous/organic continuous extractor. It was proposed that the high fluorine content of this molecule may cause it to be retained on the surface of the fluorous zirconium support when eluting products with a polar, fluorophobic solvent. This reduction would also overcome the possible problem that the selenium was being lost as a mixture of species; the seleninic acid catalyst precursor ($F_{17}C_8SeO_2H$) and the selenonic acid ($F_{17}C_8SeO_3H$). A new process was thus tested; after the catalytic run was finished 10 equivalents of base ($Na_2S_2O_5$) were added and the mixture stirred for two hours to reduce the selenium species to the diselenide. The solvent was removed under vacuum and the resulting solid washed with methanol, to elute the product, and then dried for use in the subsequent catalytic run. Fluorous zirconium phosphonate with a catalyst loading of 2 mol % was tested. The results are displayed in Table 4.19.

Entry	Solvent	Time (h)	Temperature (°C)	Conversion to Desired Product (%)	Conversion to By-products (%)
1	Et ₂ O	4	40	94%	0% by-prod
2 ^a	Et ₂ O	4	40	95%	1% by-prod
3 ^b	Et ₂ O	4	40	82%	4% by-prod
4 ^c	Et ₂ O	4	40	59%	4% by-prod

Table 4.19. Heterogeneous catalytic oxidation of *para*-nitrobenzaldehyde to *para*-nitrobenzoic acid with $F_{17}C_8SeO_2H$ supported on amorphous $[Zr(O_3P-C_6H_4-4-C_6F_{13})_2]$

^a recycle of entry 1, ^b recycle of entry 2, ^c recycle of entry 3

Conversions were considerably improved using this protocol. Levels of conversion to the desired oxidation product exceeding 80% were maintained until the fourth run, in which conversion fell to 59%. Importantly, the amount of unwanted by-product formed in each run was reduced to

almost zero. However, selenium leaching levels (Table 4.20) were slightly higher than that for the previous approach when using diethyl ether, and were almost three times that lost when acetonitrile was used. It was proposed that the reason the leaching had increased, despite improvements in conversion, was that not all of the seleninic acid had been reduced to the selenide dimer. Therefore, during the product elution wash with methanol any remaining seleninic (RSeO₂H) or selenonic (RSeO₃H) acid would be readily dissolved by the methanol and lost to the product phase. Increasing the time that the product mixture was stirred with base would allow for a greater percentage of the acid to be converted to dimer and, therefore, leaching levels should be reduced. To test this theory, a single catalytic oxidation was carried out, allowed to cool to room temperature and stirred for 6 hours with 10 equivalents of base. After filtration as described above, the product was analysed and found to contain 2.0% of the total selenium used in the reaction. Thus, by increasing the reaction time for the reduction, leaching had been halved. It was, therefore, proposed that all subsequent catalytic runs would be stirred overnight to maximise conversion to the fluoros selenide dimer and minimise selenium leaching.

The mass of support recovered after the filtration/wash step was weighed. The observed masses correspond to the initial amount of solid-supported catalyst used, minus some small mechanical losses. This indicates that, using this protocol, the majority of the product is being washed from the solid support, unlike the observations in the initial experiments.

Entry	Mass of Material Recovered by Filtration (g)	Solvent	Loss of Catalyst Per Run (%)	Loss of Catalyst Accumulative (%)
1	0.207	Et ₂ O	3.9	3.9
2 ^a	0.198	Et ₂ O	2.4	6.3
3 ^b	0.198	Et ₂ O	0.1	6.4
4 ^c	0.173	Et ₂ O	0.1	6.5

Table 4.20. Selenium leaching into product phase determined by ICP-OES

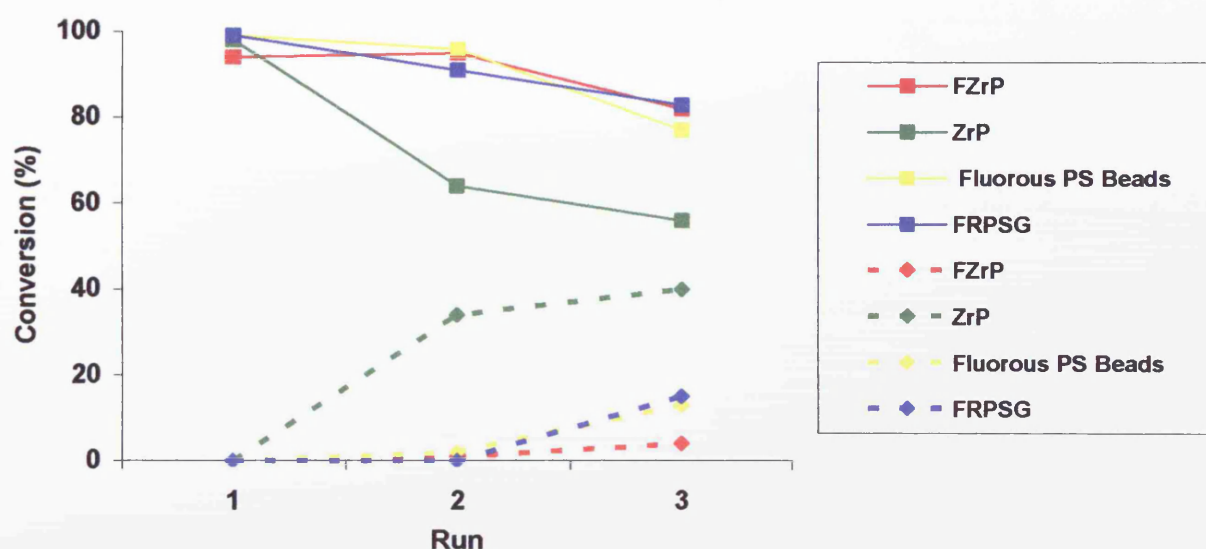
^a recycle of entry 1, ^b recycle of entry 2, ^c recycle of entry 3

4.2.4. Comparison of Catalyst Support Materials

To determine if the zirconium phosphonates perform superiorly as solid supports compared to other perfluorinated compounds, a series of catalytic oxidations was conducted using perfluorooctyl seleninic acid immobilised on the surface of four different supports. As with the dirhodium(II) perfluorocarboxylate work discussed in chapter three, commercially available fluoros reverse phase silica gel, perfluorinated polystyrene beads and fluoros and non-fluoros

zirconium phosphonates were compared. The FRPSG used was Fluoroflash® silica gel with a particle size of 40 µm. The polystyrene beads, prepared in our laboratory, were 10% cross linked with divinyl benzene and were between sieve mesh size of 10 and 40. The zirconium phosphonates used were amorphous forms of phenyl zirconium phosphonate and 4-perfluorohexylphenyl zirconium phosphonate. The fluoros silica and fluoros zirconium phosphonates possessed perfluorohexyl, C₆F₁₃, chains and the polymer beads perfluorooctyl, C₈F₁₇, chains.

The same reaction conditions as described above were used (2 mol % catalyst, Et₂O, 40 °C) and after cooling, the mixture was stirred with sodium metabisulphite overnight. The reaction solvent was then removed under vacuum and resulting solid washed with methanol and water then dried for use in the next run. The supported catalysts were recycled for three runs. The conversions for each support material are summarised in Graph 4.21 and Table 4.22.



Graph 4.21. Graph of conversion to desired product (solid line) and by-product (dashed line) using different catalyst support materials

In terms of conversion to the desired oxidation product the three fluorinated solid supports perform equally well. The first run for each is almost quantitative, with a slight fall in the second and third runs leading to final conversions of around 80%. In all cases, the amount of phenol by-product formed is negligible until the third run, in which it increases for the FRPSG and fluoros polystyrene beads systems.

As expected, the non-fluorous phenyl zirconium phosphonate performed slightly less well than the fluoros supports. The conversion in the first run starts as high as those for the other fluorinated supports but then drops substantially in the following runs. This suggests that the absence of perfluoroalkyl chains on the surface results in greater leaching of the catalyst.

Entry	Solvent	Temperature (°C)	Support Used	Conversion to Desired Product (%)	Conversion to By-products (%)
1	Et ₂ O	40	Zr(O ₃ P-C ₆ H ₄ -4-C ₆ F ₁₃) ₂	94	0
2 ^a	Et ₂ O	40	Zr(O ₃ P-C ₆ H ₄ -4-C ₆ F ₁₃) ₂	95	1
3 ^b	Et ₂ O	40	Zr(O ₃ P-C ₆ H ₄ -4-C ₆ F ₁₃) ₂	82	4
4	Et ₂ O	40	Zr(O ₃ PPh) ₂	98	0
5 ^c	Et ₂ O	40	Zr(O ₃ PPh) ₂	64	34
6 ^d	Et ₂ O	40	Zr(O ₃ PPh) ₂	56	40
7	Et ₂ O	40	Fluorous PS beads	99	0
8 ^e	Et ₂ O	40	Fluorous PS beads	96	2
9 ^f	Et ₂ O	40	Fluorous PS beads	77	13
10	Et ₂ O	40	FRPSG	99	0
11 ^g	Et ₂ O	40	FRPSG	91	0
12 ^h	Et ₂ O	40	FRPSG	83	15

Table 4.22. Heterogeneous catalytic oxidation of *para*-nitrobenzaldehyde to *para*-nitrobenzoic acid with F₁₇C₈SeO₂H supported on fluorous and non-fluorous supports

^a recycle of entry 1, ^b recycle of entry 2, ^c recycle of entry 4, ^d recycle of entry 5, ^e recycle of entry 7, ^f recycle of entry 8, ^g recycle of entry 10, ^h recycle of entry 11

Although the respective decrease and increase in product and by-product formation would suggest that loss of the catalyst through leaching is greater for the non-fluorous zirconium phosphonate than for the three fluorous supports, the data from the ICP-OES reveals that this is not the case. In fact, the amount of selenium found in the organic products from the phenyl zirconium phosphonate system is lower than that from the fluorous polystyrene beads, and equal to that for FRPSG (Table 4.23 and Graph 4.24). It is higher, however, than for the fluorous zirconium phosphonate support.

It is unclear why the non-fluorous support retains the fluorous catalyst so effectively. One possible explanation is that the phenyl zirconium phosphonate is more able to retain any unconverted seleninic or selenonic acid than the fluorous supports are. If these polar compounds account for the selenium leaching when using the fluorous supports, these losses are avoided with the non-fluorous material and its associated leaching levels would be lowered. It seems unlikely that the catalyst is immobilised through π -interactions between the phenyl rings of the zirconium phosphonate and the selenium, as was suggested for the dirhodium(II) perfluorocarboxylate complex in chapter three, although the selenium atoms adjacent to the perfluoroalkyl chains would

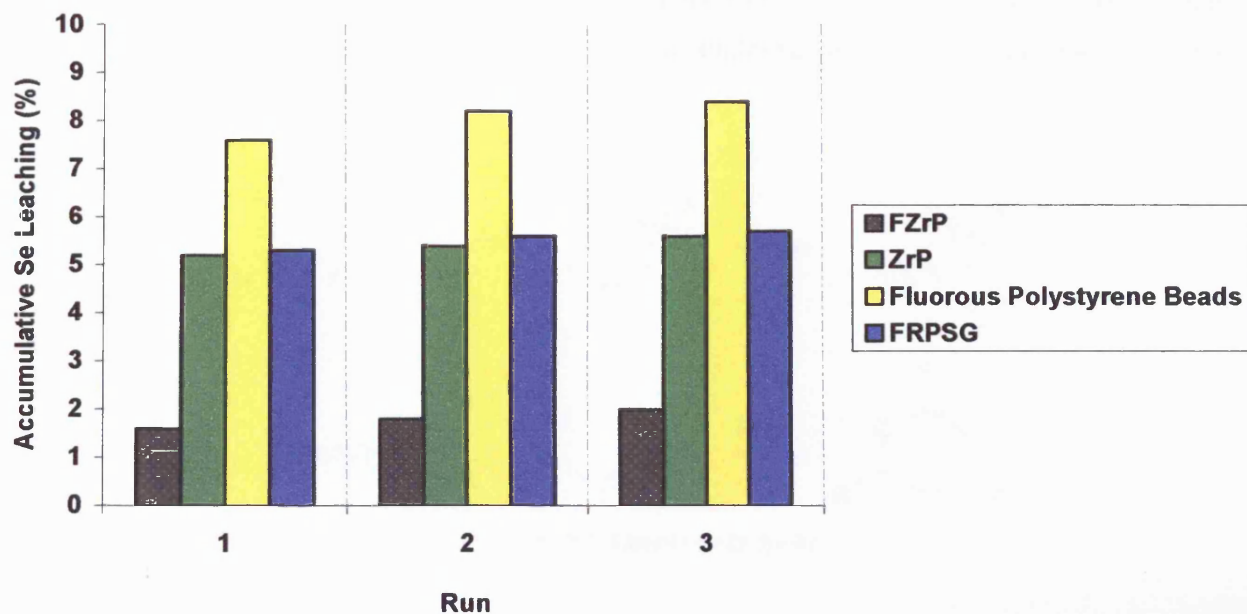
be considerably electron-deficient. The fluorous dimer, $(F_{17}C_8Se)_2$, is insoluble in methanol and, therefore, the majority of the compound will remain on the surface of the solid during the washing phase, regardless of whether the support bears perfluoroalkyl chains. Therefore, solubility may be the major factor in catalyst leaching using this protocol.

Of the three fluorinated supports, the fluorous zirconium phosphonate gives the lowest selenium losses, with a total of just 2% of catalyst lost over 3 runs (Table 4.23). This is almost 3 times less than that for FRPSG and a quarter of that lost with fluorous polystyrene beads.

Entry	Support Used	Loss of Catalyst Per Run (%)	Loss of Catalyst Accumulative (%)
1	$Zr(O_3P-C_6H_4-4-C_6F_{13})_2$	1.6	1.6
2 ^a	$Zr(O_3P-C_6H_4-4-C_6F_{13})_2$	0.2	1.8
3 ^b	$Zr(O_3P-C_6H_4-4-C_6F_{13})_2$	0.2	2.0
4	$Zr(O_3PPh)_2$	5.2	5.2
5 ^c	$Zr(O_3PPh)_2$	0.2	5.4
6 ^d	$Zr(O_3PPh)_2$	0.2	5.6
7	Fluorous PS beads	7.6	7.6
8 ^e	Fluorous PS beads	0.6	8.2
9 ^f	Fluorous PS beads	0.2	8.4
10	FRPSG	5.3	5.3
11 ^g	FRPSG	0.3	5.6
12 ^h	FRPSG	0.1	5.7

Table 4.23. Selenium leaching into product phase determined by ICP-OES

^a recycle of entry 1, ^b recycle of entry 2, ^c recycle of entry 4, ^d recycle of entry 5, ^e recycle of entry 7, ^f recycle of entry 8, ^g recycle of entry 10, ^h recycle of entry 11



Graph 4.24. Accumulative selenium leaching with different solid supports

4.3. Allylic Oxidation of Cyclooctene

Perfluorooctyl seleninic acid has been used by Crich in the catalytic allylic oxidation of a series of olefins.^[20] The substrate olefin was heated with 10 mol % catalyst and one of a range of reoxidants (Figure 4.25). Of the reoxidants tested, iodoxybenzene gave the cleanest conversion of alkenes to enones and the group reported isolated product yields of between 41 and 65%. The catalyst was recovered by reduction to the fluorous diselenide, followed by partitioning into a fluorous solvent and separation from the organic product phase using a water-cooled continuous extractor.

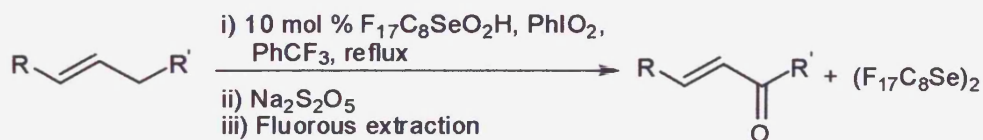


Figure 4.25. Selenium-catalysed allylic oxidation of alkenes

Crich proposed the mechanism shown in Figure 4.26 as a probable route for the oxidation. This mechanism fits well with current mechanistic understanding of selenium-based oxidation reactions.^[20]

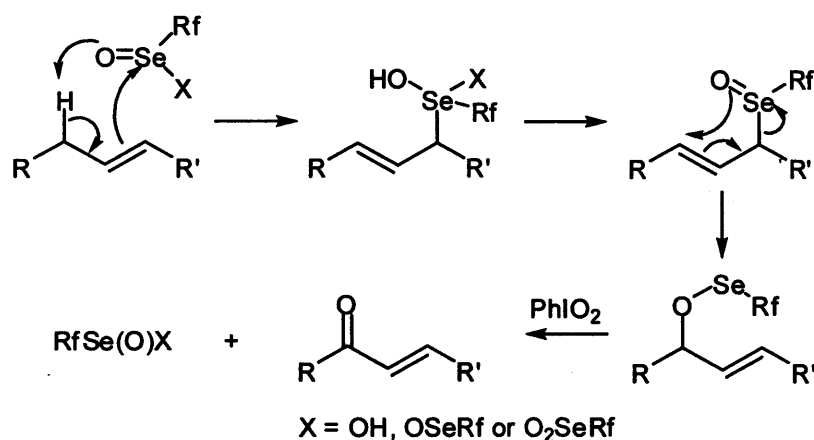


Figure 4.26. Suggested mechanism for oxidation by RfSe(O)X and PhIO_2

In an attempt to increase the applicability of our fluorinated zirconium phosphonate-based catalyst separation method for the perfluorooctyl seleninic acid we sought to apply it to the allylic oxidation of cyclooctene.

Firstly, the reaction was carried out homogeneously, using the same conditions as Crich. Cyclooctene was added to a stirred benzotrifluoride (BTF) suspension of iodoxybenzene and selenium catalyst and the mixture was heated at reflux for 6 hours. Using a stoichiometry of 3 equivalents of reoxidant and 10 mol % of perfluorooctyl seleninic acid gave virtually quantitative conversions, as determined by ^1H NMR analysis, and an 88% yield of isolated product. Even when catalyst loading was reduced to 1 mol %, conversions above 90% are attained. These values are a substantial improvement to the yields obtained for the same substrate in Crich's work, however, the report did not include reaction times.

The reaction was next conducted under supported catalysis conditions with catalyst loadings of both 1 and 10 mol %. The reaction conditions were analogous to those for the homogeneous system. At the end of the reaction 10 equivalents of sodium metabisulphite were added to reduce the seleninic acid to the perfluorooctyl selenide dimer. The solvent was then removed under reduced pressure and the resulting solid was washed with methanol to elute the product and then water to elute the iodoxybenzene and base. The solid-supported catalyst was then dried for further use. Results are shown in Table 4.27. With both 1 and 10 mol % catalyst loadings, conversions in the first run were high (85 and 90% respectively) but were expectedly lower than those for the homogeneous system. However, ^1H NMR spectroscopy studies of the second-run products showed just a trace of the enone product. As the leaching levels for both 1 and 10 mol % loadings were low,

catalyst decomposition and loss is unlikely to be responsible for the dramatic drop in conversion, and is more likely to be a result of catalyst deactivation. If the perfluorooctyl selenide dimer is not reoxidised to the seleninic acid, and thereafter the selenonic acid, by the iodoxybenzene, as it was by hydrogen peroxide in the previous oxidation system, the dimer will remain inert on the surface of the support and catalysis would not occur.

Catalyst Loading	Conversion to Desired Product (%) ^a	Selenium Leaching (%)
1 mol %	85 (<1)	0.9
10 mol %	90 (5)	1.8

Table 4.27. Supported catalytic allylic oxidation of cyclooctene

^a values in parentheses are for the 2nd run

One possible modification to circumvent this problem would be to remove the catalyst reduction step. Removal of the BTF solvent and subsequent washing of the solid by hexane, to elute the product, and elution of the iodoxybenzene may allow the catalyst to be actively recycled. However, based on the data from the previous system, leaching of the catalyst to the organic product phase will be increased. As effective separation of the catalyst from the product is one of this project's main goals, especially in the case of potentially highly toxic compounds such as perfluoroalkylated selenides, this alternative method was not investigated.

As an alternative to supported catalysis, a post-reaction fluorous solid-phase extraction methodology was adopted. At the end of the oxidation reaction the solvent was removed and the residue loaded onto a column of fluorous zirconium phosphonate. The column was first washed with hexane to elute the product and secondly with methanol to elute the catalyst. The catalyst was recovered and reused in this way for up to 3 catalytic runs and results are shown in Table 4.28.

Catalyst Loading	Conversion to Desired Product (%) ^a	Selenium Leaching (%)
1 mol %	91 (47)	19.1
10 mol %	97 (90, 18)	6.5 (9.3)

Table 4.28. Homogeneous catalytic allylic oxidation of cyclooctene

^a values in parentheses are for 2nd (and 3rd) runs

Although this approach affords an improvement in recyclability, as the catalyst is still active after use in the first run, selenium leaching levels are far greater than those for the supported method and conversions fall substantially. When a loading of 1 mol % was used, almost a fifth of the catalyst was lost in the first recycle and the conversion in the second run was halved. With a

catalyst loading of 10 mol % the situation is improved somewhat, and the proportion of catalyst lost through leaching is reduced. However the actual mass of selenium lost is similar for both 1 and 10 mol % loadings, at 0.5 mg and 1.6 mg respectively. Conversions also fall drastically over the three runs from 97 to 18%. As the leaching does not infer complete loss of the catalyst to the organic product phase, catalyst decomposition seems likely. ^{19}F NMR spectroscopy analysis of the recovered selenium compound does indeed show multiple sets of signals for the perfluorooctyl chain. Two sets of signals could result from the presence of the seleninic and selenonic acids. However, the difference in alkene oxidation products obtained with seleninic acids when a peroxide or iodoxybenzene is used as the reoxidant (epoxidation versus allylic oxidation) suggests a difference in the reactivity of the selenium-based catalyst species. Thus, the formation of perseleninic acids (so-called selenonic acids) associated with hydrogen peroxide seems not to be possible with iodoxybenzene. It is, therefore, unclear which fluorine compounds the remaining set of NMR signals arise from.

It is possible that the addition of the same reduction step as used in the aldehyde oxidation reaction previously described before the column step may help to reduce catalyst leaching/decomposition and still allow for an active catalyst in the subsequent runs, as the iodoxybenzene may reoxidise the fluorine selenium dimer more effectively under homogeneous conditions than supported. Other reoxidants, such as peroxides, may also be tested but their use is likely to lead to epoxidation products rather than allylic oxidation products. Due to time restraints, optimisation of the reaction or investigation of these variables was not conducted.

4.4. Conclusions for Chapter 4

The fluoros compound, perfluorooctyl seleninic acid, is an active catalyst for the oxidation of *para*-nitrobenzaldehyde to *para*-nitrobenzoic acid in the presence of hydrogen peroxide as a reoxidant. Under homogeneous conditions the seleninic acid gives good conversions in a range of solvents, in which it has varying solubility.

The catalyst may be supported upon a fluoros zirconium solid support and recycled by filtration at the end of reaction. Conversions to the desired product using the catalyst recovered in this way fall sharply over the course of 3 runs (from 89 to 45%), due to a combination of catalyst leaching and deactivation. The catalyst recyclability may be improved by the post-reaction addition of a weak base, sodium metabisulphite, which reduces the seleninic acid to a diselenide. The resulting compound is highly fluoros and apolar and hence is insoluble in fluorophobic, polar solvents such as methanol. Therefore, the reaction solvent is removed and the resulting solid first washed with methanol to elute the product, secondly with water to elute the base and finally more methanol. The supported catalyst is then dried for use in the next run.

The same supported methodology was implemented to conduct a comparison between a number of fluoros solid support materials. The catalyst was recoverable with all of the supports tested and was active over three runs, but leaching results show that the fluoros zirconium phosphonate performed best at retaining the fluoros selenium compound. Also, a comparison between phenyl zirconium phosphonate and its perfluorohexylated analogue, $[\text{Zr}(\text{O}_3\text{P}-\text{C}_6\text{H}_4-4-\text{C}_6\text{F}_{13})_2]$, demonstrated that the presence of the perfluoroalkyl chains on both catalyst and support reduces the amount of selenium leaching to the product as a result of better 'embedding' of the seleninic acid's fluoros chain into those of the support's surface.

The perfluorooctyl seleninic acid also catalyses the allylic oxidation of cyclooctene in the presence of iodoxybenzene. Attempts at recovery and reuse using a solid-supported catalyst on a fluoros zirconium phosphonate proved unsuccessful as the catalyst was inactive in the second run. Recovery of the catalyst by fluoros solid-phase extraction, using a short column of fluoros zirconium phosphonate proved more productive. The catalyst was reused three times but conversions fell substantially over the three runs. These results suggest that hydrogen peroxide is a more effective catalyst reoxidant than the iodoxybenzene for the perfluorooctyl seleninic acid.

References for Chapter 4

- [1] K. B. Sharpless, R. F. Lauer, *J. Am. Chem. Soc.*, **1973**, *95*, 2697.
- [2] H. L. Riley, J. F. Morley, N. A. C. Friend, *J. Chem. Soc.*, **1932**, 1875.
- [3] H. J. Reich, S. K. Shah, *J. Am. Chem. Soc.*, **1975**, *97*, 3250.
- [4] P. E. Sonnet, *Tetrahedron*, **1980**, *36*, 557.
- [5] K. B. Sharpless, R. F. Lauer, A. Y. Teranishi, *J. Am. Chem. Soc.*, **1973**, *95*, 6137.
- [6] T. Sakakibara, I. Takai, E. Ohara, R. Sudoh, *J. Chem. Soc.*, **1981**, *6*, 261.
- [7] T. Minami, H. Sako, T. Ikehira, T. Hanamoto, I. Hirao, *J. Org. Chem.*, **1983**, *48*, 2569.
- [8] S. Raucher, *Tetrahedron Lett.*, **1977**, *44*, 3909.
- [9] S. V. Ley, A. J. Whittle, *Tetrahedron Lett.*, **1981**, *22*, 3301.
- [10] S. Tomoda, Y. Takeuchi, Y. Nomura, *Synthesis*, **1985**, *2*, 212.
- [11] S. L. Schreiber, C. Santini, *J. Am. Chem. Soc.*, **1984**, *106*, 4038.
- [12] H. Gyoonhee, M. G. LaPorte, J. J. Folmer, K. M. Werner, S. M. Weinreb, *Angew. Chem. Int. Ed.*, **2000**, *39*, 3740.
- [13] T. Wirth, *Angew. Chem. Int. Ed.*, **2000**, *39*, 3740.
- [14] J. Mlochowski, M. Brzascz, M. Giurg, J. Palus, H. Wojtowicz, *Eur. J. Org. Chem.*, **2003**, 4329.
- [15] G.-J. ten Brink, J. M. Vis, I. W. C. E. Arends, R. A. Sheldon, *Tetrahedron*, **2002**, *58*, 3977.
- [16] B. Betzemeier, F. Lhermitte, P. Knochel, *Synlett.*, **1999**, *4*, 489.
- [17] J. Chen, S. Lu, *Applied Catalysis A*, **2004**, *261*, 199
- [18] D. J. Adams, J. A. Bennett, D. Duncan, E. G. Hope, J. Hopewell, A. M. Stuart, A. J. West, *Polyhedron*, **2007**, *26*, 1505.
- [19] D. Crich, Y. Zou, *J. Org. Chem.*, **2005**, *70*, 3309.
- [20] D. Crich, Z. Yekui, *Organic Lett.*, **2004**, *6*, 775.
- [21] D. A. Singleton, C. Hang, *J. Org. Chem.*, **2000**, *65*, 7554.

5. Enantioselective Fluorination Catalysed by Palladium BINAP Complexes

5.1. Introduction to Enantioselective Fluorination

The value and utility of the fluorine atom is exemplified by its presence in a multitude of everyday products. It is an important component of agrochemicals,^[1, 2] refrigerants,^[3] fire-extinguishing agents^[1] and retardants,^[4] non-stick coatings^[1, 5] and anaesthetics,^[1, 6] to name but a few. An ever increasing number of pharmaceuticals contain one or more fluorine atoms as the presence of these atoms allow for increased lipophilicity, greater activity and a reduction of oxidative metabolism of drug molecules within the body, which can lead to toxic by-products. A number of currently used fluorine-containing drugs are displayed below in Figure 5.1. However, none of these contain fluorine at a stereogenic centre, primarily because the techniques for enantioselective fluorination are much more poorly developed than many other enantioselective reactions.

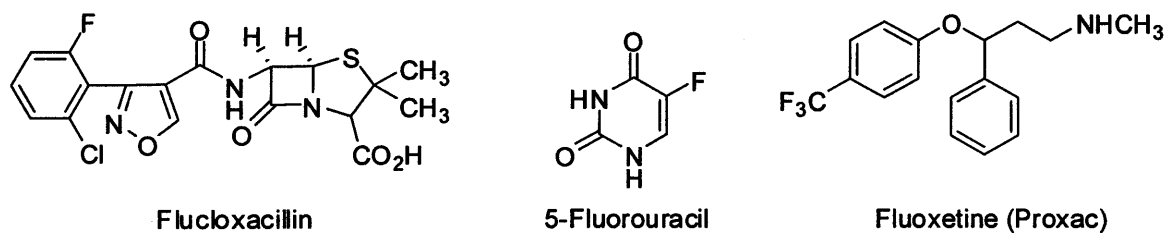


Figure 5.1. Fluorine-containing pharmaceuticals

The ability to enantioselectively prepare a drug molecule is of great importance, as the two stereo-isomers may have radically different chemistries *in vivo*, as in the case of the morning sickness treatment thalidomide, the (*S*) enantiomer of which proved to be teratogenic and led to birth defects in new-born babies.^[7] Due to the beneficial metabolic effects that a fluorine atom imparts upon pharmaceutical compounds, the field of asymmetric fluorination has received considerable interest recently.

There are two approaches to enantioselective fluorination: Firstly, use of a chiral fluorinating agent and secondly, through the use of an achiral fluorinating agent in conjunction with a chiral catalyst or auxiliary group. Clearly, the use of an auxiliary also requires its removal from the product after fluorination has been achieved. Thus, although there are examples of the successful application of these groups,^[8] the use of a chiral fluorinating agent or a chiral catalyst offers a more direct route to the desired fluorination product.

5.1.1. Fluorinating Agents

The wide variety of available fluorinating agents, ranging from elemental fluorine gas to chiral cinchona alkaloids, may be divided into two main classes; electrophilic and nucleophilic. Arguably the most commonly used fluorinating agents are Selectfluor and NFSI (*N*-fluorobenzenesulfonimide), both of which are fluoraza compounds and are electrophilic sources of fluorine (Figure 5.2). The popularity of these fluoraza compounds results from the fact that they offer improved selectivity and ease of use relative to many of the alternative fluorinating agents, such as elemental fluorine, a highly reactive, strongly oxidising toxic gas, the hypofluorites,^[9] a group of explosive, toxic gases and other fluorides such as DAST^[10] (diethylaminosulphur trifluoride) and BAST^[11] (bis{2-methoxyethylaminosulphur trifluoride}), which are thermally unstable and moisture sensitive.

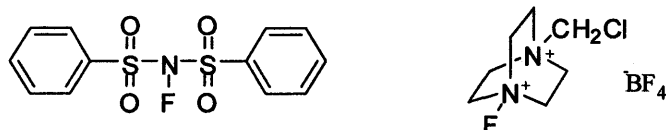


Figure 5.2. The structures of NFSI and Selectfluor

The fluoraza reagents may be neutral compounds, as is the case with NFSI, or charged quaternary ammonium salts, such as Selectfluor. Although both Selectfluor and NFSI are active fluorinating agents for a series of organic substrates such as olefins, aromatics, carbonyl compounds, enol acetates, silyl enol ethers, enamines and carbanions, neither offers the enantioselectivity required for a selective asymmetric fluorination and, therefore, require the addition of a chiral catalyst. Thus, a great deal of work has been undertaken with the aim of developing an active fluorinating reagent with built-in chirality.

5.1.2. Chiral Fluorinating Agents

5.1.2.1. Electrophilic Sources of Fluorine

The first reported example of a chiral fluorinating agent came from Differding and Lang,^[12] who in 1988 synthesised two chiral *N*-fluoro sultams, shown in Figure 5.3.

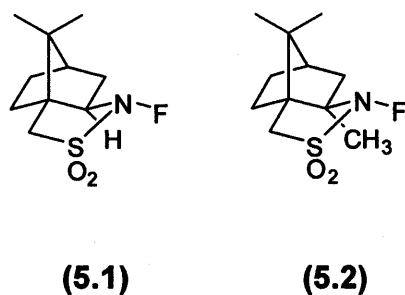


Figure 5.3. Two *N*-fluoro sultams, enantioselective fluorinating agents

These *N*-fluoro sultams were used in the electrophilic enantioselective fluorination of a series of carbonyl compounds *via* their metal enolates. The enantiomeric excesses obtained were generally poor to moderate but some success was achieved in the fluorination of ethyl cyclopentanone-2-carboxylate (Figure 5.4), which formed the major enantiomer in 85% yield. However, sultam (5.1) was found to undergo HF elimination to form its imine precursor as a side reaction. The group attempted to avoid this problem by using sultam (5.2), which replaces the vulnerable hydrogen with a methyl group. However, the resulting sultam was found to be less active and selective in the fluorinations studied.

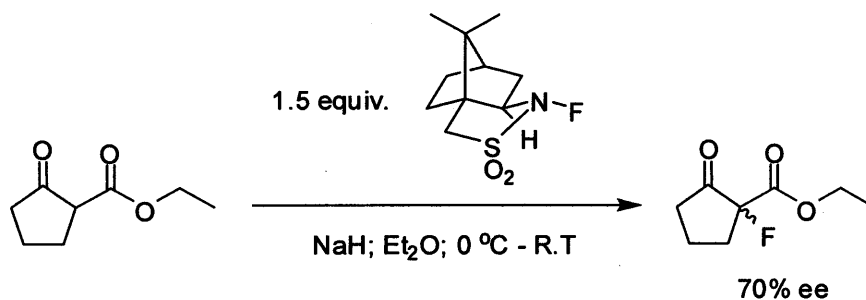


Figure 5.4. Enantioselective fluorination of ethyl cyclopentanone-2-carboxylate

Work on *N*-fluoro sultam-based chiral fluorinating agents was continued by Davis,^[13, 14] who supplemented the molecule with additional steric bulk in an attempt to increase its selectivity. The group showed that the substitution of the two hydrogen atoms on the carbon *ortho* to the nitrogen-bearing carbon for two chlorine atoms led to substantial improvements in ee's for the fluorination of a limited number of substrates. However, enantioselectivities were still poor for most of the substrates tested and in some cases were lower than those obtained by Differding and Lang.

Much research has been conducted on developing the sultam template as an electrophilic fluorinating agent, and several successful examples for non-stereoselective fluorine insertion have been reported.^[15-17] Takeuchi's group continued the evolution of saccharin-based fluorination agents, adding chiral centres in view of inferring enantioselectivity. The group reported three separate works on the synthesis and testing of several closely related fluorinating agents (Figure 5.5) designed to possess a stable but reactive N-F bond.^[17-19]

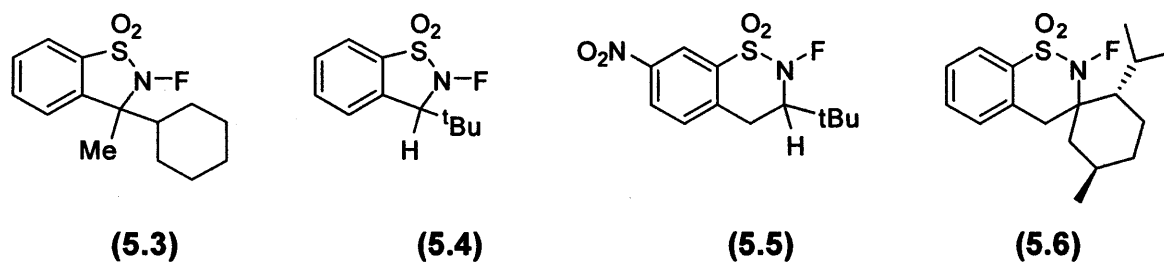
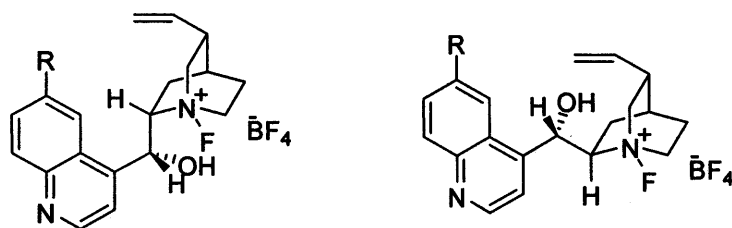


Figure 5.5. *N*-fluoro sulphonamide enantioselective fluorinating agents

Compound **(5.3)**^[17] gave modest yields and ee's of the fluorination products for the limited range of carbonyl compounds tested, except in the case of 2-benzyl-1-tetralone, which was fluorinated in 79% yield and with a promising 88% ee. This reagent was modified to give compound **(5.4)**, in which the steric bulk at the chiral carbon has been adjusted so as to be located on one face of the molecule. This modification was made in an attempt to improve selectivity but led to HF elimination, resulting in the formation of its corresponding imine and poor yields of fluorination product.

To reduce the acidity of the offending proton and prevent HF elimination, Takeuchi expanded the five-membered ring of **(5.4)** and the resulting fluorinating reagent **(5.5)** was found to be more consistently active, leading to isolated yields and ee's in the ranges of 40-79% and 43-69%.^[18] This research represented a step forward in the area as, although enantioselectivities did not exceed the 88% ee obtained with compound **(5.3)**, results were generally superior to those obtained with previous enantioselective fluorinating agents. Additional modifications to this template, leading the group to the synthesis of compound **(5.6)**, failed to further improve on their previous results, or those acquired with the original *N*-fluoro sultams of Differding and Lang.

A new class of enantioselective fluorinating agent arose from two independent reports in 2000, when Cahard^[20] and Shibata^[21] both prepared *N*-fluoro quaternary ammonium salts of cinchona alkaloids (Figure 5.6 and Figure 5.8). These charged species were more reactive than their neutral counterparts and could, therefore, fluorinate a wider range of less nucleophilic substrates, such as enol ethers. Although percentage yields were all high, most being almost quantitative, enantioselectivities for each of the substrates tested were moderate at best, between 36 and 56%.



R = H, OMe

Figure 5.6. *N*-fluoro quaternary ammonium salts prepared by Cahard *et al.*

Cahard's group was able to improve enantioselectivity through the use of a series of hydroxyl protecting groups. The free hydroxyl group of these first generation cinchona alkaloid fluorinating agents was found to protonate the enolate of the carbonyl substrates tested, thus reducing product yields. A series of protecting groups of varying steric bulk were incorporated and the resulting compounds used as reagents for the fluorination of *N*-phthaloylphenylglycine derivatives (Figure 5.7).^[22]

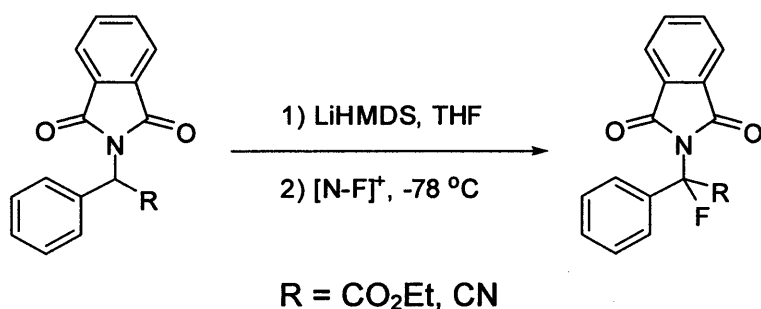


Figure 5.7. The Fluorination of *N*-phthaloylphenylglycine derivatives with *N*-fluoro cinchona alkaloid derivatives

The protected alkaloids gave moderate to good yields and excellent ee's (>90%) in the fluorination of *N*-phthaloyl phenylglycinonitrile (Figure 5.7, R = CN). Cahard's study demonstrated the necessity for the hydroxy protecting groups for the alkaloids when used as fluorinating agents but the protecting groups that gave the better ee's were found to be substrate dependent. The study also suggested that the methoxy group of the quinoline had an effect on enantioselectivity.

Shibata took a different approach to the use of the *N*-fluoro cinchona alkaloids in asymmetric fluorination. Rather than isolating the *N*-fluoro quaternary ammonium salts, the group simply fluorinated the alkaloid with Selectfluor in dry acetonitrile and then added the substrate directly (Figure 5.8). Initially, a quinine/Selectfluor combination was used,^[21] followed by a number of more complex alkaloids.^[23, 24]

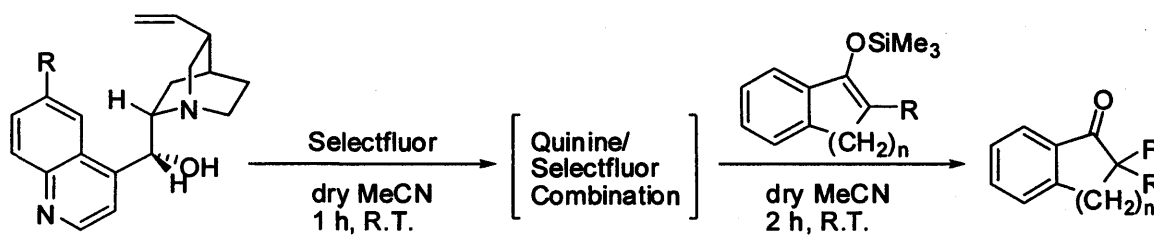


Figure 5.8. Fluorination of silyl enol ethers with a quinine/Selectfluor combination

The results from the initial quinine-based tests were promising, with excellent yields and moderate to high ee's. The reaction conditions could be altered in order to maximise enantioselectivity. By reducing the reaction temperature ee's as high as 91% could be achieved but this resulted in a slight detriment to the fluorinating agent's activity. Thus, isolated yields were lower as the temperature was decreased.

A range of alkaloid/Selectfluor combinations were screened for the fluorination of a number of different carbonyl compounds. Although some excellent yield/ee combinations were acquired for a number of the alkaloids, the results were highly substrate dependent and no clear, overall "best fluorinating agent" could be determined.

5.1.2.2. Nucleophilic Sources of Fluorine

Nucleophilic enantioselective fluorinating agents are generally less effective and less numerous than their electrophilic counterparts. The first reported example came in 1989 from Hann and Sampson,^[25] who used an enantiopure DAST derivative to achieve a low degree of enantioselectivity (16% ee) in the fluorination of ethyl 2-(trimethylsiloxy)propanoate.

In 2001, Beaumont *et al.* reported the use of an enantiopure phosphonium salt for the fluorination of 2-bromopropiophenone, producing enantiomerically enriched 2-fluoropropiophenone in just 35% yield.^[26]

5.1.3. Fluorinating Agents with Chiral Catalysts; Asymmetric Catalysis

Although chiral fluorinating agents, such as those based upon the cinchona alkaloids, have been shown to give some impressive combinations of activity and selectivity, their use requires excessive screening due to their great substrate dependence. In recent years the focus has moved to catalytic systems, to further improve the efficiency of the reaction. The acceleration and control of asymmetric fluorination reactions through chiral catalysts was first reported by Togni in 2000.^[27]

The majority of work involving chiral fluorinating agents involves the fluorination of carbonyl compounds *via* their enol or enolate. The electrophilic fluorination of 1,3 dicarbonyl compounds is catalysed by the addition of Lewis acids, as they greatly increase the enolisation process. The reaction has been targeted in recent years as a model reaction for the study of enantioselective fluorination. Tongi and Hintermann were the first to demonstrate the potential of catalytic enantioselective fluorination.^[27] An initial screen of potential Lewis acids showed that titanium-based acids, in particular TiCl_4 , were the most effective catalysts for the fluorination of the model β -ketoester tested. The group then progressed to screening a series of known enantiopure, chiral titanium Lewis acid catalysts.^[28] A Taddol-based titanium catalyst (Figure 5.9) was found to exhibit very promising activity/selectivity for a number of the substrates. Enantiomeric excesses were 62% or above, with reaction times as low as 15 minutes. When sterically hindered ester groups were present ee's were as high as 90%.

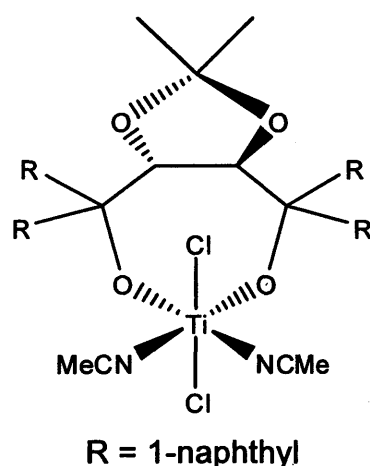


Figure 5.9. Structure of $[\text{TiCl}_2(\text{R,R-TADDOLato})]$ catalyst for enantioselective fluorination

Togni carried out extensive mechanistic studies to determine how the Ti-TADDOL complexes interact with β -ketoesters in order to establish reaction mechanisms and better understand how to engineer selectivity in these catalysts.^[29] This led to the development of new Ti-TADDOLato complex derivatives for selective halogenation reactions but no improvements to the previous ee's were attained.^[30, 31]

Sodeoka's group investigated the use of late transition metal Lewis acids in electrophilic enantioselective fluorination.^[32] Palladium complexes based on BINAP ligands were tested as catalysts for the asymmetric fluorination of β -ketoesters with NFSI (Figure 5.10).

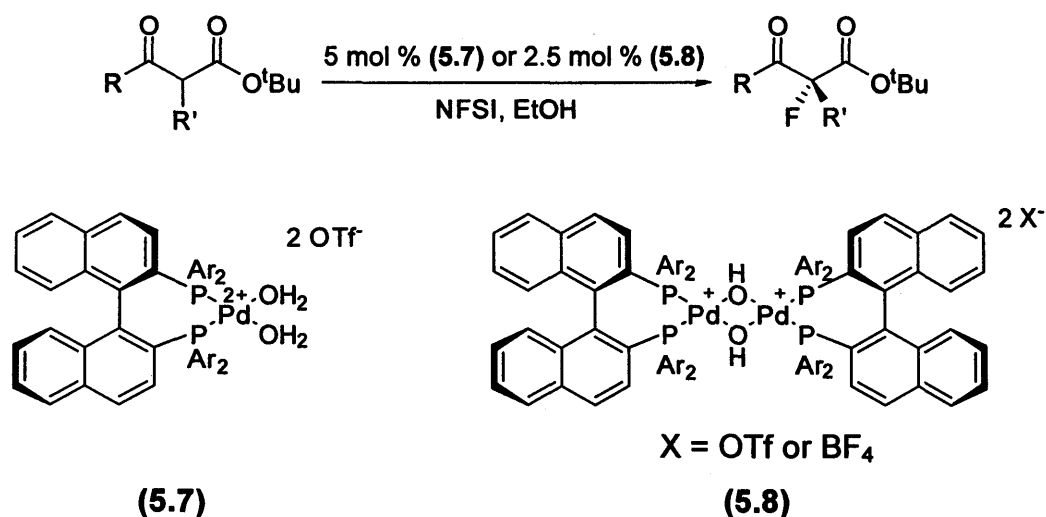


Figure 5.10. Pd-BINAP catalysed enantioselective electrophilic fluorination

The BINAP-based catalysts (5.7) and (5.8) were found to be capable of catalysing the NFSI fluorination of both cyclic and acyclic β -ketoesters in high yield (up to 96%) and enantioselectivity (up to 94%). The combination of the catalyst's excellent activities and selectivities, coupled with their more general applicability (achieving high ee did not require such great steric bulk in the substrate), stability and the mild reaction conditions represented a significant advance in the field. The proposed mechanism was equivalent to that of the titanium system described above, proceeding through an enolato-palladium species.^[33]

The stability of these palladium catalysts was demonstrated by the same group, who used ionic liquids as a medium for catalyst separation and recycling.^[34] Complex (8) immobilised in [hmim][BF₄] was actively recovered and reused in the fluorination of *tert*-butyl 2-methyl-3-oxo-3-phenylpropanoate an impressive 10 times. Although some decrease in yield was observed (93% to 67%), ee's were maintained and were still in excess of 90% for the final run.

Sodeoka's findings inspired the development of a number of late transition metal catalysts for enantioselective electrophilic fluorination. Togni^[35] and Cahard^[36] reported complexes of ruthenium and copper respectively as highly effective catalysts for enantioselective fluorination (Figure 5.11) but both failed to exceed the selectivity exhibited by the BINAP-based palladium complex.

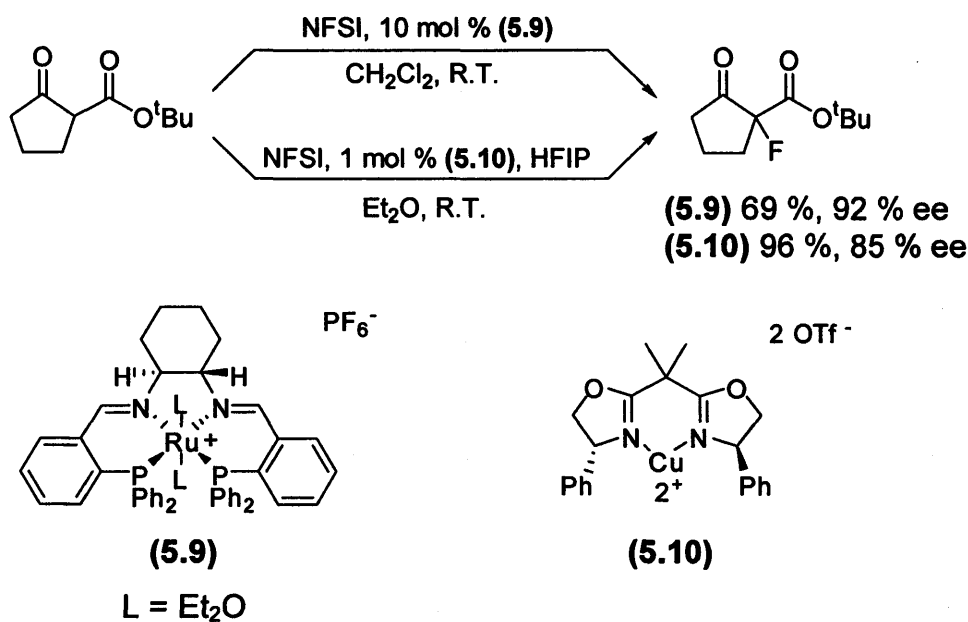


Figure 5.11. Electrophilic enantioselective fluorination of *tert*-butyl cyclopentanone-2-carboxylate

Lewis acid catalysed enantioselective fluorination using nucleophilic fluorine sources is also known.^[37, 38] Although some respectable product yield/ee combinations have been reported the results are inferior to those obtained with electrophilic reagents such as Selectfluor and NFSI.

5.1.4. Fluorous Asymmetric Catalysts

Sodeoka's fluorination work with BINAP-based palladium complexes in conjunction with the electrophilic fluorinating reagent NFSI produced some of the best combinations of product yields/ee's reported in the literature. Previous work by the Fluorine group at the University of Leicester has been conducted on the modification of BINAP ligands with perfluoroalkyl chains.^[39] These "fluorous tags" were added to the ligand in order to facilitate separation and recycle catalysts based upon them using fluorous solid-phase extraction with fluorous reverse phase silica gel. A ruthenium catalyst incorporating the fluorous ligands was tested in the asymmetric hydrogenation of methyl acetoacetate. The results indicated that activities and enantioselectivities were not impaired by the addition of the perfluoroalkyl substituents. After the reaction was complete, the product mixture was passed down a short column of FRPSG. Using methanol as the mobile phase allowed for the recovery of products free of the fluorinated BINAP ligands. Although the fluorous ligands could be also be recovered from the column by eluting with DCM, the ruthenium irreversibly bound to the surface of the silica and could not be eluted with any of the solvents tested.

In this work, we proposed to carry out enantioselective fluorinations using catalysts based upon perfluoroalkyl-derivatised BINAP ligands and recover the catalysts using fluorous techniques.

The efficacy of fluororous zirconium phosphonates as a stationary phase would be compared to that of FRPSG, which has been shown by previous work to be problematic in the recovery procedure of transition-metal catalysts.

5.2. Results and Discussion

5.2.1. Recycling of [Pd(BINAP)(OH₂)₂](OTf)₂ Using Silica Column Chromatography

In Sodeoka's original work, the group separated the catalyst from products using a silica column but did not report any attempts at catalyst recovery and recycling.^[32] We, therefore, sought to determine if the palladium catalysts were still active and/or enantioselective after purification by chromatography, and to compare the results to those from catalysts recycled with fluororous zirconium phosphonates. Therefore, the following chromatographic recycling procedure was developed; after catalysis (Figure 5.12) the crude product mixture residue was loaded onto a short silica column, first using toluene as eluent to remove any remaining fluorinating agent and associated salts, secondly with diethyl ether to recover the product and lastly with tetrahydrofuran to recover the catalyst. Between 80 - 90% by weight of the catalyst was recovered. In most cases, the crude product required further purification by column chromatography in order to obtain a sample suitable for analysis of the enantiomeric excess by chiral HPLC. Thus, determination of catalyst leaching by ICP-OES was not conducted since any leached catalyst would remain on this column, such that analysis of the organic product for palladium would no longer correspond to the actual amount of catalyst contamination.

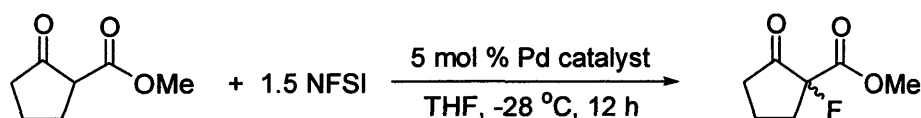


Figure 5.12. The enantioselective fluorination of methyl 2-oxo-cyclopentanecarboxylate with NFSI

However, NMR spectroscopic analysis of the recovered catalyst revealed a shift in the complex's phosphorus peak from 34 to 29 ppm, indicating a chemical change in the palladium complex. It is, therefore, impossible to quantify how much of the palladium complex, if any, was lost through the column chromatography. The dichloride precursor to the catalyst complex, [PdCl₂BINAP], has a ³¹P NMR shift of 29 ppm, suggesting that the recovered material might be an overall neutral Pd²⁺ complex. Unfortunately, a crystal suitable for X-ray analysis was unobtainable

and time did not allow for a thorough investigation into the structure of the unknown complex and therefore the complex's structure was not determined. The specific optical rotation of the catalyst changed after the first recovery but was constant in subsequent recycles.

The catalysts were then reused in subsequent runs and were shown to have remained catalytically active (Table 5.13).

Catalyst	<i>(R)</i> -5.11	<i>(S)</i> -5.11
Conversion (%)	>99 (96, 88)	>99 (94)
Yield (%)	71 (75, 65)	74 (69)
ee (%)	72 (52, 32)	58 (50)
³¹ P NMR shift (ppm)	34 (29, 29)	34 (29)
Specific optical rotation (°)	33 (23, 23)	-59 (-16)

Table 5.13 Enantioselective fluorination of methyl 2-oxo-cyclopentanonecarboxylate (MCPC), flash column recycling results

Values in parentheses represent 2nd and 3rd runs

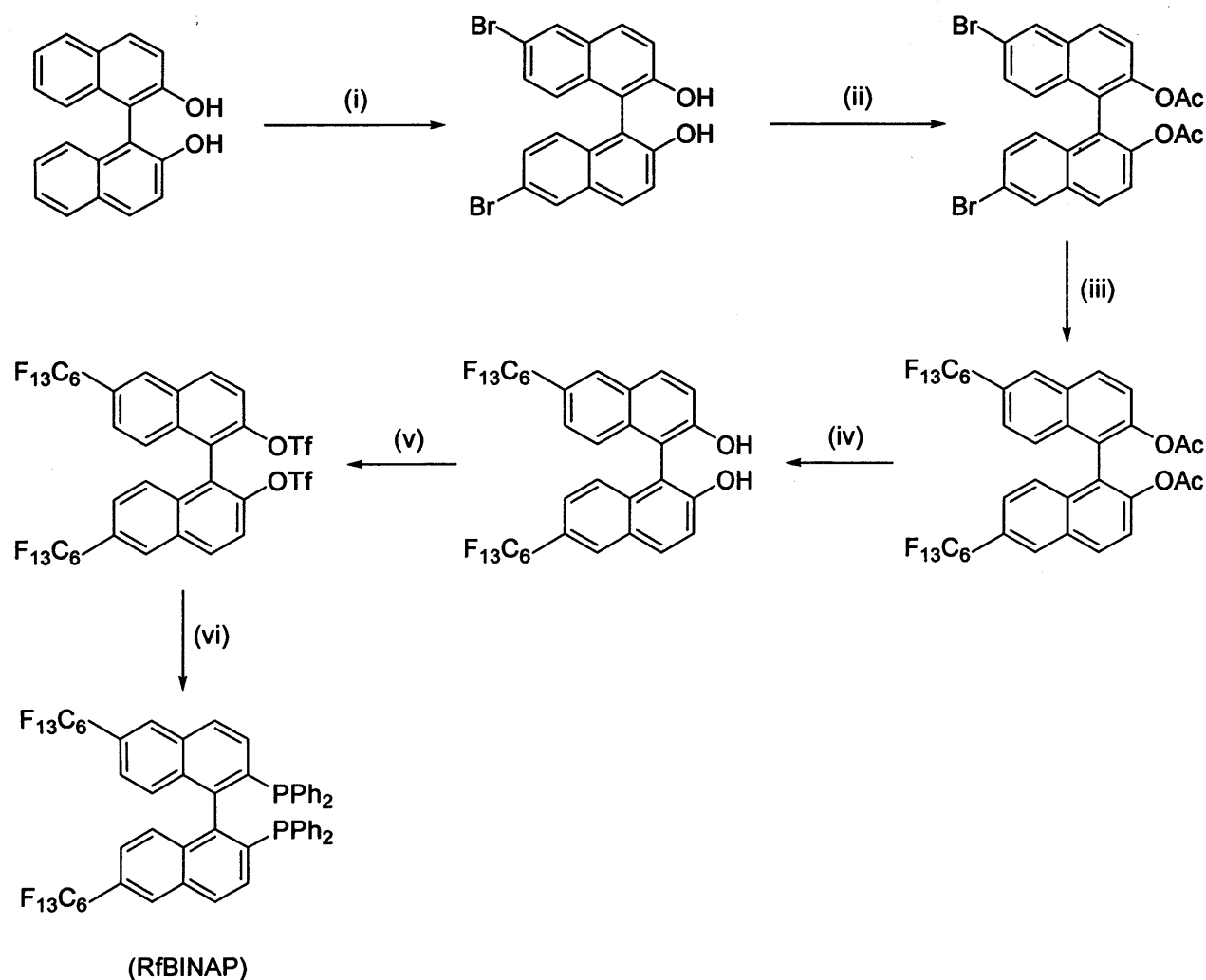


Although conversions and yields obtained showed little change, enantioselectivities fell substantially over three runs. This could be either a result of less catalyst being present for each run or could indicate catalyst decomposition, or a combination of the two factors. However, optical rotations for the recovered catalyst remained the same from run 2 to run 3, suggesting the reduction in catalyst concentration, by either mechanical losses or decomposition, is likely to be the main cause of the fall in ee. It is proposed that attack from the surface hydroxyl groups of the silica could be responsible for catalyst degradation. Since the recycling experiments involving dirhodium tetrafluorocarboxylates, discussed in chapter 3, had shown FZrP to be superior materials to silica for the separation of fluorine catalysts from organic products, we set out to prepare perfluoroalkyl derivatised analogues of the BINAP ligands in order to determine if the corresponding palladium complexes could be successfully recovered and reused using fluorine zirconium phosphonates.

5.2.2. Synthesis of Perfluoroalkyl-Derivatised BINAP Ligands

Before catalytic testing and subsequent assessment of catalyst recovery using fluorine zirconium phosphonates could begin, preparation of the perfluoroalkyl-derivatised BINAP was required, as these ligands are not commercially available. The synthesis of the fluorine BINAP

ligands may be achieved in six steps from enantio-pure 1,1'-bi-2-naphthol, as shown in Scheme 5.14. The backbone of binaphthol is first modified with bromine atoms and the hydroxyl groups protected with acetyl groups before the perfluorohexyl chains are added *via* a copper-initiated cross-coupling reaction. After removal of the acetyl protection, the perfluoroalkylated BINOL is converted to the bistriflate. Nickel-catalysed reaction with diphenylphosphine yields the desired fluororous ligand. Isolated yields were generally good to excellent, with only the cross-coupling step giving a yield substantially below 70%. Both (*R*) and (*S*) enantiomers of the ligands were prepared in overall yields of 13 and 24% respectively. The ligands and intermediates were fully characterised by multinuclear NMR and mass spectrometry and the data matched predicted and literature values.^[39]

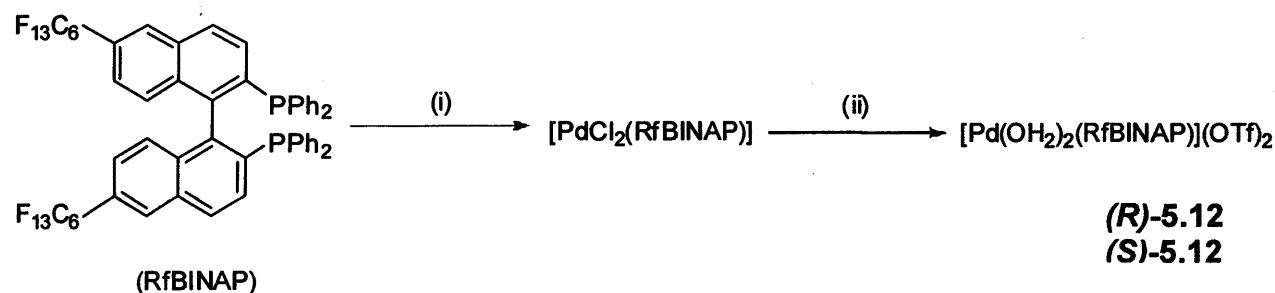


Scheme 5.14. Synthesis of perfluoroalkyl-derivatised BINAP (RfBINAP)

(i) Br_2 , $-78\text{ }^\circ\text{C}$ to R.T., DCM; (ii) Ac_2O , Et_3N , DMAP, DCM, reflux; (iii) $\text{C}_6\text{F}_{13}\text{I}$, Cu, 2,2'-bipy, DMSO, $\text{C}_6\text{H}_5\text{F}$, $80\text{ }^\circ\text{C}$; (iv) NaOEt , MeOH, R.T.; (v) $(\text{CF}_3\text{SO}_2)_2\text{O}$, pyridine, DCM, $0\text{ }^\circ\text{C}$; (vi) $[\text{NiCl}_2(\text{dppe})]$, Ph_2PH , DABCO, DMF, $110\text{ }^\circ\text{C}$.

5.2.3. Synthesis of Perfluoroalkyl-Derivatised Palladium(II) Complexes

Fluorous analogues of the palladium complexes used as asymmetric fluorination catalysts by Sodeoka^[32] were prepared using the fluorous BINAP ligands, as shown in Scheme 5.15. Ligand exchange with palladium dichloride bis(acetonitrile), followed by substitution of the chlorides for water molecules, in the presence of silver triflate, gave the desired complexes in high yield. The complexes were analysed by ¹H, ¹³C, ¹⁹F and ³¹P NMR spectroscopies and mass spectrometry. Observed phosphorus NMR shifts were as expected for the Pd²⁺ complexes and the fluorine NMR spectra displayed resonances corresponding to the perfluorohexyl chains and the triflate counteranions.



Scheme 5.15. Preparation of palladium catalysts comprising perfluoroalkyl-derivatised BINAP ligands

(i) PdCl₂(MeCN)₂, N₂, R.T., dry DCM; (ii) AgOTf, R.T., 0.5% v/v wet acetone.

5.2.4. Enantioselective Fluorination with Palladium BINAP Catalysts

The palladium catalysts based upon perfluoroalkyl-derivatised BINAP were first compared to their non-fluorous analogues to determine if the addition of the perfluoroalkyl chains had an effect upon activity or enantioselectivity. The same enantioselective fluorination of methyl 2-oxocyclopentanonecarboxylate (MCPC) with NFSI (Figure 5.12) was used to evaluate the catalysts, as this substrate is commercially available. The catalyst and substrate were stirred in THF for 10 minutes at room temperature before cooling the mixture to -25 °C and adding 1.5 equivalents of fluorinating agent and stirring for 12 hours. After quenching with saturated aqueous ammonium chloride, the organic phase was separated and the product purified by column chromatography using standard silica as the stationary phase. Enantiomeric excesses were determined by chiral HPLC.

Proton NMR spectroscopy of the crude products showed virtually quantitative conversions to the desired product. After purification by column chromatography, the isolated yield of the

mixture of enantiomers was in excess of 70%. The results for the fluoros catalyst were directly compared to those for Sodeoka's non-fluorous catalyst (Table 5.13) and the data are given in Table 5.16.

Catalyst	Conversion (%)	Yield (%)	Major:Minor Enantiomer Ratio	ee (%)
(<i>S</i>)-5.11	>99	74	79:21	58
(<i>S</i>)-5.12	>99	79	80:20	60

Table 5.16. Enantioselective fluorination of MCPC results



Despite the relatively low steric bulk of the substrate's methyl ester functionality, enantiomeric excesses were moderate to good for both the fluoros and non-fluorous catalyst and the presence of the perfluoroalkyl moiety on the BINAP backbone did not appear to have an adverse effect on the catalyst's enantioselectivity.

In order to maximise the enantioselectivity of the reaction, the tertiary-butyl ester analogue of the methyl 2-oxo-cyclopentanecarboxylate substrate was prepared, as the additional steric bulk of the ^tBu group was expected to increase product's ee. Direct trans-esterification of the methyl ester with ^tBuOH proved unsuccessful and the substrate was, therefore, prepared in two steps from adipoyl chloride (Scheme 5.17).

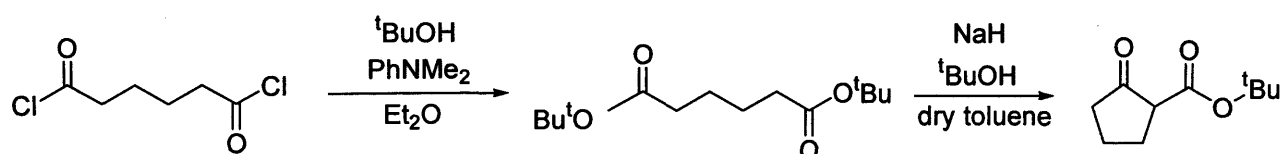


Figure 5.17. Preparation of ^tbutyl 2-oxo-cyclopentanecarboxylate from adipoyl chloride

The ^tbutyl 2-oxo-cyclopentanecarboxylate (BCPC) was fluorinated with NFSI under the same conditions used for the methyl substrate. Isolated yields and selectivities obtained (Table 5.18) were comparable to those obtained by Sodeoka's group in their enantioselective fluorination work.^[32] Product enantioselectivity was higher than that reported by Sodeoka (79%), presumably as the group conducted the reaction at a slightly higher temperature (-20 °C, as opposed to -25 °C in this work).

Catalyst	Conversion (%)	Yield (%)	Major:Minor Enantiomer Ratio	ee (%)
(S)-5.11	>99	76	98:2	96
(R)-5.11	>99	- 72 ^a	94:6	88 79 ^a
(R)-5.12	>99	-	98	96

Table 5.18. Enantioselective fluorination of BCPC

^a literature value at -20 °C^[32]



After demonstrating that the greater steric bulk of the tertiary butyl substrate significantly improved the enantioselectivity of the fluorination, all of the following catalysis experiments were conducted using BCPC.

5.2.4.1. Recycling of the Palladium BINAP Catalysts Using Column Chromatography with Fluorous Zirconium Phosphonates and FRPSG

As the results from the recycling experiments using silica columns showed a substantial fall in product ee's over just three runs, a series of experiments was conducted to determine if using alternative stationary phases in the column could avoid the problem of catalyst degradation. The two stationary phases tested were 4-perfluorohexyl phenyl zirconium phosphonates (FZrP) and fluororous reverse phase silica gel (FRPSG). Previously, we have shown that underivatized complexes have low affinities for reverse fluororous stationary phases and, therefore, the $[\text{Pd}\{(R)\text{-RfBINAP}\}(\text{OH}_2)_2](\text{OTf})_2$ complex was used for the fluorination reactions, in order to optimise the catalyst separation process.

Fluorination of ^tbutyl 2-oxo-cyclopentanonecarboxylate with NFSI was conducted under homogeneous conditions, followed by separation and recovery of the catalyst *via* column chromatography. The catalyst, $[\text{Pd}\{(R)\text{-RfBINAP}\}(\text{OH}_2)_2](\text{OTf})_2$, was reused in three successive runs and results are shown in Table 5.19 and Graph 5.20. Due to time constraints, catalysis using the (*S*)-enantiomer of the palladium complex was not performed. The (*R*)-enantiomer was chosen in preference to the (*S*)- so that a fair comparison of the results may be made to the work conducted by Sodeoka, which utilised solely the (*R*)-enantiomer.

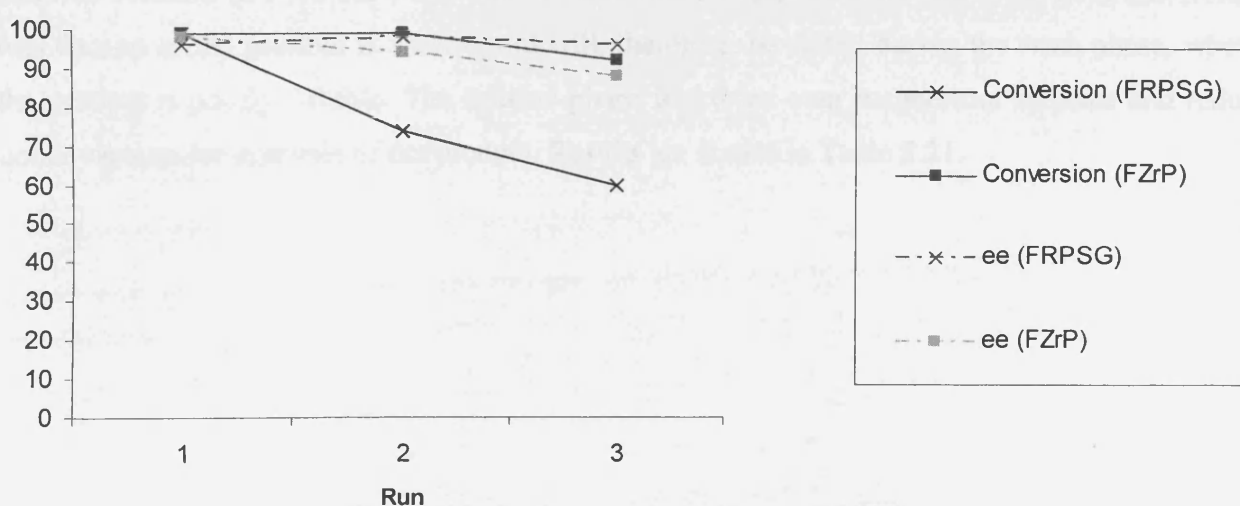
Stationary Phase Material	FZrP	FRPSG
Conversion (%)	>99 (99, 92)	>99 (74, 60)
Major:Minor Enantiomer Ratio	99:1 (97:3, 94:6)	98:2 (99:1, 98:2)
ee (%)	98 (94, 88)	96 (98, 96)
³¹ P NMR shift (ppm)	34 (29, 29)	34 (29, 29)
Mass of catalyst recovered (%)	96 (92)	83 (86)

Table 5.19. Enantioselective fluorination of BCPC, flash column recycling results

Values in parentheses represent 2nd and 3rd runs

The catalysts recovered using both stationary phases were active over the three runs but conversions were seen to fall in the fluororous silica system. This is possibly due to attack from uncapped hydroxyl groups on the silica's surface onto the catalyst's palladium centre, as the mass of recovered complex was lower with the FRPSG column than that with FZrP (83 and 86% with FRPSG, as opposed to 96 and 92% with FZrP).

Enantioselectivities, in both of the systems, did not undergo significant reductions, indicating that the recovered catalyst was unaffected by the recovery protocol. Thus, although both stationary phases allowed separation and recycle of the enantioselective palladium complex, the fluororous zirconium phosphonate's inert surface allowed for a more efficient recovery process. The small number of uncapped hydroxyl groups present on the FRPSG's surface prevent total elution of the complex from the column. However, the BINAP ligands are not detrimentally affected and the complex which is recovered from the column retains its enantioselectivity.



Graph 5.20. Conversions and enantiomeric excesses over three subsequent fluorination reaction

5.2.4.2. Recycling of Palladium BINAP Catalysts Supported on Fluorous Zirconium Phosphonates and FRPSG

Although the FZrP column recovery protocol, described in section 5.2.4.1, allowed the recycling of an active, enantioselective catalyst, a percentage of the palladium complex was lost mechanically during each step. As the starting mass of the catalyst used was small (23 mg), the accumulative losses were considerable, at almost 12% (~3 mg) of the complex's mass over two runs. Therefore, a 5% loaded solid-supported catalyst system was tested, since the palladium complex is only a small proportion of the total mass of supported material, mechanical losses of 3 mg would correspond to just 0.15 mg of catalyst, or 0.7%.

Fluorous and non-fluorous zirconium phosphonates and fluorous silica support materials were tested, for comparison purposes. Combinations of fluorous/non-fluorous catalyst and supports were tested in order to investigate if the addition of perfluoroalkyl chains to the ligands and support aided catalyst immobilisation and separation. As the initial recycling experiments (section 5.2.1.) suggested that separating the palladium complexes from organic products using non-derivatised silica led to catalyst racemisation/decomposition, silica was not tested in this series of recycling experiments.

$[\text{Pd}\{(S)\text{-BINAP}\}(\text{OH}_2)_2](\text{OTf})_2$ and $[\text{Pd}\{(S)\text{-RfBINAP}\}(\text{OH}_2)_2](\text{OTf})_2$ were loaded onto phenyl zirconium phosphonate and its fluorous analogue 4-perfluorohexylphenyl zirconium phosphonate. The supported catalysts were then used in the enantioselective fluorination of BCPC with NFSI, under the same conditions as described previously. At the end of the reaction, the crude mixture was reduced under vacuum and solid residue washed with saturated aqueous ammonium chloride solution ($2 \times 10 \text{ cm}^3$) and toluene ($2 \times 10 \text{ cm}^3$) and dried for use in the next run. Toluene was chosen as the product is soluble and will, therefore, be eluted during the wash phase, whereas the catalyst is poorly soluble. The toluene phase was dried over magnesium sulphate and reduced under vacuum for analysis of the product. Results are shown in Table 5.21.

Support	Catalyst	Conversion (%)	Major:Minor Enantiomer Ratio	ee (%)
FZrP	(S)-5.12	81 (69, 47)	98:2 (94:6, 93:7)	96 (88, 86)
	(S)-5.11	81 (71, 75)	95:5 (94:6, 92:8)	90 (88, 84)
ZrP	(S)-5.12	82 (10)	93:7 (93:7)	86 (86)
	(S)-5.11	79 (83)	93:7 (91:9)	86 (82)

Table 5.21. Enantioselective fluorination of BCPC, supported catalysis recycling results

Values in parentheses represent 2nd and 3rd runs

(S)-5.12 = [Pd{(S)-RfBINAP}(OH₂)₂](OTf)₂

(S)-5.11 = [Pd{(S)-BINAP}(OH₂)₂](OTf)₂

Conversions to the desired product were, as anticipated, lower in these supported catalysis experiments than those in the homogeneous reactions, presumably due to mass transfer issues. Enantioselectivities were maintained over the three runs, with only a small decrease in ee observed in both systems. With the fluorous zirconium support, while conversions were reasonably consistent using the non-fluorous [Pd{(S)-BINAP}(OH₂)₂](OTf)₂ catalyst, conversions with the fluorous congener dropped by over thirty percent. This difference may result from some degree of catalyst leaching, since although the fluorous catalyst should have a greater affinity for the fluorous surface of the support, it also displays a greater solubility in toluene. This is apparent from qualitative solubility tests; when 20 mg of catalyst is added to 10 cm³ of solvent a faint yellow colouration is observed after several minutes with the fluorous ligand-based catalyst. Toluene containing the non-fluorous catalyst remains colourless after standing for extended periods of time. The toluene from the washing phases of the recovery protocol was faintly yellow, supporting this theory.

The results for the phenyl zirconium phosphonate support indicate that the fluorous support offers superior catalyst immobilisation, since when the immobilising the fluorous catalyst upon the former material leads to a large drop in conversion to products in the second run. The product-containing toluene phase possessed an obvious yellow colour, indicating considerable leaching of the catalyst from the support. However, the non-fluorous BINAP complex is recoverable, despite the absence of fluorous character in both catalyst and support. The difference between the recyclability of the two complexes on this non-fluorous ZrP support is likely to be solubility based. Since the fluorous catalyst has a higher solubility in toluene and has no preferential affinity for the surface of the ZrP, whereas, the [Pd(RfBINAP)(OH₂)₂](OTf)₂ is more readily washed from the FZrP support than [Pd(BINAP)(OH₂)₂](OTf)₂.

As before, ICP-OES leaching studies of the product were not performed as further purification by column chromatography was required to obtain a sample suitable for chiral HPLC.

The same procedure was repeated with $[\text{Pd}\{(S)\text{-RfBINAP}\}(\text{OH}_2)_2](\text{OTf})_2$ supported on FRPSG. The results are shown in Table 5.22.

Support	Catalyst	Conversion (%)	Major:Minor Enantiomer Ratio	ee (%)
FRPSG	(<i>S</i>)-5.12	70 (52*, 51)	67:33 (N.R.*, 57:43)	34 (N.R.*, 4)

Table 5.22. Enantioselective fluorination of BCPC, supported catalysis recycling results

Values in parentheses represent 2nd and 3rd runs



*Not recorded. Additional dry ice added to the bath midway through the reaction. Reaction temperature did not exceed -20 °C

The data in Table 5.22 shows that the silica-based system performs less well than the zirconium phosphonate ones. Although the conversion in the final run is comparable to that for the fluorous zirconium phosphonates, the initial conversion is lower and ee's are poor. Unfortunately, the conversion observed in the second run is unreliable since the dry ice bath was refilled after several hours and the reaction temperature was, therefore, kept below -20 °C throughout the reaction. In contrast, the other fluorinations were carried out over night and, therefore, gradually warmed over the course of the reaction to around 0 °C. It is expected that enantioselectivity increases and activity decreases with decreasing temperature. Thus, the additional dry ice may have slowed conversion but allowed for a higher level of selectivity to be maintained for the entire duration of the reaction. Therefore, the ee was not recorded for this experiment.

5.5. Conclusions for Chapter 5

A fluorous equivalent of the enantioselective fluorination catalyst $[\text{Pd}(\text{BINAP})(\text{OH}_2)_2](\text{OTf})_2$, containing two perfluorohexyl chains on the BINAP backbone, was synthesised and was shown to have comparable activity and selectivity in the fluorination of methyl 2-oxo-cyclopentanonecarboxylate and ^tbutyl 2-oxo-cyclopentanonecarboxylate with NFSI.

A fluorous catalyst, $[\text{Pd}\{(R)\text{-RfBINAP}\}(\text{OH}_2)_2](\text{OTf})_2$, was recycled using columns packed with fluorous silica (FRPSG) and fluorous zirconium phosphonates (FZrP). The best results were obtained when using FZrP as a stationary phase for the recovery process, where conversions above 90% and ee's above 88% were maintained to the 3rd catalytic run. When FRPSG was used, enantioselectivities were comparable to those obtained in the FZrP system but conversions fell from 99 to 60% over the 3 runs. The non-fluorous catalyst $[\text{Pd}\{(R)\text{-BINAP}\}(\text{OH}_2)_2](\text{OTf})_2$ was recovered

using a standard silica column. In this system, conversions fell only slightly but ee fell substantially over the 3 successive runs. The data is summarised in Table 2.24.

Stationary Phase	Conversion (%)	Major:Minor Enantiomer Ratio	ee (%)
Silica ^a	>99 (96, 88)	71 (75, 65)	72 (52, 32)
FZrP ^b	>99 (99, 92)	99:1 (97:3, 94:6)	98 (94, 88)
FRPSG ^b	>99 (74, 60)	98:2 (99:1, 98:2)	96 (98, 96)

Table 2.24. Enantioselective fluorination, flash column recycling results

^a catalyst = [Pd{(R)-BINAP}(OH₂)₂](OTf)₂, substrate = methyl 2-oxo-cyclopentanonecarboxylate

^b catalyst = [Pd{(R)-RfBINAP}(OH₂)₂](OTf)₂, substrate = ^tbutyl 2-oxo-cyclopentanonecarboxylate

The palladium catalysts were also recycled *via* a supported catalysis approach. Both fluorous and non-fluorous zirconium phosphonates and FRPSG were compared as support materials. The most consistent recycling results were obtained for the fluorous zirconium phosphonate support, with both [Pd{(S)-BINAP}(OH₂)₂](OTf)₂ and [Pd{(S)-RfBINAP}(OH₂)₂](OTf)₂ catalysts recoverable and no significant loss of enantioselectivity was observed. Phenyl zirconium phosphonate was also shown to be effective as a medium for the recovery of [Pd{(S)-BINAP}(OH₂)₂](OTf)₂, although time did not allow for further recycling experiments after the 2nd run.

References for Chapter 5

- [1] W. R. Dolbier Jr., *J. Fluorine Chem.*, **2005**, *126*, 157.
- [2] D. Cartwright, *Recent Developments in Fluorine-Containing Agrochemicals*, in *Organofluorine Chemistry, Principles and Commercial Applications*, ed. R. E. Banks, B. E. Smart, J. C. Tatlow, Plenum, New York, **1994**.
- [3] T. J. Leck, P. J. Fagan, in *PCT Int. Appl.*, Du Pont, US, **2004**, p. 45.
- [4] M. Gleria, R. Bertani, R. De Jaeger, S. Lora, *J. Fluorine Chem.*, **2004**, *125*, 329.
- [5] P. R. Resnick, W. H. Buck, *Fluoropolymers*, **1999**, *2*, 25.
- [6] E. R. Larsen, *Fluorine Chem. Rev.*, **1969**, *3*, 1.
- [7] T. Eriksson, S. Bjorkman, P. Hoglund, *Eur. J. Clin. Pharm.*, **2001**, *57*, 365.
- [8] T. Iwaoka, T. Murohashi, M. Sato, C. Kaneko, *Tetrahedron: Asymmetry*, **1992**, *3*, 1025.
- [9] S. Rozen, *Chem. Rev.*, **1996**, *96*, 1717.
- [10] J. M. Shreeve, R. P. Singh, *Synthesis*, **2002**, *17*, 2561.
- [11] G. S. Lal, G. P. Pez, R. J. Pesaresi, F. M. Prozonic, H. Cheng, *J. Org. Chem.*, **1999**, *64*, 7048.
- [12] E. Differding, R. W. Lang, *Tetrahedron Lett.*, **1988**, *29*, 6087.
- [13] F. A. Davis, P. Zhou, P. J. Carroll, *J. Org. Chem.*, **1993**, *58*, 4890.
- [14] F. A. Davis, P. Zhou, C. K. Murphy, G. Sundarababu, H. Y. Qi, W. Han, R. M. Przeslawski, B. C. Chen, P. J. Carroll, *J. Org. Chem.*, **1998**, *63*.
- [15] E. L. Differding, R. W. Lang, *Helv. Chim. Acta*, **1989**, *72*, 1248.
- [16] E. Differding, G. W. Ruegg, R. W. Lang, *Tetrahedron Lett.*, **1991**, *32*, 1779.
- [17] Y. Takeuchi, T. Suzuki, A. Satoh, T. Shiragami, N. Shibata, *J. Org. Chem.*, **1999**, *64*, 5708.
- [18] Y. Takeuchi, Z. Liu, N. Shibata, *J. Org. Chem.*, **2000**, *65*, 7583.
- [19] N. Shibata, Z. Liu, Y. Takeuchi, *Chem. Pharm. Bull.*, **2000**, *48*, 1954.
- [20] D. Cahard, C. Audouard, J.-C. Plaquevent, N. Roques, *Org. Lett.*, **2000**, *2*, 3699.
- [21] N. Shibata, T. Suzuki, Y. Takeuchi, *J. Am. Chem. Soc.*, **2000**, *122*, 10728.
- [22] B. Mohar, J. Baudoux, J.-C. Plaquevent, D. Cahard, *Angew. Chem. Int. Ed.*, **2001**, *40*, 4214.
- [23] N. Shibata, T. Suzuki, T. Asahi, M. Shiro, *J. Am. Chem. Soc.*, **2001**, *123*, 7001.
- [24] N. Shibata, T. Ishimaru, T. Suzuki, K. L. Kirk, *J. Org. Chem.*, **2003**, *68*, 2494.
- [25] G. L. Hann, P. Sampson, *Chem. Comm.*, **1989**, 1650.
- [26] A. J. Beaumont, C. Kiely, D. Rooney, *J. Fluorine Chem.*, **2001**, *108*, 47.
- [27] A. Togni, L. Hintermann, *Angew. Chem. Int. Ed.*, **2000**, *39*, 4359.
- [28] R. O. Duthaler, A. Hafner, *Chem. Rev.*, **1992**, *92*, 807.
- [29] S. Piana, I. Devillers, A. Togni, U. Rothlisberger, *Angew. Chem. Int. Ed.*, **2002**, *41*, 979.

- [30] R. Frantz, L. Hintermann, M. Perseghini, D. Broggini, A. Togni, *Org. Lett.*, **2003**, *5*, 1709.
- [31] M. Perseghini, M. Massaccesi, Y. Y. Liu, A. Togni, *Tetrahedron*, **2006**, *62*, 7180.
- [32] Y. Hamashima, K. Yagi, H. Takano, L. Tamás, M. Sodeoka, *J. Am. Chem. Soc.*, **2002**, *124*, 14530.
- [33] Y. Hamashima, D. Hotta, M. Sodeoka, *J. Am. Chem. Soc.*, **2002**, *124*, 11240.
- [34] Y. Hamashima, H. Takano, D. Hotta, M. Sodeoka, *Org. Lett.*, **2003**, *5*, 3225.
- [35] C. Bonaccorsi, M. Althaus, C. Becker, A. Togni, *Pure Appl. Chem.*, **2006**, *78*, 391.
- [36] J.-A. Ma, D. Cahard, *Tetrahedron: Asymmetry*, **2004**, *15*, 1007.
- [37] S. Bruns, G. Haufe, *J. Fluorine Chem.*, **2000**, *104*, 247.
- [38] G. Haufe, S. Bruns, *Adv. Synth. Catal.*, **2002**, *344*, 165.
- [39] E. G. Hope, A. M. Stuart, A. J. West, *Green Chem.*, **2004**, *6*, 345.

6. Experimental Details

6.1. General Experimental Details

6.1.1. Nuclear Magnetic Resonance Spectroscopy

^1H , ^{19}F $\{^1\text{H}\}$, ^{31}P $\{^1\text{H}\}$, ^{13}C $\{^1\text{H}\}$ NMR spectroscopic studies were carried out on a Bruker DPX300 spectrometer at 301.37, 282.40, 121.99 and 75.47 MHz respectively. ^{77}Se NMR spectroscopic studies were carried out on a Bruker DRX400 spectrometer at 76.32 MHz. Chemical shifts are quoted in ppm using the high-frequency positive convention; ^1H and ^{13}C $\{^1\text{H}\}$ NMR spectra were referenced to external SiMe_4 , ^{19}F $\{^1\text{H}\}$ NMR spectra to external CFCl_3 , ^{31}P $\{^1\text{H}\}$ NMR spectra to external 85% H_3PO_4 and ^{77}Se NMR spectra to external Me_2Se . Perfluoroalkyl chain carbon atoms were not visible in the ^{13}C $\{^1\text{H}\}$ NMR spectra due to extensive coupling to fluorine and are, therefore, not reported. Deuterated chloroform was used as solvent unless otherwise stated.

6.1.2. Mass Spectrometry

Electron impact (EI) and fast atom bombardment (FAB) mass spectra were recorded using a Kratos Concept 1H, double focussing, forward geometry mass spectrometer. 3-Nitrobenzyl alcohol was used as the matrix for the FAB spectra. Electrospray mass spectra were recorded on a Micromass Quatro LC.

6.1.3. Elemental Analysis

All elemental analyses were conducted by Steve Boyer of the Science Technological Support Unit, London Metropolitan University.

6.1.4. Inductively Coupled Plasma Optical Emission Spectroscopy

Inductively Coupled Plasma Optical Emission Spectroscopy (ICP-OES) was conducted by the Geology Department, University of Leicester. Samples were prepared by stirring a known amount of solid in 2M HCl for 12 hours, then filtering to ensure any remaining solid was removed from the solution. The samples were analysed for metal content using a JY Horiba Ultima 2 sequential ICP-OES with generator power and flow rates optimised for sensitivity.

6.1.5. Infrared Spectroscopy

Solid-state IR spectra were obtained using a Perkin Elmer FT-IR spectrometer at 4 cm⁻¹ resolution (16 scans) with a Universal ATR sampling accessory.

6.1.6. X-Ray Crystallography

X-ray crystallography data were collected on a Bruker Apex SMART 2000 diffractometer. Crystal data and structure refinement can be found in the appendix.

6.1.7. Scanning Electron Microscopy and Energy Dispersive X-ray Analysis

Scanning electron microscopy (SEM) and energy dispersive analysis by X-ray (EDAX) studies were conducted by Graham Clark of the Engineering Department, University of Leicester.

6.1.8. X-Ray Powder Diffraction

X-ray powder diffraction studies were conducted by Dr Sandra Dann of the Chemistry Department, University of Loughborough.

6.1.9. Gas Chromatography

GC data was recorded using a Perkin Elmer Clarius 500 gas chromatogram fitted with a SGE CYDEX-B column.

6.1.10. High Pressure Liquid Chromatography

Product enantiomeric excesses were determined using chiral HPLC using a Perkin Elmer Series 200 HPLC machine fitted with a Chiralcel OD-H column using a mobile phase of 2% IPA in hexane at 1 cm³ min⁻¹ and a 220 nm detector.

6.1.11. Starting Materials

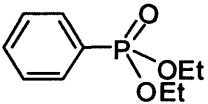
Compounds were used as supplied by Sigma-Aldrich, Lancaster or Fluorochem. Where dried solvents were necessary, DCM, hexane, Et₂O, THF, toluene and MeCN were distilled using

an Innovative Technology Pure Solv automated still and ethanol was distilled from CaH₂. All dried solvents were stored in sealed ampoules under an atmosphere of dry nitrogen over 4Å molecular sieves. Solvents were freeze-pump-thaw degassed at least three times prior to use. Pyridine and triethylamine were dried over calcium hydride and distilled into dried ampoules under nitrogen. The bases were stored under a nitrogen atmosphere over 4Å molecular sieves. [PdCl₂(MeCN)₂],^[1] [NiCl₂(dppe)],^[2] and 4-tridecafluorohexylphenyliodide,^[3] 1H,1H,2H,2H,3H,3H-perfluoroundecyliodide^[4] and iodoxybenzene^[5] were made by literature methods.

6.2. Experimental Details for Chapter Two

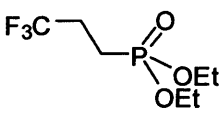
6.2.1. Synthesis of Diethyl Phosphonates *via* Simeon Protocol^[6]

6.2.1.1. Synthesis of PhPO(OEt)₂^[6]


 NaOEt (12.05 g, 0.18 mol) was added to a flame dried three neck round bottom flask under N₂. The flask was then charged with distilled EtOH (150 cm³) and the mixture was stirred until all the NaOEt was dissolved. PhPCl₂ (6.00 cm³, 0.044 mol) was then added dropwise and the solution stirred for 1 hour under N₂. I₂ (11.18 g) was added in four portions and the mixture stirred for a further 4 hours. The solution was then allowed to cool to room temperature before adding 5% aqueous HCl (50 cm³) and Et₂O (150 cm³). The organic layer was separated, washed with H₂O (2 x 50 cm³) and aqueous Na₂S₂O₅ solution (100 cm³) and then dried over MgSO₄. The solvent was removed under vacuum to yield a yellow brown oil (8.72 g, 93%); ¹H NMR (CDCl₃) δ 1.27 (6H, t, ³J_{HH} = 7.0 Hz, CH₃), 4.01 + 4.10 (4H, 2 x AB dq, ³J_{HP} = 7.3 Hz, ³J_{HH} = 7.0, ²J_{HaHb} = 10.2 Hz, 2 x CH₂), 7.41 (3H, m, Ph), 7.73 (2H, m, Ph); ¹³C {¹H} NMR (CDCl₃) δ 16.27 (d, ³J_{CP} = 7.2 Hz, CH₃), 62.09 (d, ²J_{CP} = 6.0 Hz, CH₂), 128.26 (d, ¹J_{CP} = 187.9 Hz, 1-C), 128.43 (d, ³J_{CP} = 15.6 Hz, 3-C), 131.71 (d, ²J_{CP} = 10.8 Hz, 2-C), 132.37 (d, ⁴J_{CP} = 2.4 Hz, 4-C); ³¹P {¹H} NMR (CDCl₃) δ 18.97 (S); m/z (ES⁺) 215 (MH⁺, 100%).

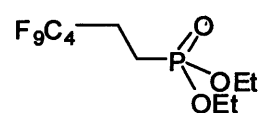
6.2.2. Synthesis of Diethyl Phosphonates *via* Michaelis-Arbuzov Reaction^[7, 8]

6.2.2.1. Synthesis of F₃C-C₂H₄PO(OEt)₂^[9]

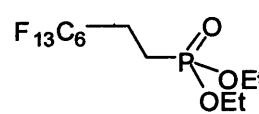

 A mixture of 1,1,1-trifluoro-4-iodo-butane (5.00 g, 0.022 mol) and P(OEt)₃ (28 cm³, 0.16 mol) was heated to 135 °C with stirring in a flame dried three neck round bottom flask equipped with distillation apparatus under nitrogen for 5 hours. The crude reaction mixture was separated between Et₂O (50 cm³) and H₂O (50 cm³) and the

aqueous layer washed with Et₂O (2 x 50 cm³) to ensure all product was extracted. The solvent was removed under vacuum and the resulting yellow liquid was Kugelröhr distilled (65 °C, 0.02 mmHg) to remove any starting materials/byproducts. This yielded a yellow oil (0.460 g, 9%); ¹H NMR (CDCl₃) δ 1.27 (6H, t, ³J_{HH} = 7.3 Hz, CH₃), 1.88 (2H, m, CH₂), 2.29 (2H, m, CH₂), 4.04 + 4.07 (4H, 2 x AB dq ³J_{HaP} = 8.2 Hz, ³J_{HbP} = 8.5 Hz, ³J_{HH} = 7.0 Hz, ²J_{HaHb} = 10.2 Hz, 2 x CH₂); ³¹P {¹H} NMR (CDCl₃) δ 27.89 (S); ¹⁹F {¹H} NMR (CDCl₃) δ -68.02 (S); ¹⁹F NMR (CDCl₃) δ -68.02 (3F, t, ³J_{FF} = 10.4 Hz); m/z (ES⁺) 235 (MH⁺, 100%).

6.2.2.2. Synthesis of F₉C₄-C₂H₄PO(OEt)₂

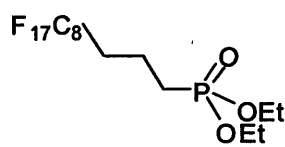
 1H, 1H, 2H, 2H-perfluorohexyl iodide (9.70 g, 0.026 mol) was heated to 135 °C with stirring in a flame dried three neck round bottom flask equipped with distillation apparatus under nitrogen. P(OEt)₃ (11.12 cm³, 0.065 mol) was added and the mixture was left to stir at 135 °C for 3 hours. The crude reaction mixture was separated between Et₂O (50 cm³) and H₂O (50 cm³) and the aqueous layer washed with Et₂O (4 x 50 cm³) to ensure all product was extracted. The solvent was removed under vacuum and the resulting yellow liquid was Kugelröhr distilled (65 °C, 0.02 mmHg) to remove any starting materials/byproducts. This yielded a clear colourless oil (5.69 g, 57%); ¹H NMR (CDCl₃) δ 1.28 (6H, t, ³J_{HH} = 7.0 Hz, CH₃), 1.91 (2H, m, CH₂), 2.31 (2H, m, CH₂), 4.04 + 4.10 (4H, 2 x AB dq ³J_{HaP} = 8.2 Hz, ³J_{HbP} = 8.5 Hz, ³J_{HH} = 7.0 Hz, ²J_{HaHb} = 10.2 Hz, 2 x CH₂); ¹H {¹⁹F} NMR (CDCl₃) δ 1.28 (6H, t, ³J_{HH} = 7.0 Hz, CH₃), 1.91 (2H, m, CH₂), 2.31 (2H, m, CH₂), 4.04 + 4.10 (4H, 2 x AB dq ³J_{HaP} = 8.2 Hz, ³J_{HbP} = 8.5 Hz, ³J_{HH} = 7.0 Hz, ²J_{HaHb} = 10.2 Hz, 2 x CH₂); ¹H {³¹P} NMR (CDCl₃) δ 1.28 (6H, t, ³J_{HH} = 7.0 Hz, CH₃), 1.91 (2H, m, CH₂), 2.31 (2H, m, CH₂), 4.04 + 4.10 (4H, 2 x AB q, ³J_{HH} = 7.0 Hz, ²J_{HaHb} = 10.2 Hz, 2 x CH₂); ¹³C {¹H} NMR (CDCl₃) δ 16.26 (d, ³J_{CP} = 6.0 Hz, 2 x CH₃), 17.05 (d, ¹J_{CP} = 147.2 Hz, CH₂), 25.03 (t, ²J_{CF} = 22.7 Hz, CH₂), 62.11 (d, ²J_{CP} = 6.0 Hz, 2 x CH₂); ³¹P {¹H} NMR (CDCl₃) δ 28.36 (S); ¹⁹F NMR (CDCl₃) δ -81.04 (3F, t, ⁴J_{FF} = 9.5 Hz CF₃), -115.53 (2F, m, α-CF₂), -124.28 (2F, m, CF₂), -126.04 (2F, m, CF₂); m/z (ES⁺) 385 (MH⁺, 100%).

6.2.2.3. Synthesis of F₁₃C₆-C₂H₄PO(OEt)₂^[10]

 1H, 1H, 2H, 2H-perfluorooctyl iodide (8.00 g, 0.017 mol) was heated to 180 °C with stirring in a flame dried three neck round bottom flask equipped with distillation apparatus under nitrogen. P(OEt)₃ (3.75 cm³, 0.22 mol) was added dropwise and the mixture was left to stir at 180 °C for 4 hours. The crude reaction mixture was purified by repeated Kugelröhr distillation (60 °C, 0.01 mmHg) to yield a clear yellow oil (3.97 g,

48%); Found: C, 29.8%; H, 2.7%; C₁₂H₁₄F₁₃O₃P requires C, 29.8%; H, 2.9%; ¹H NMR (CDCl₃) δ 1.29 (6H, t, ³J_{HH} = 7.0 Hz, CH₃), 1.92 (2H, m, CH₂), 2.30 (2H, m, CH₂), 4.07 + 4.08 (4H, 2 x AB dq, ³J_{HaP} = 7.9 Hz, ³J_{HbP} = 8.5 Hz, ³J_{HH} = 7.0 Hz, ²J_{HaHb} = 10.2 Hz, 2 x CH₂); ¹³C {¹H} (CDCl₃) δ 16.26 (d, ³J_{CP} = 6.0 Hz, 2 x CH₃), 18.71 (d, ¹J_{CP} = 143.6 Hz, CH₂), 25.14 (m, CH₂), 62.19 (d, ²J_{CP} = 6.0 Hz, 2 x CH₂); ³¹P {¹H} NMR (CDCl₃) δ 28.38 (S); ¹⁹F NMR (CDCl₃) δ -80.80 (3F, t, ⁴J_{FF} = 9.5 Hz, CF₃), -115.31 (2F, m, α-CF₂), -121.90 (2F, m, CF₂), -122.86 (2F, m, CF₂), -123.33 (2F, m, CF₂), -126.12 (2F, m, CF₂); m/z (ES⁺) 485 (MH⁺, 40%).

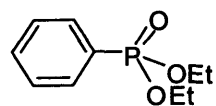
6.2.2.4. Synthesis of F₁₇C₈-C₃H₆PO(OEt)₂



A mixture of 1H, 1H, 2H, 2H, 3H, 3H-perfluoroundecyl iodide (1.00 g, 1.72 mmol) and triethyl phosphite (1.0 cm³, 5.84 mmol) were refluxed with stirring for 7 hours. H₂O (25 cm³) and Et₂O (25 cm³) were added, the ethereal layer was separated and washed with H₂O (2 x 25 cm³) and dried over MgSO₄. The solvent was then removed under vacuum and the resulting residue was Kugelröhr distilled (65 °C, 0.2 mmHg, 4 hours) to remove any starting material/by-products, yielding a yellow oil (0.63 g, 62%); Found: C, 30.0%; H, 2.7%; C₁₅H₁₆F₁₇O₃P requires C, 30.1%; H, 2.7%; ¹H NMR (CDCl₃) δ 1.26 (6H, t, ³J_{HH} = 7.0 Hz, CH₃), 1.75 (2H, m, CH₂), 1.88 (2H, m, CH₂), 2.15 (2H, m, CH₂), 3.96 – 4.14 (4H, m, 2 x CH₂); ¹³C {¹H} NMR (CDCl₃) δ 14.04 (m, CH₂), 16.26 (d, ³J_{CP} = 6.0 Hz, 2 x CH₃), 25.00 (d, ¹J_{CP} = 143.6 Hz, CH₂), 31.04 (m, CH₂), 62.00 (d, ²J_{CP} = 7.2 Hz, 2 x CH₂); ³¹P {¹H} NMR (CDCl₃) δ 30.11 (S); ¹⁹F NMR (CDCl₃) δ -80.81 (3F, t, ⁴J_{FF} = 10.0 Hz, CF₃), -114.50 (2F, m, α-CF₂), -121.71 (2F, m, CF₂), -121.92 (4F, m, 2 x CF₂), -122.70 (2F, s, CF₂), -123.55 (2F, m, CF₂), -126.11 (2F, m, CF₂); m/z (ES⁺) 599 (MH⁺, 100%).

6.2.3. Synthesis of Diethyl Phosphonates *via* Beletskaya Protocol^[11]

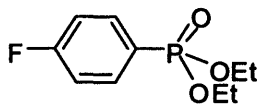
6.2.3.1. Synthesis of PhPO(OEt)₂^[11]



To a flame dried three neck round bottom flask (EtO)₂PO(H) (10.0 cm³, 0.078 mol) and NEt₃ (6.3 cm³, 0.045 mol) were added under inert conditions. The mixture was stirred for 30 minutes before adding CH₃CN/H₂O (1:1, 40 cm³), bromobenzene (4.71 g, 0.030 mol) and PPh₃ (0.47 g, 1.79 mmol). When all of the ligand had dissolved, [Pd(OAc)₂] (0.20 g, 0.89 mmol) was added and the mixture was stirred at 100 °C for 24 hours. After cooling, the mixture was filtered through 1 cm³ of silica on a glass filter frit, extracted

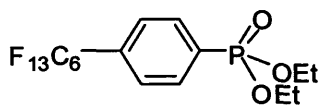
with Et₂O and dried over MgSO₄. The solvent was removed *in vacuo* to yield a brown/orange oil (2.13 g, 33%); data as for 6.2.1.1.

6.2.3.2. Synthesis of 4-F-C₆H₄-PO(OEt)₂^[12]



To a flame dried three neck round bottom flask (EtO)₂PO(H) (5.0 cm³, 0.039 mol) and NEt₃ (6.54 cm³, 0.047 mol) were added under inert conditions. The mixture was stirred for 40 minutes before adding CH₃CN/H₂O (1:1, 20 cm³), 4-fluorobromobenzene (6.125 g, 0.035 mol) and PPh₃ (0.41 g, 1.56 mmol). When all of the ligand had dissolved, [Pd(OAc)₂] (0.175 g, 0.78 mmol) was added and the mixture was stirred at 90 °C for 3 hours. After cooling, the mixture was filtered through 1 cm³ of silica on a glass filter frit, extracted with Et₂O and dried over MgSO₄. Solvent was removed *in vacuo* and the crude product was then purified by Kugelröhr distillation (60 °C, 0.01 mmHg) to yield a clear colourless oil (2.14 g, 26%); Found C, 51.7%; H, 6.2%, C₁₀H₁₄FO₃P requires C, 51.7%; H, 6.0%; ¹H (CDCl₃) δ 1.25 (6H, t, ³J_{HH} = 7.0 Hz, CH₃), 4.00 + 4.06 (4H, 2 x AB dq, ³J_{HaP} = 7.6 Hz, ³J_{HbP} = 7.9 Hz, ³J_{HH} = 7.0 Hz, ²J_{HaHb} = 10.0 Hz, 2 x CH₂), 7.08 (2H, ddd, ³J_{HP} = 12.8 Hz, ⁴J_{HF} = 8.8 Hz, ³J_{HH} = 8.8 Hz, o-C₆H₄), 7.75 (2H, ddd, ⁴J_{HP} = 3.2 Hz, ³J_{HF} = 5.5 Hz, ³J_{HH} = 8.8 Hz, m-C₆H₄); ¹H {³¹P}NMR (CDCl₃) δ 1.23 (6H, t, ³J_{HH} = 7.0 Hz, CH₃), 4.00 + 4.06 (4H, 2 x AB q, ³J_{HH} = 7.0 Hz, ²J_{HaHb} = 10.0 Hz, 2 x CH₂), 7.06 (2H, dd, ⁴J_{HF} = 8.8 Hz, ³J_{HH} = 8.8 Hz), 7.73 (2H, dd, ³J_{HF} = 5.5 Hz, ³J_{HH} = 8.8 Hz); ¹H {¹⁹F}NMR (CDCl₃) δ 1.25 (6H, t, ³J_{HH} = 7.0 Hz, CH₃), 4.00 + 4.05 (4H, 2 x AB dq, ³J_{HaP} = 7.6 Hz, ³J_{HbP} = 7.9 Hz, ³J_{HH} = 7.0 Hz, ²J_{HaHb} = 10.0 Hz, 2 x CH₂), 7.07 (2H, dd, ⁴J_{HP} = 3.5 Hz, ³J_{HH} = 8.8 Hz), 7.75 (2H, dd, ³J_{HP} = 12.8 Hz, ³J_{HH} = 8.8 Hz); ¹³C {¹H} NMR (CDCl₃) δ 16.23 (d, ³J_{CP} = 6.0 Hz, 2 x CH₃), 62.17 (d, ²J_{CP} = 6.0 Hz, 2 x CH₂), 115.79 (dd, ³J_{CP} = 15.6 Hz, ²J_{CF} = 21.5 Hz, 3-C), 124.4 (d, ¹J_{CP} = 193.2 Hz, 1-C), 134.33 (dd, ²J_{CP} = 10.8 Hz, ³J_{CF} = 8.4 Hz, 2-C), 165.53 (d, ¹J_{CF} = 252.8 Hz, 4-C); ³¹P {¹H} NMR (CDCl₃) δ 18.36 (S); ¹⁹F {¹H} NMR (CDCl₃) δ -106.04 (S); m/z (ES⁺) 232 (MH⁺, 80%).

6.2.3.3. Synthesis of 4-F₁₃C₆-C₆H₄-PO(OEt)₂



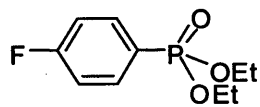
To a flame dried three neck round bottom flask were added (EtO)₂PO(H) (2.6 cm³, 0.020 mol) and NEt₃ (3.4 cm³, 0.024 mol) under inert conditions. The mixture was stirred for 40 minutes before adding CH₃CN/H₂O (1:1, 20 cm³), 4-perfluorohexyl-4-bromobenzene (8.00 g, 0.017 mol) and PPh₃ (0.210 g, 0.80 mmol). When all of the ligand was dissolved, [Pd(OAc)₂] (0.087 g, 0.40 mmol) was added and the mixture was stirred at 90 °C for 5 hours. After cooling, the mixture was filtered through 1

cm³ of silica on a glass filter frit, extracted with Et₂O and dried over MgSO₄. Solvent was removed *in vacuo* and the crude product was then purified by Kugelröhr distillation (60 °C, 0.01 mmHg) to yield a clear colourless oil (1.69 g, 19%); Found C, 35.89%; H, 2.46%, C₁₆H₁₄F₁₃O₃P requires C, 36.09%; H, 2.63%; ¹H (CDCl₃) δ 1.27 (6H, t, ³J_{HH} = 7.0 Hz, CH₃), 4.04 + 4.14 (4H, 2 x AB dq, ³J_{HaP} = 7.9 Hz, ³J_{HbP} = 7.9 Hz, ³J_{HH} = 7.0 Hz, ²J_{HaHb} = 10.2 Hz, 2 x CH₂), 7.62 (2H, dd, ³J_{HH} = 8.2 Hz, ⁴J_{HP} = 3.5 Hz, 3-H), 7.89 (2H, dd, ³J_{HH} = 8.2 Hz, ³J_{HP} = 13.2 Hz, 2-H); ¹H {³¹P} NMR (CDCl₃) δ 1.27 (6H, t, ³J_{HH} = 7.0 Hz, CH₃), 4.04 + 4.14 (4H, 2 x AB q, ³J_{HH} = 7.0 Hz, ²J_{HaHb} = 10.2 Hz, 2 x CH₂), 7.62 (2H, d, ³J_{HH} = 8.2 Hz, 3-H), 7.89 (2H, d, ³J_{HH} = 8.2 Hz, 2-H); ¹H {¹⁹F} NMR (CDCl₃) δ 1.35 (6H, t, ³J_{HH} = 7.0 Hz, CH₃), 4.13 + 4.21 (4H, 2 x AB dq, ³J_{HaP} = 7.9 Hz, ³J_{HbP} = 7.9 Hz, ³J_{HH} = 7.0 Hz, ²J_{HaHb} = 10.2 Hz, 2 x CH₂), 7.71 (2H, dd, ³J_{HH} = 8.2 Hz, ⁴J_{HP} = 3.5 Hz, 3-H), 7.89 (2H, dd, ³J_{HH} = 8.2 Hz, ³J_{HP} = 13.2 Hz, 2-H); ¹³C {¹H} NMR (CDCl₃) δ 16.14 (d, ³J_{CP} = 6.0 Hz, 2 x CH₃), 62.47 (d, ²J_{CP} = 6.0 Hz, 2 x CH₂) 126.86 (dt, ³J_{CF} = 6.0 Hz, ³J_{CP} = 14.4 Hz, 3-C), 131.93 (d, ²J_{CP} = 10.8 Hz, 2-C), 132.60 (dt, ²J_{CF} = 23.9 Hz, ⁴J_{CP} = 3.6 Hz, 4-C), 133.23 (d, ¹J_{CP} = 167.55 Hz, 1-C); ³¹P {¹H} NMR (CDCl₃) δ 16.31 (S); ¹⁹F NMR (CDCl₃) δ -80.82 (3F, t, ⁴J_{FF} = 9.5 Hz, CF₃), -111.29 (2F, t, ⁴J_{FF} = 14.2 Hz, α-CF₂), -121.42 (2F, m, CF₂), -121.69 (2F, m, CF₂), -122.79 (2F, m, CF₂), -123.33 (2F, m, CF₂); m/z (ES⁺) 533 (MH⁺, 100%).

6.2.4. Synthesis of Diethyl Phosphonates *via* Hirao Protocol^[13]

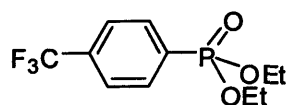
N.B: Pd(PPh₃)₄ is light and air sensitive and must be stored in a fridge and handled under argon.

6.2.4.1. Synthesis of 4-F-C₆H₄-PO(OEt)₂^[12]



HPO(OEt)₂ (6.4 cm³, 0.050 mol) and NEt₃ (7.0 cm³, 0.050 mol) were added to a flame dried 3 neck round bottom flask under N₂. A solution of Pd(PPh₃)₄ (2.65 g, 2.3 mmol) and 4-F-C₆H₄-Br (8.00 g, 0.046 mol) in toluene (20 cm³) was added under N₂ and the mixture was stirred at 90 °C for 3.5 hours. After cooling, Et₂O (50 cm³) was added and the resulting NEt₃.HBr was removed by vacuum filtration. The solvent was removed *in vacuo* and the crude product was Kugelröhr distilled to yield a clear oil (7.29 g, 69 %); Data as for 6.2.3.3.

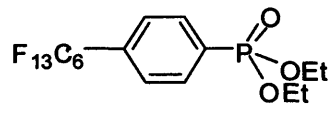
6.2.4.2. Synthesis of 4-F₃C-C₆H₄-PO(OEt)₂^[14]



HPO(OEt)₂ (5.8 cm³, 0.045 mol) and NEt₃ (6.3 cm³, 0.045 mol) were added to a flame dried 3 neck round bottom flask under N₂. A solution of

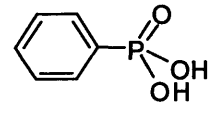
[Pd(PPh₃)₄] (2.40 g, 2.0 mmol) and 4-F₃C-C₆H₄-I (11.30 g, 0.042 mol) in toluene (75 cm³) was added under N₂ and the mixture was stirred at 90 °C for 2.5 hours. After cooling, Et₂O (100 cm³) was added and the resulting NEt₃.HI was removed by vacuum filtration. The solvent was removed *in vacuo* and the crude product was Kugelröhr distilled to yield a clear oil (8.175 g, 69 %); Found C, 46.72%; H, 4.95%, C₁₁H₁₄F₃O₃P requires C, 46.81%; H, 4.96%; ¹H (CDCl₃) δ 1.33 (6H, t, ³J_{HH} = 7.3 Hz, CH₃), 4.03 + 4.12 (4H, 2 x AB dq, ³J_{HaP} = 7.9 Hz, ³J_{HbP} = 8.2 Hz, ³J_{HH} = 7.0 Hz, ²J_{HaHb} = 10.2 Hz, 2 x CH₂), 7.88 (2H, dd, ³J_{HP} = 12.9 Hz, ³J_{HH} = 8.5 Hz, 2-H), 7.65 (2H, dd, ³J_{HP} = 3.5 Hz, ³J_{HH} = 8.2 Hz, 3-H); ¹³C {¹H} NMR (CDCl₃) δ 16.16 (d, ³J_{CP} = 6.0 Hz, 2 x CH₃), 62.44 (d, ²J_{CP} = 6.0 Hz, 2 x CH₂), 123.45 (q, ¹J_{CF} = 272.4 Hz, CF₃), 125.22 (dq, ³J_{CF} = 3.6 Hz, ³J_{CP} = 14.4 Hz, 3-C), 132.15 (d, ²J_{CP} = 10.8 Hz, 2-C), 132.76 (d, ¹J_{CP} = 187.9 Hz, 1-C), 133.95 (dq, ²J_{CF} = 32.3 Hz, ⁴J_{CP} = 3.6 Hz, 4-C); ³¹P {¹H} NMR (CDCl₃) δ 16.34 (s); ¹⁹F {¹H} NMR (CDCl₃) δ -63.31 (s); m/z (ES⁺) 282 (MH⁺, 30%).

6.2.4.3. Synthesis of 4-F₁₃C₆-C₆H₄-PO(OEt)₂

 HPO(OEt)₂ (2.6 cm³, 0.020 mol) and NEt₃ (2.8 cm³, 0.020 mol) were added to a flame dried 3 neck round bottom flask under N₂. A solution of [Pd(PPh₃)₄] (0.98 g, 0.85 mmol) and 4-F₁₃C₆-C₆H₄-Br (8.00 g, 0.017 mol) in toluene (20 cm³) was added under N₂ and the mixture was stirred at 90 °C for 3.5 hours. After cooling, Et₂O (100 cm³) was added and the resulting NEt₃.HI was removed by vacuum filtration. The solvent was removed *in vacuo* and the crude product was Kugelröhr distilled to yield a clear oil (7.65 g, 85 %); data as for 6.2.3.3.

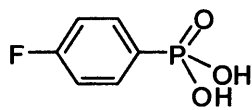
6.2.5. Synthesis of Phosphonic Acids

6.2.5.1. Synthesis of PhPO(OH)₂^[15]

 PhPO(OEt)₂ (1.01 g, 4.72 mmol) was refluxed (120 °C) with vigorous stirring for 24 hours in H₂O (20 cm³) with 12M HCl (25 cm³) as catalyst. The solvent was evaporated, and the pale orange solid was washed with chloroform and dried under vacuum to yield the product as white powder (0.73 g, 97%); Found C, 45.8%; H, 4.4%, C₆H₇O₃P requires C, 45.6%; H, 4.4%; ¹H NMR (D₂O) δ 7.48 (3H, m), 7.68 (2H, dd, ³J_{HP} = 13.1 Hz, ³J_{HH} = 8.0 Hz); ¹H NMR (C₃D₆O) δ 7.42 – 7.94 (5H, m), 4.71 (2H, bs, 2 x OH); ¹³C {¹H} NMR (D₂O) δ 128.70 (d, ³J_{CP} = 14.4 Hz), 130.09 (d, ²J_{CP} = 10.8 Hz), 130.51 (d, ¹J_{CP} = 187.2 Hz), 132.32

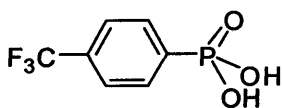
(d, $^4J_{CP} = 2.4$ Hz), ^{31}P $\{^1\text{H}\}$ NMR (D_2O) δ 15.84 (S); ^{31}P $\{^1\text{H}\}$ NMR ($\text{C}_3\text{D}_6\text{O}$) δ 19.54 (S); m/z (ES^+) 159 (MH^+ , 100%).

6.2.5.2. Synthesis of 4-F-C₆H₄-PO(OH)₂^[14]



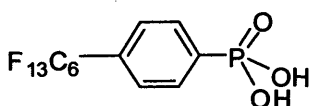
4-F-C₆H₄-PO(OEt)₂ (1.84 g, 7.93 mmol) was refluxed (120 °C) with vigorous stirring for 24 hours in H₂O (20 cm³) with 12M HCl (25 cm³) as catalyst. The solvent was evaporated, and the pale orange solid was washed with chloroform and dried under vacuum to yield the product as white powder (1.24 g, 89%); Found C, 40.8 %; H, 3.3 %, C₆H₆O₃PF requires C, 40.9 %; H, 3.4 %; ^1H NMR ($\text{C}_3\text{D}_6\text{O}$) δ 7.25 (2H, ddd, $^3J_{\text{HF}} = 8.5$ Hz, $^3J_{\text{HH}} = 8.5$ Hz, $^4J_{\text{HP}} = 2.9$ Hz, 3-H), 7.85 (2H, ddd, $^4J_{\text{HF}} = 5.8$ Hz, $^3J_{\text{HH}} = 8.7$ Hz, $^3J_{\text{HP}} = 13.1$, 2-H), 10.17 (2H, s, 2 x OH); ^{13}C $\{^1\text{H}\}$ NMR ($\text{C}_3\text{D}_6\text{O}$) δ 116.20 (dd, $^3J_{\text{CP}} = 15.2$ Hz, $^2J_{\text{CF}} = 21.4$ Hz, 3-C), 134.45 (dd, $^2J_{\text{CP}} = 12.0$ Hz, $^3J_{\text{CF}} = 8.2$ Hz, 2-C); ^{31}P $\{^1\text{H}\}$ NMR ($\text{C}_3\text{D}_6\text{O}$) δ 17.08 (S); ^{31}P $\{^1\text{H}\}$ NMR (D_2O) δ 15.14 (S); ^{19}F $\{^1\text{H}\}$ NMR ($\text{C}_3\text{D}_6\text{O}$) δ -109.22 (S); m/z (ES^+) 177 (MH^+ , 30%); m/z (ES^-) 175 (MH^- , 100%).

6.2.5.3. Synthesis of 4-F₃C-C₆H₄-PO(OH)₂^[14]



4-F₃C-C₆H₄-PO(OEt)₂ (7.00 g, 0.025 mol) was refluxed (110 °C) with vigorous stirring for 48 hours in H₂O (50 cm³) with 12M HCl (20 cm³) as catalyst. The solvent was evaporated, and the white solid was washed with hexane and dried under vacuum to yield the product as white powder (3.70 g, 67%); Found C, 37.0 %; H, 2.6 %, C₇H₆F₃O₃P requires C, 37.2 %; H, 2.7 %; ^1H NMR ($\text{C}_3\text{D}_6\text{O}$) δ 7.13 (2H, s, 2 x OH), 7.75-7.91 (m, 2H), 8.01 (m, 2H); ^{31}P $\{^1\text{H}\}$ NMR ($\text{C}_3\text{D}_6\text{O}$) δ 15.37 (S); ^{31}P $\{^1\text{H}\}$ NMR (C_6D_6) δ 14.06 (S); ^{19}F $\{^1\text{H}\}$ NMR ($\text{C}_3\text{D}_6\text{O}$) δ -63.73 (s, CF₃); ^{13}C $\{^1\text{H}\}$ NMR ($\text{C}_3\text{D}_6\text{O}$) δ 123.92 (q, $^1J_{\text{CF}} = 272.3$ Hz, CF₃), 126.05 (d, $^2J_{\text{CP}} = 10.8$ Hz, 2-C), 132.46 (d, $^3J_{\text{CP}} = 9.6$ Hz, 3-C), 132.80 (q, $^2J_{\text{CF}} = 32.3$ Hz, 2-C), 137.23 (d, $^1J_{\text{CP}} = 184.1$ Hz, 1-C); m/z (ES^-) 225 (MH^- , 100%).

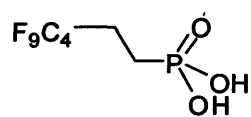
6.2.5.4. Synthesis of 4-F₁₃C₆-C₆H₄-PO(OH)₂



4-F₁₃C₆-C₆H₄-PO(OEt)₂ (2.50 g, 4.70 mmol) was refluxed (110 °C) with vigorous stirring for 72 hours in H₂O (20 cm³) with 12M HCl (30 cm³) as catalyst. The solvent was evaporated, and the brown solid was washed with chloroform and dried under vacuum to yield the product as white powder (2.24 g, 97%);

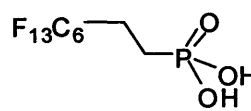
Found C, 30.2 %; H, 1.2 %, C₁₂H₆F₁₃O₃P requires C, 30.3 %; H, 1.3 %; ¹H NMR (C₃D₆O) δ 7.72 (2H, dd, ³J_{HH} = 8.5 Hz, ⁴J_{HP} = 2.9 Hz, 3-H), 7.94 (2H, dd, ³J_{HH} = 8.5 Hz, ³J_{HP} = 13.2, 2-H), 8.01 (2H, s, 2 x OH); ³¹P {¹H} NMR (C₃D₆O) δ 15.20 (S); ³¹P {¹H} NMR (C₆D₆) δ 19.59 (S); ¹⁹F {¹H} NMR (C₃D₆O) δ -81.70 (3F, t, ⁴J_{FF} = 10.4 Hz, CF₃), -111.41 (2F, t, ⁴J_{FF} = 14.2 Hz, α-CF₂), -122.00 (2F, m, CF₂), -122.20 (2F, m, CF₂), -123.47 (2F, m, CF₂), -126.83 (2F, m, CF₂); ¹³C {¹H} NMR (C₃D₆O) δ 127.71 (dt, ³J_{CP} = 6.1 Hz, ⁴J_{CF} = 14.6 Hz, 3-C), 132.33 (d, ²J_{CP} = 10.8 Hz, 2-C); m/z (ES⁻) 475 (MH⁻, 100 %).

6.2.5.5. Synthesis of F₉C₄-C₂H₄-PO(OH)₂



F₉C₄-C₂H₄-PO(OEt)₂ (3.17 g, 8.2 mmol) was refluxed (110 °C) with vigorous stirring for 48 hours in H₂O (20 cm³) with 12M HCl (20 cm³) as catalyst. The solvent was evaporated, and the white solid was washed with chloroform and dried under vacuum to yield the product as white powder (1.80 g, 67 %); Found C, 22.1 %; H, 1.7 %, C₆H₆F₉O₃P requires C, 22.0 %; H, 1.8 %; ¹H NMR (C₃D₆O) δ 2.05 (2H, m, CH₂), 2.51 (2H, m, CH₂), 10.45 (2H, s, 2 x OH); ³¹P {¹H} NMR (C₆D₆) δ 25.77 (S); ³¹P {¹H} NMR (C₃D₆O) δ 27.56 (S); ¹⁹F {¹H} NMR (C₃D₆O) δ -81.01 (3F, t, ⁴J_{FF} = 9.5 Hz, CF₃), -115.90 (2F, m, α-CF₂), -124.91 (2F, m, CF₂), -126.84 (2F, m, CF₂); ¹³C {¹H} NMR (C₃D₆O) δ 18.85 (d, ¹J_{CP} = 146.0 Hz, CH₂), 25.93 (m, CH₂); m/z (ES⁻) 327 (MH⁻, 100 %).

6.2.5.6. Synthesis of F₁₃C₆-C₂H₄-PO(OH)₂



F₁₃C₆-C₂H₄-PO(OEt)₂ (3.10 g, 6.4 mmol) was refluxed (110 °C) with vigorous stirring for 24 hours in H₂O (10 cm³) with 12M HCl (30 cm³) as catalyst. The solvent was evaporated, and the pale orange solid was washed with chloroform and dried under vacuum to yield the product as a white powder (2.51 g, 91%); Found C, 22.6 %; H, 1.4 %, C₈H₆F₁₃O₃P requires C, 22.4 %; H, 1.4 %; ¹H NMR (C₃D₆O) δ 1.92 (2H, m, CH₂), 2.36 (2H, m, CH₂), 8.59 (2H, s, 2 x OH); ³¹P {¹H} NMR (C₃D₆O) δ 27.81 (S); ³¹P {¹H} NMR (C₆D₆) δ 32.93 (S); ¹⁹F {¹H} NMR (C₃D₆O) δ -81.82 (3F, t, ⁴J_{FF} = 10.4 Hz, CF₃), -115.66 (2F, m, α-CF₂), -122.52 (2F, m, CF₂), -123.53 (2F, m, CF₂), -123.98 (2F, m, CF₂), -126.80 (2F, m, CF₂); ¹³C {¹H} NMR (C₃D₆O) δ 18.91 (d, ¹J_{CP} = 149.6 Hz, CH₂), 25.95 (s, CH₂); m/z (ES⁻) 427 (MH⁻, 100 %).

6.2.6. Synthesis of Amorphous Zirconium Phosphonates

6.2.6.1. Synthesis of $[\text{Zr}(\text{O}_3\text{PPh})_2]$ ^[16]

To a stirred solution of $[\text{ZrOCl}_2 \cdot 8\text{H}_2\text{O}]$ (0.082 g, 0.26 mmol) in H_2O (5 cm^3) was added a solution of $\text{PhPO}(\text{OH})_2$ (0.080 g, 0.51 mmol) in H_2O (1 cm^3). A white solid immediately precipitated from the solution. After 5 minutes of stirring the solid was filtered and dried under vacuum to yield a white powder (0.101 g, 99%); EDAX: C, O, P, Zr in 12:6:2:1 ratio; IR: 994, 1015, 1023 cm^{-1} $\nu(\text{P-O})$, 1144 cm^{-1} $\nu(\text{P-C})$.

6.2.6.2. Synthesis of $[\text{Zr}(\text{O}_3\text{P-C}_6\text{H}_4\text{-4-CF}_3)_2]$

To a stirred solution of $[\text{ZrOCl}_2 \cdot 8\text{H}_2\text{O}]$ (2.90 g, 0.009 mol) in H_2O (10 cm^3) was added a solution of 4- $\text{F}_3\text{C-C}_6\text{H}_4\text{-PO}(\text{OH})_2$ (4.19 g, 0.019 mol) in H_2O (10 cm^3). A white solid immediately precipitated from the solution. After 5 minutes of stirring the solid was filtered, washed well with H_2O and dried under vacuum to yield a white powder (4.10 g, 82%); IR: 1008, 1035, 1049 cm^{-1} $\nu(\text{P-O})$, 1131 cm^{-1} $\nu(\text{P-C})$.

6.2.6.3. Synthesis of $[\text{Zr}(\text{O}_3\text{P-C}_6\text{H}_4\text{-4-C}_6\text{F}_{13})_2]$

To a stirred solution of $[\text{ZrOCl}_2 \cdot 8\text{H}_2\text{O}]$ (0.34 g, 1.05 mmol) in H_2O (5 cm^3) was added a solution of 4- $\text{F}_{13}\text{C}_6\text{-C}_6\text{H}_4\text{-PO}(\text{OH})_2$ (1.00 g, 2.10 mmol) in THF (5 cm^3). A white solid immediately precipitated from the solution. After 5 minutes of stirring the solid was filtered, washed well with H_2O and THF and dried under vacuum to yield a white powder (0.978 g, 90%); IR: 1011, 1037, 1091 cm^{-1} $\nu(\text{P-O})$, 1141 cm^{-1} $\nu(\text{P-C})$.

6.2.6.4. Synthesis of $[\text{Zr}(\text{O}_3\text{P-C}_2\text{H}_4\text{-C}_4\text{F}_9)_2]$

To a stirred solution of $[\text{ZrOCl}_2 \cdot 8\text{H}_2\text{O}]$ (0.74 g, 2.29 mmol) in H_2O (5 cm^3) was added a solution of $\text{F}_9\text{C}_4\text{-C}_2\text{H}_4\text{-PO}(\text{OH})_2$ (1.50 g, 4.57 mmol) in THF (10 cm^3). A white solid immediately precipitated from the solution. After 5 minutes of stirring the solid was filtered, washed well with H_2O and THF and dried under vacuum to yield a white powder (1.68 g, 99%); IR: 1012, 1021, 1057 cm^{-1} $\nu(\text{P-O})$, 1134 cm^{-1} $\nu(\text{P-C})$.

6.2.6.5. Synthesis of $[\text{Zr}(\text{O}_3\text{P}-\text{C}_2\text{H}_4-\text{C}_6\text{F}_{13})_2]$

To a stirred solution of $[\text{ZrOCl}_2 \cdot 8\text{H}_2\text{O}]$ (0.38 g, 1.17 mmol) in H_2O (5 cm^3) was added a solution of $\text{F}_{13}\text{C}_6-\text{C}_2\text{H}_4-\text{PO}(\text{OH})_2$ (1.00 g, 2.34 mmol) in THF (5 cm^3). A white solid immediately precipitated from the solution. After 5 minutes of stirring the solid was filtered, washed well with H_2O and THF and dried under vacuum to yield a white powder (0.102 g, 93%); EDAX: C, F, O, P, Zr in 24:26:6:2:1 ratio. IR: 1008, 1035, 1062 cm^{-1} $\nu(\text{P}-\text{O})$, 1131 cm^{-1} $\nu(\text{P}-\text{C})$.

6.2.7. Synthesis of Crystalline Zirconium Phosphonates

6.2.7.1. Synthesis of Crystalline $[\text{Zr}(\text{O}_3\text{PPh})_2]$ in Glass Apparatus

A solution of $[\text{ZrOCl}_2 \cdot 8\text{H}_2\text{O}]$ (0.045 g, 0.25 mmol) in H_2O (2 cm^3) was added to a 50 cm^3 three-neck round bottom flask fitted with condenser, and N_2 flow. The condenser was connected to a Dreschel bottle containing a saturated aqueous NaOH solution to trap any evolved HF. 40% aqueous HF (0.33 cm^3 , $d = 1.13 \text{ g cm}^{-3}$, 0.15 g, 7.5 mmol) was added and the solution was stirred for 10 minutes. $\text{PhPO}(\text{OH})_2$ (0.400 g, 2.5 mmol) in H_2O (20 cm^3) was added dropwise to the solution at $90 \text{ }^\circ\text{C}$. The reaction was heated under N_2 with gentle stirring for 4 hours. After cooling, aqueous NaOH (50 cm^3) was added and the grey solid was washed with H_2O and acetone and dried under vacuum to yield a white powder (0.096 g, 95%); X-ray powder diffraction patterns: crystalline $[\text{Zr}(\text{O}_3\text{PPh})_2]$ and significant amounts of $[\text{ZrF}_6\text{H}_2]$; IR: 1012, 1039, 1092 cm^{-1} $\nu(\text{P}-\text{O})$, 1147 cm^{-1} $\nu(\text{P}-\text{C})$.

6.2.7.2. Synthesis of Crystalline $[\text{Zr}(\text{O}_3\text{P}-\text{C}_2\text{H}_4-4-\text{C}_6\text{F}_{13})_2]$ in Glass Apparatus

A solution of $[\text{ZrOCl}_2 \cdot 8\text{H}_2\text{O}]$ (0.038 g, 0.12 mmol) in H_2O (1 cm^3) was added to a 50 cm^3 three-neck round bottom flask fitted with condenser, and N_2 flow. The condenser was connected to a Dreschel bottle containing a saturated aqueous NaOH solution to trap any evolved HF. 40% aqueous HF (0.5 cm^3 , $d = 1.13 \text{ g cm}^{-3}$, 0.23 g, 11.3 mmol) was added and the solution was stirred for 10 minutes. $4-\text{F}_{13}\text{C}_6-\text{C}_2\text{H}_4-\text{PO}(\text{OH})_2$ (1.00 g, 2.3 mmol) in THF (50 cm^3) was added dropwise to the solution at $40 \text{ }^\circ\text{C}$ over 2 days. The reaction was heated under N_2 with gentle stirring for a further 2 days. After cooling, 50 cm^3 of aqueous NaOH was added and the white solid was washed with H_2O and acetone and dried under vacuum to yield a white powder (0.055 g, 50%); X-ray powder diffraction patterns: crystalline $[\text{Zr}(\text{O}_3\text{P}-\text{C}_2\text{H}_4-\text{C}_6\text{F}_{13})_2]$ and significant amounts of H_2ZrF_6 and SiO_2 ; IR: 1011, 1044, 1077 cm^{-1} $\nu(\text{P}-\text{O})$, 1144 cm^{-1} $\nu(\text{P}-\text{C})$.

6.2.7.3. Synthesis of Crystalline $[\text{Zr}(\text{O}_3\text{PPh})_2]$ in Plastic Apparatus

A solution of $[\text{ZrOCl}_2 \cdot 8\text{H}_2\text{O}]$ (0.20 g, 0.63 mmol) in H_2O (5 cm^3) was added to a Teflon conical flask fitted with a plastic syringe and a length of plastic tubing leading to a Dreschel bottle containing a saturated aqueous NaOH. 40% aqueous HF (1.4 cm^3 , $d = 1.13 \text{ g cm}^{-3}$, 0.63 g, 32.0 mmol) was added and the solution was stirred for 10 minutes then heated to $90 \text{ }^\circ\text{C}$. $\text{PhPO}(\text{OH})_2$ (1.00 g, 6.3 mmol) in THF (50 cm^3) was added dropwise to the solution at $40 \text{ }^\circ\text{C}$ over 2 days. The reaction was heated under N_2 with gentle stirring for a further 2 days. After cooling, 50 cm^3 aqueous NaOH was added and the white solid was washed with H_2O and acetone and dried under vacuum to yield a white powder (0.110 g, 44%); IR: $1012, 1039, 1092 \text{ cm}^{-1} \nu(\text{P-O})$, $1147 \text{ cm}^{-1} \nu(\text{P-C})$.

6.2.7.4. Synthesis of Crystalline $[\text{Zr}(\text{O}_3\text{P-C}_6\text{H}_4\text{-4-C}_6\text{F}_{13})_2]$ in Plastic Apparatus

A solution of $[\text{ZrOCl}_2 \cdot 8\text{H}_2\text{O}]$ (0.10 g, 0.32 mmol) in H_2O (5 cm^3) was added to a Teflon conical flask fitted with a plastic syringe and a length of plastic tubing leading to a Dreschel bottle containing a saturated aqueous NaOH. 40% aqueous HF (0.7 cm^3 , $d = 1.13 \text{ g cm}^{-3}$, 0.32 g, 16.0 mmol) was added and the solution was stirred for 10 minutes then heated to $90 \text{ }^\circ\text{C}$. 4- $\text{F}_{13}\text{C}_6\text{-C}_6\text{H}_4\text{-PO}(\text{OH})_2$ (1.00 g, 2.3 mmol) in THF (50 cm^3) was added dropwise to the solution at $40 \text{ }^\circ\text{C}$ over 2 days. The reaction was heated under N_2 with gentle stirring for a further 2 days. After cooling, 50 cm^3 aqueous NaOH was added and the white solid was washed with H_2O and acetone and dried under vacuum to yield a white powder (0.190 g, 58%); IR: $1010, 1039, 1092 \text{ cm}^{-1} \nu(\text{P-O})$, $1140 \text{ cm}^{-1} \nu(\text{P-C})$.

6.2.8. Synthesis of Platinum bis-Triphenylphosphine complexes of Phosphonic Acids

6.2.8.1. Synthesis of $[\text{Pt}\{\overline{\text{OP}(\text{O})(\text{Ph})\text{O}}\}(\text{PPh}_3)_2]$ ^[17]

Phenyl phosphonic acid (0.066 g, 41.8 mmol) and silver (I) oxide (0.580 g, 251 mmol) were added in succession to a stirred solution of $[\text{PtCl}_2(\text{PPh}_3)_2]$ (0.330 g, 41.8 mmol) in dichloromethane (40 cm^3) and the mixture refluxed for 4 hours. The cooled reaction mixture was filtered and the filtrate evaporated to dryness under reduced pressure to yield a white powder, which was recrystallised from dichloromethane-light petroleum and dried *in vacuo* (0.317 g, 87%); ^1H NMR (CD_2Cl_2) δ 9.08-9.45 (30H, m, Ph), 9.72-9.83 (5H, m, Ar); ^{31}P $\{^1\text{H}\}$ NMR (CD_2Cl_2) δ 9.2 (d, $^1J_{\text{PtP}} = 3872$, $^3J_{\text{PP}} = 7.3 \text{ Hz}$, PPh_3), 37.3 (t, $^2J_{\text{PtP}} = 126 \text{ Hz}$, $^3J_{\text{PP}} = 7.3 \text{ Hz}$, PO_3); ^{13}C $\{^1\text{H}\}$ NMR (CD_2Cl_2) δ

127.92 (d, $^2J_{CP} = 13.0$ Hz, 2-CH), 128.05 (m, C), 128.73 (m, CH), 129.51 (d, $^4J_{CP} = 2.8$ Hz, 4-CH), 131.05 (d, $^3J_{CP} = 9.3$ Hz, 3-CH), 131.74 (m, CH), 134.71 (m, CH), 140.30 (d, $^1J_{CP} = 162.9$ Hz, 1-C); m/z (FAB) 876 (MH⁺, 100 %). Crystals suitable for characterisation by X-ray crystallography were grown from DCM/petroleum ether. See appendix for structural data.

6.2.8.2. Synthesis of $[\text{Pt}\{\text{OP}(\text{O})(\text{C}_6\text{H}_4\text{-4-F})\text{O}\}(\text{PPh}_3)_2]$

4-F-C₆H₄-PO(OH)₂ (0.074 g, 41.8 mmol) and silver (I) oxide (0.580 g, 251 mmol) were added in succession to a stirred solution of [PtCl₂(PPh₃)₂] (0.330 g, 41.8 mmol) in dichloromethane (40 cm³) and the mixture refluxed for 4 hours. The cooled reaction mixture was filtered and the filtrate evaporated to dryness under reduced pressure to yield a white powder, which was recrystallised from dichloromethane-light petroleum and dried *in vacuo* (0.343 g, 92%); Found C, 55.3%; H, 3.6%, C₄₂H₃₄FO₃P₃Pt requires C, 56.4%; H, 3.8%; ¹H NMR (CD₂Cl₂) δ 6.93-7.02 (2H, m, *o*-Ar), 7.10-7.37 (30H, m, Ph), 7.66-7.76 (2H, m, *m*-Ar); ¹⁹F {¹H} NMR (CD₂Cl₂) δ -112.9 (S); ³¹P {¹H} NMR (CD₂Cl₂) δ 7.3 (d, $^1J_{\text{PtP}} = 3875$, $^3J_{\text{PP}} = 7.3$ Hz, PPh₃), 37.3 (t, $^2J_{\text{PtP}} = 125$ Hz, $^3J_{\text{PP}} = 7.3$ Hz, PO₃); ¹³C {¹H} NMR (CD₂Cl₂) δ 114.71 (dd, $^2J_{\text{CF}} = 20.6$ Hz, $^3J_{\text{CP}} = 14.4$ Hz, 3-C), 127.96 (m, C), 128.76 (m, CH), 131.84 (m, CH), 133.28 (dd, $^2J_{\text{CP}} = 10.5$ Hz, $^3J_{\text{CF}} = 7.8$ Hz, 2-C), 134.68 (m, CH), 136.58 (dd, $^1J_{\text{CP}} = 165.2$ Hz, $^4J_{\text{CF}} = 3.6$ Hz, 1-C); m/z (FAB) 894 (MH⁺, 100 %). Crystals suitable for characterisation by X-ray crystallography were grown from DCM/petroleum ether. See appendix for structural data.

6.2.8.3. Synthesis of $[\text{Pt}\{\text{OP}(\text{O})(\text{C}_6\text{H}_4\text{-4-CF}_3)\text{O}\}(\text{PPh}_3)_2]$

4-F₃C-C₆H₄-PO(OH)₂ (0.086 g, 38.0 mmol) and silver (I) oxide (0.530 g, 228 mmol) were added in succession to a stirred solution of [PtCl₂(PPh₃)₂] (0.300 g, 38.0 mmol) in dichloromethane (40 cm³) and the mixture refluxed for 6 hours. The cooled reaction mixture was filtered and the filtrate evaporated to dryness under reduced pressure to yield a white powder, which was recrystallised from dichloromethane-light petroleum and dried *in vacuo* (0.325 g, 91%); Found C, 54.6%; H, 3.8%, C₄₃H₃₄F₃O₃P₃Pt requires C, 54.7%; H, 3.6%; ¹H NMR (CD₂Cl₂) δ 7.09-7.36 (30H, m, Ph), 7.54-7.85 (4H, m, Ar); ¹⁹F {¹H} NMR (CD₂Cl₂) δ -62.8 (S); ³¹P {¹H} NMR (CD₂Cl₂) δ 7.2 (s, $^1J_{\text{PtP}} = 3879.0$ Hz), 32.7 (s, $^2J_{\text{PtP}} = 122.2$ Hz); ¹³C {¹H} NMR (CD₂Cl₂) δ 123.45 (q, $^1J_{\text{CF}} = 272.4$ Hz, CF₃), 124.32 (dq, $^3J_{\text{CF}} = 13.2$ Hz, $^3J_{\text{CP}} = 3.6$ Hz, 3-CH), 127.44 (m, C), 128.41 (m, CH), 130.54 (dq, $^2J_{\text{CF}} = 31.6$ Hz, $^4J_{\text{CP}} = 3.0$ Hz, 4-C), 130.76 (d, $^2J_{\text{CP}} = 9.4$ Hz, 2-CH), 131.48 (m, CH), 144.90 (d, $^1J_{\text{CP}} = 159.3$ Hz, 1-C); m/z (FAB) 944 (MH⁺, 100 %). Crystals suitable for characterisation by X-ray crystallography were grown from DCM/petroleum ether. See appendix for structural data.

6.2.8.4. Synthesis of $[\text{Pt}\{\text{OP}(\text{O})(\text{C}_6\text{H}_4\text{-4-C}_6\text{F}_{13})\text{O}\}(\text{PPh}_3)_2]$

4-F₁₃C₆-C₆H₄-PO(OH)₂ (0.086 g, 38.0 mmol) and silver (I) oxide (0.530 g, 228 mmol) were added in succession to a stirred solution of [PtCl₂(PPh₃)₂] (0.300 g, 38.0 mmol) in dichloromethane (40 cm³) and the mixture refluxed for 6 hours. The cooled reaction mixture was filtered and the filtrate evaporated to dryness under reduced pressure to yield a white powder, which was recrystallised from dichloromethane-light petroleum and dried *in vacuo* (0.385 g, 85%); Found C, 48.2%; H, 2.7%, C₄₈H₃₄F₁₃O₃P₃Pt requires C, 48.3%; H, 2.8%; ¹H NMR (CD₂Cl₂) δ 7.09-7.36 (30H, m, Ph), 7.54-7.85 (4H, m, Ar); ¹⁹F {¹H} NMR (CD₂Cl₂) δ -81.06 (3F, t, ⁴J_{FF} = 10.4 Hz, CF₃), -110.77 (2F, t, ⁴J_{FF} = 14.2 Hz, α-CF₂), -121.50 (2F, m, CF₂), -122.01 (2F, m, CF₂), -122.91 (2F, m, CF₂), -126.33 (2F, m, CF₂); ³¹P {¹H} NMR (CD₂Cl₂) δ 7.3 (s, ¹J_{PP} = 3881.3 Hz), 37.3 (t, ²J_{PP} = 117.2 Hz); ¹³C {¹H} NMR (CD₂Cl₂) δ 126.40 (m, CH), 127.78 (m, C), 128.81 (m, CH), 131.26 (d, ²J_{CP} = 9.4 Hz, 2-CH), 131.89 (m, C), 136.27 (m, CH), 144.90 (d, ¹J_{CP} = 160.1 Hz, 1-C); m/z (FAB) 1194 (MH⁺, 100 %).

6.2.8.5. Synthesis of $[\text{Pt}\{\text{OP}(\text{O})(\text{C}_2\text{H}_4\text{-C}_4\text{F}_9)\text{O}\}(\text{PPh}_3)_2]$

F₉C₄-C₂H₄-PO(OH)₂ (0.125 g, 38.0 mmol) and silver (I) oxide (0.530 g, 228 mmol) were added in succession to a stirred solution of [PtCl₂(PPh₃)₂] (0.300 g, 38.0 mmol) in dichloromethane (40 cm³) and the mixture refluxed for 6 hours. The cooled reaction mixture was filtered and the filtrate evaporated to dryness under reduced pressure to yield a white powder, which was recrystallised from dichloromethane-light petroleum and dried *in vacuo* (0.298 g, 75%); Found C, 48.2%; H, 3.4%, C₄₂H₃₄F₉O₃P₃Pt requires C, 48.2 %; H, 3.3 %; ¹H NMR (CD₂Cl₂) δ 1.67 (2H, m, CH₂), 2.26 (2H, m, CH₂), 7.13-7.37 (30H, m, Ph); ¹⁹F {¹H} NMR (CDCl₃) δ -81.29 (t, ⁴J_{FF} = 9.5 Hz, CF₃), -115.52 (m, α-CF₂), -124.42 (m, CF₂), -126.11 (m, CF₂); ³¹P {¹H} NMR (CD₂Cl₂) δ 7.0 (s, ¹J_{PP} = 3856 Hz), 45.12 (s, ²J_{PP} = 110.6 Hz); ¹³C {¹H} NMR (CD₂Cl₂) δ 22.14 (d, ¹J_{CP} = 199.3 Hz, CH₂), 27.29 (t, ²J_{CP} = 22.1 Hz, CH₂), 127.50 (m, C), 128.41 (m, CH), 131.45 (m, CH), 134.20 (m, CH); m/z (FAB) 1046 (MH⁺, 100 %).

6.2.8.6. Synthesis of $[\text{Pt}\{\text{OP}(\text{O})(\text{C}_2\text{H}_4\text{-C}_6\text{F}_{13})\text{O}\}(\text{PPh}_3)_2]$

F₁₃C₆-C₂H₄-PO(OH)₂ (0.163 g, 38.0 mmol) and silver (I) oxide (0.530 g, 228 mmol) were added in succession to a stirred solution of [PtCl₂(PPh₃)₂] (0.300 g, 38.0 mmol) in dichloromethane (40 cm³) and the mixture refluxed for 6 hours. The cooled reaction mixture was filtered and the

filtrate evaporated to dryness under reduced pressure to yield a white powder, which was recrystallised from dichloromethane-light petroleum and dried *in vacuo* (0.315 g, 73%); ^1H NMR (CDCl_3) δ 1.76 (2H, m, CH_2), 2.30 (2H, m, CH_2), 7.07-7.45 (30H, m, Ph); ^{19}F $\{^1\text{H}\}$ NMR (CDCl_3) δ -80.71 (t, $^4J_{\text{FF}} = 9.5$ Hz, CF_3), -115.11 (m, $\alpha\text{-CF}_2$), -121.77 (m, CF_2), -122.78 (m, CF_2), -123.40 (m, CF_2), -126.04 (m, CF_2); ^{31}P $\{^1\text{H}\}$ NMR (CDCl_3) δ 6.8 (s, $^1J_{\text{PP}} = 3867$ Hz), 47.3 (t, $^2J_{\text{PP}} = 124.3$ Hz, $^3J_{\text{PP}} = 7.3$ Hz); ^{13}C $\{^1\text{H}\}$ NMR (CD_2Cl_2) δ 21.59 (d, $^1J_{\text{CP}} = 121.5$ Hz, CH_2), 27.21 (d, $^2J_{\text{CP}} = 23.6$ Hz, CH_2), 127.85 (m, C), 128.78 (m, CH), 131.82 (m, CH), 134.58 (m, CH); m/z (FAB) 1145 [M^+] 70 %; Crystals suitable for characterisation by X-ray crystallography were grown from DCM/petroleum ether. See appendix for structural data.

6.3. Experimental Details for Chapter Three

6.3.1 Synthesis of $[\text{Rh}_2(\text{O}_2\text{C}_4\text{F}_7)_4]^{[18]}$

A solution of perfluorobutanoic acid (0.190 g, 90.5 μmol) in dry and degassed toluene (50 cm^3) was placed in a 100 cm^3 three-neck round bottomed flask equipped with a dropping funnel and a Dean-Stark trap and was heated to 105 $^\circ\text{C}$. A solution of $[\text{Rh}_2(\text{OAc})_4]$ (0.100 g, 22.6 μmol) in distilled ethanol (50 cm^3) was then added dropwise over ten minutes to the stirred toluene solution. The ethanol and liberated acetic acid were distilled from the reaction and the remaining solvent was removed under vacuum. Acetonitrile (1 cm^3) was added to resulting green residue and the purple solid was filtered and dried under vacuum at 100 $^\circ\text{C}$ for 5 hours to yield the title product as a green powder (0.168 g, 70%); ^{19}F $\{^1\text{H}\}$ NMR (CDCl_3) δ -80.95 (3F, t, $^4J_{\text{FF}} = 8.5$ Hz, CF_3), -117.20 (2F, m, $\alpha\text{-CF}_2$), -126.98 (2F, m, CF_2); m/z (FAB) 1058 (M^+ , 10 %); IR: 1641 cm^{-1} $\nu(\text{C}=\text{O})$.

6.3.2. Synthesis of $[\text{Rh}_2(\text{O}_2\text{C}_7\text{F}_{13})_4]^{[19]}$

A solution of perfluoroheptanoic acid (0.412 g, 1.13 μmol) in dry and degassed toluene (50 cm^3) was placed in a 100 cm^3 three-neck round bottomed flask equipped with a dropping funnel and a Dean-Stark trap and was heated to 105 $^\circ\text{C}$. A solution of $[\text{Rh}_2(\text{OAc})_4]$ (0.125 g, 28.3 μmol) in distilled ethanol (40 cm^3) was then added dropwise over ten minutes to the stirred toluene solution. The ethanol and liberated acetic acid were distilled from the reaction and the remaining solvent was removed under vacuum. Acetonitrile (1 cm^3) was added to resulting green residue and the purple solid was filtered and dried under vacuum at 100 $^\circ\text{C}$ for 5 hours to yield the title product as a green powder (0.240 g, 52%); ^{19}F $\{^1\text{H}\}$ NMR (CDCl_3) δ -80.08 (3F, m, CF_3), -111.41 (2F, m, $\alpha\text{-CF}_2$), -

121.17 - -122.36 (4F, m, 2 x CF₂), -123.00 (2F, m, CF₂), -126.40 (2F, m, CF₂); Infrared analysis: 1631 cm⁻¹ ν (C=O).

6.3.3. General Procedure for Alkene Cyclopropanation Under Homogeneous Conditions

A toluene solution of dimeric rhodium catalyst (0.02 mol %) was added to a 50 cm³ Schlenk flask under N₂. The olefin substrate (0.05 mol, styrene previously washed with 1 % aqueous NaOH (2 x 50 cm³) and deionised water (3 x 25 cm³)), was added as a toluene solution (10 cm³). The mixture was heated to 110 °C and ethyl diazoacetate (0.005 mol) was slowly added dropwise *via* syringe. The mixture was heated for a further 4 hours, allowed to cool and eluted through a Pasteur pipette column packed with one of the five support materials. The mixture was first eluted with toluene (10 cm³), to recover the starting materials/products, and secondly with acetonitrile (10 cm³), to recover the catalyst. The catalyst phase was added to a Schlenk flask, the solvent removed under vacuum and the catalyst reused in successive catalytic runs. The product mixture was analysed by gas chromatography and ¹H NMR spectroscopy to determine the conversion to desired products.

6.3.4. Preparation of 10 % Loaded Supported Rhodium Catalyst

A 10:1 mixture by mass of solid support material and dimeric rhodium catalyst were stirred in acetonitrile at room temperature for 30 minutes. The solvent was removed in *vacuo* and the resulting pale green support was dried to constant weight.

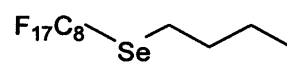
6.3.5. General Procedure for Alkene Cyclopropanation with Supported 1 mol %

[Rh₂(O₂CC₃F₇)₄]

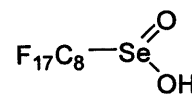
The supported rhodium catalyst (0.02 mol %) was added to a flame dried Schlenk flask under N₂. The alkene substrate (0.05 mol, styrene previously washed with 1 % aqueous NaOH (2 x 50 cm³) and deionised water (3 x 25 cm³)), was added as a toluene solution (10 cm³). The mixture was heated to 110 °C and a solution of ethyl diazoacetate (0.005 mol) was slowly added dropwise *via* syringe. The mixture was heated for a further 4 hours, allowed to cool and filtered. The flask was rinsed with toluene (5 cm³) and this solvent used to wash the solid support. The filtrate was reduced in *vacuo* and the supported catalyst was dried, added to the original Schlenk flask and reused in successive catalytic runs. The product mixture was analysed by gas chromatography and ¹H NMR spectroscopy to determine the conversion to desired products.

6.4. Experimental Details for Chapter Four

6.4.1. Synthesis of $\text{H}_9\text{C}_4\text{-Se-C}_8\text{F}_{17}$ ^[20]

 A suspension of selenium powder (1.16 g, 0.015 mol) in dried and degassed THF (50 cm³) was cooled to -78 °C under N₂. BuLi (1.6M in hexane, 9.16 cm³, 0.015 mol) was added and the mixture allowed to warm to room temperature. The selenium reacted to form a clear yellow solution. F₁₇C₈I (8.00 g, 0.015 mol) prewashed with 10% aq. NaHCO₃ solution was added, followed by H₂O (10 cm³). The solution turned dark brown. Rongalite (Sodium hydroxymethanesulphinate (4.51 g, 0.029 mol)) was added portion-wise over 5 hours and the reaction was allowed to stir for a 48 hours. The product was extracted into Et₂O (100 cm³) and the ethereal layer was washed with aq. NaHCO₃ solution (60 cm³) and H₂O (2 x 60 cm³), dried over MgSO₄ and the solvent removed under vacuum to yield a brown oil. This oil was purified by passing down a short silica column using PP3 (perfluoro-1,3-dimethylhexane) as eluant to yield the product as a pale yellow oil (2.60 g, 31%); Found C, 25.9 %; H, 1.5 %, C₁₂H₉F₁₇Se requires C, 26.0 %; H, 1.6 %; ¹H NMR (CDCl₃) δ 0.87 (3H, t, ³J_{HH} = 7.46 Hz, CH₃), 1.36 (2H, sextet, ³J_{HH} = 7.37 Hz, CH₂), 1.69 (2H, quintet, ³J_{HH} = 7.45 Hz, CH₂), 2.96 (2H, t, ³J_{HH} = 7.46 Hz, CH₂); ¹⁹F {¹H} NMR (CDCl₃) δ -80.79 (3F, t, ⁴J_{FF} = 10.4 Hz, CF₃), -86.77 (2F, m, CF₂), -118.26 (2F, m, CF₂), -121.22 (2F, m, CF₂), -121.86 (4F, m, 2 x CF₂), -122.70 (2F, m, CF₂), -126.10 (2F, m, CF₂); ¹³C {¹H} NMR (CDCl₃) δ 13.20 (s, CH₃), 22.67 (s, CH₂), 24.83 (s, CH₂), 32.16 (s, CH₂); ⁷⁷Se NMR (D₂O) δ 413.7 (m); m/z (ES⁻) 555 (MH⁻, 100 %).

6.4.2. Synthesis of $\text{F}_{17}\text{C}_8\text{SeO}_2\text{H}$ ^[20]

 Hydrogen peroxide (30% aq. w/w, 1.15 cm³, 37.8 mmol) was added to a stirred solution of F₁₇C₈SeBu (2.10 g, 3.78 mmol) in F₃CCH₂OH (20 cm³) at 0 °C. The mixture allowed to warm to room temperature and was stirred overnight. The solvent was removed under vacuum to yield the product as a white solid, which was recrystallised from hexane (1.77 g, 88%); Found C, 17.9%; H, 0.1%, C₈HF₁₇O₂ requires C, 18.1 %; H, 0.2 %; ¹H NMR (CD₃CN) δ 2.39 (bs, OH); ¹⁹F {¹H} NMR (CD₃CN) δ -81.45 (3F, t, ⁴J_{FF} = 10.4 Hz, CF₃), -119.21 (2F, m, CF₂), -120.25 (2F, m, CF₂), -122.27 (6F, m, 3 x CF₂), -123.08 (2F, m, CF₂), -126.52 (2F, m, CF₂); ⁷⁷Se NMR (C₂D₆SO) δ 1245.6 (s); m/z (ES⁻) 531 (M⁻, 100 %), Mp 132 – 135 °C (lit = 135 – 137 °C^[20]).

6.4.3. Preparation of 10 % Loaded Supported Perfluorooctyl Seleninic Acid

Perfluorooctyl seleninic acid (0.210 g) and solid support material (1.890 g) were stirred in THF (15 cm³) at room temperature for 30 minutes. The solvent was removed in *vacuo* and the resulting white powder support was dried to constant weight.

6.4.4. General Procedure for Oxidation of *para*-Nitrobenzaldehyde Catalysed by Supported Perfluorooctyl Seleninic Acid

A 50 cm³ Schlenk flask was charged with 10 % loaded supported perfluorooctyl seleninic acid (2 mol %), solvent (25 cm³) and hydrogen peroxide (4 mmol, 0.4 cm³ 35% aq. w/w). The mixture was heated to 40 °C, *para*-nitrobenzaldehyde (2 mmol, 0.302 g) added and was stirred for 4 hours. The mixture was allowed to cool, sodium metabisulphite (20 mmol, 0.075 g) added and was stirred overnight. The mixture was filtered and the solid washed with MeOH (15 cm³), water (10 cm³), and further MeOH (10 cm³), dried and reused in successive catalytic runs. The MeOH phase was reduced under vacuum analysed by ¹H NMR spectroscopy to determine the conversion to the desired product.

6.4.5. General Procedure for Allylic Oxidation of Cyclooctene Catalysed by Supported Perfluorooctyl Seleninic Acid

Cyclooctene (0.050 g, 0.45 mmol), iodoxybenzene (0.319 g, 1.35 mmol) and 10% loaded supported perfluorooctyl seleninic acid (1 mol %, 0.240 g, 0.045 mmol) in benzotrifluoride (15 cm³) were stirred at reflux for 6 hours. After cooling, the mixture was filtered, the solid washed with benzotrifluoride (10 cm³) and dried for use in subsequent runs. The benzotrifluoride phase was removed under vacuum and the product analysed by ¹H NMR spectroscopy.

6.4.6. General Procedure for Allylic Oxidation of Cyclooctene Catalysed by Perfluorooctyl Seleninic Acid under Homogeneous Conditions

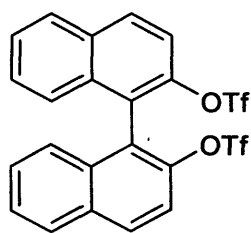
Cyclooctene (0.050 g, 0.45 mmol), iodoxybenzene (0.319 g, 1.35 mmol) and perfluorooctyl seleninic acid (1 mol %, 0.024 g, 0.045 mmol) in benzotrifluoride (15 cm³) were added to a 50 cm³ round-bottomed flask and stirred at reflux for 6 hours. After cooling, the mixture was eluted through a Pasteur pipette column packed with fluorinated zirconium phosphonate, first washing with hexane to elute products and secondly with methanol to elute the catalyst. The methanol phase was

added to a flask, removed under vacuum and used in subsequent catalytic runs. The hexane phase was reduced under vacuum and the product analysed by ^1H NMR spectroscopy.

6.5. Experimental Details for Chapter Five

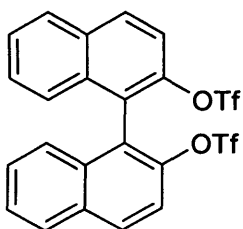
6.5.1. Non-fluorous BINAP

6.5.1.1. Synthesis of (*R*)-2,2'-di-(trifluoromethane-sulphonyloxy)-1,1'-binaphthyl^[21]



Triflic anhydride (3.36 cm³, 0.020 mol) was added dropwise to a solution of (*R*)-1,1'-bi-2-naphthol (2.31 g, 8.08 mmol) and pyridine (1.96 cm³, 0.024 mmol) at 0 °C under N₂ in dry dichloromethane (100 cm³) and the mixture was stirred for 4 hours. The solvent was removed under reduced pressure and the product extracted into ethyl acetate (50 cm³). This solution was washed with 5 % hydrochloric acid (100 cm³), saturated NaHCO₃ (100 cm³), 10 % NaCl solution (100 cm³) and water (100 cm³). The organic phase was dried over magnesium sulphate, filtered and the solvent removed under reduced pressure. The crude product was recrystallised from hexane (4.12 g, 93 %); ^1H NMR (CDCl₃) δ 7.18 (2H, d, $^3J_{\text{HH}} = 9.1$ Hz, ArH), 7.32 (2H, t, $^3J_{\text{HH}} = 8.2$ Hz, ArH), 7.49 (2H, t, $^3J_{\text{HH}} = 8.2$ Hz, ArH), 7.53 (2H, d, $^3J_{\text{HH}} = 9.4$ Hz, ArH), 7.91 (2H, d, $^3J_{\text{HH}} = 8.2$ Hz, ArH), 8.01 (2H, d, $^3J_{\text{HH}} = 9.1$ Hz, ArH); ^{19}F { ^1H } NMR (CDCl₃) δ -74.45 (s, CF₃); ^{13}C { ^1H } NMR (CDCl₃) δ 118.20 (q, $^1J_{\text{CF}} = 320.7$ Hz, OSO₂CF₃), 119.39 (CH), 123.54 (C), 126.78 (CH), 127.38 (C), 128.05 (CH), 128.43 (CH), 132.10 (CH), 132.40 (C), 133.18 (C), 145.45 (C).

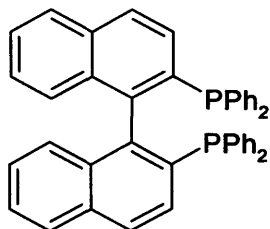
6.5.1.2. Synthesis of (*S*)-2,2'-di-(trifluoromethane-sulphonyloxy)-1,1'-binaphthyl^[21]



Triflic anhydride (6.75 cm³, 0.040 mol) was added dropwise to a solution of (*S*)-1,1'-bi-2-naphthol (4.60 g, 0.016 mol) and pyridine (3.91 cm³, 0.048 mol) at 0 °C under N₂ in dry dichloromethane (100 cm³) and the mixture was stirred for 4 hours. The solvent was removed under reduced pressure and the product extracted into ethyl acetate (50 cm³). This solution was washed with 5 % hydrochloric acid (100 cm³), saturated NaHCO₃ (100 cm³), 10 % NaCl solution (100 cm³) and water (100 cm³). The organic phase was dried over magnesium sulphate, filtered and the solvent removed under reduced pressure. The crude product was isolated as an oil which solidified after prolonged drying under high vacuum and was then recrystallised from hexane (8.40 g, 95 %); ^1H NMR (CDCl₃) δ 7.18 (2H, d, $^3J_{\text{HH}} = 8.5$ Hz, ArH), 7.34 (2H, t, $^3J_{\text{HH}} = 8.2$ Hz, ArH), 7.51 (2H, t, $^3J_{\text{HH}} = 8.2$ Hz, ArH), 7.54 (2H, d, $^3J_{\text{HH}} = 9.4$ Hz, ArH), 7.93 (2H, d, $^3J_{\text{HH}} = 8.4$ Hz, ArH), 8.06 (2H,

d, $^3J_{\text{HH}} = 9.1$ Hz, ArH); ^{19}F $\{^1\text{H}\}$ NMR (CDCl_3) δ -74.61 (s, CF_3); ^{13}C $\{^1\text{H}\}$ NMR (CDCl_3) δ 118.19 (q, $^1J_{\text{CF}} = 320.7$ Hz, OSO_2CF_3), 119.37 (CH), 123.53 (C), 126.78 (CH), 127.38 (C), 128.04 (CH), 128.42 (CH), 132.10 (CH), 132.40 (C), 133.18 (C), 145.45 (C).

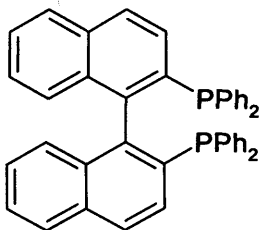
6.5.1.3. Synthesis of (*R*)-2,2'-bis-(diphenylphosphino)-1,1'-binaphthyl^[22]



To a dry and degassed DMF solution of $[\text{NiCl}_2(\text{dppe})]$ (0.496 g, 9.45×10^{-4} mol in 100 cm^3) under N_2 was added diphenylphosphine (1.97 cm^3 , 11.3 mmol). The brown solution was heated to $150 \text{ }^\circ\text{C}$ for 30 minutes before adding (*R*)-2,2'-di-trifluoromethane sulphonyl-oxy-1,1'-binaphthyl (5.20 g, 9.45 mmol) and DABCO (3.81 g, 0.034 mol) in DMF (100 cm^3). The resulting green solution was stirred at $110 \text{ }^\circ\text{C}$ for a further 4 hours. An additional portion of diphenylphosphine (1.97 cm^3 , 11.3 mmol) was then added *via* syringe. Heating and stirring was continued for 72 hours.

The DMF was distilled from the reaction mixture and the resulting brown solid was stirred in MeOH (200 cm^3) for 30 minutes, filtered, washed with MeOH and dried *in vacuo*. The off-white solid was recrystallised from DCM/MeOH to yield the pure product as white crystals (3.32 g, 56 %); ^1H NMR (CDCl_3) δ 6.75 (2H, d, $^3J_{\text{HH}} = 8.2$ Hz, ArH), 6.83 (2H, t, $^3J_{\text{HH}} = 8.2$ Hz, ArH), 6.95-7.14 (20H, m, Ph), 7.26 (2H, t, $^3J_{\text{HH}} = 7.9$ Hz, ArH), 7.37 (2H, d, $^3J_{\text{HH}} = 8.5$ Hz, ArH), 7.75 (2H, d, $^3J_{\text{HH}} = 7.9$ Hz, ArH), 7.81 (2H, d, $^3J_{\text{HH}} = 8.5$ Hz, ArH); ^{31}P $\{^1\text{H}\}$ NMR (CDCl_3) δ -15.38 (S); ^{13}C $\{^1\text{H}\}$ NMR (CDCl_3) δ 125.75 (CH), 126.49 (CH), 127.46 (CH), 127.53 (CH), 127.65 (CH), 127.97 (CH), 128.00 (CH), 128.05 (CH), 128.35 (CH), 130.51 (CH), 132.83 (CH), 133.19 (C), 133.38 (C), 134.17 (CH), 135.47 (C), 137.42 (C), 137.93 (C), 145.22 (C).

6.5.1.4. Synthesis of (*S*)-2,2'-bis-(diphenylphosphino)-1,1'-binaphthyl^[22]



To a dry and degassed DMF solution of $[\text{NiCl}_2(\text{dppe})]$ (0.401, 7.64×10^{-4} mol in 100 cm^3) under N_2 was added diphenylphosphine (1.59 cm^3 , 9.17 mmol). The brown solution was heated to $150 \text{ }^\circ\text{C}$ for 30 minutes before adding (*S*)-2,2'-di-trifluoromethane sulphonyl-oxy-1,1'-binaphthyl (4.20 g, 7.64 mmol) and DABCO (3.70 g, 0.034 mol) in DMF (100 cm^3). The resulting green solution was stirred at $110 \text{ }^\circ\text{C}$ for a further 4 hours. An additional portion of diphenylphosphine (1.59 cm^3 , 9.17 mmol) was then added *via* syringe. Heating and stirring was continued for 72 hours.

The DMF was distilled from the reaction mixture and the resulting brown solid was stirred in MeOH (200 cm³) for 30 minutes, filtered, washed with MeOH and dried *in vacuo*. The off-white solid was recrystallised from DCM/MeOH to yield the pure product as white crystals (3.1 g, 65 %); ¹H NMR (CDCl₃) δ 6.75 (2H, d, ³J_{HH} = 8.5 Hz, ArH), 6.83 (2H, t, ³J_{HH} = 8.2 Hz, ArH), 6.93-7.15 (20H, m, Ph), 7.26 (2H, t, ³J_{HH} = 7.0 Hz, ArH), 7.37 (2H, d, ³J_{HH} = 8.6 Hz, ArH), 7.75 (2H, d, ³J_{HH} = 8.2 Hz, ArH), 7.81 (2H, d, ³J_{HH} = 8.5 Hz, ArH); ³¹P {¹H} NMR (CDCl₃) δ -15.38 (S); ¹³C {¹H} NMR (CDCl₃) δ 125.80 (CH), 126.53 (CH), 127.58 (CH), 127.70 (CH), 127.65 (CH), 127.97 (CH), 128.01 (CH), 128.03 (CH), 128.35 (CH), 130.51 (CH), 132.83 (CH), 133.19 (C), 133.38 (C), 134.30 (CH), 135.47 (C), 137.42 (C), 137.92 (C), 145.20 (C).

6.5.1.5. Synthesis of [PdCl₂{(R)-BINAP}]^[23]

[PdCl₂(MeCN)₂] (0.416 g, 1.61 mmol) and (R)-BINAP (1.00 g, 1.61 mmol) were dissolved in dry and degassed DCM (20 cm³) and stirred under N₂ for 2 hours at room temperature. The solvent was removed under vacuum to yield the product as a vibrant yellow powder (1.18 g, 92%); ¹H NMR (CDCl₃) δ 6.69 (4H, m, Ph), 6.78 (2H, d, ³J_{HH} = 8.5 Hz, ArH), 6.88 (2H, t, ³J_{HH} = 7.3 Hz, ArH), 7.15 (2H, t, ³J_{HH} = 7.0 Hz, Ph), 7.31 (2H, t, ³J_{HH} = 9.6 Hz, Ph), 7.38 - 7.49 (8H, m, Ph), 7.52 (2H, t, ³J_{HH} = 7.9 Hz, ArH), 7.59 (2H, d, ³J_{HH} = 8.2 Hz, ArH), 7.68 (4H, m, Ph), 7.83 (2H, d, ³J_{HH} = 8.2 Hz, ArH), 7.87 (2H, d, ³J_{HH} = 8.2 Hz, ArH); ³¹P {¹H} NMR (CDCl₃) δ 28.69 (S); ¹³C {¹H} NMR (CDCl₃) δ 121.84 (C), 122.58 (C), 126.79 (CH), 127.29 (CH), 127.49 (CH), 127.74 (CH), 127.88 (CH), 128.12 (CH), 128.24 (CH), 128.88 (CH), 129.74 (C), 130.37 (CH), 130.83 (CH), 132.90 (C), 134.02 (C), 135.12 (CH), 135.25 (CH), 138.70 (C); m/z (FAB) 763 [M-Cl]⁺ (100 %).

6.5.1.6. Synthesis of [PdCl₂{(S)-BINAP}]^[23]

[PdCl₂(MeCN)₂] (0.416 g, 1.61 mmol) and (R)-BINAP (1.00 g, 1.61 mmol) were dissolved in dry and degassed DCM (20 cm³) and stirred under N₂ for 2 hours at room temperature. The solvent was removed under vacuum to yield the product as a vibrant yellow powder (1.18 g, 92%); ¹H NMR (CDCl₃) δ 6.62 (4H, m, Ph), 6.70 (2H, d, ³J_{HH} = 8.5 Hz, ArH), 6.80 (2H, t, ³J_{HH} = 7.5 Hz, ArH), 7.07 (2H, t, ³J_{HH} = 7.6 Hz, Ph), 7.24 (2H, t, ³J_{HH} = 9.4 Hz, Ph), 7.30 - 7.43 (8H, m, Ph), 7.44 (2H, t, ³J_{HH} = 8.5 Hz, ArH), 7.51 (2H, d, ³J_{HH} = 7.9 Hz, ArH), 7.60 (4H, m, Ph), 7.75 (2H, d, ³J_{HH} = 7.3 Hz, ArH), 7.79 (2H, d, ³J_{HH} = 7.6 Hz, ArH); ³¹P {¹H} NMR (CDCl₃) δ 28.70 (S); ¹³C {¹H} NMR (CDCl₃) δ 121.89 (C), 122.64 (C), 126.85 (CH), 127.34 (CH), 127.46 (CH), 127.72 (CH),

127.88 (CH), 128.18 (CH), 128.24 (CH), 129.04 (CH), 129.80 (C), 130.57 (CH), 130.83 (CH), 132.92 (C), 134.09 (C), 135.07 (CH), 135.19 (CH), 138.76 (C); m/z (FAB) 763 [M-Cl]⁺ (100 %).

6.5.1.7. Synthesis of [Pd(OH)₂]{(R)-BINAP}](OTf)₂^[24]

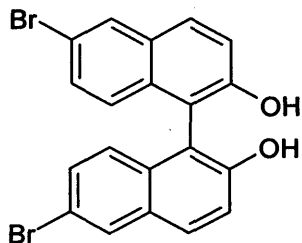
To a solution of [PdCl₂]{(R)-BINAP} (1.00 g, 1.25 mmol) in wet acetone (40 cm³, 5 % v/v H₂O) was added AgOTf (0.643 g, 2.50 mmol) under nitrogen and the mixture stirred at room temperature for 12 hours. The mixture was then filtered through Celite to remove any AgCl, washed with DCM (10 cm³) and the solvent removed under vacuum to yield the product as an orange brown powder (1.30 g, 98%); ¹H NMR (CDCl₃) δ 4.59 (4H, bs, 2 x H₂O) 6.64 (2H, d, ³J_{HH} = 8.5 Hz, ArH), 6.80 (4H, m, Ph), 6.95 (2H, t, ³J_{HH} = 7.3 Hz, ArH), 7.13 (2H, t, ³J_{HH} = 8.5 Hz, Ph), 7.36 - 7.76 (22H, m, ArH/Ph); ¹⁹F {¹H} NMR (CDCl₃) δ -77.92 (S); ³¹P {¹H} NMR (CDCl₃) δ 34.14 (S); ¹³C {¹H} NMR (CDCl₃) δ 118.08 (C), 118.95 (C), 122.80 (C), 123.65 (C), 126.96 (CH), 127.51 (CH), 127.66 (CH), 128.48 (CH), 129.06 (CH), 129.43 (CH), 129.59 (CH), 130.32 (CH), 132.04 (CH), 132.81 (C), 133.01 (CH), 134.59 (CH), 134.74 (CH), 139.61 (C).

6.5.1.8. Synthesis of [Pd(OH)₂]{(S)-BINAP}](OTf)₂^[24]

To a solution of [PdCl₂]{(S)-BINAP} (0.760 g, 53.0 mmol) in wet acetone (40 cm³, 5 % v/v H₂O) was added AgOTf (0.272 g, 1.06 mmol) under nitrogen and the mixture stirred at room temperature for 12 hours. The mixture was then filtered through Celite to remove any AgCl, washed with DCM (10 cm³) and the solvent removed under vacuum to yield the product as an orange brown powder (0.860 g, 96%); ¹H NMR (CDCl₃) δ 4.71 (4H, bs, 2 x H₂O), 6.62 (2H, d, ³J_{HH} = 8.5 Hz, ArH), 6.80 (4H, m, Ph), 6.94 (2H, t, ³J_{HH} = 7.2 Hz, ArH), 7.11 (2H, t, ³J_{HH} = 8.5 Hz, Ph), 7.38 - 7.80 (22H, m, ArH/Ph); ¹⁹F {¹H} NMR (CDCl₃) δ -78.06 (S); ³¹P {¹H} NMR (CDCl₃) δ 33.98 (S); ¹³C {¹H} NMR (CDCl₃) δ 118.11 (C), 118.97 (C), 122.82 (C), 123.67 (C), 126.99 (CH), 127.54 (CH), 127.69 (CH), 128.51 (CH), 129.09 (CH), 129.45 (CH), 129.61 (CH), 130.28 (CH), 132.06 (CH), 132.79 (C), 133.01 (CH), 134.62 (CH), 134.77 (CH), 139.63 (C).

6.5.2. Fluorous BINAP

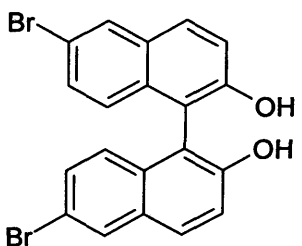
6.5.2.1. Synthesis of (*R*)-6,6'-Dibromo-1,1'-bi-2-naphthol^[25]



(*R*)-1,1'-bi-2-naphthol (4.60 g, 16.0 mmol) was dissolved in dichloromethane (50 cm³) and cooled to -78 °C with constant stirring. Bromine (2.5 cm³, 48.4 mmol) in dichloromethane (20 cm³) was added dropwise over 30 minutes. The solution was then allowed to warm to room temperature and was stirred overnight.

The excess bromine was quenched with aqueous sodium metabisulphite (10 % solution, 50 cm³) and the solid was filtered from the mixture (6.98 g, 98%); ¹H NMR (CDCl₃) δ 4.97 (2H, s, OH), 6.89 (2H, d, ³J_{HH} = 9.1 Hz, ArH), 7.30 (2H, dd, ³J_{HH} = 9.1 Hz, ⁴J_{HH} = 2.0 Hz, ArH), 7.32 (2H, d, ³J_{HH} = 8.1 Hz, ArH) 7.81 (2H, d, ³J_{HH} = 9.1 Hz, ArH), 7.97 (2H, d, ⁴J_{HH} = 2.0 Hz, ArH); ¹³C {¹H} NMR (CD₂Cl₂) δ 110.71 (s, C), 118.01 (s, C), 118.99 (s, CH), 126.13 (s, CH), 130.45 (s, CH), 130.57 (s, CH), 130.67 (s, CH), 130.86 (s, C), 131.91 (s, C), 153.39 (s, C-O); m/z (ES⁻) 443 [M-H]⁻ (100 %).

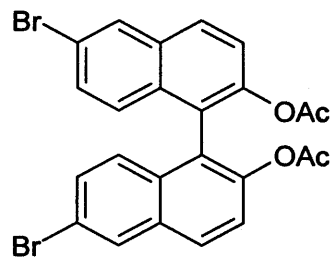
6.5.2.2. Synthesis of (*S*)-6,6'-Dibromo-1,1'-bi-2-naphthol^[25]



(*S*)-1,1'-bi-2-naphthol (10.04 g, 35.0 mmol) was dissolved in dichloromethane (120 cm³) and cooled to -78 °C with constant stirring. Bromine (5.06 cm³, 98.0 mmol) in dichloromethane (30 cm³) was added dropwise over 30 minutes. The solution was then allowed to warm to room temperature and was stirred overnight.

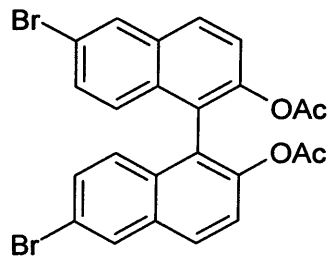
The excess bromine was quenched with aqueous sodium metabisulphite (10 % solution, 50 cm³) and the solid was filtered from the mixture (14.29 g, 92%); ¹H NMR (CDCl₃) δ 4.94 (2H, s, OH), 6.89 (2H, d, ³J_{HH} = 8.8 Hz, ArH), 7.30 (2H, dd, ³J_{HH} = 9.1 Hz, ⁴J_{HH} = 2.0 Hz, ArH), 7.32 (2H, d, ³J_{HH} = 8.8 Hz, ArH) 7.81 (2H, d, ³J_{HH} = 9.1 Hz, ArH), 7.98 (2H, d, ⁴J_{HH} = 2.0 Hz, ArH); ¹³C {¹H} NMR (CD₂Cl₂) δ 110.70 (s, C), 118.00 (s, C), 118.97 (s, CH), 126.13 (s, CH), 130.45 (s, CH), 130.56 (s, CH), 130.67 (s, CH), 130.84 (s, C), 131.91 (s, C), 153.41 (s, C-O); m/z (ES⁻) 443 [M-H]⁻ (100 %).

6.5.2.3. Synthesis of (*R*)-6,6'-Dibromo-2,2'-diacetoxy-1,1'-binaphthyl^[25]



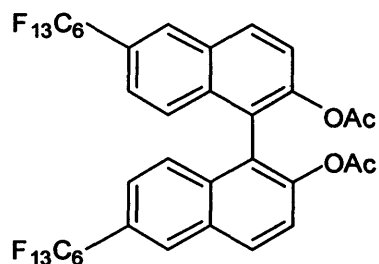
Acetic anhydride (2.30 g, 22.52 mmol) in dichloromethane (5 cm³) was added dropwise to a stirred solution of (*R*)-6,6'-dibromo-1,1'-bi-2-naphthol (5.00 g, 11.26 mmol), triethylamine (6.82 g, 67.56 mmol) and DMAP (0.016 g, 0.13 mmol) in dichloromethane (50 cm³). The solution was refluxed for 1 hour. After cooling to room temperature, the solution was washed with 1M HCl (50 cm³), 5 % w/w sodium carbonate solution (50 cm³) and water (50 cm³), dried over magnesium sulphate, filtered and the solvent removed under reduced pressure to yield a pale yellow solid, which was recrystallised from ethanol (5.65 g, 95 %); M.p. 175 – 177 °C; ¹H NMR (CDCl₃) δ 1.80 (6H, s, COCH₃), 6.93 (2H, d, ³J_{HH} = 9.1 Hz, ArH), 7.29 (2H, dd, ³J_{HH} = 9.1 Hz, ⁴J_{HH} = 2.0 Hz, ArH), 7.37 (2H, d, ³J_{HH} = 9.1 Hz, ArH), 7.83 (2H, d, ³J_{HH} = 9.1 Hz, ArH), 8.02 (2H, d, ⁴J_{HH} = 2.0 Hz, ArH); ¹³C {¹H} NMR (CD₂Cl₂) δ 20.54 (s, CH₃), 120.09 (s, C), 123.10 (s, CH), 123.25 (s, C), 127.76 (s, CH), 128.86 (s, CH), 130.12 (s, CH), 130.30 (s, CH), 131.72 (s, C), 132.61 (s, C), 147.04 (s, C), 169.17 (s, C-O); m/z (FAB) 529 [MH]⁺ (63 %), 486 [MH - Ac]⁺ (83 %), 444 [MH - 2 x Ac]⁺ (91 %).

6.5.2.4. Synthesis of (*S*)-6,6'-Dibromo-2,2'-diacetoxy-1,1'-binaphthyl^[25]



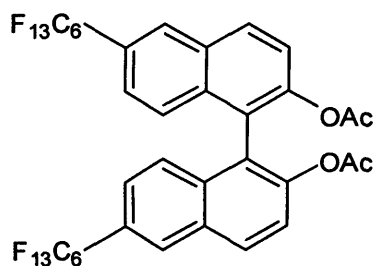
Acetic anhydride (5.98 g, 59.0 mmol) in dichloromethane (25 cm³) was added dropwise to a stirred solution of (*R*)-6,6'-dibromo-1,1'-bi-2-naphthol (13.03 g, 29.0 mmol), triethylamine (17.76 g, 0.176 mol) and DMAP (0.045 g, 0.36 mmol) in dichloromethane (75 cm³). The solution was refluxed for 1 hour. After cooling to room temperature, the solution was washed with 1M HCl (50 cm³), 5 % w/w sodium carbonate solution (50 cm³) and water (50 cm³), dried over magnesium sulphate, filtered and the solvent removed under reduced pressure to yield a pale yellow solid, which was recrystallised from ethanol (13.88 g, 91 %); M.p. 175 – 177 °C; ¹H NMR (CDCl₃) δ 1.79 (6H, s, COCH₃), 6.92 (2H, d, ³J_{HH} = 9.1 Hz, ArH), 7.28 (2H, dd, ³J_{HH} = 9.1 Hz, ⁴J_{HH} = 2.0 Hz, ArH), 7.36 (2H, d, ³J_{HH} = 8.8 Hz, ArH), 7.83 (2H, d, ³J_{HH} = 8.8 Hz, ArH), 8.02 (2H, d, ⁴J_{HH} = 2.0 Hz, ArH); ¹³C {¹H} NMR (CDCl₃) δ 20.56 (s, CH₃), 120.09 (s, C), 123.05 (s, CH), 123.14 (s, C), 127.69 (s, CH), 128.79 (s, CH), 130.04 (s, CH), 130.22 (s, CH), 131.64 (s, C), 132.54 (s, C), 147.06 (s, C), 169.15 (s, C-O).

6.5.2.5. Synthesis of (*R*)-6,6'-Bis-(perfluoro-*n*-hexyl)-2,2'-diacetoxy-1,1'-binaphthyl^[25]



A mixture of (*R*)-6,6'-dibromo-2,2'-diacetoxy-1,1'-binaphthyl (2.00 g, 3.79 mmol), perfluoro-*n*-hexyl iodide (5.06 g, 0.113 mol), copper powder (2.41 g, 38.0 mol), 2,2'-bipyridine (0.300 g, 1.9 mmol), fluorobenzene (50 cm³) and DMSO (50 cm³) under N₂ was stirred for 72 hours at 80 °C. After cooling to room temperature, the reaction mixture was diluted with water (150 cm³) and diethyl ether (150 cm³) and filtered. The organic layer was washed with 1M HCl (3 x 100 cm³) and water (2 x 100 cm³), dried over MgSO₄, filtered and the solvent removed under reduced pressure to yield a yellow solid, which was recrystallised from hexane (1.22 g, 32 %); ¹H NMR (CDCl₃) δ 1.79 (6H, s, COCH₃), 7.20 (2H, d, ³J_{HH} = 8.8 Hz, ArH), 7.37 (2H, d, ³J_{HH} = 9.1 Hz, ArH), 7.49 (2H, d, ³J_{HH} = 8.8 Hz, ArH), 8.07 (2H, d, ³J_{HH} = 9.1 Hz, ArH), 8.17 (2H, s, ArH); ¹⁹F {¹H} NMR (CDCl₃) δ -80.74 (6F, t, ⁴J_{FF} = 10.4 Hz, 2 x CF₃), -110.23 (4F, m, 2 x CF₂), -121.42 (8F, m, 4 x CF₂) -122.73 (4F, m, 2 x CF₂), -126.07 (4F, m, 2 x CF₂); ¹³C {¹H} NMR (CDCl₃) δ 20.34 (s, CH₃) 122.98 (s, C), 123.51 (s, CH), 123.74 (s, CH), 126.42 (s, C), 126.69 (s, CH), 128.02 (m, CH), 130.42 (s, C), 130.81 (s, CH), 134.65 (s, C), 148.72 (s, C), 169.00 (s, C-O); m/z (FAB) 922 [M-2Ac]⁺ (100 %), 964 [M-2Ac]⁺ (50 %), 1007 [MH]⁺ (45 %).

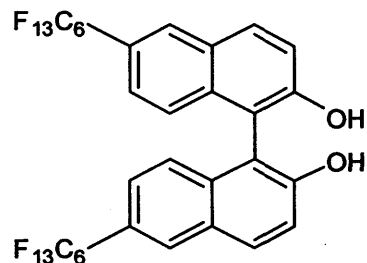
6.5.2.6. Synthesis of (*S*)-6,6'-Bis-(perfluoro-*n*-hexyl)-2,2'-diacetoxy-1,1'-binaphthyl^[25]



A mixture of (*S*)-6,6'-dibromo-2,2'-diacetoxy-1,1'-binaphthyl (6.01 g, 11.40 mmol), perfluoro-*n*-hexyl iodide (15.21 g, 0.341 mol), copper powder (7.24 g, 0.114 mol), 2,2'-bipyridine (0.912 g, 5.7 mmol), fluorobenzene (100 cm³) and DMSO (150 cm³) under N₂ was stirred for 72 hours at 80 °C. After cooling to room temperature, the reaction mixture was diluted with water (150 cm³) and diethyl ether (150 cm³) and filtered. The organic layer was washed with 1M HCl (3 x 100 cm³) and water (2 x 100 cm³), dried over MgSO₄, filtered and the solvent removed under reduced pressure to yield a yellow solid, which was recrystallised from hexane (6.35 g, 55 %); ¹H NMR (CDCl₃) δ 1.79 (6H, s, COCH₃), 7.19 (2H, d, ³J_{HH} = 8.8 Hz, ArH), 7.36 (2H, d, ³J_{HH} = 8.8 Hz, ArH), 7.48 (2H, d, ³J_{HH} = 9.1 Hz, ArH), 8.05 (2H, d, ³J_{HH} = 8.8 Hz, ArH), 8.16 (2H, s, ArH); ¹⁹F {¹H} NMR (CDCl₃) δ -80.90 (6F, t, ⁴J_{FF} = 10.4 Hz, 2 x CF₃), -110.32 (4F, m, 2 x CF₂), -121.48 (8F, m, 4 x CF₂) -122.81 (4F, m, 2 x CF₂), -126.18 (4F, m, 2 x CF₂); ¹³C {¹H} NMR (CDCl₃) δ 20.37 (s, CH₃) 123.00 (s, C), 123.54 (s, CH), 123.77 (s, CH), 126.45 (s, C), 126.72 (s, CH), 128.05 (m, CH), 130.44 (s, C), 130.84 (s, CH), 134.68 (s, C), 148.75

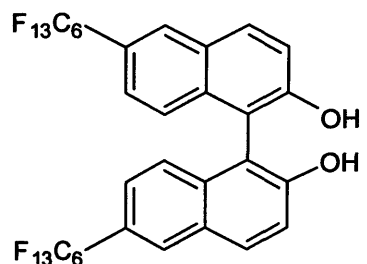
(s, C), 169.02 (s, C-O); m/z (FAB) 922 [M-2Ac]⁺ (100 %), 964 [M-2Ac]⁺ (50 %), 1007 [MH]⁺ (40 %).

6.5.2.7. Synthesis of (*R*)-6,6'-Bis-(perfluoro-*n*-hexyl)-1,1'-binaphthol^[25]



Sodium ethoxide (0.55 g, 7.96 mmol) was added to a stirred solution of (*R*)-6,6'-bis-(perfluoro-*n*-hexyl)-2,2'-diacetoxy-1,1'-binaphthyl (2.00 g, 1.99 mmol) in methanol (75 cm³) for 10 minutes at room temperature and then quenched with 2M hydrochloric acid (100 cm³). The solution was extracted with dichloromethane (2 x 50 cm³), the organic phase separated, dried over magnesium sulphate and filtered. The solvent was removed under vacuum and the resulting off-white solid recrystallised from dichloromethane/hexane to yield the product as white crystals (1.72 g, 94%); Mp 78-80 °C; ¹H NMR (CDCl₃) δ 5.20 (2H, s, OH), 7.15 (2H, d, ³J_{HH} = 8.9 Hz, ArH), 7.37 (2H, d, ³J_{HH} = 9.1 Hz, ArH), 7.44 (2H, d, ³J_{HH} = 9.1 Hz, ArH), 8.09 (2H, d, ³J_{HH} = 9.1 Hz, ArH), 8.20 (2H, s, ArH); ¹⁹F {¹H} NMR (CDCl₃) δ -80.89 (6F, t, ⁴J_{FF} = 10.4 Hz, 2 x CF₃), -110.09 (4F, m, 2 x CF₂), -121.51 (8F, m, 4 x CF₂) -122.89 (4F, m, 2 x CF₂), -126.14 (4F, bs, 2 x CF₂); ¹³C {¹H} NMR (CDCl₃) δ 110.48 (s, C), 119.29 (s, CH), 124.56 (s, CH), 124.75 (s, CH), 125.06 (s, C), 128.24 (s, C), 128.37 (m, CH), 132.74 (s, CH), 135.01 (s, C), 154.73 (s, C).

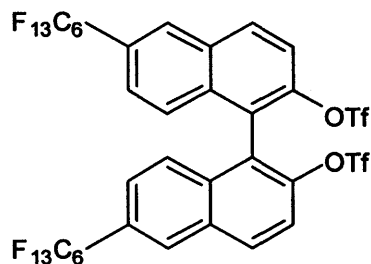
6.5.2.8. Synthesis of (*S*)-6,6'-Bis-(perfluoro-*n*-hexyl)-1,1'-binaphthol^[25]



Sodium ethoxide (1.51 g, 0.022 mol) was added to a stirred solution of (*S*)-6,6'-bis-(perfluoro-*n*-hexyl)-2,2'-diacetoxy-1,1'-binaphthyl (5.50 g, 5.47 mmol) in methanol (75 cm³) for 10 minutes at room temperature and then quenched with 2M hydrochloric acid (100 cm³). The solution was extracted with dichloromethane (2 x 50 cm³), the organic phase separated, dried over magnesium sulphate and filtered. The solvent was removed under vacuum and the resulting off-white solid recrystallised from dichloromethane/hexane to yield the product as white crystals (4.85 g, 96%); Mp 80-82 °C; ¹H NMR (CDCl₃) δ 5.17 (2H, s, OH), 7.13 (2H, d, ³J_{HH} = 8.8 Hz, ArH), 7.37 (2H, d, ³J_{HH} = 9.1 Hz, ArH), 7.40 (2H, d, ³J_{HH} = 9.1 Hz, ArH), 8.02 (2H, d, ³J_{HH} = 9.1 Hz, ArH), 8.16 (2H, s, ArH); ¹⁹F {¹H} NMR (CDCl₃) δ -80.83 (6F, t, ⁴J_{FF} = 10.4 Hz, CF₃), -110.06 (4F, m, 2 x CF₂), -121.44 (8F, m, 4 x CF₂) -122.79 (4F, m, 2 x CF₂), -126.14 (4F, bs, 2 x CF₂); ¹³C {¹H} NMR (CDCl₃) δ 110.48 (s, C), 119.27 (s, CH), 124.54 (s, CH),

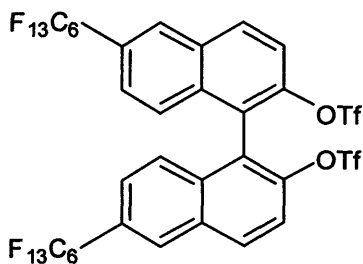
124.72 (s, CH), 125.03 (s, C), 128.32 (s, C), 128.34 (m, CH), 132.72 (s, CH), 134.98 (s, C), 154.71 (s, C).

6.5.2.9. Synthesis of (*R*)-6,6'-Bis-(perfluoro-*n*-hexyl)-2,2'-di(trifluoromethane-sulphonyloxy)-1,1'-binaphthyl^[25]



Triflic anhydride (0.69 g, 2.44 mmol) was added dropwise to a solution of (*R*)-6,6'-bis-(perfluoro-*n*-hexyl)-1,1'-bi-2-naphthol (0.90 g, 0.98 mmol) and pyridine (0.24 cm³, 2.93 mmol) at 0 °C in dry dichloromethane (50 cm³) and the mixture was stirred for 4 hours. The solvent was removed under reduced pressure and the product extracted into ethyl acetate (50 cm³). This solution was washed with 5 % hydrochloric acid (100 cm³), saturated NaHCO₃ (100 cm³), 10 % NaCl solution (100 cm³) and water (100 cm³). The organic phase was dried over magnesium sulphate, filtered and the solvent removed under reduced pressure. The crude product was isolated as an oil which solidified after prolonged drying under high vacuum and was then recrystallised from hexane (0.80 g, 69 %); Mp 120-122 °C; ¹H NMR (CDCl₃) δ 7.30 (2H, d, ³J_{HH} = 8.8 Hz, ArH), 7.50 (2H, d, ³J_{HH} = 8.8 Hz, ArH), 7.70 (2H, d, ³J_{HH} = 9.1 Hz, ArH), 8.24 (2H, d, ³J_{HH} = 9.1 Hz, ArH), 8.26 (2H, s, ArH); ¹⁹F {¹H} NMR (CDCl₃) δ -74.47 (6F, s, OTf), -80.90 (6F, t, ⁴J_{FF} = 10.4 Hz, 2 x CF₃), -110.68 (4F, t, ³J_{FF} = 13.3 Hz, 2 x CF₂), -121.50 (8F, m, 4 x CF₂), -122.80 (4F, m, 2 x CF₂), -126.19 (4F, m, 2 x CF₂); ¹³C {¹H} NMR (CDCl₃) δ 118.08 (q, ¹J_{CF} = 320.1 Hz CF₃), 121.00 (s, CH), 123.11 (s, C), 125.05 (s, CH), 127.34 (s, CH), 128.19 (s, C), 128.38 (s, CH), 131.33 (s, C), 133.43 (s, CH), 134.45 (s, C), 147.00 (s, C); m/z (FAB) 1186 [M]⁺ (21 %), 1054 [MH - Tf]⁺ (11%), 868 [MH - C₆F₁₃]⁺ (12 %).

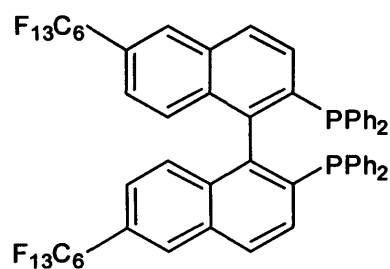
6.5.2.10. Synthesis of (*S*)-6,6'-Bis-(perfluoro-*n*-hexyl)-2,2'-di(trifluoromethane-sulphonyloxy)-1,1'-binaphthyl^[25]



Triflic anhydride (2.29 g, 8.13 mmol) was added dropwise to a solution of (*S*)-6,6'-bis-(perfluoro-*n*-hexyl)-1,1'-bi-2-naphthol (3.00 g, 3.25 mmol) and pyridine (0.78 cm³, 9.76 mmol) at 0 °C in dry dichloromethane (100 cm³) and the mixture was stirred for 4 hours. The solvent was removed under reduced pressure and the product extracted into ethyl acetate (75 cm³). This solution was washed with 5 % hydrochloric acid (100 cm³), saturated NaHCO₃ (100 cm³), 10 % NaCl solution (100 cm³) and water (100 cm³). The organic phase was dried over magnesium sulphate, filtered and the solvent

removed under reduced pressure. The crude product was isolated as an oil which solidified after prolonged drying under high vacuum and was then recrystallised from hexane (2.94 g, 76 %); Mp 118-120 °C; ^1H NMR (CDCl_3) δ 7.29 (2H, d, $^3J_{\text{HH}} = 9.1$ Hz, ArH), 7.50 (2H, d, $^3J_{\text{HH}} = 8.8$ Hz, ArH), 7.69 (2H, d, $^3J_{\text{HH}} = 9.1$ Hz, ArH), 8.22 (2H, d, $^3J_{\text{HH}} = 9.1$ Hz, ArH), 8.24 (2H, s, ArH), ^{19}F $\{^1\text{H}\}$ NMR (CDCl_3) δ -74.47 (6F, s, OTf), -80.90 (6F, t, $^4J_{\text{FF}} = 10.4$ Hz, 2 x CF_3), -110.68 (4F, t, $^3J_{\text{FF}} = 13.3$ Hz, 2 x CF_2), -121.50 (8F, m, 4 x CF_2) -122.80 (4F, m, 2 x CF_2), -126.19 (4F, m, 2 x CF_2); ^{13}C $\{^1\text{H}\}$ NMR (CDCl_3) δ 118.10 (q, $^1J_{\text{CF}} = 320.2$ Hz CF_3), 121.02 (s, CH), 123.13 (s, C), 125.05 (s, CH), 127.37 (s, CH), 128.18 (s, C), 128.38 (s, CH), 131.34 (s, C), 133.43 (s, CH), 134.45 (s, C), 147.01 (s, C); m/z (FAB) 1186 $[\text{M}]^+$ (19 %), 1054 $[\text{MH} - \text{Tf}]^+$ (15%), 868 $[\text{MH} - \text{C}_6\text{F}_{13}]^+$ (10 %).

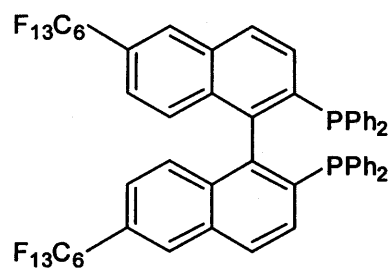
6.5.2.11. Synthesis of (*R*)-6,6'-Bis-(perfluoro-*n*-hexyl)-2,2'-bis(diphenylphosphino)-1,1'-binaphthyl^[25]



To a dry and degassed DMF solution of $[\text{NiCl}_2(\text{dppe})]$ (0.033 g, 6.24×10^{-5} mol in 50 cm^3) under N_2 was added diphenylphosphine (0.13 cm^3 , 7.49×10^{-4} mol). The solution was then heated to $150 \text{ }^\circ\text{C}$ for 1 hour. A DMF solution of (*R*)-6,6'-bis-(perfluoro-*n*-hexyl)-2,2'-di-(trifluoromethane-sulphonyloxy)-1,1'-binaphthyl (0.740 g , 6.24×10^{-4} mol in 50 cm^3) and DABCO (0.245 g , 2.18×10^{-5} mol) was added and the mixture stirred at $110 \text{ }^\circ\text{C}$ under N_2 for 4 hours. An additional portion of diphenylphosphine (0.13 cm^3 , 7.49×10^{-4} mol) was added by syringe and heating and stirring was continued for a further 72 hours.

The reaction was allowed to cool to room temperature and the DMF distilled under reduced pressure. The resulting brown solid was stirred in MeOH (50 cm^3) for 1 hour, filtered, washed with MeOH and dried *in vacuo* to yield an off-white powder. The crude product was recrystallised from DCM/MeOH (0.540 g , 69 %); Mp $253\text{-}256 \text{ }^\circ\text{C}$; ^1H NMR (CDCl_3) δ 6.58 (2H, d, $^3J_{\text{HH}} = 8.8$ Hz, ArH), 6.78 (2H, d, $^3J_{\text{HH}} = 8.8$ Hz, ArH), 6.85-7.33 (20H, m, Ph), 7.50 (2H, d, $^3J_{\text{HH}} = 8.6$ Hz, ArH), 7.93 (2H, d, $^3J_{\text{HH}} = 8.5$ Hz, ArH), 8.01 (2H, s, ArH); ^{19}F $\{^1\text{H}\}$ NMR (CDCl_3) δ -80.74 (6F, t, $^4J_{\text{FF}} = 10.4$ Hz, 2 x CF_3), -110.28 (4F, m, 2 x CF_2), -121.36 (8F, m, 4 x CF_2) -122.74 (4F, m, 2 x CF_2), -126.08 (4F, m, 2 x CF_2); ^{31}P $\{^1\text{H}\}$ NMR (CDCl_3) δ -13.39 (s); ^{13}C $\{^1\text{H}\}$ NMR (CDCl_3) δ 121.42 (CH), 125.43 (C), 126.40 (CH), 126.55 (CH), 127.07 (CH), 127.19 (CH), 127.34 (CH), 128.07 (CH), 128.17 (CH), 130.37 (CH), 130.94 (C), 131.76 (CH), 133.18 (C), 133.80 (CH), 134.15 (C), 136.26 (C), 138.86 (C), 142.20 (C).

6.5.2.12. Synthesis of (*S*)-6,6'-Bis-(perfluoro-*n*-hexyl)-2,2'-bis(diphenylphosphino)-1,1'-binaphthyl^[25]



To a dry and degassed DMF solution of $[\text{NiCl}_2(\text{dppe})]$ (0.111 g, 2.11×10^{-4} mol in 100 cm^3) under N_2 was added diphenylphosphine (0.44 cm^3 , 2.53 mmol). The solution was then heated to $150 \text{ }^\circ\text{C}$ for 1 hour. A DMF solution of (*S*)-6,6'-bis-(perfluoro-*n*-hexyl)-2,2'-di-(trifluoromethane-sulphonyloxy)-1,1'-binaphthyl (2.5 g, 2.11 mmol in 50 cm^3) and DABCO (0.827 g, 7.39 mmol) was added and the mixture stirred at $110 \text{ }^\circ\text{C}$ under N_2 for 4 hours. An additional portion of diphenylphosphine (0.44 cm^3 , 2.53 mmol) was added by syringe and heating and stirring was continued for a further 72 hours.

The reaction was allowed to cool to room temperature and the DMF distilled under reduced pressure. The resulting brown solid was stirred in MeOH (100 cm^3) for 1 hour, filtered, washed with MeOH and dried *in vacuo* to yield an off-white powder. The crude product was recrystallised from DCM/MeOH (1.85 g, 70 %); Mp $256\text{-}259 \text{ }^\circ\text{C}$; ^1H NMR (CDCl_3) δ 6.65 (2H, d, $^3J_{\text{HH}} = 8.8 \text{ Hz}$, ArH), 6.87 (2H, d, $^3J_{\text{HH}} = 9.1 \text{ Hz}$, ArH), 6.95-7.40 (20H, m, Ph), 7.59 (2H, d, $^3J_{\text{HH}} = 8.8 \text{ Hz}$, ArH), 8.02 (2H, d, $^3J_{\text{HH}} = 8.2 \text{ Hz}$, ArH), 8.09 (2H, s, ArH); ^{19}F $\{^1\text{H}\}$ NMR (CDCl_3) δ -80.72 (6F, t, $^4J_{\text{FF}} = 9.5 \text{ Hz}$, 2 x CF_3), -110.26 (4F, m, 2 x CF_2), -121.34 (8F, m, 4 x CF_2), -122.71 (4F, m, 2 x CF_2), -126.06 (4F, m, 2 x CF_2); ^{31}P $\{^1\text{H}\}$ NMR (CDCl_3) δ -13.37 (s); ^{13}C $\{^1\text{H}\}$ NMR (CDCl_3) δ 121.42 (CH), 125.43 (C), 126.41 (CH), 126.54 (CH), 127.07 (CH), 127.19 (CH), 127.40 (CH), 128.07 (CH), 128.16 (CH), 130.37 (CH), 130.94 (C), 131.76 (CH), 133.19 (C), 133.80 (CH), 134.23 (C), 136.27 (C), 138.83 (C), 142.08 (C).

6.5.2.13. Synthesis of $[\text{PdCl}_2\{(\text{R})\text{-RfBINAP}\}]$

$[\text{PdCl}_2(\text{MeCN})_2]$ (0.031 g, 11.92 mmol) and (*R*)-RfBINAP (0.150 g, 11.92 mmol) were dissolved in dry and degassed DCM (20 cm^3) and stirred under N_2 for 3 hours at room temperature. Hexane (10 cm^3) was added, the resulting precipitate was filtered and dried under vacuum to yield the product as a vibrant yellow powder (0.102 g, 60%); ^1H NMR (CDCl_3) δ 6.66 – 6.80 (6H, m, ArH/Ph), 6.85 (2H, m, ArH), 7.26 (2H, d, $^3J_{\text{HH}} = 9.0 \text{ Hz}$, ArH), 7.38 - 7.82 (18H, m, ArH/Ph), 7.87 (2H, s, ArH); ^{19}F $\{^1\text{H}\}$ NMR (CDCl_3) δ -80.67 (6F, t, $^4J_{\text{FF}} = 9.5 \text{ Hz}$, 2 x CF_3), -110.72 (4F, m, 2 x CF_2), -120.79 (4F, m, 2 x CF_2), -121.26 (4F, m, 2 x CF_2), -122.68 (4F, m, 2 x CF_2), -126.01 (4F, m, 2 x CF_2); ^{31}P $\{^1\text{H}\}$ NMR (CDCl_3) δ 28.69 (s); ^{13}C $\{^1\text{H}\}$ NMR (CDCl_3) δ 115.44 (C), 121.61 (C), 122.34 (C), 123.89 (CH), 127.70 (CH), 128.00 (CH), 128.01 (CH), 128.17 (CH), 128.83 (C),

129.77 (CH), 130.20 (CH), 130.85 (CH), 131.47 (CH), 132.79 (C), 133.90 (C), 135.12 (CH), 135.26 (CH), 137.79 (C); m/z (FAB) 1399 [M-Cl]⁺ (100 %).

6.5.2.14. Synthesis of [PdCl₂{(S)-RfBINAP}]

[PdCl₂(MeCN)₂] (0.175 g, 67.57 mmol) and (S)-RfBINAP (0.850 g, 67.57 mmol) were dissolved in dry and degassed DCM (20 cm³) and stirred under N₂ for 2 hours at room temperature. The solvent was removed under vacuum to yield the product as a vibrant yellow powder (0.919 g, 95%); ¹H NMR (CDCl₃) δ 6.56 – 6.70 (6H, m, Ar/Ph), 6.85 (2H, m, Ph), 7.23 (2H, d, ³J_{HH} = 9.0 Hz, ArH), 7.34 - 7.68 (14H, m, ArH/Ph), 7.75 (2H, d, ³J_{FF} = 7.9 Hz, ArH), 7.79 (2H, d, ³J_{FF} = 7.9 Hz, ArH), 7.83 (2H, s, ArH); ¹⁹F {¹H} NMR (CDCl₃) δ -80.68 (6F, t, ⁴J_{FF} = 10.4 Hz, 2 x CF₃), -110.66 (4F, m, 2 x CF₂), -120.84 (4F, m, 2 x CF₂), -121.73 (4F, m, 2 x CF₂), -122.69 (4F, m, 2 x CF₂), -126.03 (4F, m, 2 x CF₂); ³¹P {¹H} NMR (CDCl₃) δ 28.90 (S); ¹³C {¹H} NMR (CDCl₃) δ 115.26 (C), 121.61 (C), 122.34 (C), 123.89 (CH), 127.70 (CH), 127.99 (CH), 128.02 (CH), 128.17 (CH), 128.85 (C), 129.72 (CH), 130.14 (CH), 130.86 (CH), 131.45 (CH), 132.85 (C), 133.90 (C), 135.15 (CH), 135.29 (CH), 137.82 (C); m/z (FAB) 1399 [M-Cl]⁺ (100 %).

6.5.2.15. Synthesis of [Pd(OH₂)₂{(R)-RfBINAP}](OTf)₂

To a solution of [PdCl₂{(R)-RfBINAP}] (0.150 g, 10.45 mmol) in wet acetone (40 cm³, 5 % v/v H₂O) was added AgOTf (0.054 g, 20.91 mmol) under nitrogen and the mixture stirred at room temperature for 12 hours. The mixture was then filtered through Celite to remove any AgCl, washed with DCM (10 cm³) and the solvent removed under vacuum to yield the product as an orange brown powder (0.173 g, 98%); ¹H NMR (CDCl₃) δ 3.60 (4H, bs, 2 x H₂O), 6.71 (2H, d, ³J_{HH} = 8.7 Hz, ArH), 6.83 (4H, m, Ph), 6.93 (2H, m, Ph), 7.28 (2H, t, ³J_{HH} = 8.7 Hz, Ph), 7.54 - 7.86 (18H, m, ArH/Ph), 7.92 (2H, s, ArH); ¹⁹F {¹H} NMR (CDCl₃) δ -78.11 (6F, s, OTf), -80.68 (6F, t, ⁴J_{FF} = 9.5 Hz, 2 x CF₃), -110.86 (4F, m, 2 x CF₂), -120.79 (4F, m, 2 x CF₂), -121.23 (4F, m, 2 x CF₂), -122.68 (4F, m, 2 x CF₂), -126.02 (4F, m, 2 x CF₂); ³¹P {¹H} NMR (CDCl₃) δ 33.94 (S); ¹³C {¹H} NMR (CDCl₃) δ 115.02 (C), 117.78 (C), 118.64 (C), 121.76 (C), 122.56 (C), 124.44 (q, ¹J_{CF} = 327.2 Hz, OSO₂CF₃), 124.71 (CH), 127.44 (CH), 128.54 (CH), 129.10 (CH), 129.82 (CH), 129.98 (CH), 131.50 (CH), 132.31 (CH), 133.50 (CH), 133.69 (C), 134.38 (C), 134.61 (CH), 134.76 (CH), 138.64 (C).

6.5.2.16. Synthesis of [Pd(OH₂)₂{(S)-RfBINAP}](OTf)₂

To a solution of [PdCl₂{(S)-RfBINAP}] (0.760 g, 53.0 mmol) in wet acetone (40 cm³, 5 % v/v H₂O) was added AgOTf (0.272 g, 1.06 mmol) under nitrogen and the mixture stirred at room temperature for 12 hours. The mixture was then filtered through Celite to remove any AgCl, washed with DCM (10 cm³) and the solvent removed under vacuum to yield the product as an orange brown powder (0.860 g, 96%); ¹H NMR (CDCl₃) δ 3.12 (4H, bs, 2 x H₂O) 6.72 (2H, d, ³J_{HH} = 9.1 Hz, ArH), 6.83 (4H, m, Ph), 6.94 (2H, m, Ph), 7.29 (2H, t, ³J_{HH} = 9.1 Hz, Ph), 7.54 - 7.86 (18H, m, ArH/Ph), 7.92 (2H, s, ArH); ¹⁹F {¹H} NMR (CDCl₃) δ -78.18 (6F, s, OTf) -80.67 (6F, t, ⁴J_{FF} = 9.5 Hz, 2 x CF₃), -110.87 (4F, m, 2 x CF₂), -120.79 (4F, m, 2 x CF₂), -121.21 (4F, m, 2 x CF₂), -122.66 (4F, m, 2 x CF₂), -126.03 (4F, m, 2 x CF₂); ³¹P {¹H} NMR (CDCl₃) δ 33.94 (S); ¹³C {¹H} NMR (CDCl₃) δ 115.25 (C), 117.80 (C), 118.66 (C), 121.79 (C), 122.60 (C), 124.44 (q, ¹J_{CF} = 327.2 Hz, OSO₂CF₃), 124.74 (CH), 127.45 (CH), 128.56 (CH), 129.12 (CH), 129.85 (CH), 130.00 (CH), 131.46 (CH), 132.33 (CH), 133.48 (CH), 133.68 (C), 134.38 (C), 134.64 (CH), 134.78 (CH), 138.66 (C).

6.5.3. Preparation of 10 % Loaded Supported Palladium Catalyst

A 10:1 mixture by mass of solid support material and the palladium BINAP catalyst were stirred in THF (15 cm³) at room temperature for 30 minutes. The solvent was removed in *vacuo* and the resulting pale yellow support was dried to constant weight.

6.5.4. General Procedure for Enantioselective Fluorination With NFSI Under Homogeneous Conditions

A 50 cm³ round-bottomed flask was charged with β-ketoester substrate (27.2 mmol), palladium catalyst (5 mol %, 1.36 mmol) and THF (20 cm³) and the mixture stirred at room temperature for 10 minutes. The flask was cooled to -25 °C, NFSI (0.128 g, 40.8 mmol) added and the mixture stirred for 12 hours before quenching with saturated aqueous ammonium chloride (20 cm³). The organic phase was separated, dried over MgSO₄ and reduced under vacuum. The resulting residue was passed through a short column packed with support material, first eluting with toluene to remove NFSI and any related salts, secondly with Et₂O to recover products and lastly with THF to recover the catalyst.

6.5.5. General Procedure for Enantioselective Fluorination With NFSI With Supported Catalyst

A 50 cm³ round-bottomed flask was charged with β -ketoester substrate (27.2 mmol), supported palladium catalyst (5 mol %, 1.36 mmol) and THF (20 cm³) and the mixture stirred at room temperature for 10 minutes. The flask was cooled to -25 °C, NFSI (0.128 g, 40.8 mmol) added and the mixture stirred for 12 hours before quenching with saturated aqueous ammonium chloride (20 cm³). The mixture was filtered, the solid washed with H₂O (10 cm³), toluene (3 x 10 cm³), and then dried for use in subsequent catalytic runs. The toluene phase was reduced under vacuum and the residue purified by flash column chromatography using a silica column and the product ee determined by chiral HPLC.

References for Chapter 6

- [1] M. A. Andrews, T. C.-T. Chang, C.-W. F. Cheng, T. J. Emge, K. P. Kelly, T. F. Koetzle, *J. Am. Chem. Soc.*, **1984**, *106*, 5913.
- [2] R. Busby, M. B. Hursthouse, P. S. Jarrett, C. W. Lehrmann, K. M. A. Malik, C. Phillips, *J. Chem. Soc., Dalton Trans.*, **1993**, 3767.
- [3] D. J. Adams, E. G. Hope, A. M. Stuart, A. J. West, 'Handbook of Fluorous Chemistry', ed. J. A. Gladysz, D. P. Curran, I. T. Hórvath, Wiley-VCH, Germany, **2004**.
- [4] J. M. Vincent, A. Rabion, V. K. Yachandra, R. H. Fish, *Angew. Chem., Int. Ed. Engl.*, **1997**, *36*, 2346.
- [5] J. G. Sharefkin, H. Saltzman, *Organic Syntheses*, **1973**, *Coll. Vol. 5*, 665.
- [6] F. Siméon, P.-A. Jarffrès, D. Villemin, *Tetrahedron*, **1998**, *54*, 10111.
- [7] A. Michaelis, R. Kaehne, *Chem. Ber.*, **1898**, *31*, 1048.
- [8] A. E. Arbuzov, *J. Russ. Phys. Chem. Soc.*, **1906**, *38*, 687.
- [9] R. N. Haszeldine, D. L. Hobson, D. R. Taylor, *J. Fluorine Chem.*, **1976**, *8*, 115.
- [10] C. Emnet, J. A. Gladysz, *Synthesis*, **2005**, *6*, 1012.
- [11] I. P. Beletskaya, M. M. Kabachnik, M. D. Solnsteva, *Russ. J. Org. Chem.*, **1999**, *35*, 71.
- [12] P. Machnitzki, T. Nickel, O. Stelzer, C. Landgrafe, *Eur. J. Inorg. Chem.*, **1998**, *7*, 1029.
- [13] T. Hirao, T. Masunaga, N. Yamada, Y. Ohshiro, T. Agawa, *Bull. Chem. Soc. Jpn.*, **1982**, *55*, 909.
- [14] R. C. Grabiak, J. A. Miles, G. M. Schwenzer, *Phosphorus Sulfur*, **1980**, *9*, 197.
- [15] C. Yuan, H. Feng, *Synthesis*, **1990**, 140.
- [16] M. B. Dines, P. M. Giacomo, *Inorg. Chem.*, **1981**, *20*, 92.
- [17] R. W. Kemmitt, S. Mason, J. Fawcett, D. R. Russell, *J. Chem. Soc., Dalton Trans.*, **1992**, 851.
- [18] R. S. Drago, J. R. Long, R. Cosmano, *Inorg. Chem.*, **1982**, *21*, 2196.
- [19] A. Biffis, E. Castello, M. Zecca, M. Basato, *Tetrahedron*, **2001**, *57*, 10391.
- [20] D. Crich, Y. Zou, *J. Org. Chem.*, **2005**, *70*, 3309.
- [21] L. Kurz, L. Gray, D. Morgans, M. J. Waldyke, T. Ward, *Tetrahedron Lett.*, **1990**, *31*, 6321.
- [22] H. Takaya, K. Mashima, K. Koyano, M. Yagi, H. Kumobayashi, T. Taketomi, S. Akutagawa, R. Noyori, *J. Org. Chem.*, **1986**, *51*, 629.
- [23] T. Hayashi, Y. Matsumoto, Y. Ito, *J. Am. Chem. Soc.*, **1988**, *110*, 5579.
- [24] Y. Hamashima, K. Yagi, H. Takano, L. Tamás, M. Sodeoka, *J. Am. Chem. Soc.*, **2002**, *124*, 14530.
- [25] E. G. Hope, A. M. Stuart, A. J. West, *Green Chem.*, **2004**, *6*, 345.

Appendix

Crystal data and structure refinement for [Pt{OP(O)(Ph)O}(PPh₃)₂]

Empirical formula	C ₄₃ H ₃₇ Cl ₂ O ₃ P ₃ Pt	
Formula weight	960.63	
Temperature	150(2) K	
Wavelength	0.71073 Å	
Crystal system	Triclinic	
Space group	P-1	
Unit cell dimensions	a = 10.709(4) Å	α = 110.509(6)°
	b = 12.694(5) Å	β = 91.607(6)°
	c = 16.659(6) Å	γ = 110.300(5)°
Volume	1960.4(12) Å ³	
Z	2	
Density (calculated)	1.627 Mg/m ³	
Absorption coefficient	3.877 mm ⁻¹	
F(000)	952	
Crystal size	0.16 x 0.11 x 0.09 mm ³	
Theta range for data collection	1.82 to 25.00°.	
Index ranges	-12 ≤ h ≤ 12, -15 ≤ k ≤ 14, -19 ≤ l ≤ 19	
Reflections collected	13392	
Independent reflections	6788 [R(int) = 0.0789]	
Completeness to theta = 25.00°	98.3 %	
Absorption correction	Empirical	
Max. and min. transmission	0.862 and 0.677	
Refinement method	Full-matrix least-squares on F ²	
Data / restraints / parameters	6788 / 0 / 469	
Goodness-of-fit on F ²	1.132	
Final R indices [I > 2σ(I)]	R1 = 0.0637, wR2 = 0.1347	
R indices (all data)	R1 = 0.0753, wR2 = 0.1395	
Largest diff. peak and hole	2.678 and -2.420 e.Å ⁻³	

Crystal data and structure refinement for [Pt{OP(O)(C₆H₄-4-F)O}(PPh₃)₂]

Empirical formula	C ₄₉ H ₅₀ Cl ₂ F O ₃ P ₃ Pt
Formula weight	1064.79
Temperature	150(2) K
Wavelength	0.71073 Å
Crystal system	Triclinic
Space group	P-1
Unit cell dimensions	a = 10.750(3) Å α = 88.632(4)° b = 12.715(3) Å β = 80.066(4)° c = 18.134(4) Å γ = 69.989(3)°
Volume	2292.5(9) Å ³
Z	2
Density (calculated)	1.543 Mg/m ³
Absorption coefficient	3.327 mm ⁻¹
F(000)	1068
Crystal size	0.23 x 0.16 x 0.09 mm ³
Theta range for data collection	2.02 to 26.00°.
Index ranges	-13 ≤ h ≤ 13, -15 ≤ k ≤ 15, -22 ≤ l ≤ 22
Reflections collected	17788
Independent reflections	8864 [R(int) = 0.0349]
Completeness to theta = 26.00°	98.3 %
Absorption correction	Empirical
Max. and min. transmission	0.802 and 0.622
Refinement method	Full-matrix least-squares on F ²
Data / restraints / parameters	8864 / 0 / 451
Goodness-of-fit on F ²	0.987
Final R indices [I > 2σ(I)]	R1 = 0.0294, wR2 = 0.0659
R indices (all data)	R1 = 0.0351, wR2 = 0.0670
Largest diff. peak and hole	1.573 and -1.056 e.Å ⁻³

Crystal data and structure refinement for [Pt{OP(O)(C₆H₄-4-CF₃)O}(PPh₃)₂]

Empirical formula	C ₄₆ H ₃₉ Cl ₇ F ₃ O ₃ P ₃ Pt	
Formula weight	1232.92	
Temperature	150(2) K	
Wavelength	0.71073 Å	
Crystal system	Triclinic	
Space group	P-1	
Unit cell dimensions	a = 12.762(2) Å	α = 75.523(3)°
	b = 13.973(3) Å	β = 89.498(3)°
	c = 14.618(3) Å	γ = 65.859(3)°
Volume	2290.3(7) Å ³	
Z	2	
Density (calculated)	1.788 Mg/m ³	
Absorption coefficient	3.631 mm ⁻¹	
F(000)	1216	
Crystal size	0.21 x 0.16 x 0.06 mm ³	
Theta range for data collection	1.76 to 25.00°.	
Index ranges	-15 ≤ h ≤ 15, -16 ≤ k ≤ 16, -17 ≤ l ≤ 17	
Reflections collected	16683	
Independent reflections	8011 [R(int) = 0.0325]	
Completeness to theta = 25.00°	99.1 %	
Absorption correction	Empirical	
Max. and min. transmission	0.862 and 0.651	
Refinement method	Full-matrix least-squares on F ²	
Data / restraints / parameters	8011 / 0 / 514	
Goodness-of-fit on F ²	0.981	
Final R indices [I > 2σ(I)]	R1 = 0.0314, wR2 = 0.0630	
R indices (all data)	R1 = 0.0369, wR2 = 0.0643	
Largest diff. peak and hole	1.413 and -0.886 e.Å ⁻³	

Crystal data and structure refinement for $[\text{Pt}\{\text{OP}(\text{O})(\text{C}_2\text{H}_4\text{-C}_6\text{F}_{13})\text{O}\}(\text{PPh}_3)_2]$

Empirical formula	C ₄₅ H ₃₆ Cl ₂ F ₁₃ O ₃ P ₃ Pt	
Formula weight	1230.64	
Temperature	150(2) K	
Wavelength	0.71073 Å	
Crystal system	Triclinic	
Space group	P-1	
Unit cell dimensions	a = 10.742(2) Å	α = 91.262(3)°
	b = 12.570(2) Å	β = 96.664(3)°
	c = 19.076(4) Å	γ = 111.477(3)°
Volume	2374.9(8) Å ³	
Z	2	
Density (calculated)	1.721 Mg/m ³	
Absorption coefficient	3.258 mm ⁻¹	
F(000)	1208	
Crystal size	0.21 x 0.17 x 0.07 mm ³	
Theta range for data collection	1.75 to 26.00°.	
Index ranges	-13 ≤ h ≤ 13, -15 ≤ k ≤ 15, -23 ≤ l ≤ 23	
Reflections collected	18537	
Independent reflections	9192 [R(int) = 0.0388]	
Completeness to theta = 26.00°	98.3 %	
Absorption correction	Empirical	
Max. and min. transmission	0.802 and 0.585	
Refinement method	Full-matrix least-squares on F ²	
Data / restraints / parameters	9192 / 400 / 622	
Goodness-of-fit on F ²	1.031	
Final R indices [I > 2σ(I)]	R1 = 0.0517, wR2 = 0.1319	
R indices (all data)	R1 = 0.0645, wR2 = 0.1373	
Largest diff. peak and hole	2.259 and -1.256 e.Å ⁻³	

Seminars, Conferences and Lecture Courses Attended

2003

Monday 6th October, Dr Chris Richards (Queens Mary, University of London), *Very Active Planar Chiral Catalysts for Asymmetric Synthesis*

Wednesday 8th October, Prof. Iain Campbell, FRS (University of Oxford), 2nd Tim Norwood Memorial Lecture, *NMR and Proteins*

Monday 20th October, Dr Sandie Dann (University of Loughborough), *Unusual Complex Oxides and Sulfides*

Monday 27th October, Dr Chris Hayes (University of Nottingham), *Natural and Non-natural Products: Total Synthesis and Biological Applications*

Friday 14th November, Prof. Walter Leitner (Max Planck Institute, Mülheim), Greiss Lecture (RSC)

Monday 24th November, Prof. Thomas Wirth (Cardiff University), *Scope and Potential of Chiral Electrophiles in Stereoselective Synthesis*

Monday 8th December, Prof. Peter Hore (University of Oxford), *Real-time NMR Techniques for Studying Protein Structure and Folding*

2004

Monday 12th January, Dr Liam Cox (University of Birmingham), *Exploiting Silicon Reagents in Asymmetric Reactions*

Monday 19th January, Prof. Bill Levason (University of Southampton), *Recent Developments in the Chemistry of Antimony Ligands*

Monday 9th February, Dr Michael Whitlesey (University of Bath), *Stoichiometric and Catalytic Ruthenium Carbene Systems*

Monday 1st March, Dr Iain Coldham (University of Sheffield), *Stereoselective Synthesis of Cyclic Amines using Chiral Organolithium Species and Cycloaddition Reactions*

Monday 26th April, Dr Graham Sandford (University of Durham), *Polyfunctional Heterocycles and Macrocycles*

Monday 10th May, Dr Dominic Wright (University of Cambridge), *Torocyclic Ligands*

Monday 24th May, Dr Steve Allin (Loughborough University), *New Asymmetric Routes to Chiral Heterocycles*

Monday 7th June, Prof. Peter Scott (University of Warwick), *Catalysis with Chiral Metal Complexes*

Monday 15th October, Prof. Eric Herbst (Ohio State University), *Chemistry and Star Formation*

Monday 25th October, Prof. Alan Armstrong (Imperial College, London), *New Methods and Synthetic Applications of Asymmetric Heteroatom Transfer*

Monday 11th November, Dr Helen Aspinall (University of Liverpool), *Chiral Lanthanides Complexes for Organic Synthesis*

Monday 15th November, Dr Gareth J. Pritchard (University of Loughborough), *New Routes to Heterocyclic Systems From Vinylcyclopropanes*

2005

Monday 17th January, Dr Stuart McGregor (Heriot-Watt University, Edinburgh), *Non-innocent N-Heterocyclic Carbene and Phosphine Ligands*

Monday 7th February, Dr Mike Hill (Imperial College, London), *Molecular Catalysis with Group 2 Metals*

Monday 14th June, Dr Simon Jones (University of Sheffield), *Fiddling With Phosphorus*

Monday 10 October, Dr. Christopher Frost (University of Bath), *Exploring New Strategies in Organic Synthesis via Catalytic Conjugate Addition*

Monday 17 October, Prof Gary Attard (University of Cardiff), *Aspects of Chiral Surface Chemistry: an Electrochemical Perspective*

Wednesday 26 October, Prof. R.H. Holm (Harvard University), *Structural and Functional Analogues of Molybdenum and Tungsten Oxotransferases/Hydroxylases: What can be Learned?*

Monday 31 October, Prof. Matthew Davidson (University of Bath), *Metal and Metal-free Phenolates: Catalysts, Sensors and Surprises*

Monday 7 November, Prof. Richard Templar (Imperial College London), *How Cells Survive- from Lipids to Liquid Crystals*

Wednesday 9 November, Prof.. Peter H. Seeberger (ETH, Zurich), *Chemical Glycomics: Automated Synthesis of Carbohydrates as a Platform for Biological and Medical Research*

Monday 14 November, Dr. Richard S. Grainger (University of Birmingham), *Harnessing Reactive Intermediates for Organic Synthesis*

Tuesday 29 November, Prof. Tim Softley (University of Oxford), *From Highly Excited to Ultracold Molecules: Chemical Dynamics in the Extreme*

Monday 5 December, Prof. Tom Simpson (University of Bristol), *Chemical and Biochemical Studies on Polyketide Natural Products*

2006

Monday 30 January, Prof. Michiel Sprik (University of Cambridge), *Density Functional Based Molecular Dynamics Simulation of Redox Reactions in Solution*

Monday 20 February, Prof. Colin Creaser (Nottingham-Trent University), *Ion Mobility Spectrometry: Shaping up for the Structural and Trace Analysis*

Monday 6 March, Prof. Mikiko Sodeoka (Tohoku University, Japan), *Rosalind Franklin Lectureship 2006*

Monday 13 March, Dr. Paul Howes (Department of Physics, University of Leicester), *Nanoparticle Toxicology*

Monday 3rd April, Prof. Jonathan Williams (University of Bath), *C-C Bond Formation from Alcohols*

Conferences Attended

Crystal Faraday Associates Induction Workshop. University of Loughborough, December 2003

3rd Leicester Catalysis Symposium. University of Leicester, February 2004

10th Merck Case Conference. Botleigh Grange Hotel, Southampton, April 2004

Crystal Faraday Associates Workshop. University of Leicester, April 2004

4th Bristol Synthesis Meeting. University of Bristol, April 2004

Coordination Chemistry Discussion Group Meeting. University of Leicester, July 2004

4th RSC Fluorine Subject Group Meeting. University of Durham, September 2004

Sheffield Stereochemistry Meeting. University of Sheffield, December 2004

Inorganic Chemistry Meeting. University of Warwick, March 2005

11th Merck Case Conference. Botleigh Grange Hotel, Southampton, April 2005

5th Bristol Synthesis Meeting. University of Bristol, April 2005

RSC Fluorine Group Postgrad Symposium, Oxford University, September 2005

Green Chemistry Summer School, Venice University, September 2005

Catalysis Summer School, Liverpool University, September 2005

Half-day Synthesis Symposium, University of Leicester, February 2006

12th Merck CASE Conference, Botleigh Grange Hotel, Southampton, April 2006

22nd Organometallic Chemistry Conference, Zaragoza, Spain, July 2006

Presentations Made

Poster entitled “Fluorous Zirconium Phosphonates” presented at the Crystal Faraday Workshops, Merck Case Conference and Leicester Catalysis Symposium. Brief presentation, also entitled “Fluorous Zirconium Phosphonates”, presented at the Crystal Faraday Associates Induction Workshop. Poster entitled “Fluorous Zirconium Phosphonates as Novel Materials for Catalyst Recovery” presented at the Green Chemistry and Catalysis Summer Schools and at the 22nd Organometallic Chemistry Conference. Oral presentation entitled “Fluorous Zirconium Phosphonates as Novel Materials for Catalyst Recovery” given at the RSC Fluorine Group Postgrad Symposium and the 12th Merck CASE Conference.

Publications and Awards

D. J. Adams, J. A. Bennett, D. J. Cole-Hamilton, E. G. Hope, J. Hopewell, J. Kight, P. Pogorzelec, A. M. Stuart, *J. Chem. Soc. Dalton Trans.*, **2005**, 3862.

D. J. Adams, J. A. Bennett, D. Duncan, E. G. Hope, J. Hopewell, A. M. Stuart A. J. West, *Polyhedron*, **2007**, *26*, 1505.

Winner of the oral presentation prize at the 11th Merck Case Conference, Botleigh Grange Hotel, Southampton, April 2005.

Lecture Courses Attended (2003 to 2004)

Title	Convenor	Term	Credits
Retrosynthetic Analysis	Dr. P, Jenkins	1	5
Crystallography	Dr. D, Russel	2	5
Exploring Reaction Mechanisms	Dr M, Harger / Prof. P, Cullis	2	5